LATE PLEISTOCENE TECHNOLOGICAL CHANGE AND HUNTER GATHERER BEHAVIOR AT MOCHE BORAGO ROCKSHELTER, SODO-WOLAYTA, ETHIOPIA: FLAKED STONE ARTIFACTS FROM THE EARLY OIS 3 (60 – 43 KA) DEPOSITS

By

ERICH C. FISHER

A DISSERTATION PRESENTED TO THE GRADUATE SCHOOL
OF THE UNIVERSITY OF FLORIDA IN PARTIAL FULFILLMENT
OF THE REQUIREMENTS FOR THE DEGREE OF
DOCTOR OF PHILOSOPHY

UNIVERSITY OF FLORIDA

2010

To the Wolayta people living at Moche Borago today. Tosimo.

ACKNOWLEDGEMENTS

I thank my committee chair, and friend, Dr. Steven Brandt first and foremost for his support, advice, and wisdom these past few years. I also thank my doctoral committee for their advice throughout the entire Ph.D. process. My research was graciously funded by the J. William Fulbright U.S. student program, and I would particularly like to thank my Fulbright program adviser, Jermaine Jones as well as Yohannes Birhanu at the U.S. Embassy in Addis Ababa. I also acknowledge the support of Dr. Zinabu Gebremariam, Markos Tekle, and the faculty and staff at Hawassa University who warmly received me, gave me space to work, and accommodation. Similarly, I thank Wezeru Mamitu Yilma and Ato Menker Bitew at the National Museum of Ethiopia for providing space to analyze the collections, and the Sodo Bureau of Culture, SNNPR Bureau of Culture, and, most importantly, the Authority for Research and Conservation of Cultural Heritage for their continued support of SWEAP research. In particular, I thank Ato Jara Hailemariam, Director of ARCCH, and Dr. Yonas Beyene, Head of Archaeology. I would be remiss not to acknowledge my appreciation to Ms. Anna Fernyhough and Dr. Gebre Yntiso for accommodation and friendship while I was living in Ethiopia. I also thank Stephen Burns, Jason Cosford, Hai Cheng, Antje Voelker, Syee Weldeab, Seifu Kebede, Mohammed Umer, and Henry Lamb for providing ideas and/or data about paleolclimates related to my research. Lastly, I extend my most gracious thank you to my parents, my family, and my friends who have supported me tirelessly throughout these past few years.

TABLE OF CONTENTS

Page

LIST OF TABLES

LIST OF FIGURES

Abstract of Dissertation Presented to the Graduate School
of the University of Florida in Partial Fulfillment of the
Requirements for the Degree of Doctor of Philosophy

LATE PLEISTOCENE TECHNOLOGICAL CHANGE AND HUNTER GATHERER BEHAVIOR AT MOCHE BORAGO ROCKSHELTER, SODO-WOLAYTA, ETHIOPIA: FLAKED STONE ARTIFACTS FROM THE EARLY OIS 3 (60 – 43 KA) DEPOSITS

By

ERICH C. FISHER

August 2010

Chair: Steven A. Brandt
Major: Anthropology

The current archaeological evidence suggests that hunter-gatherers living in Africa during the Late Pleistocene rapidly expanded into Europe and Asia by 50 – 40 ka. It is widely believed that these populations of humans practiced a modern behavioral repertoire that included, among other things, complex social and technological skills. However, there are only a handful of sites across the Horn of Africa that date to this critical time period, known as Oxygen Isotope Stage 3. Consequently, very few studies have been able to comment on any of the behavioral or environmental preconditions that may have influenced or affected these populations prior to, and during, the hypothesized migrations via the Horn and out of Africa.

This dissertation presents new data from the Moche Borago rockshelter, located on the western flank of the volcano Mt. Damota near the current town of Sodo in Wolayta, southwest Ethiopia. Moche Borago has been studied since 2006 by the Southwest Ethiopia Archaeological Project and the sequence provides an intact series of archaeological deposits dating to early OIS 3, ~54 – 40 ka. This dissertation focuses on the analysis of stone tools from the lower deposits at Moche Borago dating from ~54 – 43 ka to infer technological behavioral change in southwest Ethiopia during this time period.

These findings are compared against broader paleoclimatic proxy records, which suggest that there may have been rapid and repeated fluctuations in the West African and Southwest Asian monsoon systems at this time. Monsoonal flux may have affected local ecology and resources, and it is hypothesized here that changes in the stone tools reflect local behavioral adaptations to monsoon-driven local environmental change around Moche Borago. The rapid and repeated nature of the climatic and environmental flux during this time period may have forced resident human populations in the Horn of Africa to develop a flexible behavioral strategy that allowed these people to quickly adopt their existing social and technical behaviors to suite changing contexts. Behavioral adaptations to monsoon-driven environmental changes may partially explain the unique stone tool record in the Horn of Africa during the Late Pleistocene.

CHAPTER 1
INTRODUCTION

During the Last Glacial period (73.5-14.7 ka), anatomically and behaviorally modern hunter-gatherers moved out of Africa. Archaeological evidence shows that these colonizers spread into Australia by 60 to 40 ka (Roberts et al., 1999; Thorne et al., 1999; Bowler et al., 2003) and into Europe by 45 to 40 ka (Zilhão, 2006; Zilhão et al., 2007). Eventually, the descendants of these hunter-gatherers arrived in North America by ~20 ka (Forster et al., 1996; Oppenheimer, 2003).

The many environments these people moved through underscore their innate ability to adapt to and exploit diverse ecological conditions successfully. The main reason attributed to these successes is the development of "modern human behaviors" toward the end of the Middle Pleistocene and into the Late Pleistocene (~300-30 ka). These behaviors are broadly seen as a suite of new social, technological, and symbolic tools that gave African hunter-gatherers the ability to contend with a wider range of natural and social environments and exploit resources more effectively and efficiently. A subject of current debate is the specific nature of these "modern human behaviors" and why and how they evolved (McBrearty and Brooks, 2000; Wadley, 2001; Marean and Assefa, 2005).

My interest in this debate focuses upon what role(s) Late Quaternary paleoenvironmental changes may have had in the establishment of these modern human behaviors. Numerous scholars hypothesize that these behavioral changes were direct or indirect responses by African hunter-gatherers to either the long, cold, arid conditions of the Penultimate Glacial (195-128 ka), and/or the Last Glacial periods (73.5-14.7 ka), or to the long stretches of warm and humid climates that characterized the Last Interglacial period (128-73.5 ka) (Clark, 1960; Clark, 1988; McBrearty and Brooks, 2000; Ambrose et al., 2002; Barton et al., 2009). Many of the models

generated by these scholars argue for direct causal relationships between paleoenvironmental change and behavioral change. However, these models may be too simplistic because they fail to recognize the variability and instability that characterized Glacial and Interglacial climates of the Late Quaternary. These climates have been revealed by newer and more detailed climatic records (Wolff et al., 2010; Capron et al., 2010).

Multiple marine and terrestrial proxies from North America, Europe, and Asia reveal Oxygen Isotope Stage 3 (OIS 3) (~59-28 ka), as one of the most climatically unstable oxygen isotope stages of the last 200,000 years—if not the most climatically unstable oxygen isotope stage. Although relatively warmer and more humid than the cold and arid Oxygen Isotope Stage 4 (~72-59 ka) that preceded it, OIS 3 was punctuated by numerous short periods of even warmer and wetter climates called Dansgaard-Oeschger (D-O) events, as well as significantly colder and more arid events called Heinrich events.

The climatic fluctuations during OIS 3 are known to have changed European and African vegetation (Sanchez-Gone et al., 2008; Hessler et al., 2010). Across eastern Africa[1] these climatic variations are widely believed to have influenced the intensity of monsoonal moisture originating from the Atlantic and Indian oceans (Wang et al., 2001; Burns et al., 2003; Weldeab et al., 2007; Revel et al., 2010). These fluctuations in turn affected vegetation patterns across the region (Kiage and Liu, 2006).

How African hunter-gatherer subsistence, settlement, and social strategies may have responded to OIS 3 fluctuations, as well as what role(s) early OIS 3 (60-45 ka) climatic instability may have played in the development of modern human behavior at the threshold of

[1] Burundi, Eritrea, Ethiopia, Djibouti, Kenya, Rwanda, Somalia, Tanzania, and Uganda.

hunter-gatherer migrations through and out of Africa, have never been seriously considered. This lack of study is due in part to:

- scientists questioning whether or not any secure terrestrial paleoclimatic data from Africa can be correlated definitely to Heinrich and D-O events

- the complete absence of African archaeological sites firmly dated to the end of OIS 4 and early OIS 3

However, recent excavations by the Southwest Ethiopian Archaeological Project (SWEAP) at Moche Borago (MB) rockshelter, located in the highlands of Southwestern (SW) Ethiopia, have revealed a radiocarbon-dated archaeological sequence that spans the critical time period from 60 to 40 ka (Brandt et al., 2006; Hildebrand et al., 2008; Brandt et al., 2010). My dissertation draws upon this new database by posing four major research questions:

- What is the evidence at global, continental, and local scales for climatic fluctuations during early and middle OIS 3?

- How might these climatic changes have affected the local ecology around Moche Borago?

- If evidence exists at various scales for climatic and environmental fluctuations during OIS 3, how did the mobility patterns, subsistence strategies, and social organization of hunter-gatherers vary in response to paleoenvironmental instability?

- If evidence exists at various scales for climatic and environmental fluctuations during OIS 3, how did hunter-gatherer stone tool technology vary in response to paleoenvironmental fluctuations?

By addressing these major questions, the goal of this dissertation is to provide data at the local scale that can contribute to a better understanding of human behavioral adaptations during OIS 3 on the regional, continental, and global scales. In the future, the data from Moche Borago can be

used to develop more informed hypotheses relating to the establishment of modern human behavior in the Late Pleistocene.

This dissertation is organized into nine chapters. Following this introductory chapter, Chapter 2 provides an overview of current research on Late Pleistocene paleoclimates and environments of Europe, Asia, and Africa in order to answer the first and second of the dissertation's four major questions: What is the evidence at global, continental, regional, and local scales for major and rapid climatic fluctuations in eastern Africa during early OIS 3? I use a multi-scalar approach to tackle this question.

At the broadest scale are high-latitude ice cores from Greenland that can be linked to continental records in Europe and Africa showing mostly concurrent climatic and environmental changes (Grootes et al., 1993; Stuiver and Grootes, 2000; Sanchez-Gone et al., 2008; Hessler et al., 2010; Fletcher et al., 2010). Records from the northwest (NW) African Atlantic margin, Mediterranean coast, the Nile Basin, the Levant, and the circum-Indian Ocean area show similar paleoclimatic fluctuations during OIS 3, which affected the intensity of monsoon systems (Bar-Matthews et al., 2000; Burns et al., 2003; Weldeab et al., 2007; Revel et al., 2010). Lake cores (Livingstone, 1975; Gasse, 2000; Kebede et al., 2005) and pollen assemblages (Kiage and Liu, 2006; Hessler et al., 2010) provide data on a regional level. At the most proximal scale, the geomorphological history of the deposits at Moche Borago reveals periods of much wetter conditions in the area. These wetter periods are hypothesized to be due to increased monsoonal moisture.

Chapter 3 summarizes the intellectual history of models linking arid climatic events and human behavior in African archaeology, and also reviews ethnographic observations about how African hunter-gatherers adapt to arid environments. This intellectual history is applied to

Questions 3 and 4, which concern how the archaeological data from Moche Borago can be used to infer hunter-gatherer responses to Late Pleistocene paleoenvironmental change.

Chapter 4 gives summary background information about archaeology in the Horn of Africa dating from OIS 4 to OIS 3. A relatively few archaeological sites date to OIS 3, and many of the currently available sites are poorly dated or have gaps in the depositional sequence. The lack of archaeological data makes comparisons between sites difficult, and knowing where and how hunter-gatherers were living in the Horn is still largely unresolved.

Chapter 5 provides descriptions of the region around Moche Borago, the current inhabitants, and excavations at the site. The site was first excavated in 1996 by a research team from the Centre National de la Recherche Scientifique whose main interest was Holocene archaeology. Their excavations revealed Pleistocene deposits below the Holocene layers, which have been the focus for the Southwest Ethiopia Archaeology Project (SWEAP) since 2006. My interpretations of the site stratigraphy and context are based on SWEAP research at the site during four field seasons. The dataset of stone artifacts used in this study comes from the main SWEAP excavation area called the "Block Excavation Area" or the BXA. The nearby Esay rockshelter is also introduced in this chapter. Esay is notable for a shallow stream of water that flows across the floor of the site, providing a modern-day analog to past fluvial features, as evident in the geomorphic history of Moche Borago.

Chapter 6 details the litho-stratigraphic sequence at Moche Borago and site-specific evidence for climatic change during early OIS 3. The depositional history of the Pleistocene layers at the site is complex, showing contributions by fluvial, aeolian, and volcanic process. The Pleistocene layers subdivided naturally into litho-stratigraphic units by thick, archaeologically sterile volcanic ashes. Evidence for fluvial features at the site are found in one

of the litho-stratigraphic units called the "S-Group," which shows that the local area was much wetter at this time.

Chapter 7 provides the analysis of lithic raw materials, cores, and debitage. The stone artifact assemblage is made mainly of locally available obsidian. The oldest and deepest litho-stratigraphic unit is characterized by abundant debitage and relatively few cores, which is unlike the S-Group that has little debitage and many more cores.

Chapter 8 discusses the unshaped and shaped tools, focusing specifically upon points. Relatively few unshaped and shaped tools in the lowest litho-stratigraphic unit are found at Moche Borago compared to the overlying S-Group that has more types of tools. The points show technological and typological patterns put into a regional context, suggesting that hunter-gatherers employed regional cultural traditions during OIS 3.

Chapter 9 returns to the original four research questions and hypotheses to explain what the data from Moche Borago may reveal about hunter-gatherer responses to paleoenvironmental changes during OIS 3. Each of these four research questions is posed in turn, and relevant data from each chapter are synthesized into a succinct answer describing how hunter-gatherers may have been living and behaving at Moche Borago during OIS 3.

CHAPTER 2
THE PALEOCLIMATIC AND PALEOENVIRONMENTAL CONTEXT IN THE HORN OF AFRICA FROM OIS 4 TO OIS 3

This chapter presents a summary of the available paleoclimatic and paleoenvironmental data from across the Northern Hemisphere that date from OIS 4 to OIS 3. The purpose of this chapter is to contextualize the findings of my flaked stone artifact analysis from Moche Borago and interpretations of these data about behavioral variability during OIS 3.

This chapter will focus on changes that may have affected the ecological conditions across the Horn of Africa and southwestern Ethiopia during OIS 3. However, few direct data sources are available from the Horn so I have adopted a multi-scalar approach that draws together data from across the Northern Hemisphere, the region, and more local surroundings to Moche Borago. This approach relies on a top-down chain of evidence starting from the high-latitude ice core records to regional and local data sources that enable me to speculate about what the climatic and environmental conditions around Moche Borago may have been like at various time periods during OIS 3. Following the findings of Burns (2003; 2004), Cai (2006), and Revel (2010), I believe that hemispheric and regional climatic instability during OIS 3 induced monsoonal variability across the circum-Indian Ocean region and the Horn of Africa. I speculate that the changes in monsoonal precipitation across the southwestern Ethiopian highlands altered the local ecology and that local bands of hunter-gatherers adapted their lithic behaviors to suit.

Glacial and Interglacial Cycling

The Last Glacial period occurred from 73.5 to 14 ka. It is part of the broader cycling of the world's climates which are thought to be due to variations in the earth's orbit around the sun, the tilt of the earth, and the wobble in the earth's axial rotation (Milankovitch, 1941). These variations of movement affect the radiation that reaches the earth's surface, which is known as insolation (Bradley, 1999). By studying the distribution of insolation across the earth,

Milankovitch (1941) found periodic anomalies above 65° north latitude that were in phase with continental ice sheet growth. He hypothesized that when the position and movement of the earth around the sun minimize insolation above 65° north latitude, then the northern latitudes become cooler and the continental ice sheets expand. The timing of insolation anomalies is calculated to occur approximately every 100,000 years, which is coincident with the historical phases of glacial/interglacial cycles seen in the paleoclimatic proxy records dating to the Pleistocene.

Today, stable oxygen isotopes are a commonly employed method to classify the natural glacial/interglacial cycling of the earth's climates in the past. Stable oxygen isotopes can be studied from numerous sources containing fossil water, but these records are still most often reconstructed from marine biogenic materials such as corals or shell and high-latitude ice cores.

Oxygen isotope records rely on variations in the ratio ($\delta^{18}O$) of naturally occurring ^{18}O and ^{16}O to classify glacial and interglacial climates. The variations in the atomic weights of the different oxygen isotopes (^{18}O is heavier than ^{16}O) mean that when temperatures drop during glacial periods, ^{18}O is naturally distilled from precipitation via the process of fractionation (Dansgaard, 1964). The process of fractionation creates lower oxygen isotope ratios during glacial periods, which makes the classification possible (Bradley, 1999).

According to the stable oxygen isotope record, the Last Glacial is composed of three distinct stages. The ages I use to define each stage are drawn from the most recent calculations, which are described in Sanchez-Goni et al. (2010). The earliest stage, known as Oxygen Isotope Stage 4 (OIS 4), lasted from 73.5 to 59.4 ka, and this stage was associated with generally cold and arid conditions. The next stage was OIS 3 (59.4-27.8 ka). Climatic conditions were slightly warmer and wetter during OIS 3. Multiple records suggest an intensified seasonality and general climatic instability across Africa during this time (Flores et al., 2000; Kiage and Liu, 2006). The

latest period was OIS 2, lasting from 27.8 to 14 ka. OIS 2 coincides with the end of the Pleistocene epoch and the beginning of the Holocene epoch. OIS 2 is generally known for cold and arid conditions that culminated in the Last Glacial Maximum between 27.2 and 23.5 ka.

Major Data Sources

Voelker (2002) provided a comprehensive summary of the current available climatic and environmental proxy data for OIS 3. The locations of Voelker's data sources and newer sources are represented in Figure 3-1 and Table 3-1. In total, ~250 sites have yielded various types and qualities of data pertaining to climatic fluctuations during OIS 3. The distribution of sites shows a bias for data derived from high-latitude locations such as ice sheets and for marine cores leaving large absences of data interior to most continents. The emphasis on ice cores is because these data types provide a wealth of isotopic and other climatic proxy data spanning long time frames within well understood formation processes and contexts. Marine records also do not suffer many of the complicating effects of diagenesis that terrestrial records may undergo (Bradley, 1999).

Three primary issues regarding most of these data sources include dating, resolution, and local influences. Ice and marine cores typically rely on accelerator mass spectrometry ^{14}C dating to ~40 ka, but thereafter these records are tuned orbitally using layer counting and age models (Bradley, 1999; Svensson et al., 2006; Svensson et al., 2008). This relative dating method is prone to error and the chronologies are often revisited and adjusted. The most recent readjustment is the Greenland Ice Core Chronology 2005 (GICC05) (Andersen et al., 2006; Svensson et al., 2006; Svensson et al., 2008; Wolff et al., 2010).

Speleothem records are now being dated using Uranium-series, which provides an independent and direct dating method. However, these records are sensitive to the context of formation (hydrological, geological, chemical, and climatic), and they require a closed system to

minimize re-crystallization of calcite, thereby limiting porosity and detrital contamination. Low uranium content in the parent material can also limit the resolution of speleothem records (Lundblad and Holmgren, 2005).

Other terrestrial proxy records provided by lake cores, palynology, and phytoliths can provide regional and local climatic records given the right circumstances. Terrestrial freshwater lake core records are largely dependent upon the existence and fluctuations of the lake sediments through time and are generally only dated using ^{14}C up to ~40 ka (e.g. Gasse, 1977; Kiage and Liu, 2006). Experimental methods such as $^{230}Th/^{232}Th$ dating are being applied at sites such as Sacred Lake, Kenya (Olago et al., 2001).

Local influences may mask or enhance certain paleoclimatic signals in these data sources. The Greenland $\delta^{18}O$ ice core records, for example, all show similar patterns of air temperature flux that occurred above Greenland (Dansgaard et al., 1993). Similar climatic patterns are seen in the $\delta^{18}O$ records from Hulu cave (China) and Moomi cave (Socotra Island) speleothems, but these records are also believed to show the regional fluctuations in monsoon systems (Burns et al., 2003; Cai et al., 2006).

Millennial Scale Events During OIS 4 and OIS 3

Beginning during OIS 4, ~75 ka, Northern Hemisphere climates started to become increasingly unstable (Wolff et al., 2010). The climatic fluctuations take two forms. On the one hand, periods of intense cold and arid conditions called Heinrich events (H) occurred. These events were likely caused by massive discharges of freshwater ice from the Hudson Strait (Canada) into the North Atlantic Ocean. The freshwater influx may have slowed or shut down the North Atlantic thermohaline circulation, which regulates oceanic temperatures and, by proxy, terrestrial temperatures and precipitation (Hemming, 2004). On the other hand, rapid increases

in Northern Hemisphere temperatures and humidification called Dansgaard-Oeschger events (D-O) also occurred.

Heinrich and Dansgaard-Oeschger events began during OIS 4 and increased in intensity during OIS 3, affecting both the Northern and Southern hemispheres (Hessler et al., 2010; Sanchez-Gone and Harrison, 2010). Heinrich and Dansgaard-Oeschger events are linked phenomenon and the combined effects of ice-sheet and ocean-atmosphere interactions by both maintained a frequently fluctuating climatic regime during the Late Pleistocene (especially OIS 3). These fluctuations occurred up to the decadal level, and the general patterning forms the foundation for the saw-toothed, stepwise pattern of climatic changes seen during this period (Leuschner and Sirocko, 2000; Sanchez-Gone and Harrison, 2010; Hessler et al., 2010; Wolff et al., 2010).

Heinrich Events

Heinrich events are quasi-periodic excursions (~7,200 years) of massive amounts of Laurentide and Scandinavian sheet ice, which discharged from the Hudson Strait (Canada) into the Atlantic Ocean. The provenance of the ice source is established from high detritral carbonate concentrations, which were carried within the ice and deposited along a belt in the Atlantic Ocean approximately 40 to 55° north latitude (Ruddiman, 1977; Broecker et al., 1992; Grousset et al., 1993; Leuschner and Sirocko, 2000; Hemming, 2004).

The causal factors for Heinrich events are debated. Broecker (1994) suggested that Heinrich events were caused by exogenous orbital fluctuations which facilitated ice sheet growth and eventual expansion. MacAyeal (1993), however, proposed an endogenous explanation. He argued that following a period of increased ice growth (i.e. binge) the ice sheet became unstable and was purged.

Building upon these ideas, Maslin (2001) put forth a stepwise model based on freshwater influx from minor ice sheet discharges in the North Atlantic Ocean. According to his model, minor ice sheet discharges disrupted the North Atlantic Deep Water Circulation (NADW) which regulates oceanic temperature. The disruption of the NADW caused Southern Hemisphere heat piracy that, in turn, melted Antarctic ice and disrupted the Antarctic Bottom Water Current (AABW). Thus, heating in the Southern Hemisphere is inversely related to cooling in the Northern Hemisphere. After several bi-hemispheric cycles, the progressive ice-melting phases in the Northern Hemisphere undercut the Laurentide ice sheet, forcing a full-fledged Heinrich excursion.

Regardless of the exact reason behind the formation of Heinrich events, two points appear certain. First, Heinrich events occur on a roughly 7,200-year periodicity. The duration of Heinrich events ranges from centennial to millennial scales, but lasts no longer than ~2,200 years (Hemming, 2004). Second, climatic changes attributed to Heinrich cooling events are abundant in terrestrial and marine records. For example, during Heinrich events depletion of the δ^{18}O signature in foraminifera indicates massive influxes of freshwater ice during these events, which lowered Atlantic oceanic salinity up to 4‰ and sea surface temperatures by 1 to 2°C (Bond et al., 1993; Leuschner and Sirocko, 2000; Hemming, 2004).

These data are supported by modeling results, which also suggest that massive influx of freshwater into the Atlantic decreases NADW circulation, slowing or shutting down entirely the thermohaline circulation system in the Atlantic (Van Campo et al., 1990; Vidal and Arz, 2004; Weldeab et al., 2007). Sea surface temperatures (SST) also decrease, thereby changing the location of the Inter-tropical Convergence Zone (ITCZ) which controls the intensity and patterns of monsoonal winds across Africa and SW Asia (Vidal and Arz, 2004; Tierney et al., 2008).

Leuschner and Sirocko (2000) and Voelker (2002) each demonstrated that cooling episodes associated with Heinrich events also are found in both hemispheres and on every continent, though records pertaining directly to Africa are especially scarce.

Dansgaard-Oeschger Events

Dansgaard-Oeschger (D-O) events are cyclic warming events that occurred throughout the Last Glacial (Dansgaard et al., 1993; Grootes et al., 1993). Table 3-2 lists D-O cycles occurring between 53 and 46 ka and these events are represented graphically in Figure 3-2 alongside the oxygen isotope stages.

The beginnings of D-O events are often punctuated. High-resolution records from Moomi Cave (Socotra Island) in the Indian Ocean indicate, for example, that the transition from the arid H5 event (~48 ka) to D-O12 (~55-44 ka) occurred only within the span of 25 years (Burns et al., 2003; Burns et al., 2004). In northern high latitudes, at least, evidence also suggests dramatic temperature fluctuations at the onset of D-O events. These fluctuations are estimated between 8°C (DO13) and 16°C (DO19), but they seem to fall most commonly between 10 and 12°C (Wolff et al., 2010).

Individual D-O events occur on a roughly 1,470-year periodicity (Bond et al. 1997). However, a larger pattern may be involved. Heinrich events often precede initial D-O events, followed by a triplet of subsequent D-O events. Each of the subsequent D-O events generally appears smaller than the prior event, indicating a gradual cooling over the subsequent 1,000 to 3,000 years leading up to the next Heinrich event (Burns et al., 2003; Huber et al., 2006; Cosford et al., 2008). This triplet pattern of D-O events and subsequent Heinrich events supports the hypothesis for a stepwise recursive relationship between Northern Hemisphere and Southern Hemisphere oceanic circulation and phases of punctuated Laurentide ice sheet discharge (Bond et al., 1997; Maslin et al., 2001).

West African and SW Asian Monsoonal Systems

Today, the highlands of the Horn of Africa receive the majority of annual precipitation from the African (Atlantic or West African) boreal summer monsoon systems. The northerly movement of the ITCZ between July and August draws moisture-rich air masses via the mid-latitude westerlies from the Atlantic Ocean off the coast of NW Africa and across the continent (Figure 3-3). As these air masses hit the highlands of the Horn, the moisture is released as precipitation (Mohammed et al., 2004; Revel et al., 2010). In SW Ethiopia the orographic influence of the highlands on the monsoon air masses results in >2,000 mm annual average precipitation (Livingstone, 1975; Gasse, 2000; Mohammed et al., 2004) (Figure 3-4).

The SW Asian (Indian) monsoons influence the highlands of the Horn in other ways. The SW Asian monsoons are part of the larger Asian monsoon system. The East Asian monsoons derive their precipitation mainly from tropical western Pacific waters whereas the SW Asian water source is the Indian Ocean (Cosford et al., 2008). The Qinghai-Tibet Plateau isolates the precipitation from the two monsoonal systems, but these systems are both driven primarily by a land-sea thermal gradient during the boreal summer and the northward movement of the ITCZ (Burns et al., 2003).

Recent isotopic research on meteoric water shows a latitudinal gradient across the Horn that may relate to differences in precipitation source-waters, hence monsoon systems. Freshwater lakes and groundwater from southern Ethiopia and Kenya appear to be more strongly influenced from an Indian Ocean water source than more northerly locations of the Horn (Kebede et al., 2005; Kebede et al., 2008; Kebede et al., 2009). These locations may therefore be more influenced by the SW Asian monsoons than the more northerly locations. Kebede (per comm.) hypothesized that past deviations in the annual intensity and pattern of the West African monsoonal system over the southern Ethiopian highlands may have been buffered by the SW

Asian monsoons. When discussing the SW Ethiopian highlands then, it is prudent to consider the fluctuation of both the African and SW Asian monsoons.

The $\delta^{18}O$ cave speleothem records from Xiabailong, Hulu, and Xiangshui caves in China (Wang et al., 2001; Cai et al., 2006; Cosford et al., 2008), Moomi Cave (Socotra Island) in the Indian Ocean (Burns et al., 2003; Burns et al., 2004), and also Arabian Sea cores (Schulz et al., 1998) indicate that the SW Asian and East Asian monsoon systems were affected by climatic variability during the Late Pleistocene. Nile paleohydrology, West African Atlantic marine cores, and continental records provide a contemporaneous and synchronous account of African monsoonal variability during this time period (Lezine and Casanova, 1991; Flores et al., 2000; Weldeab et al., 2007; Revel et al., 2010).

As numerous studies have noted, the timing and duration of the climatic variability evident from these records are in step with high-latitude millennial-scale Dansgaard-Oeschger and Heinrich events found in the Greenland ice cores (Wang et al., 2001; Burns et al., 2003; Burns et al., 2004; Cai et al., 2006; Cosford et al., 2008; Revel et al., 2010). The link between these records is that insolation increased during D-O events, changing the land-sea thermal gradient and intensifying the monsoons from West Africa to Western Asia. The Horn of Africa and the highlands of the Horn—being uniquely positioned between the confluence of the African and Asian monsoons—very likely experienced increased monsoonal precipitations during D-O events that are in phase with the broader regional and hemispheric patterns.

In summary, changing orbital conditions during the Pleistocene forced a succession of glacial and interglacial periods with a roughly 100,000-year periodicity. Among the most common climatic changes during the Late Pleistocene were the dramatic and rapidly occurring millennial scale events such as Heinrich stadials and Dansgaard-Oeschger interstadials. These

events are found synchronously in high-latitude ice core records and numerous multi-proxy low-latitude records. Dansgaard-Oeschger events, in particular, may have affected regional monsoons systems across Africa and Asia. The influence of the African and Asian monsoons in the Horn of Africa today, and especially the SW Ethiopia highlands, indicates that this area likely experienced monsoonal variability during the Late Pleistocene

The Paleoclimatic and Paleoenvironmental Context of Europe, Asia, and Africa Between 65 and 43ka

This section synthesizes paleoclimates (PC) and paleoenvironments (PE) in Europe, Asia, and Africa ~65 to 43 ka, which covers the end of OIS 4 and the early and middle stages of OIS 3. This synthesis is subdivided into three subsections, 65 to 55 ka, 55 to 48 ka, and 48 to 43 ka, following the natural subdivisions proposed by Huber (2006:508) using D-O events. Accordingly, period 65 to 55 ka corresponds with D-O18-15 and H6; period 55 to 48 ka corresponds with D-O14-13 and H5; and period 48 to 40 ka corresponds with D-O12-9 (cf. Wolff et al., 2010). I have structured each section so that the descriptions start from the broadest regional scale and move toward the local conditions in the Horn of Africa and, as best as possible, the SW Ethiopia highlands.

OIS 4: 73.5 to 65 ka

OIS 4 was a period of cold and arid glacial conditions across the Northern Hemisphere. The environmental conditions across Africa during OIS 4 are often described using the better documented glacial OIS 2 (27.8-14.7 ka) analog, which was the last stage of the Last Glacial. Generally speaking, annual temperatures across the continent were cooler, precipitation was lower, and vegetation zones contracted while deserts expanded.

In the Horn of Africa, lake cores show that mean annual temperature was up to 5ºC cooler during OIS 2 than today (Gasse, 2000). Lower temperatures also led to decreased precipitation

rates. The water levels at many of the rift valley lakes dropped significantly. Lake Tanganyika dropped up to 300 m, Lake Mobuto Sese Seko (Albert) was 46 m lower, while Lake Victoria and Lake Abhe (Ethiopia) may have been desiccated (Gasse, 2000).

Across North Africa, the expansion of the Sahara desert during OIS 2 followed widespread desiccation of the Last Interglacial grasslands (Close et al., 1996). Decreased discharge and increased sediment load in the Atbara river and the Blue Nile and White Nile resulted in the blockage and occasional cessation of these riverine systems (Wendorf and Schild, 1989; Close et al., 1996). In Central Africa, the once widespread tropical rainforests fragmented and were replaced by patchy woody grasslands (Cornelissen, 2002).

OIS 4 to OIS 3: 65 to 55 ka

Northern Hemisphere climates were becoming increasingly unstable by the end of OIS 4. The GISP2, GRIP, and NGRIP $\delta^{18}O$ ice cores show that across the Northern Hemisphere high-latitude cold and arid conditions during H6 (~60 ka) were followed in rapid succession by D-O events 17 (~59 ka) and 16 (~58 ka) (Grootes et al., 1993; Sowers et al., 1993; Meese et al., 1994; Stuiver and Grootes, 2000; North Greenland Ice Core Project, 2004). North Atlantic sea surface temperatures (SSTs) from core CH73-139c corroborate these findings (Labeyrie et al., 1991).

These climatic fluctuations appear to have had widespread influence on local paleoenvironments across Europe. Atlantic marine core records (MD95-2042; SU81-18; MD99-2331; MD04-2845) show a rapid expansion of the Mediterranean forest regime in SW Iberia during D-O 17 to 16 (Sanchez-Gone et al., 2008).

The expansion in Mediterranean forest cover in Europe during D-O events indicates that the climatic patterns were likely reminiscent of the current Mediterranean climate with hot and dry summers and winter rainfall (Sanchez-Gone et al., 2008). Similar influences in winter rainfall patterns are found also in the Soreq cave (Israel) speleothem records. These records

show periodic low $\delta^{18}O$ and $\delta^{13}C$ values that are correlated to sapropel events in the eastern Mediterranean Sea (Bar-Matthews et al., 2000). Sapropels are pluvial events that reflect changes in Mediterranean Sea SST or salinity due to increased rainfall and freshwater riverine runoff.

Bar-Matthews et al. (2000) believed that the sapropels and fluctuations in Soreq cave $\delta^{18}O$ and $\delta^{13}C$ are influenced by monsoonal activity. Similarly, total organic carbon (TOC) records from Arabian Sea cores (111KL; 136KL) show fluctuations in TOC that are consistent with the pattern of sapropel, D-O, and H climatic shifts during this period (Schulz et al., 1998). Schulz et al. (1998) identified these TOC-rich bands to show greater precipitation that was likely due to increased monsoonal activity.

Early OIS 3: 55 to 48 ka

The intensity of D-O events 17 to 15 declined sequentially after H6. By D-O 15, the magnitude of annual temperature increases above Greenland may have been only 9 to 10ºC above current conditions (Wolff et al., 2010). However, D-O 14 (~54 ka) appears to be as strong as D-O 17 with a 12.5ºC mean annual temperature spike (Wolff et al., 2010).

Atlantic marine core records (MD95-2042; SU81-18; MD99-2331; MD04-2845) show that mid-Atlantic forests across NW Iberia and western France expanded significantly during D-O 14 (Sanchez-Gone et al., 2008). Mediterranean forests, however, do not show significant changes implying that the effects of millennial-scale events across western Europe were also strongly influenced by regional influences, including the varying effects of orbital orientation (Sanchez-Gone et al., 2008).

The eastern Mediterranean Sea and Arabian Sea were also experiencing wetter conditions during this period. At Soreq cave, low $\delta^{18}O$ and $\delta^{13}C$ speleothem values at 54 ka may correlate to the poorly studied sapropel 2 event (Bar-Matthews et al., 2000). This time is coincident to D-

O 14. A high lake level stand from Lake Lisan, the precursor to the current Dead Sea, corroborates these findings (Neev and Emery, 1967; Stein et al., 1998; Bar-Matthews et al., 2000).

Total organic carbon (TOC) records from the Arabian Sea provide a particularly clear sequence of D-O events during this period.[2] TOC peaks are present at ~56 ka (D-O 16), ~53 ka (D-O 15), ~51 ka (D-O 14), and ~47 ka (D-O 13) (Schulz et al., 1998). The very sudden and large increase in TOC at the onset of D-O 14 is analogous to the similarly identified D-O 14 event above Greenland where a 12.5ºC mean annual temperature spike occurred (Wolff et al., 2010). While the TOC records do not record paleothermometry, the similarities between D-O 14 in the Arabian Sea and above Greenland lend credence to the hypothesis that similar temperature shifts were occurring between these two areas during D-O events.

What do these patterns reveal about monsoonal variability at this time? The Arabian TOC records and speleothems from Moomi cave and Xiaobailong cave indicate coupling between millennial-scale interstadial (i.e. D-O) events and the SW Asian monsoons. Schulz et al. (1998) believed the TOC records to be strongly correlated to monsoonal variability. Organic rich bands (high TOC) are formed during periods of monsoon-induced biological productivity. The $\delta^{18}O$ speleothem records from Moomi cave (Socotra Island) and Xiaobailong cave (SW China) both show isotopic changes relating to precipitative influences derived from the SW Asian summer monsoons (Burns et al., 2003; Burns et al., 2004; Cai et al., 2006). Thus, during this period, SW Asian monsoonal variability was clearly linked to D-O events in the circum-Indian Ocean region.

Proxy records pointing to West African monsoonal variability show similar patterns to SW Asian monsoonal variability, though the records are generally of lower resolution. Continental

[2] Discrepancies occurr between D-O ages in the TOC records and other records, such as Wolff (2010), because the TOC records use an orbitally-tuned age model based on layer counting.

North Africa records indicate a broad humid phase from 52 to 44 ka attributed to increased West African monsoonal activity (Lezine and Casanova, 1991). Sediment cores from the coast of West Africa suggest a period of high riverine runoff ~55 ka that is also interpreted to indicate increased West African monsoons at this time (Weldeab et al., 2007). This time period is approximate to D-O 15. Recent and unpublished $\delta^{18}O$ records from the Gulf of Guinea, however, may contradict the decoupling hypothesis of the monsoons proposed by Weldeab (2007). These newer records show that West African monsoonal variability is tightly linked to Greenland temperature instabilities during OIS 3 (Weldeab per comm.).

The pattern of sapropel events correlated to the Soreq cave records shows the influence of millennial-scale climatic variability on the West African monsoons in the eastern Mediterranean region (Bar-Matthews et al., 2000). Low $\delta^{18}O$ and $\delta^{13}C$ values at 54 ka are coincident to sapropel 2 and D-O 14. Most importantly, the formation of Mediterranean sapropels is linked to increased precipitation in the Nile source region, the Ethiopian highlands (Bar-Matthews et al., 2000). Nile paleohydrology records provide another independent data source that is also directly correlated to the Ethiopian highlands. These records show a broad period of pluvial conditions from 60 to 50 ka that are interpreted as increased monsoonal activity in the Ethiopian highlands at this time (Revel et al., 2010).

Taken together, since the beginning of OIS 3, and certainly from 55 to 48 ka, a series of D-O events in the Northern Hemisphere occurred that had a clear impact on the intensity of both the African and SW Asian monsoons systems. This impact included large-magnitude temperature fluctuations of D-O events above Greenland to concurrent increases in regional monsoonal precipitation across North Africa, the eastern Mediterranean Sea, the circum-Indian Ocean, and finally the Horn of Africa. No concurrent terrestrial records exist from the SW

Ethiopian highlands dating to this period. However, these data provide strong supporting evidence that regional monsoonal variability changed the precipitation patterns across the Horn of Africa and, by proxy, SW Ethiopia in sync with D-O events. Most importantly, I believe these precipitation changes almost certainly impacted the local ecology in the Horn and SW Ethiopia.

Early-Mid OIS 3: 48 to 43 ka

By 48 ka, the glacial aridity of H5 was present across Europe, Arabia, Asia, and North and East Africa. Multiple Greenland ice cores each show severely depleted $\delta^{18}O$ between ~48 and 47 ka (Grootes et al., 1993; Greenland Ice-core Project, 1993; Stuiver and Grootes, 2000; North Greenland Ice Core Project, 2004). Atlantic Ocean SSTs adjacent to western Europe were >10°C cooler than prior periods, and pollen records indicate contractions of the European mid-Atlantic forests and the Mediterranean forests (Sanchez-Gone et al., 2008). The Lago Grande di Monticchio sediment cores from southern Italy similarly show decreases in the relative abundance of woody taxa at this time (Allen et al., 1999).

The TOC records from the Arabian Sea sediment cores suggest similarly cool conditions at this time. These records show a ~1.5 ka period of drastically lower TOC, pterapod-rich sediments implying colder conditions during H5 (Schulz et al., 1998). The SSTs derived from marine cores near the Eastern Maldives (MD90963) and Somalia (TY93929/P; MD85668; MD85674), and eastern Mozambique's marine cores (MD79257) are also lower (Bard et al., 1997; Rostek et al., 1997; Bard, 2003).

Climatic conditions improved quickly at the onset of D-O 12, 46.8 ka. In France, the Villars cave $\delta^{18}O$ speleothem shows the highest growth rates and greatest variation in $\delta^{18}O$ at this time (Genty et al., 2003). The findings indicate a sudden shift from cooler to warmer and more humid conditions on par with a 10°C (50°F) temperature increase during D-O 12, which is similarly seen in other marine and terrestrial records at this time (Guiot et al., 1993; Cayre et al.,

1999; Genty et al., 2003). Concurrently, Atlantic forests across western France and NW Iberia expand at this point (Sanchez-Gone et al., 2008) while woody taxa increased in abundance across southern Italy (Allen et al., 1999).

The D-O 12 event had a similar impact across the circum-Indian Ocean region. The Moomi cave $\delta^{18}O$ speleothem record indicates gradually improving climatic conditions after 50 ka until 47.2 ka when a rapid enrichment of $\delta^{18}O$ occurs during D-O 12. The Moomi M1-2 speleothem was sampled in 8-year increments across this period, and the resolution of this record shows that the shift from cold and arid H5 to the warmer and wetter D-O 12 occurred within 25 years (Burns et al., 2003). Mean annual temperatures above Greenland increased 12ºC during D-O 12 (Wolff et al., 2010).

Around 43 ka, the D-O 11 events are evident in both high-latitude ice cores and regional records surrounding the Horn of Africa. Above Greenland, D-O 11 is associated with the greatest increase in mean annual temperatures known during OIS 3, 15°C (Wolff et al., 2010). However, for reasons that are still unclear, the D-O 11 event is poorly seen in the Arabian Sea TOC records (Schulz et al., 1998) and Xiaobailong speleothem records (Cai et al., 2006). Nile paleohydrology records indicate a broad period of pluvial conditions at this time with flood maxima from 38 to 30 ka (Revel et al., 2010). Continental North Africa records show a similar broad pluvial event from 52 to 44 ka (Lezine and Casanova, 1991).

Conclusions

What do these data imply about ecology changes and hunter-gatherer adaptation in SW Ethiopia during OIS 3? First, a clear relationship is evident between high-latitude ice-core records, mid-latitude terrestrial and marine records, and low-latitude tropical marine and terrestrial records from across Africa and the circum-Indian Ocean region. These similarities may extend to parallels between the paleothermometry of these regions during D-O events,

which would also help to explain the increase in monsoonal activities during these times. If the teleconnection that I have laid out between regions and records holds true, then D-O 12 (46.8 ka) and D-O 11 (43.3 ka) almost certainly had a major impact on the Horn of Africa. Mean annual temperatures are estimated to have increased up to 12°C during D-O 12 and up to 15°C during D-O 11 (Wolff et al., 2010). During D-O 12, these changes may have taken place within 25 years (Burns et al., 2003; Burns et al., 2004). Even if the magnitude of these changes was ameliorated in lower latitudes, it is still very likely that the intensity and rapidity of these two D-O events, in particular, had appreciable effects on the climate across the circum-Indian Ocean region and the Horn of Africa .

Second, a clear relationship is evident between millennial-scale climatic instability, seen in high-, mid-, and low-latitude records, and monsoonal variability. Paleoclimates (PC) and paleoenvironments (PE) records from the coast of West Africa, North Africa, the Mediterranean Sea, and the circum-Indian Ocean region all show that pluvial events, including D-O events and sapropels, are associated with coeval increases in African and SW Asian monsoonal intensity and precipitation. The Moomi cave record and Arabian Sea TOC show SW Asian monsoonal flux during D-O events (Schulz et al., 1998; Burns et al., 2003; Burns et al., 2004). Marine core records from the Gulf of Guinea show West African monsoonal flux during D-O events (Weldeab et al., 2007). Unpublished $\delta^{18}O$ data from the same location are also tightly linked to temperature changes above Greenland during OIS 3 (Weldeab per comm.). The fluctuations in both the African and SW Asian monsoons appear in sync with each other and, significantly, in sync with temperature flux above Greenland during H and DO events of OIS 3.

Most importantly, however, we must consider the unique position of the Horn of Africa and the highlands in the Horn. Today, the distribution of precipitation across the Ethiopian

highlands is controlled by orographic influences (Mohammed et al., 2004). Similar orographic forces must have controlled the spatial distribution of rains across the highlands during OIS 3. Therefore, the SW Ethiopian highlands must have had relatively greater amounts of precipitation during periods of monsoonal intensity of OIS 3. The Mediterranean records from Soreq cave and the Nile paleohydrology records provide clear evidence to support this idea (Bar-Matthews et al., 2000; Revel et al., 2010). The only way to increase Nile River discharge naturally is at the source locations, in the Ethiopian highlands and Lake Victoria.

Third, the increase in monsoonal precipitation during D-O events of OIS 3 almost certainly had an effect on local environments of the Horn and hunter-gatherer resources. In particular, fluctuations in the monsoon rains would alter the distribution of the vegetation zones around Moche Borago. During D-O events, I believe that more diverse and abundant resources were available around Moche Borago. The montane woodlands would have probably moved toward lower elevations, more marshy grasslands might have appeared on the plains below the site, and Lake Abaya almost certainly was present. Therefore, it is during pluvial times, and, in particular, D-O 12 (46.8 ka) and D-O 11 (43.3 ka) that I expect to find changes in stone artifacts at Moche Borago as the local hunter-gatherer populations adapted to more abundant resources.

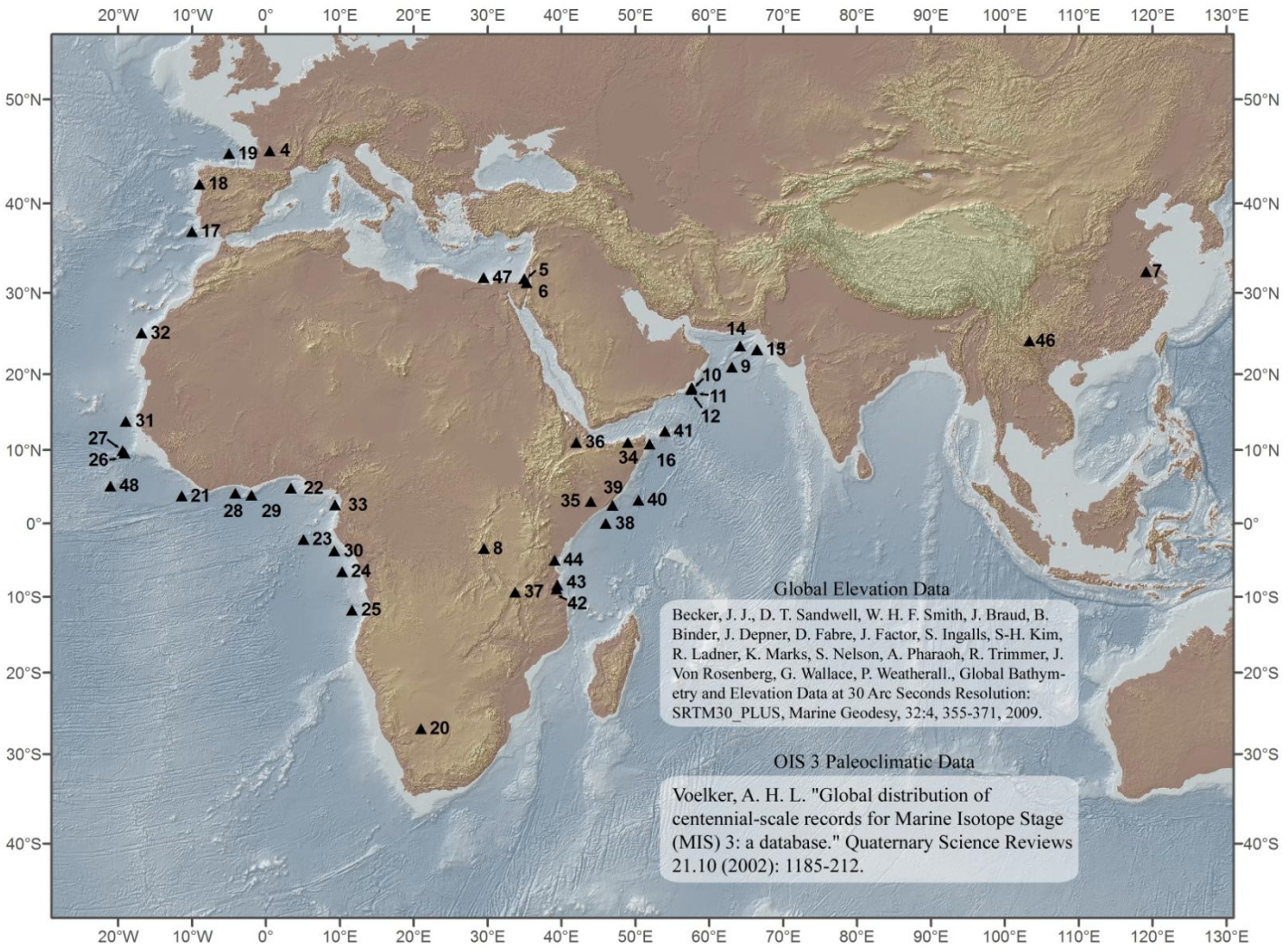

Figure 3-1: Paleoclimatic proxy sites across the circum-Indian Ocean area that are described in the text.

Table 3-1: Description of Paleoclimatic Sites in Figure 3-1

No.	Location	Core number	Latitude	Longitude	References
1	Central Greenland	GISP2	72.6	-38.5	Grootes et al. 1993; JGR special volume and CD-
2	Central Greenland	GRIP	72.58	-37.63	Dansgaard et al. 1993; Johnsen et al. 1992; JGR
3	Greenland	NGRIP	75.1	-42.3	Johnsen et al. 2001; NGRIP members 2004; http://www.glaciology.gfy.ku.dk/ngrip/; Johnsen et al. 1992; Hansson 1994
4	Villars Cave, France	Vil 9	45.3	0.5	Genty et al. 2003; Grootes et al. in prep.
5	Soreq cave, Israel	speleothems	31.7	35	Bar-Matthews et al. 1999
6	Lake Lisan, Paleo-Dead Sea,	Perazim valley out-	31.21	35.31	Schramm 1997; Schramm et al. 2000;
7	Hulu Cave, China	PD, MSD, MSL, H82 and YT	32.5	119.17	Wang et al. 2001
8	Kashiru, Burundi, Africa	Ka-1	-3.45	29.53	Bonnefille et al. 1990, 1992; Bonnefille and Chalie 2000
9	Arabian Sea	SO42-57KL	20.9	63.12	Leuschner et al. 2000;
10	Arabian Sea off Oman	RC27-14	18.25	57.66	Altabet et al. 2002
11	Arabian Sea off Oman	RC27-23	17.99	57.59	Altabet et al. 2002
12	Arabian Sea off Oman	ODP site 723B	18.05	57.61	Altabet et al. 1999, 2002
13	Arabia Sea	SO90-88KL	23.1	66.48	Shulz et al. 1998
14	Arabia Sea	SO90-111KL	23.58	64.22	Shulz et al. 1998
15	Arabia Sea	SO90-136KL	23.12	66.5	Shulz et al. 1998
16	Arabian Sea	Piston core 905	10.77	51.95	Klocker et al. 2006
17	Atlantic Ocean	MD95-2042; SU81-18	37	-10	Sanchez Goni et al. 2008
18	Atlantic Ocean	MD99-2331; MD03-2697	42	-9	Sanchez Goni et al. 2008
19	Atlantic Ocean	MD04-2845	45	-5	Sanchez Goni et al. 2008
20	Namib Desert		-27	21	Stokes et al. 1997
21	Atlantic Ocean	GIK 16776	3.73	-11.4	Dupont et al. 2000
22	Atlantic Ocean	GIK16856	4.8	3.4	Dupont et al. 2000
23	Atlantic Ocean	GIK16876	-2.2	5.1	Dupont et al. 2000
24	Atlantic Ocean	GeoB1008	-6.58	10.32	Dupont et al. 2000
25	Atlantic Ocean	GeoB1016	-11.77	11.68	Dupont et al. 2000
26	Atlantic Ocean	GIK16415	9.57	-19.1	Dupont et al. 2000
27	Atlantic Ocean	GIK16416	9.9	-19.38	Dupont et al. 2000

Table 3-1: Continued

No.	Location	Core number	Latitude	Longitude	References
28	Atlantic Ocean	KS84067	4.13	-4.12	Dupont et al. 2000
29	Atlantic Ocean	KS12	3.87	-1.93	Dupont et al. 2000
30	Atlantic Ocean	KW23	-3.77	9.28	Dupont et al. 2000
31	Atlantic Ocean	V22-196	13.83	-18.95	Lezine and Casanova 1991
32	Atlantic Ocean	M12392-1	25.17	-16.83	Lezine and Casanova 1991
33	Atlantic Ocean	MD03-2707	2.5	9.39	Weldeab et al. 2007
34	N. Somalia		11	49	Brook et al. 1995
35	S. Somalia		3	44	Brook et al. 1995
36	Lake Abhe		11	42	Gasse 1977
37	Lake Masako	M96A	-9.33	33.75	Barker et al. 2003
38	Indian Ocean	MD85-668	-0.02	46.04	Meynadier et al. 1992
39	Indian Ocean	MD85-669	2.49	46.92	Meynadier et al. 1992
40	Indian Ocean	MD85-674	3.19	50.44	Meynadier et al. 1992
41	Oman margin	RC27-14	18.25	57.66	Altabet et al. 2002
42	Oman margin	RC27-23	17.99	57.59	Altabet et al. 2002
43	Moomi cave, Socotra Island	M1-2	12.5	54	Burns et al. 2003
44	Kilwa cave system		-8.93	39.35	Lundblad and Holmgren 2005
45	Songo-Songo Island cave system		-8.42	39.48	Lundblad and Holmgren 2005
46	Tanga cave system		-5.03	39.08	Lundblad and Holmgren 2005
47	Xiangshui Cave	X3	110.92	25.25	Cosford et al. 2008
48	Xiaobailong Cave	XBL-1	24.2	103.35	Cai et al. 2006
49	Medite4rranean Sea	MS27PT	31.81	29.47	Revel et al. 2010
50	Sierra Leone Rise	CAMEL-1	5.11	-21.04	Flores et al. 2000

Note: For added sites and descriptions, see Voelker (2002).

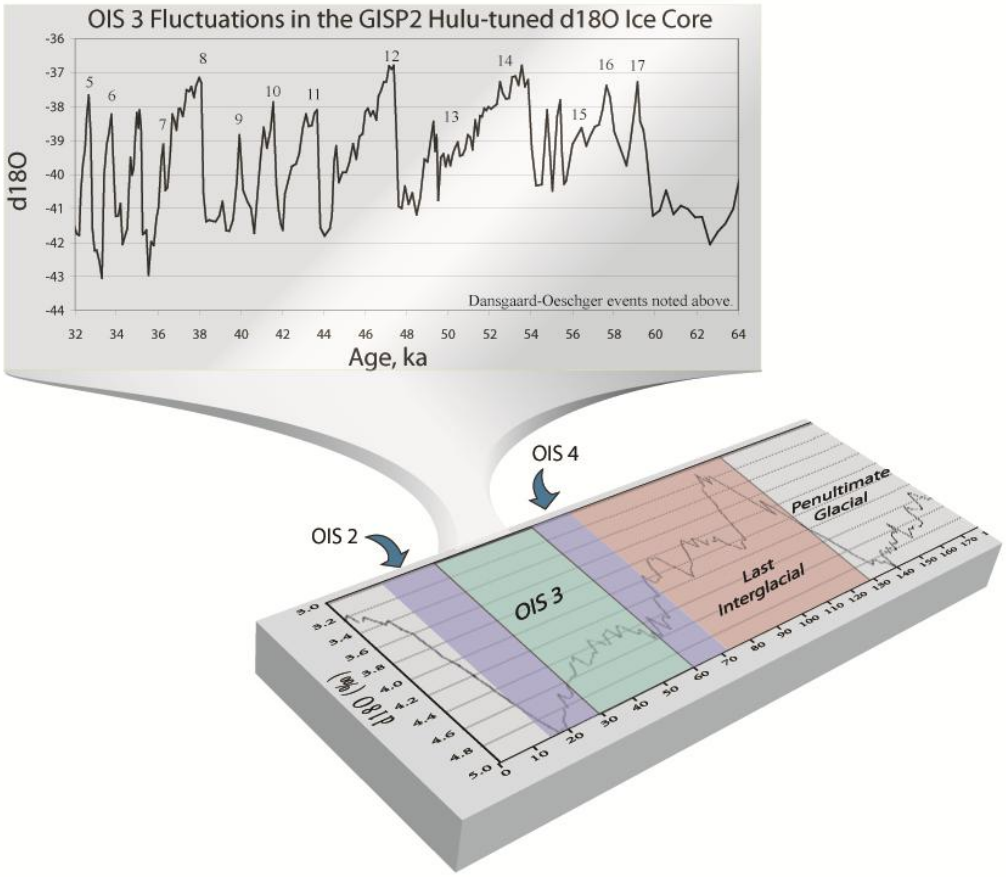

Figure 3-2: Timeline of the Last Glacial showing the boundaries of Oxygen Isotope Periods and Dansgaard-Oeschger events.

Table 3-2: List of Dansgaard-Oeschger Events from the Last Glacial to the Present

Event	Age Range, BP	Temperature Increase, ◦C	Age Reference	Temperature Reference
Younger Dryas	11,513 - 11,613	10 ± 4	Rasmussen et al. 2006	Grachev and Severinghaus 2005
1	14,549 - 14,735	11 ± 3	Rasmussen et al. 2006	Grachev and Severinghaus 2005
2	22,992 - 23,588	-	Andersen et al. 2006	
3	27,314 - 28,146	-	Andersen et al. 2006	
4	28,401 - 29,299	12 ± 5	Andersen et al. 2006	Sanchez-Goni et al. 2008
5	31,884 - 33,016	7 ± 5	Andersen et al. 2006	Sanchez-Goni et al. 2008
6	33,084 - 34,296	7 ± 3	Andersen et al. 2006	Sanchez-Goni et al. 2008
7	34,769 - 36,091	9 (+3;-6)	Andersen et al. 2006	Sanchez-Goni et al. 2008
8	37,445 - 38,895	11 (+3;-6)	Andersen et al. 2006	Huber et al. 2006
9	39,320 - 40,900	9 (+3;-6)	Andersen et al. 2006	Huber et al. 2006
10	40,593 - 42,227	11.5 (+3;-6)	Andersen et al. 2006	Huber et al. 2006
11	42,422 - 44,158	15 (+3;-6)	Svensson et al. 2008	Huber et al. 2006
12	45,854 - 47,766	12 (+3;-6)	Svensson et al. 2008	Landais et al. 2004b
13	48,215 - 50,245	8 (+3;-6)	Svensson et al. 2008	Huber et al. 2006
14	52,974 - 55,366	12.5 (+3;-6)	Svensson et al. 2008	Huber et al. 2006
15	54,494 - 57,006	10 (+3;-6)	Svensson et al. 2008	Huber et al. 2006
16	56,943 - 59,517	9 (+3;-6)	Svensson et al. 2008	Huber et al. 2006
17	ca. 59,390	12 (+3;-6)	Svensson et al. 2008	Huber et al. 2006
18	ca. 64,045	11 ± 2.5	Estimated	Landais et al. 2004a
19	ca. 72,280	16 ± 2.5	Estimated	Landais et al. 2004a
20	ca. 76,400	11 ± 2.5	Estimated	Landais et al. 2004a

Note: This chart follows the definitions of D-O events after Wolff et al., 2010.

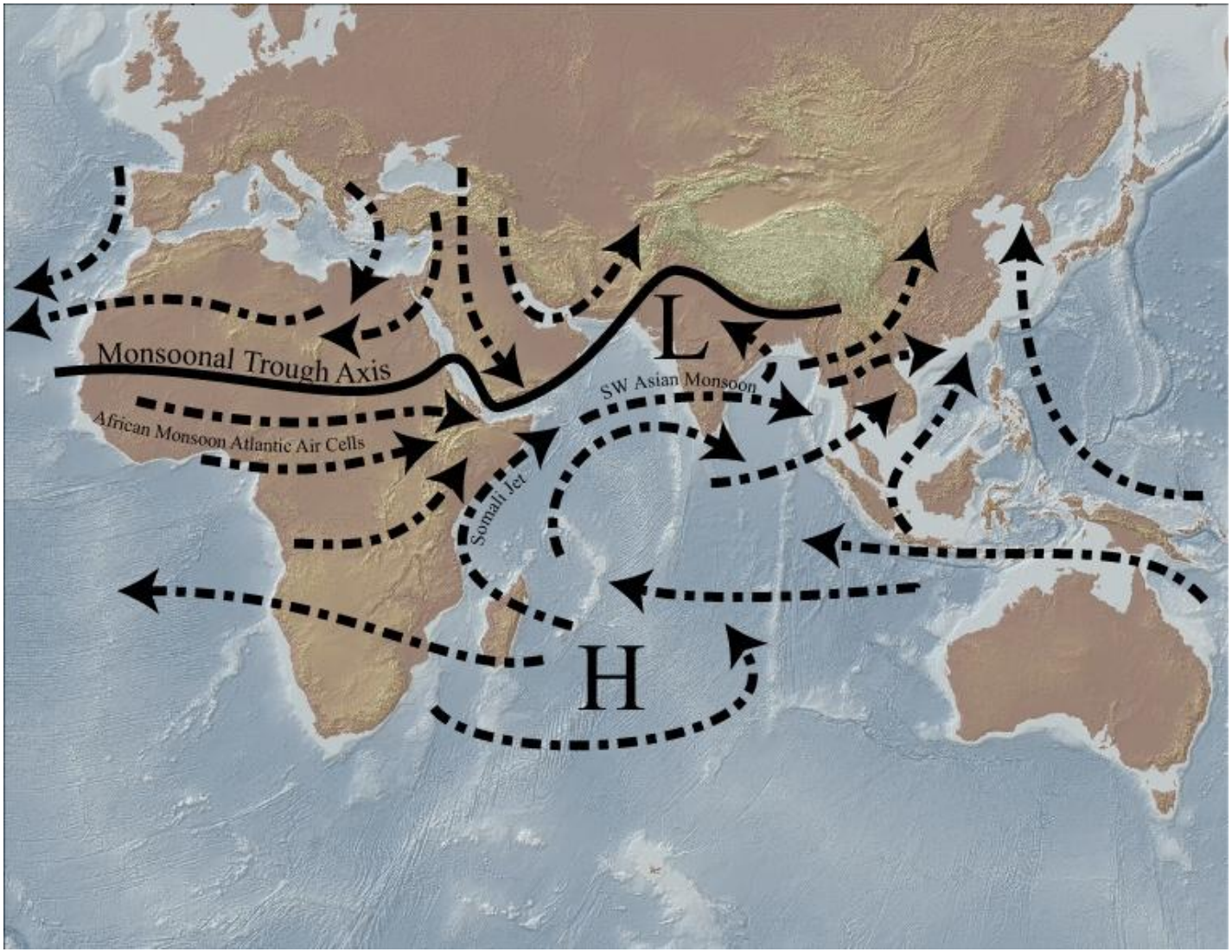

Figure 3-3: Generalized wind patterns of the summer monsoon systems in Africa and SW Asia.

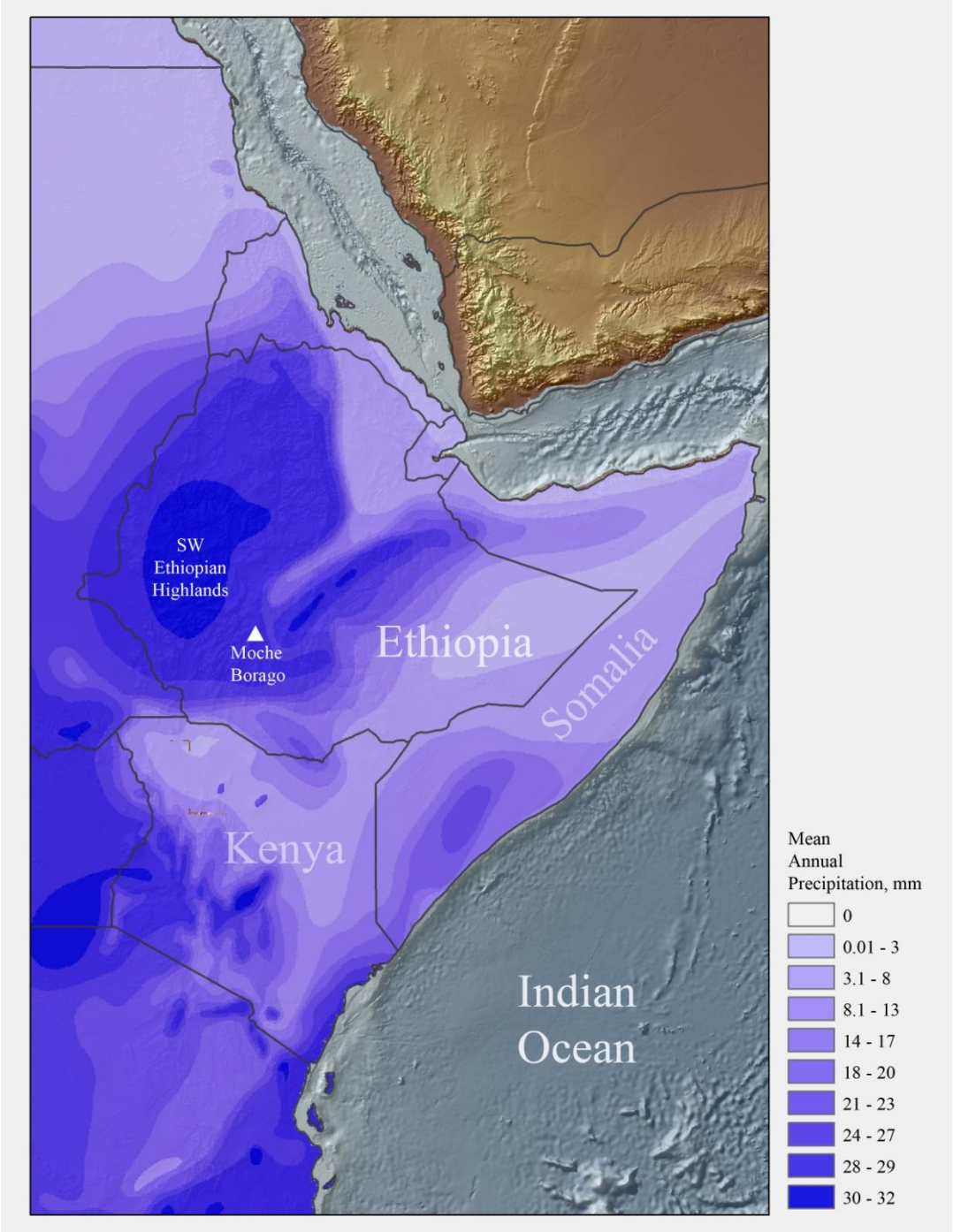

Figure 3-4: Contemporary mean annual precipitation rate across the Horn of Africa. Data credit: FAO / UNEP Desertification and Mapping Project

CHAPTER 3
A BRIEF HISTORY OF THEORETICAL IDEAS ABOUT HUNTER-GATHERER BEHAVIORAL VARIABILITYAND ARID CLIMATIC EVENTS DURING THE LATE PLEISTOCENE

This chapter briefly reviews the history of theoretical thought that has framed scholarly inquiry into the relationship between Late Pleistocene human behavior variability in Africa and environmental change. Since the early 20th century, much of this research has focused on the relationship between arid climatic events and human behavior change. I contend that arid-adaptation ideas are popular to this day because of the theoretical history and also because we know with greater certainty that glacial climates were most common during the Middle and Late Pleistocene.

Modern Human Behaviors

Just as with any other natural organism, humans rely on climates to regulate our environment, subsistence resources, and even comfort. We differ from other organisms, however, in the complex array of modern behaviors developed since the Middle Pleistocene to modify our environments to our benefit. These behaviors broadly include new social, technological, and symbolic tools that allowed hunter-gatherers the ability to contend with a wider range of environments and exploit resources more effectively and efficiently (McBrearty and Brooks, 2000; Marean and Assefa, 2005).

Several overviews of modern human behaviors have been discussed about how these behaviors can be identified materially in the archaeological record (McBrearty and Brooks, 2000; Wadley, 2001; Henshilwood and Marean, 2003; Marean and Assefa, 2005). The main issues in these discussions relate to concerns about methodologies to identify the behaviors in archaeological contexts, as well as the ontology of the behaviors, regarded both individually and as a group package. McBrearty and Brooks (2000), for example, provided the most detailed

synthesis to date about behavioral modernity, including the list of traits that may define behavioral modernity in African contexts, the timing and speed of the behavior changes, and the relationship between the African and European archaeological records. Henshilwood and Marean (2003), however, questioned the widely used trait list approach and the empirical tests employed to assess behavioral modernity in the archaeological record. Wadley (2001) argued that intangible symbolic systems are the indisputable evidence for modern behavior, and she suggested several methods to identify symbolism in material culture.

I view modern behaviors, as they were developed, as a buffer to protect humans from the uncertainties of the natural world. On the one hand, this buffer can be envisioned materially. Such technologies as air conditioners and air heaters create artificial and stable environments. The bow and arrow would also fall into this category. Projectile hunting weapons likely provided a security factor when firing an arrow at a distance from potentially dangerous prey. On the other hand, the buffer can also be conceptualized less tangibly. Exchange systems provide a multi-locus insurance for resources. Symbolic systems also help to make sense of the unpredictable and inexplicable events in the natural world. As modern humans, we have developed new social and technological behaviors to ultimately detach ourselves from the unpredictable natural world to ensure our resources and the security of our offspring.

Late Pleistocene Behavioral Variability in the Archaeological Record

Hunter-gatherers may have adapted their behavior to varying ecological conditions brought about by glacial or interglacial phases during the Middle and Late Pleistocene. For example, the variable use of marine resources in relationship to sea stand and coastline fluctuations during the Middle Pleistocene in South Africa shows context-dependent hunter-gatherer adaptations (Henshilwood et al., 2004; Jacobs et al., 2006; Marean et al., 2007; Fisher et al., 2010). The highly mobile subsistence strategies developed by Aterian hunter-gatherers in the Saharan

grassland during the Last Interglacial (128-75 ka) period of the Late Pleistocene are other examples of the unique behavioral adaptations of people in Africa during this time (Garcea and Giraudi, 2006; Barton et al., 2009).

Furthermore, many of the behavioral changes seen during the Middle and Late Pleistocene appear to be associated with innovations among African hunter-gatherer populations to create and maintain social relationships (McBrearty and Brooks, 2000; Wadley, 2001; Ambrose, 2002; Henshilwood and Marean, 2003; Marean and Assefa, 2005). These relationships may have provided a self-maintained and multi-locus system to minimize any risk associated with living in diverse or degraded environmental conditions, often hypothesized for arid, glacial periods in Africa (Ambrose, 1998a; Ambrose, 1998b; Ambrose, 2002; Ambrose, 2003).

Adaptation to local environmental conditions may also reflect the development of cultural patterning in stone tool technologies across Africa during the Late Pleistocene (Clark, 1964; Clark, 1988; Brooks et al., 2006). The social and technological behaviors, which are first seen in Later Stone Age (LSA) hunter-gatherers during the Late Pleistocene in Africa, are also part-in-parcel of the greater development of modern behaviors. Generally speaking, LSA behaviors include broadening social and symbolic systems and expressions, expanded habitat and resource use, and new ways of making and using stone artifacts (McBrearty and Brooks, 2000). Cultural patterning in stone tools may also relate to genetic and cultural isolation due to catastrophic climatic events (Ambrose, 2002; Ambrose, 2003).

Arid-Adaptation Ideas Since the Early 20th century

The earliest known anatomically modern humans (White et al., 2003) and much of the earliest evidence for behavioral modernity are now known to date to glacial MIS 6 (195-128 ka) (McBrearty and Brooks, 2000). The glacial-interglacial cycling that followed has been seen by

some researchers to be a major influence on modern human behavioral adaptations (Clark, 1988).

Scholars in the first half of the 20th century were aware of a similar pattern of glacial-interglacial cycling during the Pleistocene, but they were at a disadvantage from the lack of accurate chronological information available after the advent of radiocarbon dating in the 1950s. In the second half of the 20th century, radiocarbon and potassium-argon dating enabled researchers to emplace arid-adaptation ideas within chronological frameworks. The result was the development of a generalized sequence of cultural "speed-up" associated with arid "inter-pluvial" events and cultural "slow-down" associated with more ameliorated conditions.

1900-1940

As early as 1901, Max Blanckenhorn in *Neues zur Geologie un Paleontologie Aegyptens, IV* used the term "pluvial" to denote periods of increased rainfall (Blanckenhorn, 1901). At the same time, other German scholars had developed a theoretical teleconnection between glacial climates in the Northern Hemisphere and "pluvial" conditions in the middle and lower latitudes (Flint, 1959). According to these ideas, mid- and low-latitude heating increased evaporation, which caused increased amounts of snowfall and cooler temperatures in higher latitudes such as in Europe. Conversely, glacial conditions in Europe were also believed to cause increased precipitation in Africa because storms were deflected toward Africa (Flint, 1959)

In 1914, Brooks adopted the term "pluvial" into the English-based scholarship (Brooks, 1914). It was Wayland's research in Uganda in the 1920s and 1930s, however, which had the most significant influence on pluvial research in Africa at this time. Wayland used river gravel deposits to establish a series of two pluvial events (Kamasian and Gamblian) and an epi-pluvial event in Uganda, which he then used to correlate to inter-pluvial (glacial) events in Europe (Wayland, 1929; Wayland, 1930; Wayland, 1934).

Wayland's "pluvial" method, as it became known, was highly influential on the work of other early Africanists including Louis Leakey (Leakey and Solomon, 1929) and Erik Nilsson (1929). This is because the pluvial method was more than just a means for relative dating. It was also one of the first methods to tie perceived cultural changes seen in the African Stone Age archaeological record to a paleoenvironmental record (Wayland, 1929; Wayland, 1930; Wayland and Burkitt, 1932; Wayland, 1934). Key to this chronology was the link between culture change and the environment. Wayland (1934) suggested that perceived rapid cultural changes were associated with arid (inter-pluvial) events. Examples, of these rapidly-changing cultural industries include the Chellean, Aurignacian, Capsian, and Stillbay.

1940-Present-Day

At the First Pan-African Congress on Prehistory in 1947, the nomenclature of the Pleistocene pluvials was revised from Wayland's terminology (Kageran, Kamasian, and Gamblian) to "the First," "the Great," and "the Last," respectively (Nilsson, 1949). The biggest development at this time, however, was the advent of absolute dating methods.

In the 1950s, radiocarbon dating confirmed the relative timing of the latest pluvial events (Arnold and Libby, 1949; Libby and Arnold, 1950; Libby, 1951; Flint, 1959). Around this same time, Cole (1954) provided an updated account of the pluvial hypothesis, reiterating the links between arid, inter-pluvial environments, and rapid cultural change in African Stone Age archaeology.

Of particular importance was the way that Cole regarded the "Upper Paleolithic." According to Cole (1954), "Upper Paleolithic" was characteristic to Stone Age Industries exhibiting rapid changes in the frequencies of types of stone artifacts or techniques used to make stone artifacts. This phrase was not a cultural-chronological or even a cultural-spatial term, such as "Upper Paleolithic" (or Later Stone Age) is used today. The phrase represented a period of

rapid cultural change (inferred from stone tool technology), and for this reason Cole was able to identify the East African Fauresmith, Stillbay, Sangoan, and Kenya Capsian Industries as "Upper Paleolithic."

Furthermore, Cole's "Upper Paleolithic" Stone Age Industries were all dated to inter-pluvial events. The implication is twofold. First, Cole's (1954) use of the term "Upper Paleolithic" reified the link between rapid cultural change and arid, inter-pluvial events. Second, and less obvious, is the idea that the term "Upper Paleolithic" became associated with rapid cultural change in Africa. It has only been within the last decade, and following much intensive scholarly inquiry, that the transition to the African "Upper Paleolithic (i.e. the Later Stone Age) was found to be neither rapid nor punctuated (McBrearty and Brooks, 2000).

By the 1960s, the pluvial hypothesis was discredited due largely to the efforts of Flint (1959) who argued that the pluvial method was unsupported by existing evidence. He also stated that climates were an unsuitable primary basis for a geo-stratigraphic sequence. Culture ecology became the next dominant theoretical grounding in African Stone Age archaeological research at this time. As part of the broader processualist movement, culture ecology studies integrated ethnographic and environmental research within archaeological investigations. The purpose of this integration was to study the systemic processes of humans past and present adapting to their environment using an explicit and positivist scientific methodology (Binford, 1962; Binford, 1965; Trigger, 1989).

Clark (1964) was among the most ambitious and influential proponents of the early culture ecology approach. He advocated a direct relationship between environmental change and human evolution suggesting that it was the "contrasting environments of glacial and tropical Africa that were responsible for the basic differences in the stone cultures" (White, 1959; Clark, 1964:177).

Furthermore, and perhaps more than any other mid-20th century researcher, Clark championed the link between arid environments and rapid behavioral change by suggesting that the challenges of early humans were wrought by environmental deterioration and met by the development of new behaviors (Clark, 1960; Clark, 1963; Clark, 1965; Clark, 1988). For example, Clark (1960: 309-310) suggested:

> These drier periods seem to have been times of cultural "speed-up"--times of relatively short duration compared with the intervening wet periods, when new ideas and new forms were able to spread with greater ease throughout the continent and when less favourable living conditions stimulated man's powers of invention towards improved methods of securing food and more comfortable living quarters [an example that J. G. D. Clark has pointed out, of Toynbee's concept of "Challenge and Response," as a main explanation of the historical development of human society].

> On the other hand, as soon as technical ability permitted [that is to say from the end of the Earlier Stone Age onwards], the long periods of wetter climate made for stability, slow development, and isolation of groups, and so resulted in a number of contemporary regional cultural variants.

Conclusions

Today, arid-adaptation ideas similar to Clark's can be found in the resurgence of special interest discussions concerning African cultural-environmental refugia (Brandt, 1988:840; Shea, 2006; Brandt et al., 2006; Cohen et al., 2007; Hildebrand et al., 2008) and past climatic catastrophes such as the Toba super-eruption in SE Asia (Ambrose 1998a, 1998b, 2003; Rose and Chesner 1990; but see Oppenheimer 2002; Gathorne-Hardy and Harcourt-Smith 2003). However, a problem with studying just arid-adaptation is that it may be only one perspective of a much larger phenomenon. This phenomenon was recognized by Clark (1988:251) who also implied that Last Interglacial hunter-gatherers were as adapted to their environment as were hunter-gatherers in glacial periods. Furthermore, the ethnographic record provides a vital

account of how contemporary hunter-gatherers adapt to arid or unpredictable environmental conditions.

A number of studies have addressed hunter-gatherer behavioral variability, and both Lee and Devore (1968) and Kelly (1995) have provided thorough descriptions of this research. In Africa, some of the seminal studies of hunter-gatherer living outside of tropical forests include Wiessner's (1977; 1980; 1982) accounts of the !Kung San (Kalahari), and Woodburn's (1968) and Marlowe's (2010) research among the Hadza (Tanzania).

Kelly (1995) provided a detailed discussion of the various 20th Century theoretical approaches in anthropology that have been used in hunter-gatherer studies. Binford's (1980) seminal study showed that hunter-gatherer organization around resources can be projected onto, or interpreted from, archaeological assemblages. Yellen and Harpending (1972) have shown that !Kung band aggregation and cultural homogeneity can be attributed to resource availability, which is also observable in the archaeological material culture record.

According to Yellen (1977), however, it is the predictability of resources in an area rather than resource diversity that can affect hunter-gatherer behavior. In variable and unpredictable conditions, like deserts, Yellen (1977) finds that people living in these areas proffer a flexible behavioral strategy that enables them to adapt to, and exploit, numerous environments and available resources. People living in variable and unpredictable conditions are also more resistant to change. Behavioral conservatism, therefore, is a product of successful adaptation to unpredictable environments, which contradicts many ideas about behavioral change to arid and glacial times in the Late Pleistocene archaeological record.

In environments where resources are unpredictable and highly variability, ethnographic and archaeological cultures should evidence consistent and rarely changing behaviors and

material culture. But, what might be expected during OIS 3? The climate during OIS 3 may have been unstable and resources in the Horn of Africa might have become unpredictable. Under these conditions a more conservative material culture archaeological record could be expected following a period of adaptation to the new environmental conditions. However, the logic here assumes that the environmental changes from good to bad, hence from resource abundance to a lack of resources and unpredictable resources. More intense monsoons during OIS 3 almost certainly would have introduced a degree of unpredictability into the environment, but the added moisture may have also helped to increase resource diversity and abundance in the area. Therefore, increased unpredictability coupled with increased resources may have created a situation where it was not only advantageous for hunter-gatherers to diversify into new resource niches but it was timely to experiment with new ways to more effectively collect diverse resources.

To develop this idea further it is useful to look towards the available archaeological data, which will be discussed in the following chapter. Here, I have briefly reviewed the history of theoretical thought about arid-adaptation ideas in African Stone Age research since the early 20th century. I have focused intently on these ideas because this genre of thought has been such a predominant force in African Stone Age archaeology throughout much of the last century to today.

CHAPTER 4
ARCHAEOLOGICAL SITES IN EASTERN AFRICA DATING TO THE LATE PLEISTOCENE (OIS 4 AND OIS 3)

This chapter summarizes the archaeological data about hunter-gatherer occupation of the Horn of Africa and East Africa during OIS 4 and OIS 3. The OIS 3 archaeological record, in particular, is minimal, being characterized by large spatial and temporal gaps in the data. Many of these sites are also poorly dated with the result that little data currently are available to discuss how hunter-gatherers were living in this region during this period.

OIS 3 Archaeological Record: Limitations

Two reasons for the dearth of archaeological data in eastern Africa during OIS 3 include chronology and sampling issues and prehistoric human behavior. The first problem, chronology and sampling, relates not only to the historical lack of research in this area and in this period in general (cf. Brandt, 1986), but also to the lack of dating techniques that have been, until recently, available to date sites of Late Pleistocene age. As both Clark (1954) and Brandt's (1986) reviews of the Horn show, a number of sites are known in the region but many still remain undated. The second reason draws upon current estimates for low population densities across Africa during the Last Glacial (Ambrose, 1998b), and the likelihood that human populations across this region were located in only specific localities during glacial periods (Brandt et al., 2006; Hildebrand et al., 2008; Basell, 2008).

Chronological and Sampling Problems

Radiocarbon dating has been widely used to date Holocene and Late Pleistocene sites, but apart from this technique, other methods have not been available to date Late Pleistocene sites until relatively recently. Obsidian hydration used to be fairly common, but it is now known to be problematic, if not unreliable entirely. The complicating factor for obsidian hydration is due to the variability of hydroxyl ions within the obsidian (Mazer et al., 1991; Anovitz et al., 1999;

Hull, 2001; Rogers, 2008). Other techniques had minimum-age limits in excess of the Late Pleistocene, such as Potassium-Argon dating. Today, new techniques, such as Argon-Argon and optically stimulated luminescence dating, provide more options for researchers but even these techniques are dependent upon specific environments and sample types.

The use of radiocarbon has sustained Late Pleistocene archaeology in eastern Africa up to the present day. However, even radiocarbon has had limitations when dealing with Late Pleistocene-aged materials. Until relatively recently, a ~40 ka cap on the maximum age limit has been in place for radiocarbon analysis because no calibration curves existed beyond this time period.

Radiocarbon (^{14}C) is a product of atmospheric interactions with cosmic rays and geomagnetism, as well as fluctuations in the global carbon reservoirs (Hughen et al., 2004). Several notable deviations of cosmogenic nuclides (^{14}C, ^{10}BE, ^{36}CL) occurred during the Late Pleistocene due to solar activity and geomagnetic flux (Baumgartner et al., 1998; Hughen et al., 2004; Muscheler et al., 2005; Chiu et al., 2007). Within the last decade new calibrations have been developed using independent dating methods such as U-series on marine fossil coral, and speleothem records that extend the calibration curves up to 50 to 60 ka (Hughen et al., 2006; Chiu et al., 2007; Weninger and Joris, 2008; Reimer et al., 2009). The 40 ka cap not only limited the usefulness of radiocarbon dating, but it also required researchers to publish only uncalibrated radiocarbon ages from many Late Pleistocene sites in eastern Africa (cf. Clark, 1954; Mehlman, 1989). To avoid confusion, extra vigilance is now required when discussing these ages to differentiate between calibrated and uncalibrated dates.

Many dated Late Pleistocene archaeological sites in Africa were also excavated prior to the development of improved collection techniques and radiocarbon pre-treatment methods, which

are now known to help ensure more accurate and precise results (Brandt et al., 2010). Today, it is important to know what material is being sampled for radiocarbon dating. Bone, for example, poses dating problems due to potential contamination and weathering (Hedges and Vanklinken, 1992). The collection of radiocarbon samples can also affect results. Samples taken from sieves at Moche Borago, for example, provided widely inaccurate and imprecise results due to contamination (Brandt et al., 2010).

Methodological problems also occur in dating many Late Pleistocene sites in eastern Africa. Many Late Pleistocene sites are dated from a single sample or at the most two or three samples, (cf. Brandt, 1986). In Ethiopia, for example, Porc Epic, K'one, and FeJx 4 at Lake Besaka are the only sites dating to the Late Pleistocene in which each has more than three absolute dates. However, only the topmost deposits of the 11 m sequence at K'one are dated, which leaves the entire lower two-thirds of the sequence to be inferred (Kurashina, 1978; Clark and Williams, 1978; Brandt, 1986). At Porc Epic, questions arise about the accuracy of the ages, as well as the context of the archaeological deposits (Brandt, 1986).

Problems Arising from Late Pleistocene Demography and Settlement Patterns

While the lack of Late Pleistocene archaeological data in eastern Africa can be attributed to an absence of research or methods, the prehistoric distribution of people across this landscape may also be a major factor. Human populations across Africa during the Last Glacial were already very low, possibly due to the aftereffects of catastrophic events such as the Toba super-volcano eruption (Ambrose, 1998b). These populations would have been spread thinly across the landscape, and current methods may be unable to identify the archaeological signatures of these occupations.

Furthermore, human populations may have moved into or out of specific areas during glacial periods such as OIS 4 and OIS 2 (Barham and Mitchell, 2008). Among the best known

examples of population movements is the widespread abandonment of previously occupied areas in the Sahara during OIS 4, ~74 ka, (Wendorf and Schild, 1992). These populations may have moved east into the Nile valley, but even these occupations appear to have been ephemeral (Van Peer, 1998; Van Peer and Vermeersch, 2000). In Somalia, early Holocene hunter-gatherers may have been targeting isolated inselberg formations (large rocky outcrops) instead of living further abroad these features (Brandt, 1986). In Kenya, Late Pleistocene hunter-gatherers may have followed specific environmental ecotones (Ambrose, 2001). Humans likely also congregated in isolated environmental refugia across the Horn and East Africa during the especially arid periods of OIS 4 and OIS 2 (Ambrose, 1998b; Brandt et al., 2006; Basell, 2008). The lack of Late Pleistocene archaeology in eastern Africa may not just be an artifact of the region's research history, but the lack of sites itself may be a real pattern also.

OIS 3 Archaeological Record: Available Data

Basell (2008) noted approximately 60 sites in eastern Africa that contain Middle Stone Age archaeological materials. Of these sites, only 14 have deposits dated directly to OIS 3 and artifacts that span the major technological change at this time to microlithic tools. These 14 sites across this region equate to only 1 site for every ~420,000 square km (Figure 4-1). To compound the problem, many of these sites have dating or context issues. For convenience, I have provided a summary in Appendix B of sites from across the Horn, East Africa, and North Africa that date to OIS 3. These sites have archaeological deposits which span the transition to microlithic tools at this time. This summary includes published ages and brief descriptions of archaeological materials. I also provide additional details about the archaeological sites from the Horn and East Africa that date to OIS 3 and that have early microlithic technology.

Mode 4 and Mode 5 Stone Tools

Microliths are blunted (backed) on one lateral edge for purposes likely related to hafting or handling the tool. These artifacts often take the form of crescents or geometric trapezoids. The development of microliths during OIS 3 signals a major change in technology and subsistence strategies among hunter-gatherers at this time. Microlith technology enabled hunter-gatherers to build multi-component tools to more effectively use raw materials. It is also likely that the development of these artifacts signals the development of other important technologies such as the bow and arrow (Ambrose, 2002). Microliths may even have been used in early social exchange systems (Ambrose, 2002).

The earliest microliths date to the South African Howiesons Poort Industry, but current evidence suggests that the Howiesons Poort ended after 60 ka (Jacobs et al., 2008). The appearance of microliths in East Africa, 50 to 40 ka, marks the re-appearance of the technology, which continued into the Holocene (Ambrose, 2002). Microliths are one technological hallmark for the Later Stone Age of eastern Africa (Clark, 1954; Brandt, 1986). Another technological hallmark for Pleistocene and Holocene Later Stone Age (LSA) technology is the use of blade and bladelet technology, which itself is seen as an increasingly more economical use of raw materials than prior stone tool technologies (McBrearty and Brooks, 2000).

Following J. G. D. Clark's (1971) classification of Stone Age lithic technology, blade and microlithic/bladelet tools are classified as Mode 4 and Mode 5, respectively. Clark's typology is useful because it considers only technological changes. Middle Stone Age (MSA) and LSA, by comparison, imply both cultural and technological changes. The shift from MSA to LSA, for example, signifies technological and subsistence changes and also transformations in hunter-gatherer cultures, including language, symbolism, and identities (McBrearty and Brooks, 2000; Wadley, 2001). The MSA and LSA also have different characteristics at various times or places.

For instance, in southern Africa, some Pleistocene LSA assemblages do not have microliths whereas they are often present in Holocene LSA assemblages (Mitchell, 2002). The term "Mode 4/5" refers to technology that includes the presence of both blade/bladelet and microlith technologies, which are common to both Late Pleistocene and Holocene LSA assemblages in eastern Africa and the Horn of Africa.

The earliest published age for Mode 4/5 technology is for Mumba rock shelter in Tanzania where a number of chronometric ages have been provided (25 conventional radiocarbon, 4 AMS, 1 amino acid racemization, 6 uranium-series, and 5 potassium-thorium) (Mehlman, 1989; Marks and Conard, 2006; Prendergast et al., 2007). However, despite these efforts, the age of the site is still contentious (Marks and Conard, 2006; Prendergast et al., 2007).

Much of the discussion revolves around the dating of Layer V, which includes early Mode 5 technology. This layer is generally taken to date to ~65 ka, but this age is based on a single U-Th date (with an error of at least 6,049 years). However, different results can be calculated if all of the various dates from Layer V are considered (n = 11; cf. Prendergast et al. 2007), and then run through a central age model (Galbraith and Laslett, 1993; Van der Touw et al., 1997; Galbraith et al., 1999; Galbraith et al., 2005). Based on the central age model, which considers both the average and standard deviations of a sample, the weighted mean is only 32,961 ± 3,347, with an error approximately half that of the supposedly more accurate U-Th age. Unless substantive evidence suggests a certain technique or a range of ages is more accurate than any other technique, the age of Layer V at Mumba must remain inconclusive.

The most securely dated early Mode 4/5 deposits are currently found at Enkapune Ya Muto (Tanzania), dating >50 to 46 ka. The Enkapune Ya Muto sequence is dated using 35 conventional radiocarbon and AMS ages plus 3 obsidian hydration ages (Ambrose, 1998a). The

earliest Mode 4/5 deposits (>50-46 ka), however, are not directly dated. Rather, the published ages are estimates based on sediment deposition rates calculated from the obsidian hydration chronology (Ambrose, 1998a). Considering the well-cited problems with obsidian hydration (Mazer et al., 1991; Anovitz et al., 1999; Hull, 2001; Rogers, 2008), the ^{14}C ages on ostrich eggshells in overlying deposits may be a more confident minimum age estimate from 39 to 37 ka.

Only four sites in Ethiopia have stratified early Mode 4/5 deposits. Near Dire Dawa, Porc Epic cave has a 2.5 m sequence, which is capped by cemented breccia (Clark et al., 1984; Assefa, 2006). The lithic technology from Porc Epic has been studied closely (Pleurdeau, 2001; Pleurdeau, 2005), but serious concerns linger about the context and dating results at the site (Brandt, 1986). Already mentioned, K'one has an 11 m sequence, but only the topmost portion of the stratigraphically highest loam deposit has been dated (Kurashina, 1978; Clark and Williams, 1978; Brandt, 1986). The Bulbula River site in central Ethiopia (near Ziway) has a single conventional radiocarbon date of 27,050 ± 1,540 ^{14}C BP for the Mode 4/5-bearing paleosol (Gasse and Street, 1978; Brandt, 1986). Liben Bore in southern Ethiopia has been studied closely (Brandt, 2000; Negash, 2004; Fisher, 2005), however, it is currently undated. Also worth mentioning, locality FeJx at Lake Besaka (central Ethiopia) has slightly younger Mode 4/5 artifacts in Terminal Pleistocene deposits dating from 19 to 22 ^{14}C BP (Brandt, 1986).

In Somalia, the dating and context is no better. The stratified Mode 3 and Mode 4/5 deposits at Midhishi 2 (NE Somalia) are dated by two radiocarbon samples with the oldest, >40 ka, providing only the minimum age for the deposits (Brandt and Brook, 1984). At Gud-Gud, the deposits are dated to >40 ka by a single radiocarbon sample, but the assemblage is also small, being composed of less than 50 mostly undiagnostic artifacts (Brandt and Brook, 1984; Brandt,

1986). At Gogoshiis Qabe in southern Somalia, the Mode 3 deposits are stratified under terminal Pleistocene and Holocene assemblages, but the Mode 3 deposits themselves are undated (Brandt, 1988).

Conclusions

Archaeological data are sparse for the Late Pleistocene in eastern Africa due partly to the historical record of research in this area. The methods and techniques available to prior researchers may also have contributed to the lack of data today. At the very least, the absence of dating methods and methodological advances commonplace today makes much of the prior findings difficult, but not impossible, to compare with new data. But the lack of sites might reveal something about the nature of human populations in the region or where they were located during the Late Pleistocene. Resolving these issues requires new research at previously studied sites, as well as the analysis of new sites. Toward this goal, the findings from Moche Borago provide an important new record of human occupation in the Horn during OIS 3 of the Late Pleistocene. In Chapter 5, I will introduce the Sodo-Wolayta region where Moche Borago is located and describe the prior research which has been conducted at the site.

Figure 4-1: Map of the Horn of Africa (red) and East Africa (yellow) showing the archaeological sites discussed in the text.

CHAPTER 5
MOCHE BORAGO ROCKSHELTER: LOCATION, ORAL HISTORY, AND PRIOR ARCHAEOLOGICAL RESEARCH

Mochena Borago Sodwa translates as "Moche, son of Borago of Sodo." In the local Wolayta language of the Wolayta people, the traditional designation for the rockshelter takes its name from Moche Borago. According to oral history, Moche Borago was among the first owners of the land around the rockshelter, and, unknown to most outsiders, his name also commands a unique place in southern Ethiopian history. Reportedly, Moche, and perhaps his father Borago, was an adviser to King T'ona, the last king of Wolayta, before he was defeated by Emperor Menelik in 1894 at the battle of Chelsha in Borada (Tema Asele, Balcha Basa, and Alaro Asele, per comm.). The unique oral history surrounding this site and nearby rockshelters complement the prehistoric record being revealed in the current archaeological excavations. This chapter introduces the Wolayta region, its people, and the local history of Moche Borago rockshelter. The second half of this chapter provides an overview of prior scientific research at Moche Borago, including the Southwest Ethiopia Archaeological Project (SWEAP) excavations from 2006 to 2008.

Physiography of the Wolayta Region

Wolayta is located within the Southern Nations, Nationalities, and People's Region (SNNPR) of Ethiopia. This region is currently one of the most densely populated areas of Ethiopia, which includes a diverse collection of spoken languages and cultures. Sodo is the capital city of Wolayta, found at the southern foothills of Mt. Damota approximately 3 km from Moche Borago. Wolayta itself is located between the lowland Rift Valley and lake country and southern Ethiopian highlands. Variations in elevation,

temperature, and rainfall here create a series of altitudinal ecological zones that provide an abundant source of plant and animal resources (Lesur-Gebremariam, 2008).

Ethiopian Rift Valley System

Ethiopia is dominated by the tectonic activities of the East African Rift System. The country is positioned just off the epicenter of three divergent tectonic plates, which form the East African Rift system to the south, the Red Sea to the north, and the Gulf of Aden to the northeast. The intersection of these plate boundaries is the Afar triple junction—and the most prominent feature other than the Rift Valley—is the depressed and hyper-arid Danakil depression in northern Ethiopia and Eritrea.

Within the Rift Valley, the divergent action of the African and Arabian plates forms a north-south series of normal fault grabens that have been in-filled to form the Ethiopian lake country (Di Paola, 1972). Along the peripheries of the Rift systems tectonic uplift produced the Ethiopian highlands around 75 million years ago, elevating these areas on average >1,500 m above sea level (asl). The Rift Valley subdivides the highlands into western and southeastern components in Ethiopia.

Climate

Ethiopia's climate is determined by the seasonal movements of the Inter-Tropical Convergence Zone (ITCZ) and monsoonal moisture (Kebede, 2004). From October to March, the ITCZ is positioned south of Ethiopia, allowing cold, dry air to flow in from Arabia. During April and May, the ITCZ moves northward drawing in moisture from the Indian Ocean that accounts for ~25% of the total annual rainfall in Ethiopia. From July to August, 75% of Ethiopia's rainfall occurs when the ITCZ is located north of the country drawing moisture-rich monsoonal air masses from the Atlantic Ocean across Ethiopia and the Horn (Kebede, 2004).

Highland areas, such as southern and southwestern Ethiopia, receive greater amounts of rainfall than lowlands due to the orographic influence of the highlands on the monsoon air masses (Livingstone, 1975; Gasse, 2000; Mohammed et al., 2004). Moche Borago is located near the eastern limit of the southern highlands in a transitional zone to the lowland lake country. The city of Awassa, which is located in the Rift Valley lake country to the east, receives ~120 mm per month from July to August whereas the city of Jimma to the west in the highlands receives >200 mm (National Meteorlogical Agency, 2010).[3] In Obe Jage, north of Mt. Damota, the average annual rainfall is ~1,250 mm (Le Gal and Molinier, 2006) and rainfall around Moche Borago should have a similar average annual rainfall.

Physiography and Vegetation

Moche Borago is situated ~2,200 m asl on the western flank of the volcano massif Mt. Damota. This mountain is a major freshwater resource in the area because precipitation at higher elevations of the mountain drains via numerous stream channels into the valleys below (Borena, 2008). The location of Moche Borago makes it accessible to lowland zones and resources to the south and east, including the Omo gorge and Lake Abaya, as well as highland resources to the west. On clear days, the western ridge of the highlands is visible from the Moche Borago site to the west, and Lake Abaya can sometimes be seen to the southeast.

The natural vegetation of the area has been replaced largely by farming and eucalyptus (*Eucalyptus globulus*). Today, the slopes of Mt. Damota, and much of the surrounding countryside, are heavily cultivated by seasonal crops of domesticated maize

[3] The meteorological station at Sodo was closed in 1986. Awassa and Jimma are the nearest major stations.

(*Zea mays)*, barley (*Hordeum vulgare)*, sorghum (*Sorghum bicolor)*, finger millet (*Eleusine coracana)*, teff (*Eragostis tef)*, and ensete (*Ensete ventricosum*), as well as numerous other crops (Le Gal and Molinier, 2006).

The predominant natural vegetation of the area is Ethiopian Afromontane forest. However, the distribution of these forests is now heavily restricted and fragmented due to farming. Hildebrand (2003) provided a comprehensive summary of vegetation species common to Afromontane forests. In general, Afromontane forests occur from 1,500 to 2,600 m asl. The extant Afromontane forests around Moche Borago are dominated by the conifer *Podocarpus falcatus* and *Juniperus procera*.

The lowlands below Mt. Damota consist of patchy Afromontane forest and grasslands. This area possibly relates to the "transitional" forest zone, as defined by Hildebrand (2003), which occurs from 500 to 1,500 m asl. This forest zone includes species such as euphorbia (*Euphorbia candelabrum*) and acacia (*Acacia Abyssinia*) known to occur around Sodo. Based on firsthand observations, our SWEAP team speculated that the grasslands below Moche Borago may be relict marshlands from wetter periods of the past.

This region might have sustained abundant natural resources in the past. The most obvious is freshwater, which would have precipitated at high elevations of Mt. Damota and collected into stream channels that eventually drained into the lowlands. During periods of aridity today, precipitation still collects on top of the mountain. During previous glacial periods, it is likely that the same phenomenon might have occurred.

Afromontane forests include a number of edible wild plants. To date, no study has been published of the extant or archaeological wild plant types from the Wolayta

region, though these studies are part of ongoing SWEAP research. Le Gal and Molinier (2006) provided descriptions of agro-economy from 1940 to present day, but they did not focus on wild plant resources. The best survey of edible highland plant resources in the SW Ethiopian highlands is Hildebrand (2003). However, her study targeted the Bench-Maji area in extreme SW Ethiopia, which is located at a higher elevation than Wolayta and also receives greater annual rainfall. Hildebrand (2003) also noted that Afromontane forest in the far southwest Ethiopian highlands differ from Afromontane forests elsewhere in the highlands. However, the species diversity of Afromontane forests in Bench-Maji should still approximate the species found in Afromontane forests in Wolayta.

The wild edible plants found by Hildebrand (2003) to be common in Afromontane forests include seasonally available greens, fruits, oil seeds, and tubers. Certain resources are available only at certain times of the year. Greens, for example, are most widespread today during the spring rains (March to May) whereas oil seed is most common in the dry seasons (Hildebrand, 2003).

Tubers are known from ethnographic sources to be a primary subsistence resource of African hunter-gatherers (Vincent, 1984). While yams are present in Afromontane forests, it is the false banana, known as enset (*Enset ventrocosum*), that is a staple crop today and often regarded as a famine food during drought (Hildebrand, 2003). Besides being a food resource, enset also provides wood, fibers for clothing and binding, and freshwater (Hildebrand, 2003).

Language

Omotic and Cushitic are the only indigenous language families found in the Wolayta area today (Lamberti and Sottile, 1997). Amharic, a Semitic language, is the

primary language today for commerce and trade across Ethiopia and the Wolayta region. The use of Amharic in the Southern Nations, Nationalities, and People's Region (SNNPR) of Ethiopia today can be traced back to the Amhara expansion and subjugation of southern kingdoms by Emperor Menelik in the late 19th century.

The Wolayta language is part of the Ometo sub-branch of the Omotic language family (Lamberti and Sottile, 1997). To the west, northwest, and east of Wolayta are highland Cushitic speakers (Kambaata, Haddiya, and Sidamo, respectively) (Lamberti and Sottile, 1997). To the south and west, the Gamo and Gofa peoples share a similar Omotic language with the Wolayta.

Brief mention should be made about the use of the term "Wolayta" in this dissertation. Wolayta, as the name for the language and culture in the Wolayta region, is plural for "Wolamo"/"Wellamo." Some researchers (cf. Cerulli, 1956) have argued that Wolamo is more accurate to use when speaking about language and culture. Lamberti and Sottile (1997), however, contended that local people today prefer the term Wolayta. The use of this term in this region is interesting because this Omotic name uses the Cushitic singular "-tta" suffix.

Political History

Until the late 19th century, the Wolayta region was a feudal kingdom, part of the wider network of Gibe kingdoms that included the Sidamo, Kafa, and Jimma states. Records indicate that Wolayta was a subsidiary of the Kindgom of Kafa. Trade was an important staple for the Wolayta Kingdom, owing to its location at the juncture of the more northerly Cushitic-speaking peoples and southerly Omotic peoples (Cerulli, 1956; Lamberti and Sottile, 1997).

Beckingham and Huntingford (1954) stated that the Wolayta Kingdom was established in the mid-13th century with the Damot Dynasty. The second dynasty (Wolaitamola) dealt with repeated Islamic invasions (Shinn and Ofcansky, 2004). The foundation of the third dynasty in the mid-16th century began in Tigray (northern Ethiopia and Eritrea). Kawo (King) Damota (1835-1845) of the Tigray Dynasty shares the same name as the volcanic mountain on which Moche Borago is located.

Local History of Moche Borago Rockshelter

According to local history, the rockshelter and surrounding land was purchased by Moche Borago from Ato Wara and Wyseru K'arare. Ato Moche[4] was originally from Sodo. Ato Moche, and perhaps his father Ato Borago, was an adviser to the Wolayta King T'ona. Moche and Borago were members of the Maka clan of the Dogala branch of the Wolayta. The rockshelter may have been unnamed before either Moche or Borago received it, meaning that name likely predates 1894 when T'ona was captured.

Before Moche Borago purchased the land around the rockshelter, it might have been used as a sacred place for ritual sacrifices of goat and sheep. In the Wolayta region, ritual sacrifice is recorded in Cerulli (1956) who noted that the practice was most common to Tälehê, the spirit of the Omo River,[5] but it is also present in other ceremonies.

It is unclear if Moche Borago ever inhabited the rockshelter. Remnant wall foundations have survived on the south side of the rockshelter, but these are widely believed to date to the 19th century when Menelik occupied the area, or to the 1930s and

[4] "Ato" is the male titular prefix for "Mister" in Amharic.

[5] This is only an example because Cerulli (1956) mentioned that ritual sacrifice to the spirit Tälehê was made in the Omo River.

1940s during the Italian occupation (1936-1941) of Ethiopia. Both ideas may be correct since recent archaeological evidence in Moche Borago supports the use of the site during the early 19th century (e.g. coins) and use of the site within the past few hundred years.

Prior Archaeological Research at Moche Borago

In 1995, Roger Joussaume of the Centre National de la Recherche Scientifique (National Center for Scientific Research) in Nanterre, France, developed the Groupe d'étude de la Protohistoire dans la Corne de l'Afrique (GEPCA) (the Protohistoric Study Group in the Horn of Africa). The focus of this project was to study the origins and processes underlying plant and animal domestication in the Horn of Africa during the Neolithic, and how these developments related to underlying environmental changes (Gutherz et al., 2000a). The project was subdivided into multiple components, including teams studying rock art and megalithic monuments in the region and archaeological excavations in Djibouti and Ethiopia of which Moche Borago was one element.

GEPCA Excavations: 1998 and January-February 2000

The first excavations at Moche Borago were undertaken under the leadership of Xavier Gutherz of the University of Montpelier (France) in 1998, and again in January and February of 2000 (Gutherz et al., 2000a). Between these two field seasons, Gutherz's team took geological samples of the shelter floor and walls and created three 4 m^2 test excavation areas (Figure 5-1). From the geological samples, the team was able to show the presence of volcanic deposits in and around the site and that the formation of the rockshelter was likely an abscess of softer materials within ancient and highly heterogeneous volcanic lahar deposits.

Excavations in three areas revealed stratified archaeological deposits containing abundant pottery, burnt and unburnt bone, and "MSA and LSA" lithics within stratified

sandy and silty deposits, including numerous well-defined hearth features (Gutherz et al., 2000a). The lithic artifacts included large amounts of blade and flake debitage (Poisblaud, 2000). The findings in Test Pit 1 were particularly rich, and this area was subsequently expanded to 6 m^2 during the 2000 field season. Excavation in Test Pit 2 revealed fluvial activity and reworked deposits with interstratified volcanic layers.

In unit G10 of Test Pit 1, Gutherz's team excavated a narrow 0.5 m x 1 m sondage from approximately 1.5 to 1.8 m below the current cave floor. The sondage excavations stopped after a hard, dense rocky deposit was discovered, which Gutherz and his team believed to be bedrock. Mode 3 lithics were also recovered in G10, suggesting that stratified Middle Stone Age (MSA) deposits might underlie the Holocene deposits above. Radiocarbon samples taken below the well-defined tephra 11 deposit[6] were dated to 28,700 ± 1,100 BP (31,184 ± 906 cal. BP, using Cal-Pal Hulu). The Holocene sequence above tephra 11 dated from 4,370 ± 70 BP (3,062 ± 124 cal. BP) to 1,480 ± 60 BP (852 ± 67 cal. BP).

GEPCA Excavation: November 2000

A third excavation in November 2000 focused on stratigraphic and sedimentological analysis of the Holocene deposits at the site, including correlations between various profiles in the excavation areas (Sordoillet and Pouzolles, 2000). Post hole structures were also identified in the stratigraphic profiles of Holocene deposits in Test Pit 3. A ring of post holes was uncovered during lateral excavations at Test Pit 1, which may date to the first millennium (Jallot and Pouzolles, 2000). A large amount of

[6] SWEAP later renamed Tephra 11 "BWT" (see Chapter 6).

charcoal was recovered near this area, which led Jallot and Pouzolles (2000) to suggest on-site metallurgy even though no other evidence, such as slag, supported this theory.

Research during the 2000 season also included a micromorphology analysis that found phytoliths, carbonized and uncarbonized plant remains, and carbonized seeds in the Holocene deposits (Gutherz et al., 2001). Faunal materials from these deposits, which were also preliminarily studied, included a large percentage of bovine remains but also artiodactyls and carnivore remains including *Panthera pardus, Colobus guereza,* and *Dendrohyrax arboreyeus*. Crocodiles, fish, and shellfish (species not provided) were also recovered (Lesur, 2000).

The November 2000 excavation also provided more information on the ceramic sequence in this area. Analysis suggested an aceramic Holocene occupation at the site, which is dated via radiocarbon on charcoal to 4,370 ± 70 BC (3,062 ± 124 cal. BP) (Gutherz et al., 2001). Overlying the aceramic Holocene layers were deposits containing a variable amount of ceramics, often having curvilinear decorations. In the uppermost deposits, traditional ceramic *jebena* (coffee pot) and *cha'ati* (spice jars) fragments were recovered (Jallot and Pouzolles, 2000).

GEPCA Excavation: December 2001

In December 2001, GEPCA carried out a final excavation at the site. During this season, Test Pit 1 and Test Pit 3 were connected in order to clarify ambiguities between the stratigraphic profiles of these areas (Gutherz et al., 2001). This correlation also helped to resolve the stratigraphic lateral associations of a rich bone and ash layer discovered in Test Pit 3. This layer contained two-thirds of the total faunal material found at Moche Borago, and that faunal material has been relatively dated via stratigraphic correlation to approximately the early 5th millennium BC. Lesur (in Gutherz

et al., 2001) noted that the faunal samples are dominated by Bovinae, especially buffalo (*Syncerus caffer*), but a distinct Bovidae component includes Gazella, Tragelaphis, and possibly Kobus. Lesur found domestic cow (*Bos taurus)* in the upper and most recent layers at the site. Lesur's (Gutherz et al., 2001) impression of the Holocene fauna is that the fauna reflects a predominant hunting subsistence strategy focused on Bovidae, especially buffalo, and that domesticated animals, such as cow, arrived in this area only within the last millennium.

Other faunal identifications include the remains of primates (*Papio cynocephalus, Colobus guereza*), hyena (*Crocuta crocuta*), suides (*Potomocheroerus larvatus* and *Phacochoerus africanus*), and hyrax (*Heterohyrax brucei*) (Lesur 2001). Several human teeth were also found in the deposits, but no known study has been published on this discovery. Most faunal remains have been fire-altered, as the interpretation of the Holocene faunal assemblage suggests. The diversity of the fauna remains also indicates the exploitation of two distinct biomes during the Holocene: the humid plains along the Weja River below Mt. Damota and a forest biome (Gutherz et al., 2001). A similar subsistence strategy between highland woodlands and lowland grasslands is speculated for Pleistocene hunter-gatherers occupying the site.

SWEAP Excavations: 2006-2008

The Southwest Ethiopia Archaeological Project (SWEAP) began excavating Moche Borago in 2006. This multi-national project, led by Co-PIs Dr. Steven Brandt (SB) (University of Florida) and Dr. Elisabeth Hildebrand (EH) (Stony Brook University), was funded by the U.S. National Science Foundation. Research conducted by SWEAP focused on assessing the context of the stratigraphic and archaeological sequences (pre-Holocene) at Moche Borago, as reported by Gutherz (Gutherz et al.,

2000a; Gutherz et al., 2000b; Gutherz et al., 2001), and continuing excavations into Pleistocene deposits across the site in a systematic and knowledgeable manner (Figure 5-2).

The original focus for SWEAP research at Moche Borago was human adaptation during arid periods of the Late Pleistocene, including OIS 4 and OIS 2/Last Glacial Maximum (LGM). Brandt et al. (2006) and Hildebrand et al. (2008) hypothesized that humans moved into wetter regions of the Horn, such as southwestern Ethiopia, during the early Last Glacial (~74-60 ka) and Last Glacial Maximum (~18 ka) because these areas may have sustained greater resource diversity at these times. The confluence of people moving into SW Ethiopia may have affected the genetic, linguistic, and cultural demography in this region, thus spurring the development of Later Stone Age social and technological behavioral innovations.

Since 2006, radiocarbon dating—both accelerator mass spectrometry (AMS) and conventional—of the site's deposits suggests that OIS 2/LGM layers at the site may not exist anymore (see Chapter 6 for more detail). The oldest, currently dated deposits at the site also fall within early OIS 3, meaning that OIS 4 layers are also unlikely. The sequence is unique, however, because these deposits preserve among the most complete records of OIS 3 occupation in the Horn.

To simplify the discussions of the deposits across the site, SWEAP placed all excavation units on site (both GEPCA and SWEAP) into three main excavation groups: 1) Block Excavation Area (BXA), 2) TU2 (Test Unit 2 area of GEPCA) ~9 m southeast

of BXA, and 3) the newer area known as N42, ~9 m southeast of TU2 and ~18 m from BXA. N42 is currently the most southerly excavation at the site (Figure 3-2).[7]

The SWEAP team rediscovered, exposed, photographed, and mapped, using a Total Station, all the GEPCA excavation units and stratigraphic profiles. During the initial mapping of the GEPCA excavation units, the SWEAP team noticed that the grid system used by the GEPCA team was offset 30° from true north, most likely done intentionally to accommodate the natural orientation of the site.[8]

Geodetic control for SWEAP research is based on the UTM system (zone 37N). Unlike the arbitrary grid used by GEPCA, the global UTM system allows local site data to be more easily articulated into regional and global contexts without requiring coordinate transformations in most circumstances. The SWEAP team preserved the orientation of the pre-existing GEPCA excavation units, but new excavation areas are oriented according to the true north UTM system. The variation between the GEPCA and SWEAP grids means that cardinal directions, which conform to the GEPCA units, are not equivalent to those in the newer SWEAP units. Therefore, in the following discussions, any cardinal orientation that is relative to the 30º North angled offset of the GEPCA grid is indicated with the prefix "GG" (GEPCA Grid), for example, G10 GG north profile, whereas orientations relative to newer SWEAP units do not have a designate and are aligned to true north (e.g. N42E38 north profile).

The alphanumeric designate of the GEPCA excavation units was also retained (e.g. G10). Newer UTM-based excavation units use a Northing-Easting schema (e.g.

[7] In this chapter, and subsequent chapters, a unique three-letter name is used to define stratigraphic layers within each excavation area, like BWT. For further information on the stratigraphy and descriptions of particular layers, please see Chapter 6.

[8] Magnetic declination from 1995 to 2000 was less than 2° at Moche Borago.

N42E38), relying on the coordinates of the southeast corner of an excavation unit that are truncated to two significant digits to the left of the decimal. All spatial data, regardless of excavation area orientation, are recorded using UTM coordinates.

SWEAP Excavations: 2006

In 2006, SWEAP focused primarily on new excavations in unit N42E38 while continuing GEPCA excavations into the Pleistocene deposits in the BXA unit G10 and TU2. G10 had been dug originally as a 1 m x 0.5 m sondage to a depth of ~2 m below surface by GEPCA in 1998 (Gutherz et al., 2000a; Gutherz et al., 2001). In 2006, SWEAP excavated the remaining northern half of G10 relatively quickly in order to assess firsthand the stratigraphic and general archaeological sequence in the Pleistocene deposits at the site. Archaeological materials recovered from this 1 m x 0.5 m area were minimally piece-plotted, except for charcoal samples. The SWEAP excavations in nearby units G9, H9, and I10 proceeded at a slower pace, and every artifact found *in situ* was plotted using the total station, which is normal SWEAP protocol.

At the close of the 2006 SWEAP field season, excavations in G10 had reached a depth of 1.60 m below the current rockshelter surface,[9] but excavations still had not hit the "bedrock," as described by Gutherz et al. (2000a). I began analysis of lithic material from G10 in July 2006 with assistance from William Wright and Kochito Kero. Preliminary results from this analysis showed that the deepest excavated areas from G10 contained Mode 3 and Mode 4/5 lithic artifacts. Strata from the upper G10 Pleistocene deposits, however, appeared to have Mode 4/5 lithics only.

[9] This depth is equivalent to 1.05 m below tephra BWT, which defines the Holocene/Pleistocene boundary in the BXA deposits.

In TU2, a dense layer of heavily rolled and abraded pebbles and stone artifacts within a reddish silty-clay layer (RGX) were found stratigraphically below a compact volcanic tephra that was assumed to correlate to tephra BWT in the BXA area. The TU2 sequence appeared deflated relative to the BXA excavations, and sediments here seemed to be more frequently derived from volcanic activities.

The stratigraphic sequence in the N42 area completely contradicted the strata from the BXA. The excavations here revealed ~1 m of stratified, archeologically sterile volcanic tephra/ash deposits (some with blocky clasts exceeding 10 cm diameter) overlying another 1 m of dense, stratified volcanic lahar deposits. Only a relatively thin series of three silty-sand layers (layers: UPFC, MPFC, and LPFC), unconformably placed atop the uppermost lahar layer (ULF), contained deposits similar to those in the BXA unit where archaeological materials might be expected to be found.

In late 2006, five charcoal radiocarbon samples were sent to Dr. Hong Wang at the Illinois Geological Survey. Due to the small sizes of charcoal, multiple pieces of charcoal from the same stratigraphic layer were aggregated into a single sample. The calibrated ages of these samples suggested that the deposits underlying tephra BWT at Moche Borago dated to OIS 3 (samples SWAP06-1 to SWAP06-5). These same results also indicated a possible unconformity dating to the Terminal Pleistocene between the uppermost Pleistocene deposits (layers: RCA, RGCA, and RGCB) and the BWT tephra, which marks the Holocene/Pleistocene transition.[10]

[10] Samples of the BWT tephra were also collected by Dr. Leah Morgan for Ar^{40}/Ar^{39} dating analysis in 2006. The results of this analysis provided an age of 3.16 MA. The Mt. Damota volcano is known to have been active during the Pliocene (Woldegabriel et al. 1990), and this age may be due to feldspars that were derived by erosion from the pre-existing older volcanic sources and do not reflect the true depositional age of BWT (L. Morgan, 2008 per comm.).

SWEAP Excavation: 2007

The 2007 field season focused on resolving many of the questions raised by the prior 2006 field season, including the lateral correlations of stratigraphic deposits across the site, the depth of the Pleistocene deposits in the BXA, and the ages of the Pleistocene deposits across each excavation area. Prior excavations were continued in the BXA (G10, G09, and H09), TU2 (TU2S), and N42 (N42E38).

The "bedrock" layer, as described by Gutherz et al. (2000a, 2001), was also reached in 2007 in unit G10 ~2 m below the rockshelter surface. This stratigraphic layer, which was named PKT, appeared to be more like a lahar deposit than bedrock due to the clast sizes, texture, color, and homogeneity.

At the completion of the 2007 field season, nearly 2,500 stone artifacts, faunal material, ochre, and charcoal had been plotted from units G10, G9, and H9.[11] Every stratigraphic profile in the BXA had also been mapped, described, and sampled. Excavations in G10 reached the sterile PKT lahar. In G9, the excavations ended within the RCA deposit whereas in H9 the excavations reached stratigraphic layer VDBS. In TU2, both GG east and west profiles were mapped, described, and sampled. Excavations in N42E38 were stopped 2.2 m below surface, still within archaeologically-sterile volcanic deposits.

The anthropogenic pits/possible paleo-fluvial features first noticed in G10 GG north in 2006 were seen also in TU2 and N42. In TU2, the LFX1 lahar had been truncated, and the underlying LFX2 lahar deposit had been undercut by fluvial action before the YBSX tephra had in-filled this area. Similarly, in N42E38, the anomalous

[11] The current total following the March 2008 field season is 6,520 plotted pieces of lithics, charcoal, bone, and ochre.

UPFC, MPFC, and LPFC silty-clay deposits first noticed in 2006 were found to contain size-sorted cobbles, also likely fluvially deposited. The N42E38 silty-clay deposits unconformably overlie the ULF lahar deposit, which is similarly believed to have been eroded fluvially.

In December 2007, an additional 13 radiocarbon samples on charcoal (SAWP07-01 - SWAP07-13) were processed and analyzed by Dr. Hong Wang at the Illinois Geological Survey. Unlike the prior five radiocarbon samples submitted in 2006, the new samples were all piece-plotted and collected *in situ*, and they were not aggregated into larger sample sizes. Five samples targeted the possible unconformity underlying tephra BWT and the age range of the deposits immediately underlying BWT (RCA, RGCA, and RGCB). Five charcoal samples were selected from across the other BXA Pleistocene deposits, and two charcoal samples were taken from TU2. The results of this assay confirmed the Terminal Pleistocene unconformity between RCA and BWT at the top of the Pleistocene sequence. Furthermore, the CTTC deposits, among the deepest at the site, were dated to ~53 ka and the remaining samples from BXA confirmed the nearly complete OIS 3 chronological sequence. The samples from TU2 helped to establish a stratigraphic/chronological correlation between the BWT and YBS tephras in these two areas.

SWEAP Excavation: 2008

Following the 2007 field season, the chronology and composition of the Pleistocene deposits at Moche Borago were sufficiently well known to be classified into five major stratigraphic aggregates, following the sequence seen in the FG G10 north profile. These stratigraphic groups are described in Chapter 6.

In early March 2008, an additional eight radiocarbon samples (SWAP08-1 - SWAP08-8) were processed by Dr. Hong Wang at the Illinois Geological Survey. Many of these samples were prudently chosen to target the very top of the RCA deposits, which were carefully excavated from units H9 and G9. The rest of the new radiocarbon samples were selected to help define the age of the YBT tephra in the BXA area.

In late March 2008, I returned to Moche Borago with Kochito Kero and Menassis Girma to continue the excavation of H9 in the BXA. The 2008 excavations were designed to increase the artifact sample size between the YBS and YBT tephras, dating to ~43 ka. These excavations were part of the doctoral field research for this dissertation, which was funded by the J. William Fulbright Foundation as part of the 2007-2008 Ph.D. Research Scholarship Program.

During the 2008 excavations, a semi-circular feature of burnt and discolored sediment was found in H9 containing a loose in-filling of abundant bone and stone artifacts. This feature was interpreted to be a series of hearth deposits, repeatedly excavated and refilled with anthropogenic materials during the occupation of the site ~43 ka.

The depth of the highly consolidated PKT deposit was also explored more extensively using a 0.5 x 0.5 m test excavation. This endeavor was halted after the test unit reached a depth of 1 m below the upper surface of PKT. Following the 2008 field season, four more radiocarbon samples (SWAP08-9 - SWAP08-12) were sent to Dr. Hong Wang at the Illinois Geological Survey. These samples increased the total radiocarbon array of the Moche Borago Pleistocene deposits to 29, making this excavation location among the most chronologically secure sites in the Horn of Africa.

Esay Rockshelter

During the March 2008 field season, myself, Kochito Kero, and Menassis Girma also visited the nearby Esay rockshelter, about a 30-minute walk south of Moche Borago. Esay rockshelter is smaller than Moche Borago, being approximately 28.5 m long and 20 m deep. The site is located at the head of a deep, steep ravine such as Moche Borago. However, unlike Moche Borago, a shallow stream percolates out of the rear cave wall at Esay, bisecting the site. This site is a useful modern analog for possible paleo-fluvial channels seen at Moche Borago. The implications of the observations at Esay will be discussed in Chapter 6.

Today, Muslim residents of the area visit Esay rockshelter because the stream at the site is believed to contain holy water, as evidenced by three modern fire hearths seen near the entrance to the site in 2008. From a geomorphological perspective, staining on the rockshelter walls and roof (especially around joints and cracks) suggests that either water flow may increase during the wet seasons or was increased during more humid periods in the past. The current stream channel is headed by a 15 cm joint in the rear rockshelter wall 1.2 m above the current cave floor surface. At the base of this joint is a small pool. The stream channel itself is ~2 m wide and is bordered with small plants and shrubs (sp. unknown). A distinctive algal mat lines both banks of the stream. The channel base is composed of heavily abraded pebbles that are size-sorted and intermixed with obsidian and chert stone tools. The stone artifacts did not appear to be heavily abraded, however, and no diagnostic tool types were observed.

Conclusions

In total, Gutherz and his team excavated more than 20 sq m at Moche Borago, mainly in the northwest section of the site. The GEPCA excavations exposed a broad

lateral area, which allowed the team to identify the presence of post holes, fire hearths, and other spatial patterning often not easily seen in vertical excavations. The excavations done by GEPCA also facilitated the predominantly Pleistocene-focused research of SWEAP, which started in 2006, because much of the Holocene deposits in the various excavation areas had been previously removed.

The SWEAP excavations continued the GEPCA research in the BXA and TU2 areas while concurrently starting new excavations in the N42 area. An array of specialized analyses and radiocarbon samples now provides a detailed perspective into the depositional history and stratigraphic context of the Pleistocene archaeological materials at the site. Furthermore, it is now confirmed that Moche Borago contains OIS 3 archaeological deposits. The progressive radiocarbon strategy used to date these deposits is also unique among similarly aged sites in Africa, and Moche Borago is now the best dated OIS 3 sequence in the Horn of Africa.

In Chapter 6, the stratigraphy and cultural sequence of the Pleistocene deposits will be provided in detail. The stratigraphic descriptions will offer context to the stone artifact analyses that will be presented in Chapters 7 and 8.

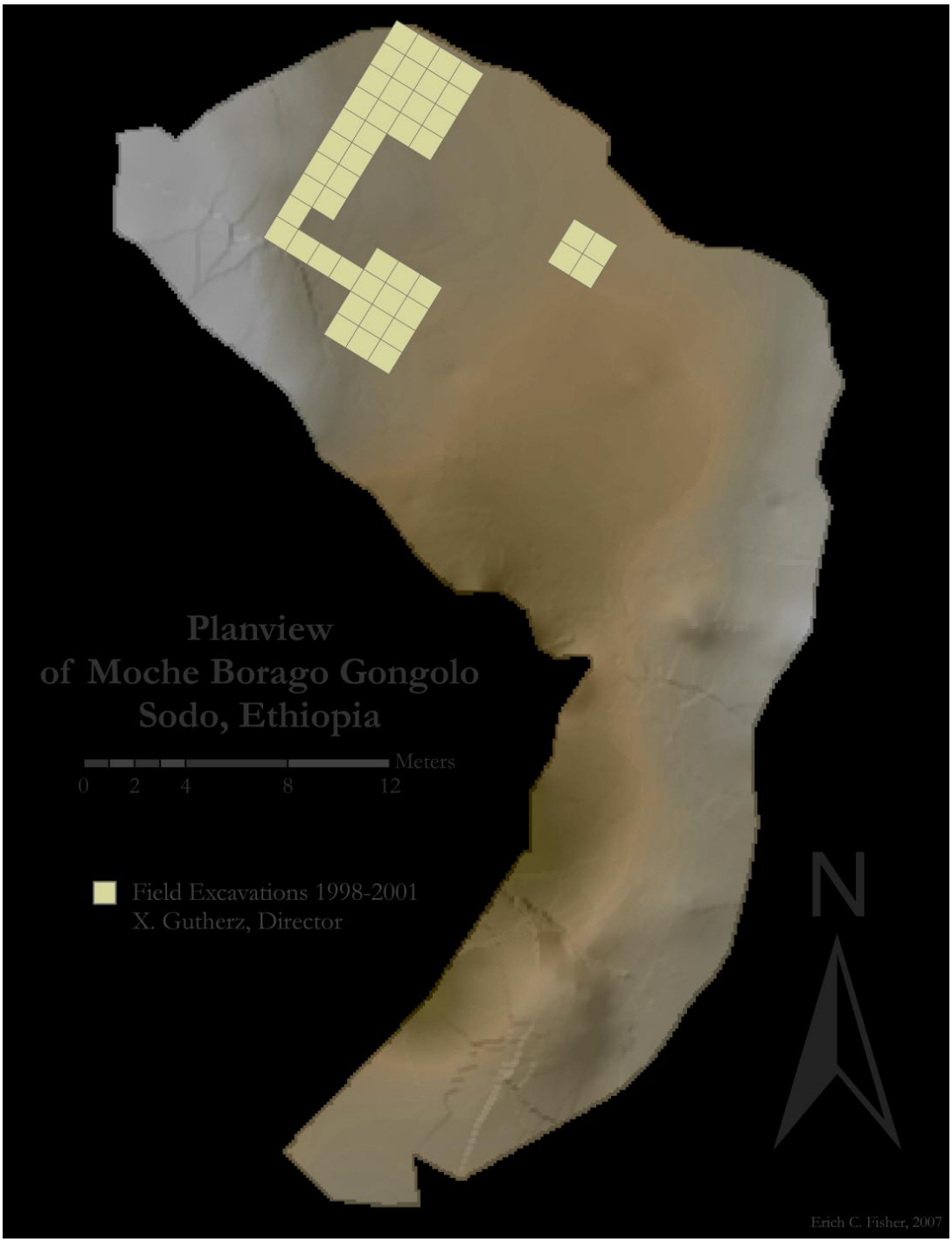

Figure 5-1: GEPCA excavation areas at Moche Borago from 1998 to 2001.

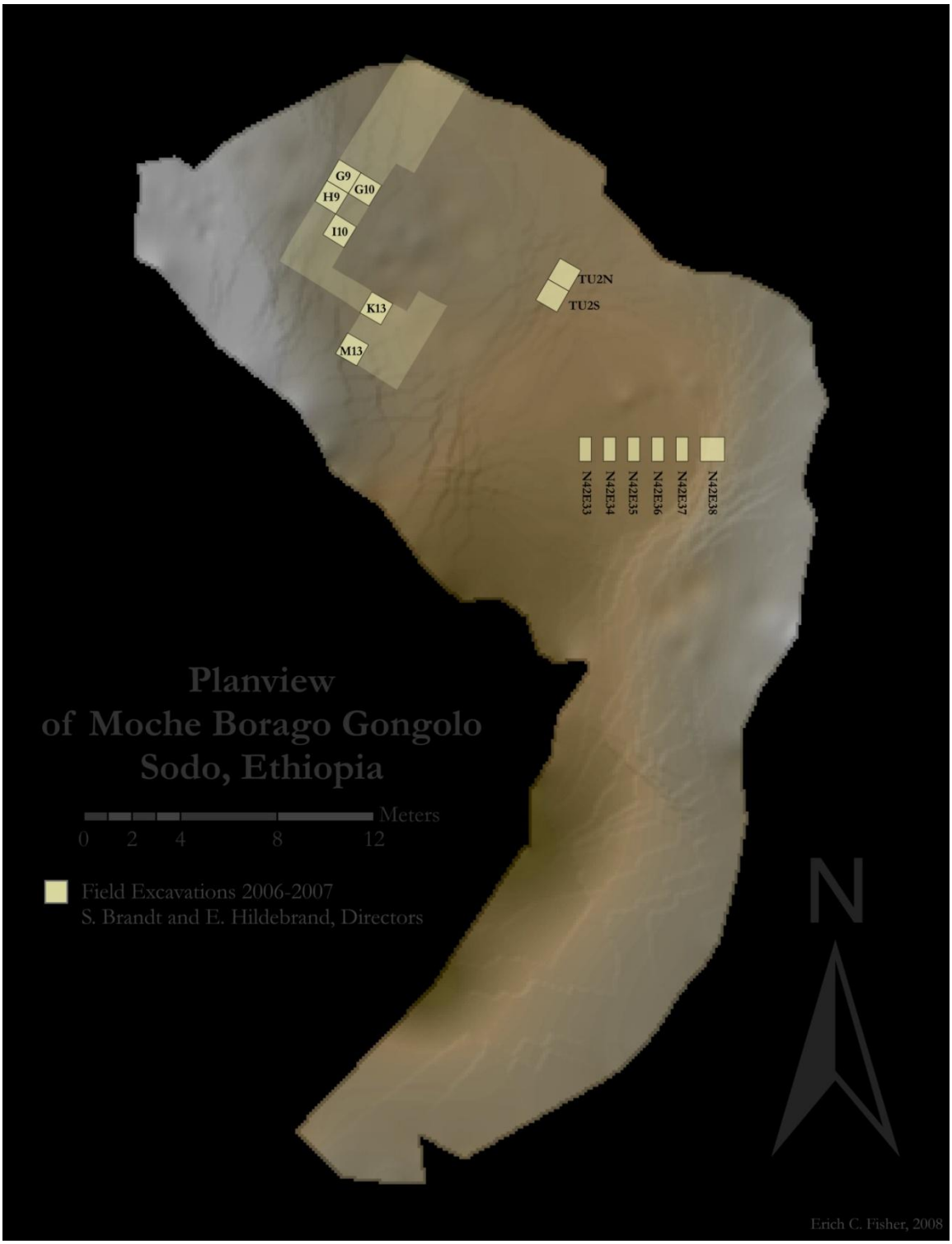

Figure 5-2: SWEAP excavations from 2006 to the present.

CHAPTER 6
THE LITHO-STRATIGRAPHIC SEQUENCE AT MOCHE BORAGO ROCKSHELTER DURING EARLY OIS 3

This chapter provides detailed descriptions of the Late Pleistocene litho-stratigraphic sequence at Moche Borago, which showed a nearly continuous deposition from early OIS 3 to the Holocene when there is a major unconformity in the main BXA excavation area. I provide a high level of detail for three reasons. First, very few African archaeological deposits date to OIS 3, so that Moche Borago provides unique information on OIS 3 depositional environments. Second, although well-defined interstratifications are visible within the deposits that provided consistent and clear litho-stratigraphic divisions, a great deal of stratigraphic variability exists between excavation areas, indicating the depositional history at Moche Borago is complex. Third, the detailed descriptions contextualize the archaeological findings described in Chapters 7 and 8. Since sedimentary and geomorphic evidence suggest that certain time periods were wetter than other periods, at the end of this chapter, I will compare what is currently known about the depositional history of the deposits at Moche Borago to the known paleoenvironmental and paleoclimatic sequence across the region.

Litho-Stratigraphic Units Versus Culture-Stratigraphic Units

The descriptions of stratigraphic sequences at archaeological sites have two main common sources to draw upon: 1) geomorphology and lithology and 2) archaeology. Litho-stratigraphic methodology focuses on the depositional history and diagenesis of the lithologic deposits. Culture-stratigraphic methodology, however, prioritizes changes in the material culture accrued from human occupation at the site. Both methods provide useful information in understanding a site's history, and they are also not mutually exclusive.

However, they must be defined *a priori* and separated out *a posteriori* because litho-stratigraphic sequences may not parallel changes in material culture as is the case with the oldest lithologic deposits at Moche Borago, detailed in Ch. 8. In this chapter, I therefore rely on a strictly litho-stratigraphic methodology. Descriptions of the archaeology within any group are presented here only for referential purposes.

Methods

Many processes can alter or remove a site's deposits in 40,000 years, including mechanical processes (e.g. fluvial, aeolian, root, human, and animal actions) and geochemical processes (e.g. soil formation, leaching, and percolation). The volcanic bedrock and ashes common to the Wolayta area (Di Paola, 1972) create alkaline sediment conditions, which affects bone preservation (Berna et al., 2004).

A number of methods are now employed in modern archaeology to discern the minute processes that have affected a site's deposits in order to better interpret the litho-stratigraphic and archaeological history at a site. The SWEAP team relied on a large and diverse international collaboration of researchers to bring reliable, cutting-edge methods to bear on the study of Moche Borago.

Stratigraphic Descriptions and Profiles

A stratigraphic unit is a single, unique layer of sediment. Stratigraphic units can be identified vertically from the layers above and below it, and they can be defined laterally from surrounding sediments. Stratigraphic units that share similar features (e.g. color, texture, consolidation, sediment type) are grouped into larger litho-stratigraphic units or "groups". At Moche Borago, each litho-stratigraphic group shares similar sediment characteristics, and group divisions are all well-defined by volcanic ash layers.

We gave each new stratigraphic unit a unique name consisting of a short combination of letters (e.g. PKT), which sometimes acted as an acronym (e.g. BWT is "Big White Tephra"). If a stratigraphic unit was also numbered, it was part of a specific depositional sequence. Descriptions of individual stratigraphic units were collected during the excavations as they were found. Detailed information was recorded about the topology, topography, and sedimentology of each stratum. Sedimentological information included the color (dry and wet), texture, consolidation, and inclusions of the layer. Topological information related to the location of the stratigraphic unit relative to other layers above and below and to possible correlated units in other areas. Topographical information about the top, middle, and base of every stratigraphic unit was collected using the total station, and was also useful for creating detailed 3D models of the strata. Photographs were also taken of each stratigraphic unit.

Stratigraphic profiles were recorded using a total station and concurrently noted down onto paper graphs.[12] Point spacing within the profiles was approximately 10 cm. The stratigraphic profile data were integrated into the site multidimensional GIS alongside the lateral topographical strata data and archaeological data.

Multidimensional GIS (mDGIS) Modeling

A Trimble TS-305 total station was used on-site by the SWEAP team since 2006. A TDS Recon drove the total station and customized drop-down menus within the TDS Foresight software and provided prompts to record thematically-based attribute information for every point taken. All archaeological and faunal materials in H09, G09,

[12] E. Hildebrand was instrumental in describing, maintaining, and mapping the Holocene and Pleistocene stratigraphic profiles.

and I10[13] were plotted *in situ* during excavations. These data were integrated daily into a mDGIS database built within ESRI ArcGIS 9.3, which was cross-checked for accuracy of the recording methods and spatial patterning within the data.

Stratigraphic survey points collected during the excavations were imported into the mDGIS to create 2.5D elevation models of the horizontal stratigraphy and vertical wall profiles. The vertical profiles were created in 2.5D vector format using a custom Python script because ESRI ArcGIS does not accommodate vertically geo-referenced raster imagery. Planimetric photographs taken of each stratigraphic unit and level, however, could be geo-referenced in ArcGIS and were often draped onto the elevation models to create photo-realistic representations of the site.

Bulk Sample Analysis

Representative samples of each stratigraphic unit were collected into individual 4" x 6" plastic bags. The location of each sample was recorded using the total station at the time the sample was collected. Sub-samples were exported internationally for various analyses.

Inductively Coupled Plasma-Mass Spectrometry

Inductively Coupled Plasma-Mass Spectrometry was attempted on sediment samples from the site to assess geochemical variability. Sample preparation procedures followed Kamenov et al. (2009). The samples were processed and analyzed by Dr. Jonathon Walz, with assistance by Dr. George Kamenov, at the University of Florida Department of Geological Science ICP-MS laboratory. Seventeen samples were processed in 2008, and an additional 28 samples were analyzed in 2009. Both groups of

[13] G10 and TU2 were considered test excavations and only charcoal was plotted.

samples were analyzed using an Element 2 (Thermo-Finnigan) ICP-MS. The 2008 samples were heated prior to analysis whereas the 2009 samples were not cooked before analysis. No discernible difference occurred between cooking the samples prior to analysis. Quantification of the samples in parts per million was made using the USGS reference standard (J. Walz per comm.).

X-Ray Florescence

The x-ray florescence (XRF) analysis was also used to identify spatial geochemical variability within the sediments. Energy dispersive x-ray florescence analysis was done using a Bruker Tracer III-V portable XRF. The Tracer III-V used an X-ray tube excitation source with a Rhodium target. A silicon detector converts the incoming analog x-ray pulses into proportionally-sized digital signals. The Tracer III-V variably measured incoming x-ray energy between 0 and 45 keV.

Sediment samples were placed into 31 mm diameter polyethylene rings with 0.16 mm ultralene film ends directly atop the Tracer sensor. Spectra data were collected systematically for 180 seconds using a .006" Cu / .01" Ti / .012" Al composite filter at 40 keV and 15 μA. These settings allowed all incoming x-rays between 17 keV and 40 keV to reach the sample, but the filter focused the sensitivity of the measurements only to elements between 5 keV and 17 keV.

Spectra were analyzed visually using Bruker S1PXRF ver.3.8.27 and Artax ver.5.3.15.1 software. The software was used to export the raw spectra x-ray abundance counts (1,024 rows long with 0.04 keV / row) into individual *.csv files. These data were subsequently collated into a single database for statistical analysis. The data were normalized using the Rh K_{α} raw spectrum abundance values of sample CTTC, which had the lowest Rh K_{α} abundance.

Statistical analysis of the normalized spectrum abundance data was accomplished using SPSS 17.0. Quantile-quantile (QQ) plots showed that the data were not normally distributed. Therefore, bivariate relationships were derived using one-tailed correlation matrices of the full spectra data (1,024 variables/sample) based on Spearman's ρ. The correlation coefficient was squared to produce the coefficient of determination, R^2, which was then converted to a percentage (R^2 x 100) to describe the amount of shared variation in ranks between samples. All significant values were reported $p < .01$.

Overall, the bivariate relationship between all unique pairs of samples was directional (one-tailed) and very high (mean of shared ranked variation between samples = 95.4%; SD = 2.0, $p < .01$). The high relationship among samples was due to the overall chemical similarity within the deposits. However, some chemical variation was still expected and seen due to heterogeneity within the samples themselves or because of likely post-depositional processes that affected the chemistry of the samples differently.

Analysis of within and between-sample variations helped to identify the minimum value of shared ranked variation between two samples that were derived from the same source. This analysis looked at multiple cases of homogenous strata sampled from different excavation areas (e.g. tephra BWT sampled from the Block Excavation Area and TU2) and unhomogenized, heterogeneous strata samples taken from a single area (e.g. N42 ULF which had numerous inclusions). For each type of strata (homogenous, different area or heterogeneous, same area), the results consistently showed that each sample group shared at least 97% of the ranked variation, meaning that R^2 values $\geq$ 97% were most likely derived from the same source. Therefore, all R^2 values described in the

text here that were ≥ 97% (0.97) were assumed to derive from the same parent material and thus regarded as the same stratigraphic layer.

Magnetic Susceptibility

Magnetic susceptibility was used to identify geomagnetic changes in the sediments that may be due to anthropogenic or geogenic factors. Samples were sieved, ground, air-dried, and packed into standard Bartington plastic sample boxes (2.5 cm diameter, 10 cc). Each sample was subjected to a suit of mineral magnetic tests as per Herries and Fisher (in press). These tests included dual frequency and low temperature magnetic susceptibility measurements using the Bartington MS2 equipment and IRM (isothermal remanent magnetization) acquisition curves and backfields, hysteresis loops, and thermomagnetic curves applying a Magnetic Measurements variable field translation balance (VFTB) (Herries per comm.).

Radiocarbon

H. Wang at the University of Illinois at Urbana-Champaign Geochronology Laboratory processed and dated the Moche Borago radiocarbon samples. The standard procedure acid-base-acid (ABA) pretreatment was used for accelerator mass spectrometry (AMS) ^{14}C dating of Moche Borago charcoal samples. The same pretreatment was also applied to the ^{14}C-free wood background sample and working standard wood samples, which included IAEA C5 (Two Creek forest wood), FIRI- D (Fifth International Radiocarbon Inter-comparison D wood), and one ISGS ^{14}C dating lab working standard (Reily AC wood) samples.

All samples were boiled for 1 hour in 2M HCl and rinsed to neutrality using deionized water (DI-water). The samples were then soaked in 0.125 M NaOH for 1 hour and rinsed to neutrality using DI-water. Thereafter, the samples were soaked again in 2M

HCl for 30 minutes and rinsed to pH 6 using DI-water. The samples were dried overnight in an oven set at 70°C. Then ~5 mg of each unknown sample and the background and working standard wood samples were placed into pretreated quartz tubes for sealed quartz tube combustion at 800°C with 0.1 g Cu, 0.5 g CuO granules and a few grains of Ag foil. The quartz tubes had been preheated at 800°C for 2 hours and the CuO granules had been preheated at 800°C one day before usage. The Cu grains and Ag foils were reduced using hydrogen gas under vacuum at 800°C. The combustion was programmed for 2 hours at 800°C. The samples were subsequently cooled from 800°C to 600°C for 6 hours to allow the Cu to reduce the NxO to nitrogen gas. The purified CO_2 was then collected cryogenically for AMS ^{14}C analysis. Purified CO_2 was submitted to the Keck Carbon Cycle AMS Laboratory of the University of California-Irvine for AMS ^{14}C analysis using the hydrogen-iron reduction method. At the University of Illinois at Urbana-Champaign, a split of purified CO_2 was also analyzed for $\delta^{13}C$ values using the Finnegan 252 IRMS (isotope ratio mass spectrometer) with a dual inlet device. Sample preparation backgrounds were subtracted based on the measurements of ^{14}C-free wood. All results were corrected for isotopic fractionation, according to the conventions of Stuiver and Polach (1977), with $\delta^{13}C$ values measured on prepared graphite using the AMS. The AMS analysis indicated that all working standards of wood were within two standard deviations and all background wood samples were older than 53,300 ^{14}C yr BP, which led us to believe that charcoal samples with ^{14}C ages from 48,850 to 41,580 were true ages and all other results were reliable. The accelerator mass spectrometry results are provided in Table 6-1 (H. Wang per comm.).

Litho-Stratigraphic Groups of the Block Excavation Area

The Block Excavation Area (BXA) was the main focus for both the GEPCA and SWEAP excavation teams. This excavation area, the most northerly at the site, occupies 24 sq m^2, being mostly within the upper 1 meter of deposits[14]. The SWEAP excavations were focused closest on a 3 sq m area between excavation units G10, G09, and H09 and also almost exclusively on the deeper Pleistocene deposits (Figure 5-2).

Half of unit G10 was first excavated by GEPCA as a 0.5 m x 1 m sondage to test the total depth of the archaeological deposits at Moche Borago. The SWEAP team continued these excavations in the remaining 0.5 m x 1 m of deposits, and the depositional sequence became the backbone of the stratigraphic research at Moche Borago, including naming conventions, litho-stratigraphic groups, and correlations.

Next, the stratigraphic units are described in groups. Deeper, older deposits are explained first and the discussion moves upward within each stratigraphic sequence. A composite profile, which shows the stratigraphic sequences and correlation of deposits between each excavation area, is provided in Figure 6-1.

PKT

Location: BXA
Stratigraphic Units: PKT
Age: Unknown

The PKT deposit is the lowest within the BXA. It is a mottled pink (5YR6/2) consolidated ash deposit with abundant, poorly sorted clasts. The deposit was heavily consolidated and attempts to excavate it required a hammer and chisel. The deposits were first described by Gutherz (Gutherz et al., 2001) as possible bedrock. This seems

[14] This calculation does not consider the connection made between the GEPCA Test Unit 1 and Test Unit 3 made in 2001. Was this area to be considered, the BXA surface area becomes 36 sq. meters.

unlikely because PKT appeared to be dissimilar to the parent rock in the rockshelter walls. The total depth of the PKT deposit is still unknown. In 2008, a 0.5 m x 0.5 m test pit was dug to a depth of 1 m below the top surface of PKT, but little change was noted within the deposit.

PKT was the only stratigraphic unit at Moche Borago which was not aggregated into a larger litho-stratigraphic group due mainly to the unique characteristics of this layer. The x-ray fluorescence spectra of PKT showed the highest recorded amount of rubidium across all stratigraphic samples from each excavation area collected from the site. Iron and zirconium concentrations, generally found in high amounts across the site, were also lower in PKT. By comparison, the iron concentration is much higher within the overlying T-Group deposits when compared to PKT, suggesting that the T-Group did not derive from the PKT deposit.

T-Group Deposits

Location: BXA
Stratigraphic Units: VHG, CTTC, CTT, MHD, and DCC
Age: >53 to 45 ka

Located stratigraphically above PKT was a series of sandy-silt (VHG, CTT, MHD) and clayey (DCC) layers that represented a period of dense human occupation at the site. These layers were collectively aggregated into the "T-Group" litho-stratigraphic unit, which was bracketed by tephra YBT (above) and (PKT) below.

The T-Group could be subdivided into Upper and Lower, based on sedimentological and chronological grounds. The T-Group Lower (VHG, CTT, CTTC) deposits were characterized by hard, gravelly ashes and clayey-sands that appeared to be more heavily weathered than overlying deposits. The age of the T-Group Lower has been minimally dated 53,224 ± 2,662 cal. BP because we have currently dated only a

single sample, which came from CTT in the uppermost T-Group Lower deposits. The lower deposits, which are mainly represented by VHG, remained undated.

The T-Group Upper deposits (MHD and DCC) were characterized by an increased clay content and red coloration of the sediments. The T-Group Upper included numerous stratified hearth deposits that showed a banded profile in the excavation unit walls. While the hearth deposits represented sedimentological deposition, the anthropogenic process by which they were deposited blurs the boundary between purely litho-stratigraphic and culture-stratigraphic classifications. The weighted mean age[15] of the T-Group Upper was estimated to be 45,164 ± 982 cal. BP using radiocarbon.

Layer descriptions

Micromorphological analysis showed that the contact between PKT and the lowest T-Group deposit, VHG, was very sharp. Currently, we are unsure if the contact between PKT and VHG is unconformable. VHG was a layer of moderately abundant gravels in a hard, mottled clay matrix, containing microscopic clasts of variably weathered volcanic ashes, charcoal, and reworked clay fillings suspected to be from water in the cave.

The upper surface of VHG was eroded and capped by CTT, a compacted, localized ash lens in G10 surrounded by a clay berm (CTTC). CTT may have been disturbed. Numerous irregular clasts of weathered tuff, charcoal grains, iron-stained bone fragments, and organic matter were revealed in micromorphology (P. Goldberg per comm.).

CTT was likely a basal sub-deposit associated with the MHD hearth features found stratigraphically above it. Charcoal recovered from CTT was dated directly to 53,224 ±

[15] All weighted mean ages presented here rely on the Central Age model (Galbraith and Laslett, 1993; Van der Touw et al., 1997; Galbraith et al., 1999; Galbraith et al., 2005).

2,662 cal. BP, which is currently the oldest and deepest absolute age at the site. The underlying 20+ cm of archaeological deposits, which are mainly VHG, are currently undated.

MHD is a series of stratified archaeological hearth deposits that indicated a repeated human presence in this section of the rockshelter during early OIS 3, ~53 to 45 ka. The MHD deposit was characterized by numerous compacted aggregates of fine, iron-rich illuvial clay bands deposited through colluvial activities. The upper surfaces of some of the clay bands appeared to have been moderately eroded and stabilized (P. Goldberg, per comm.).

Stratigraphically above MHD was the slightly thicker layer DCC. DCC was the topmost layer of the T-Group. The XRF analysis showed that DCC had the highest iron content[16] of the T-Group deposits, including the overlying YBT tephra. The weighted mean radiocarbon age for DCC was estimated at 45,164 ± 982 cal. BP, which provides the upper age estimate of the T-Group deposits.

Occupational Hiatus #1

Location: BXA
Stratigraphic Unit: YBT
Age: ~43 ka

The first major occupational hiatus at the site was found within the tephra YBT that overlay DCC and capped the T-Group. YBT was a ~20 cm thick yellow-brown (2.5YR6/3), prominently-graded ash that was variably intermixed with soil aggregates (sandy-silt) (P. Goldberg, per comm.). Statistical comparisons using whole XRF spectra showed that the chemical composition of the YBT tephra is very similar to that of the

[16] According to XRF analysis, the iron content appeared to increase incrementally within the T-Group, starting with the lowest iron abundance values at the base, VHG.

BWT tephra dating to the early Holocene, $R^2 = 0.984$, $p < .01$ (Spearman's ρ). This observation was further supported by mineral magnetic analysis which also pointed to similar sources for these layers (A. Herries per comm.). BWT and YBT shared similar reversible thermomagnetic curves, which are also unique compared to other strata at the site.[17] Currently, the source for BWT and YBT is unknown though it is presumed to be local. BWT was correlated chemically via XRF to open-air tephra up to 18 km northeast of Moche Borago and Mt. Damota.

Charcoal was found in YBT, which may have become carbonized as the hot ash was deposited into the site. Multiple radiocarbon samples from YBT dated this volcanic event between 41 and 45 ka, providing a weighted mean, calibrated radiocarbon age of 43,403 ± 1,213 cal. BP. The duration of the YBT volcanic event is still undetermined. Artifact densities were high before and after YBT, while the tephra layer itself was effectively sterile (1 stone artifact was recovered in YBT from unit G10).

S-Group Deposits

Location: BXA
Stratigraphic Units: OBMB, LVDBS, LMGV, VDBS
Age: 44 to 43 ka

Above YBT were a series of distinct stratigraphic units, which formed the S-Group aggregate in the BXA. The S-Group is believed to represent a single, rapid, and continuous depositional context in between two major volcanic episodes (YBT and YBS) at Moche Borago. This interpretation is supported by XRF, mineral magnetic analysis, and radiocarbon results. The XRF and mineral magnetic analysis showed that each of the

[17] The magnetic mineralogy between BWT and YBT differed slightly, but overall test results showed that both layers were dominated by small, stable, single domain ferromagnetic grains.

S-Group layers had slightly varying chemistry, but these deposits were similar overall.[18] The mean R^2 in a Spearman's ρ correlation matrix, which analyzed full XRF spectra of all S-Group samples, was 0.967 (SD = 0.188, $p < .01$). Frequency dependence of magnetic susceptibility (X_{FD}%) also showed a continuity of fine-grained magnetite across the S-Group deposits, which was also unlike the magnetic signature of the underlying YBT tephra (A. Herries per comm.) The dating of the S-Group deposits was also precise. Three radiocarbon samples taken from a ~20 cm vertical span within various S-Group layers provided a tightly constrained weighted mean age of 43,480 ± 443 cal. BP.

Layer descriptions

At the base of the S-Group (and directly overlying tephra YBT) was OBMB, a mottled blend of ash and silty clay. The lateral extent of OBMB is currently being questioned because this layer is well represented in G10 but nearly absent elsewhere in the BXA and completely absent in other excavation areas. The limited extent of OBMB might indicate that it was incised or removed by natural or anthropogenic process.

Micromorphology showed that OBMB is a massive, weakly bedded tuff with lenses of soil aggregates rich in organic matter (P. Goldberg, per comm.). Intersecting OBMB and the underlying tephra YBT was LVDBS, which is loosely consolidated dark brown silt. LVDBS was interpreted originally as a pit feature cut into OBMB and YBT due mainly to micromorphological analysis and a lack of abrasion on the abundant lithic materials found within the stratigraphic unit. Micromorphology seemed to support this interpretation and showed an unsorted heterogeneous mix of charcoal, phytoliths, plant

[18] In contrast, correlations to YBT were elementally very dissimilar from the S-Group, and particularly for Rare Earth Elements (REE). YBT had much larger zirconium counts with moderately larger counts of rubidium, yttrium, niobium, and molybendum. Strontium appeared all but absent in YBT as opposed to S-Group deposits.

tissues, and bone fragments, which suggested colluviation and possible trampling of these deposits (P. Goldberg, per comm.). However, it is equally likely that these processes were more indicative of the sample location (near the top edge of the pit) feature rather than being indicative to the feature itself.

In 2007 and 2008 new evidence suggested we re-look at LVDBS and our original interpretation that it was an anthropogenic pit. The reinterpretation of LVDBS now suggests that it is a fluvial feature, which is consistent with similarly aged fluvial features found across the site. Furthermore, in nearby excavation unit H09, a much more likely anthropogenic pit was excavated in 2008 in equivalent S-Group deposits,[19] and it was very dissimilar to the possible G10 LVDBS pit feature. First, the H09 pit is much smaller than the LVDBS pit, being ~40 cm diameter and 10 cm deep. The LVDBS feature was at least 70 cm wide and more than 30 cm deep. Second, the H09 pit was formed within a relict hearth feature that included an underlying patch of burnt, hardened clay (layer HCLMGV). No underlying discolored or hardened sediment in or around LVDBS was found to suggest it was ever excavated as a hearth. The subsequent fill deposits within the H09 pit (layer LMGV) were loosely consolidated silty-clay sediments with abundant lithics, charcoal, and the highest concentration of heavily burnt, friable bone found in the BXA. Here, we can see some similarity with LVDBS, as indicated by the micromorphology and excavations, that is, an abundance of lithics, charcoal, and bone overall. But much of the bone and lithic materials from H09 were oriented vertically near to 90°, most likely due to repeated excavation and mixing within the feature. This pattern was not seen in LVDBS.

[19] The H09 pit was found in LMGV which underlay LVDBS in H09. The base of the H09 pit was HCLMGV and the next major stratigraphic unit underneath appeared to be OBMB.

LVDBS therefore seemingly represents low-energy channel fill rather than an anthropogenic pit. The H09 feature, on the other hand, is currently believed to represent the use of an *in situ* hearth that was dug out repeatedly and re-used. Further support for the LVDBS fluvial interpretation was found in the stratigraphically equivalent S-Group deposits in TU2 and N42, and clear cut-and-fill activity was associated within the lowest S-Group deposits and the underlying YBT tephra. Furthermore, stone artifacts found in the active stream channel in nearby Esay rockshelter provide a modern analog to the past fluvial features at Moche Borago. At Esay, stone artifacts found in the shallow stream channel were also not rolled because it is a low energy fluvial environment. Therefore, at Moche Borago, abrasion may not be a clear signal for fluvial activity in the BXA.

The overlying VDBS deposits consisted of dark silts with abundant stone tools, bone, and charcoal. VDBS appeared to cap the channel fill, but this conclusion is not yet definitive.

Occupational Hiatus #2

Location: BXA
Stratigraphic Unit: YBS
Age: 43,121 ± 692 cal. BP

The second volcanic event, called YBS, overlay VDBS to cap the S-Group. Charcoal taken from the YBS ash directly dated this deposit to 43,121 ± 692 cal. BP. YBS was a series of yellow-brown (2.5YR5/3), archaeologically sterile, ash layers 10 to 20 cm thick interstratified with darker, thinner lenses.

Compared to other major tephra at Moche Borago, YBS had a unique elemental and magnetic signature. The elemental composition of YBS showed lower iron and Rare Earth Elements (REE) (especially zirconium), except for strontium which is much higher in YBS. Statistical comparisons between full XRF spectra data using Spearman's ρ R^2

values ($p < .01$) showed that YBS and BWT shared only 92% of their ranked variability whereas correlation between YBS and YBT accounted for only 88.6% of the ranked variability. Being less than 97%, these R^2 values suggested that the YBS tephra did not share the same parent material as either BWT or YBT.

Mineral magnetic analysis provided additional information on the depositional history of the YBS tephra. These data showed that YBS contained titanium, which occurred rarely in sampled Moche Borago sediments (the overlying R-Group had slightly elevated titanium abundance, however). The X_{LF} (magnetic susceptibility) values of YBS were higher than other tephra at Moche Borago and similar to the magnetic characteristics of most other clay and silt-based strata at the site. Currently, the only explanation for the titanium within YBS is that this tephra was deposited originally outside of Moche Borago in a titanium-rich environment and then secondarily weathered and transported into the rockshelter (A. Herries per comm.).

R-Group

Location: BXA
Stratigraphic Units: RGCB, RCGA, RCA
Age: ~41 ka

Positioned stratigraphically above YBS was the R-Group, composed of the RGCB, RGCA, and RCA deposits. The R-Group sediments were among the most homogenous found at Moche Borago. Using a Spearman's ρ correlation matrix of full XRF spectra, the mean ranked variability between R-Group deposits was 96.7% ($p < .01$; SD = 0.6).

The R-Group sediments were characteristically red to reddish brown clays and silty clays. The distinct red color of the R-Group sediments suggested a change in the oxidation of the iron within these deposits, perhaps due to sub-aerial exposure as a paleosol. Round to sub-rounded inclusions varied in abundance, but the inclusions were

present throughout the R-Group, as were abundant, unabraded archaeological materials. R-Group sediments shared similar X_{LF} (magnetic susceptibility) and X_{FD}% with the T-Group deposits, which might indicate that these sediments were deposits under similar climatic contexts (A. Herries per comm.).

Currently, the R-Group has 11 radiocarbon ages, which were derived from charcoal in the BXA and TU2. The weighted mean age was 41,159 ± 783 cal. BP. This age accords well with the overall Pleistocene chronology at Moche Borago.

Late and Terminal Pleistocene Unconformity

Location: BXA
Stratigraphic Units: R-Group to BWT
Age: Terminal Pleistocene/OIS 2

Above the uppermost R-Group deposit (RCA) was the tephra BWT, which is described in more detail in the next sub-section (see Occupational Hiatus #3: BXA H-Group). This ash was a marker tephra for GEPCA (GEPCA called it "Tephra 11") and it remained one of the key marker tephras for the SWEAP team. The importance of BWT was its age. Although the GEPCA team recognized that Holocene sediments overlay BWT, they did not date BWT directly. The SWEAP team collected samples of charcoal within BWT from TU2, G9, and H9 for radiocarbon analysis. These samples provided a weighted mean age of 8,051 ± 594 cal. BP that confirmed the early Holocene age of the tephra.

Originally, the R-Group deposits underlying BWT were believed to date to the Terminal Pleistocene. The basis for this hypothesis was a GEPCA radiocarbon sample, dated 28,700 ± 1,100 BP, which was noted in GEPCA's 2000 report (Gutherz et al., 2000a). It is unclear if this age was calibrated and, if so, what radiocarbon calibration curve did GEPCA use. The position of the GEPCA sample shown in Gutherz' (Gutherz

et al., 2000a) profile drawings appeared to be from sediments underlying Tephra 11/BWT (presumably R-Group).

Subsequent radiocarbon analysis by SWEAP since 2006 consistently showed that the R-Group was much older, ~41 ka. The gap in time from the R-Group (~41 ka) to BWT (~8 ka) suggested a major unconformity that effectively spanned the Terminal Pleistocene/OIS 2. Currently, this gap in the sequence is the only known major (i.e. > 10,000 years) unconformity within the Later Pleistocene deposits at Moche Borago. Equivalent strata in TU2 also revealed an unconformity (i.e. TU2 BWT and RGX).

The cause of the unconformity is currently unknown. Volcanic activity and fluvial action are both being considered. Fluvial action may be supported by micromorphology, which shows that RCA (the uppermost R-Group deposit) had a highly porous microstructure with voids filled by oriented and laminated reddish orange clay (P. Goldberg, per comm.). The contact with the overlying BWT tephra was also sharp, but the base of BWT was weathered and iron-stained. Water flowing at the contact between these units may explain the discoloration, but no evidence existed for post-depositional movement of archaeological materials. The 3D plots of archaeological and faunal materials from the R-Group deposits in G09, H09, and I10 revealed fine vertical stratification consistent with continuous, undisturbed deposition of the recognized stratigraphic layers and hearth lenses. The hearths, in particular, were denoted by the absence of lithics. If vertical movement of archaeological materials occurred when the Terminal Pleistocene deposits were eroded, we would not expect vertical spatial patterning. Furthermore, vertical movement might create lag deposits of artifacts, especially at the contact with BWT, or size-sorting, neither of which was evident.

Occupational Hiatus #3/BXA H-Group

Location: BXA
Stratigraphic Units: BWT
Age: Early Holocene

The other hypothesis to explain the Terminal Pleistocene unconformity is volcanic activity, which can also be associated with increased precipitation. So perhaps it is prudent to jointly consider both ideas. The evidence for a major volcanic event, which may have removed the Terminal Pleistocene deposits, was found in the presence of the BWT tephra and the H-Group, which were found in all three excavation areas.

Layer Descriptions

H-Group deposits were found in all current excavation areas. The H-Group was best represented in the BXA by stratified ash, lapilli, and bombes found in the north GG profile of units J/K 11-13 (GG TU3), TU2, and N42 and also BWT. The H-Group was unique for the size of pyroclastic materials and also for the apparent lateral size-sorting within these deposits. In N42, the H-Group was composed mainly of bombe and lapilli clasts, but no clear BWT ash was present. In TU2, larger bombe and lapilli clasts of the H-Group gave way to smaller lapilli and ash, and a clearly defined BWT ash layer was also found. In BXA, lapilli and bombes were infrequent and the BWT ash was thicker.

Currently, we believe that BWT was one event within the large H-Group volcanic series. BWT was always found in association with H-Group deposits (overlying). BWT was a 20 cm thick, dense, homogenous, and archaeologically sterile white ash dating to the early Holocene. BWT was among the clearest marker tephras throughout the site deposits. Tentatively, this tephra has been correlated chemically via XRF to tephra up to 18 km NE of Moche Borago and Mt. Damota.

Stratigraphic Summary of TU2

Approximately 8 m east-southeast of the BXA, TU2 was re-opened by SWEAP in 2006 to observe the stratigraphic profiles described by Gutherz et al. (2001) and integrate these data into the SWEAP database. Aspects of the stratigraphy were reminiscent of both the BXA and N42 areas. In 2007, SWEAP extended the TU2 excavations 1 m to the south to increase the profile length and archaeological sample size from this area. These excavations yielded high densities of lithics within R-Group sediments, as well as additional supporting geomorphic evidence for fluvial channels.

L-Group

Location: TU2
Stratigraphic Units: LFX 1 and 2
Age: >45 kya?

At the base of TU2S (the deepest of the two TU2 units) was LFX1, a lahar deposit composed of numerous sub-angular clasts of ash and other detritus suspended within an orange (7.5YR5/3) homogenous matrix. Above LFX1, LFX2 was marked by larger clasts of ash but retained much of the coloration and composition of LFX1. Both LFX1 and LFX2 were archaeologically sterile. The XRF correlation analysis ($p < .01$) using Spearman's R^2 showed that the TU2 L-Group shared more than 97% of ranked variation with the L-Group deposits identified in N42 (ULF and LLF). The L-Group deposits, however, have not been identified within the BXA.

Both LFX1 and LFX2 had been truncated and, in the case of LFX1, undercut LFX2. The cause of the truncation is believed to be fluvial erosion though detailed analyses are pending. A single radiocarbon date of a thin lens (BGC) between LFX2 and the overlying tephra YBSX dated these L-Group deposits minimally to 44,888 ± 786 cal. BP.

S-Group

Location: TU2
Stratigraphic Units: BGC
Age: ~43 ka

The S-Group was represented in TU2 in only a single, thin lens of clayey sediments (BGC) that contained an abundance of gravel inclusions and abraded lithics. The gravel inclusions were poorly sorted and had rounded to sub-rounded edges. A single charcoal sample collected from BGC provided a radiocarbon age of 44,888 ± 786 cal. BP for this layer. This age was similar to the weighted mean age of the BXA S-Group (43,480 ± 443 cal. BP). The shared post-depositional context made it more likely that the intrusive TU2 L-Group fluvial channel was contemporary with the BXA S-Group fluvial channel (LVDBS).

Occupational Hiatus #2

Location: TU2
Stratigraphic Units: YBSX
Age: 42 to 43 ka

Stratigraphically above LFX2 was tephra YBSX. This thick ash and lapilli lens was in-fill within the TU2 L-Group fluvial channel. Radiocarbon dating of charcoal from the YBSX tephra provided a single date of 42,776 ± 526 cal. BP. Taken together with the BGC radiocarbon age, YBSX likely was deposited sometime between 44,888 ± 786 cal. BP and 42,776 ± 526 cal. BP. This age placed YBSX concurrent to the BXA S-Group and tephra YBS deposits. The XRF analysis supported a correlation between TU2 YBSX and BXA YBS. These layers shard 97.3% ranked variation ($p < .01$). YBSX also shared > 97% ranked variation with BXA LVDBS, and nearly as much with VDBS (96.4%).

R-Group

Location: TU2

Stratigraphic Units: RGX
Age: >Early Holocene to <~40,000

Stratigraphically above YBSX was RGX. RGX had a similar red color and composition to the R-Group found in the BXA. While it is currently correlated into the R-Group, based on composition, dating, and stratigraphic placement, neither XRF nor ICP-MS showed ≥97% statistical correlation between TU2 RGX and BXA R-Group deposits. The mean R^2 value with BXA R-Group deposits (RCA, RGCA, RGCB) indicated only 96% share variation within ranks (SD = 0.9, $p < .01$).

TU2 RGX shared > 97% ranked variability with TU2 YBSX (97.6%), BXA YBS (97.4%) and LVDBS (97.4%), suggesting that it may have derived some of its sedimentology from these underlying deposits. The Rare Earth Elements (REE) and iron counts were also similar between RGX and these layers. Furthermore, RGX was notable for containing high frequencies of heavily abraded lithics. Data also suggested that RGX was deposited via fluvial processes. Unlike the probable low-energy fluvial event seen in the BXA (LVDBS), fluvial processes in RGX may have been more energetic, as evidenced by the abrasion on the lithics. The RGX channel may have also re-deposited lithics from other areas of the site or washed away major portions of the original R-Group sequence of sediments in TU2, leaving only the heavier fractions of the deposit behind.

Occupational Hiatus #3/TU2 H-Group

Location: TU2
Stratigraphic Units: HEP1 and 2
Age: Early Holocene

Stratigraphically above RGX was the TU2 BWT tephra. The XRF R^2 ($p < .01$) analysis indicated that 98.7% of the ranked variability was shared with BXA's BWT, providing one the highest correlations between Moche Borago sediments. Independent

radiocarbon samples were all similar between BXA and TU2 BWT samples, and each of these dates was incorporated into the BWT weighted mean age of 8,051 ± 594 cal BP.

Two layers were stratigraphically above TU2 BWT that were part of the Holocene H-Group volcanic event (HEP1 and HEP2). Both TU2 H-Group layers were composed of ash and lapilli. HEP2 appears to have a higher frequency of lapilli than the overlying HEP1.

Stratigraphic Summary of N42E38

The stratigraphy of the southernmost excavation area is currently defined using the sequence in N42E38, a 1 x 1 m pit ~8 m southeast of TU2 and ~16 m southeast of the BXA. N42E38 was excavated > 2 m below the surface and the majority of deposits appeared to be volcanic (both tephra and lahar). N42E38 was unique because nearly all deposits were archaeologically sterile, except for the most recent and topmost 5 to 10 cm of sediment and a series of silt and clay channel fill deposits, known as the N42 S-Group.

Also, N42E38 was unique for being located on a small rise (~20 cm above the surface of TU2 and BWT) near the rear rockshelter wall. The geology of this area is currently poorly understood. However, the massive volcanic deposits found in N42E38 may have backed up against the rockshelter wall and built up the shelter floor in this area. It is currently not known why these thick deposits are not found in the other excavated areas of the site.

Current Basal Sediments

Location: N42E38
Stratigraphic Units: MPT, SRS, and DRB
Age: Undated

MPT is the current base of the N42E38 sequence. This lens was undated and archaeologically sterile. Above MPT was speckled red sand (SRS) with dark reddish

brown sand (DRB) above it. SRS is reminiscent of similarly speckled red sand found stratigraphically between YBSX and LFX2 in TU2 (TU2 SRS)[20]. XRF analysis showed that N42 SRS and MPT shared > 97% ranked variation ($p < .01$) with TU2 SRS, as well as with the overlying TU2 LFX1 and LFX2 deposits (TU2 L-Group). This correlation may be misleading because the N42 L-Group deposits (LLF and ULF) also shared >97% ranked variation with the TU2 L-Group deposits. Therefore, the N42 basal sediments are currently uncorrelated laterally across the site.

L-Group

Location: N42E38
Stratigraphic Unit: LLF, ULF
Age: Undated

Two distinct lahar features above the N42 basal sediments constituted the N42 L-Group deposits. The L-Group had two subdivisions: lower lahar feature LLF and upper lahar feature ULF. LLF exhibited numerous inclusions of semi-angular ash and lapilli and other detritus up to ~20 cm diameter within a fairly homogenous orange (10YR4/4) clay matrix. ULF was similar to LLF but had more abundant inclusions that were more angular in shape. Both ULF and LLF shared >97% ranked variation ($p < .01$) with the TU2 L-Group (LFX1 and LFX2). While the TU2 L-Group deposits appeared to contain smaller-sized inclusions than those seen within the N42 L-Group deposits, similarities occurred overall in texture, composition, color, and hardness that strongly suggested these deposits derived from the same event. If so, then the radiocarbon sample from the top of TU2 LFX2 provided a minimal date of 44,888±786 cal. BP for the N42 L-Group.

[20] TU2 SRS is a thin, red lens that was found only in isolated areas within TU2S. It did not appear to represent a contiguous stratigraphic layer, and therefore it was not included within the descriptions.

The L-Group deposits between N42 and TU2 were also likely altered post-depositionally by fluvial activity. The top of ULF had been truncated sharply and clasts within ULF were visibly sheared off. The east and west N42 profile walls showed that the truncation occurred on an approximately 30° irregular slope facing the rear cave wall. The north profile walls revealed a shallow (<20 cm) semi-circular depression at the base of the slope. In-filling this shallow depression were the N42 S-Group deposits.

S-Group

Location: N42E38
Stratigraphic Units: COL, LPFC, MPFC, UPFC
Age: Undated. Possibly ~42 to 45 ka, based on correlation

Overlying the L-Group is the lowermost S-Group deposit in N42—a thin lens of manganese-rich sediment, labeled COL. Originally, COL was thought to be organic, and the algal mat at the base of the shallow stream in nearby Esay rockshelter was suggested as a likely analog. However, attempts to radiocarbon date COL showed no organic materials present (Hong Wang, per comm.) and XRF analysis thereafter indicated high amounts of manganese, which could be due to fluvial deposition.

As with the S-Groups in the BXA and TU2, the N42 S-Group was a series of silt and clay channel-fill deposits (layers LPFC, MPFC, UPFC). Each of the layers recorded a different phase of stream activity. We can see a distinct fining upward size-sorting of abraded cobbles between these layers with LPFC containing the highest density and largest cobble size. Infrequent but heavily abraded, archaeological materials were found within these deposits, supporting the fluvial hypothesis on the one hand and, on the other hand, the correlation to other S-Group deposits at Moche Borago. These correlations were further supported by XRF analysis. LPFC, MPFC, and UPFC each shared >97% ranked variation ($p < .01$) with channel-fill LVDBS in the BXA.

Occupational Hiatus #3/N42E38 H* Group

Location: N42E38
Stratigraphic Units: HEP1 and 2
Age: Undated, possibly Early Holocene based on correlation

Stratigraphically above the S-Group were two massive tephras (~1 m total thickness) that constituted the N42 H-Group (HEP1 and HEP2). The N42 H-Group contained abundant bombes within a loosely consolidated lapilli and ash matrix. The larger fraction between the two layers was found within the lower unit (HEP1). HEP2 was less consolidated, and numerous large (5-20 cm) cavities were found between the clasts.

A Working Model of the OIS 3 Depositional History at Moche Borago Rockshelter

Moche Borago was occupied at least 53-51,000 years ago, but occupation also likely occurred earlier since the lowest 20-40 cm of archaeological deposits remain undated. Concurrent ice core records showed that across the Northern Hemisphere, high latitude cold and arid conditions during Heinrich (H) 6 (~60 ka) were followed in rapid succession by Dansgaard-Oeschger (D-O) events 17 (~59 ka), 16 (~58 ka), and 15 (~56 ka) (Grootes et al., 1993; Sowers et al., 1993; Meese et al., 1994; Stuiver and Grootes, 2000; North Greenland Ice Core Project, 2004). The intensity of these D-O events (17-15) was declining sequentially after H6, but the magnitude of annual temperature increases above Greenland was still ~9 to 10ºC above current conditions (Wolff et al., 2010).

As Chapter 2 detailed, the Ethiopian highlands were experiencing wetter conditions concurrent to the D-O events and sapropels of OIS 3, and these conditions may have been influenced by regional monsoonal flux. Paleoclimatic and paleoenvironmental records from the coast of West Africa, North Africa, the Mediterranean Sea, and the circum-

Indian Ocean region all show that pluvial events, including D-O events and sapropels, during OIS 3 are associated with coeval increases in African and SW Asian monsoonal intensity and precipitation (Schulz et al., 1998; Bar-Matthews et al., 2000; Burns et al., 2003; Burns et al., 2004; Weldeab et al., 2007; Revel et al., 2010). The formation of Mediterranean sapropels and the Nile paleohydrology records are linked to increased precipitation in the Nile source region, which is the Ethiopian highlands (Bar-Matthews et al., 2000; Revel et al., 2010).

~60 ka to 45 ka

The T-Group deposits are among the least well understood at Moche Borago, which makes it difficult to do comparisons of these layers to the broader climatic context of the Horn at this time. The basal layer (PKT) is still uncorrelated to other layers and the chronology of the T-Group Lower is only very broadly defined. Also, a ~5,000-year gap exists between the upper error age estimate of the T-Group Lower and the lower age error estimates of the T-Group Upper.

What little contextual information that can be gleaned from the T-Group suggests that this group began during a wet phase and ended during another wet phase. The basal deposits of the T-Group (VHG, in particular) included reworked clay fillings, indicating that these layers were deposited during humid conditions. The T-Group Upper deposits (especially MHD) presented numerous aggregates of fine, iron-rich illuvial clay bands (P. Goldberg, per comm.), showing that these deposits were also laid down in a humid environment.

However, if a strict interpretation of the chronology is adhered to, then the current age for the T-Group Upper is coeval to H5. The dating of the T-Group Upper deposits is substantiated by three radiocarbon samples that show continuity from the T-Group

Upper, into YBT and the S-Group. Therefore, if I were to speculate broadly about the T-Group, I would place the T-Group Upper contemporary to D-O 12 (46.8 ka). The age of D-O 12 is within the statistical margin of error for the current weighted mean age estimates of the T-Group Upper, and correlation to D-O 12 would also explain the evidence that these deposits collected in wetter conditions. I am hesitant to speculate about the chronology of the T-Group Lower at this time because too much uncertainty still surrounds these deposits.

45 ka to 43 ka

After 45 ka, a volcanic eruption laid down the first major OIS 3 tephra found at Moche Borago (YBT). No evidence suggests human occupation at the site during the time of the eruption. The volcano deposited ~20 cm of homogenous ash and lapilli across the site, which would have made the rockshelter uninhabitable for an unknown duration of time. The YBT deposit is characteristic of the pyroclastic volcanic activity found across the western margin of the Main Ethiopian Rift. The majority of volcanoes here share a felsic magma composition that has produced numerous explosive ignimbrite and rhyolite deposits across the region (Di Paola, 1972; WoldeGabriel et al., 1990). The source of the YBT tephra is currently unknown but XRF analysis suggests that YBT shares the same source as the Holocene-aged BWT tephra.

The timing of the YBT tephra is linked closely to the overlying S-Group and tephra YBS deposits. These layers were apparently deposited within one millennium of each other, ~43 ka.[21] At this time (~43 ka), substantial evidence suggests that climatic

[21] YBT is dated to 43,403 ± 1,213 cal. BP. The overlying S-Group deposits are dated 43,480 ± 443 cal. BP. YBS is dated 43,121 ± 692 cal. BP. YBT and YBS do not share a similar source, according to XRF analysis.

conditions around Moche Borago were among the wettest in our OIS 3 record. This evidence is drawn mainly from fluvial geomorphic features found in each excavation area: 1) in the BXA, the S-Group LVDBS channel; 2) in TU2, the S-Group channel that cut into the L-Group; and 3) at N42, the L-Group was truncated with overlying S-Group channel-fill deposits. Between the N42 S-Group and LVDBS in the BXA, these deposits shared >97% ranked variation ($p < .01$), making the S-Group correlation between each excavation area at Moche Borago among the most secure.

In the BXA, LVDBS (S-Group) represented channel-fill deposits that were cut into OBMB and tephra YBT. Sections of YBT were even missing in the BXA, and we currently believe this was cut-and-fill activity from the LVDBS channel. Even clearer evidence exists for fluvial activity in TU2, though the age is less certain. Fluvial activity appears to have truncated and undercut the TU2 L-Group. The age of the fluvial activity here can be limited to the time period 45 to 43 ka. Radiocarbon dating of layer BGC between YBSX (above) and the L-Group (below) dates the fluvial cutting to a maximum of ~45 ka. The minimal age of the channel cutting (~43 ka) can be inferred via stratigraphic correlation between tephra YBSX (TU2) and YBS (BXA). BGC is believed to be remnant S-Group deposits that contained an abundance of heavily abraded lithics, which may indicate increased stream activity, rolling, and fluvial abrasion here (unlike in the BXA).

In N42, the most well-defined channel-fill deposits at Moche Borago (LPFC, MPFC, UPFC) unconformably overlay the undated upper L-Group deposit (ULF). The lowermost fluvial unit, LPFC, contained the highest density and largest cobble size of the group, and we can see a distinct fining upward size-sorting of abraded cobbles.

Infrequent but heavily abraded archaeological materials were also found within these deposits, supporting another instance of high energy fluvial deposition on the one hand and, on the other hand, the correlation to other S-Group deposits.

Therefore, from ~44 ka to ~43 ka, a series of high and low energy fluvial features were present at Moche Borago. The source of the water is likely due to percolation from joints within the rear cave walls, which is similar to the current stream conditions at Esay rockshelter. It is unknown if the channels seen in each excavation area were interconnected from a single source or multiple sources. Based on the morphology of the channel features, it appears that the channels were spatially-limited phenomenon at the site and the energy of the stream flow was lower around the BXA and greatest at N42. It seems highly unlikely that the channels disturbed the entire site and I speculate that the source of the freshwater at this time may have been a major incentive for occupation of the site at this time.

This same time period coincides almost precisely with wetter and warmer climatic conditions that would have occurred during D-O 11 (43.4 ka). The D-O 11 event is evident in both high-latitude ice cores and regional records surrounding the Horn of Africa. Above Greenland, D-O 11 is associated with the greatest increase in mean annual temperatures known during OIS 3, 15°C (Wolff et al., 2010). Across Africa, monsoonal activity may also have increased at this time. West African marine core records indicate that monsoonal precipitation was greater at 43 ka just prior to a dry event at 42.5 ka, though the changes are subtle (S. Weldeab per comm.). The Moomi cave records show a similar, subtle pattern of monsoonal increase ~43 ka (Burns et al., 2003; Burns et al.,

2004). Nile paleohydrology records also indicate a broad period of pluvial conditions at this time, which show wetter conditions in the Ethiopian highlands (Revel et al., 2010).

Conclusions

Fluvial channels are known only in the S-Group deposits at Moche Borago even though other litho-stratigraphic units, such as the T-Group Upper, may be associated with wet climatic conditions. The presence of the channels suggests that the climatic context of the S-Group was significantly wetter than other periods in our OIS 3 records from Moche Borago. The timing of the S-Group in the BXA is among the most precise and accurate of all litho-stratigraphic groups, and this chronology is further supported by the ages for the YBT tephra (below) and YBS tephra (above). Regional and local evidence for monsoonal intensity increase is not as robust for D-O 11 as it is for other millennial-scale events. However, based on the available facts, I am confident that the S-Group deposits show localized evidence for increased monsoonal activity due to D-O 11.

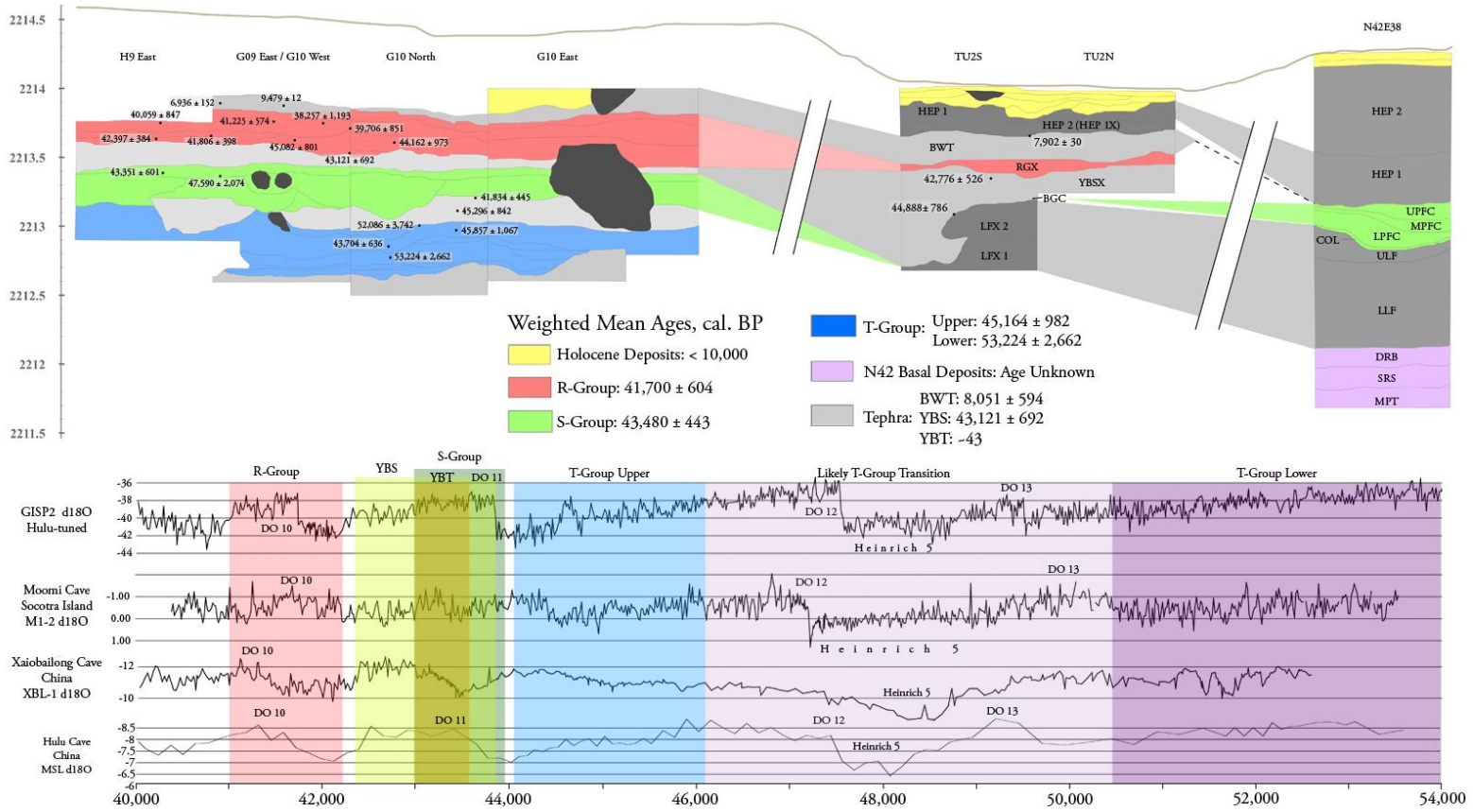

Figure 6-1: This composite image shows the stratigraphic profiles from the BXA (left), TU2 (center) and N42 (right) excavation areas. Selected calibrated radiocarbon ages are placed in their approximate 2D position along the profile walls. Selected climatic curves are represented at the bottom for comparison to the Moche Borago chronology (Sowers et al., 1993; Grootes et al., 1993; Meese et al., 1994; Stuiver and Grootes, 2000; Wang et al., 2001; Burns et al., 2003; Burns et al., 2004; Cai et al., 2006)

Table 6-1: The AMS Radiocarbon Assay from Moche Borago

Bag Number	Sample #	XU	Strat Unit	Level	d31C	pMC	±	D14C		14C age	±	Cologne CalPal, BP	±
		N42E											
4711	SWAP07-01	36	HEP	9	-25.5	0.9835	0.0014	-16.5	1.4	135	15	133	101
2575	SWAP07-02	G9	RCA	2	-23.7	0.3497	0.0007	-650.3	0.7	8440	20	9479	12
2200	SWAP07-03	H9	RCA	15	-23.7	0.0128	0.0004	-987.2	0.4	35010	270	40059	847
2290	SWAP07-04	TU2S	OST	6	-25.1	0.4156	0.0008	-584.4	0.8	7055	20	7902	30
2596	SWAP07-05	H9	RCA	18	-23.3	0.0089	0.0004	-991.1	0.4	37930	370	42397	384
3334	SWAP07-06	H9	RGCA	19	-22.9	0.0057	0.0004	-994.3	0.4	41580	590	45082	801
4039	SWAP07-07	H9	VDBS	26	-28.9	0.0076	0.0004	-992.4	0.4	39200	440	43351	601
2261	SWAP07-08	TU2S	YBSX/ BWT	11	-24	0.0085	0.0004	-991.5	0.4	38320	390	42776	526
2105	SWAP07-09	G10	YBT	17	-26.8	0.0055	0.0004	-994.5	0.4	41830	600	45296	842
2206	SWAP07-10	TU2S	BGC	16	-26.9	0.0058	0.0004	-994.2	0.4	41370	570	44888	786
2117	SWAP07-11	G10	DCC	19	-23.7	0.0051	0.0004	-994.9	0.4	42400	650	45857	1067
3112	SWAP07-12	G10	DCC	23	-22.2	0.0069	0.0004	-993.1	0.4	39920	480	43704	636
3123	SWAP07-13	G10	CTT	25	-24.2	0.0023	0.0004	-997.7	0.4	48850	1420	53224	2662
3135	SWAP08-1	G10	DCC	24	-24.3	0.0374	0.0008	-962.6	0.8	26400	180	31198	360
2109	SWAP08-2	G10	YBT	18	-23.3	0.0026	0.0008	-997.4	0.8	47700	2500	52086	3742
2037	SWAP08-3	G10	YBT	17		0.01	0.0008	-990	0.8	36960	650	41834	445
4002	SWAP08-4	H9	VDBS	26	-23.9	0.0042	0.0008	-995.8	0.8	44000	1600	47590	2074
3346	SWAP08-5	H9	RGCA	19	-25.2	0.0065	0.0008	-993.5	0.8	40500	1000	44162	973
2141	SWAP08-7	H9	RCA	15	-24.8	0.0111	0.0008	-988.9	0.8	36120	590	41225	574
2237	SWAP08-8	H9	RCA	15	-22.2	0.0157	0.0008	-984.3	0.8	33370	420	38257	1193
2248	SWEAP 08-9	G10	YBS		-25.1	0.008	0.0007	-992	0.7	38750	680	43121	692
3834	SWEAP 08-10	G9	RCA		-23.6	0.0139	0.0007	-986.1	0.7	34360	400	39706	851
3424	SWEAP 08-11	G9	RCA		-21.1	0.0097	0.0007	-990.3	0.7	37200	560	41956	419
2804	SWEAP 08-12	H9	RCA		-25.5	0.0101	0.0007	-989.9	0.7	36900	540	41806	398
7241	SWAP09-2	I10	YBT		-21.9	0.0509	0.0006	-949.1	0.6	23920	90	26831	383
7242	SWEAP 09-1	I10	YBT		-26.7	0.0094	0.0005	-990.6	0.5	37480	470	40158	396

CHAPTER 7
DESCRIPTIVE AND STATISTICAL ANALYSES OF THE T-GROUP AND S-GROUP ASSEMBLAGES AT MOCHE BORAGO: RAW MATERIALS, CORES, AND LITHIC DEBITAGE

Chapters 7 and 8 focus upon the analyses of flaked stone artifacts recovered from the early OIS 3 deposits of excavation unit G10 in the main Block Excavation Area (BXA). As previously discussed in Chapter 5, G10 provides a link to prior GEPCA excavations, as half of this $1m^2$ unit formed the 1998 sondage that first exposed Moche Borago's Late Pleistocene deposits.

My analytical sample comes from the remaining 50 cm^2 section of G10, excavated during the 2006-2008 field seasons. Although this unit represents only one of five $1m^2$ excavation units into Late Pleistocene deposits so far excavated at Moche Borago, G10 is the site's deepest archaeological unit as well as its lithological type section, as every major Late Pleistocene litho-stratigraphic unit is exposed in its profiles.

The G10 "lithics"[22] that form my analytical sample come from the T Group deposits, further subdivided into T-Group Lower and T-Group Upper, and the S-Group deposits stratified below the YBS tephra dated to ~43ka. Artifacts found in the later OIS 3 strata above YBS, the R-Group, were not included in this dissertation (except for a small sample of points discussed in Chapter 8), as they were originally thought to be of OIS 2 (Terminal Pleistocene) age.

[22] I use the term "lithics" interchangeably with "flaked stone artifacts", both of which exclude ground stone artifacts.

General Description of the Assemblages

This chapter follows a general lithic reduction sequence, in that I begin with a discussion of hammerstone percusors, followed by raw materials and nodules, cores and debitage.

The flaked stone artifact assemblages from the T-Group and S-Group contain 2,913 total pieces (Table 7-1). The highest frequency of lithics are found in the T-Group (n=2351), with T-Group Lower (n = 1,061) and T-Group Upper (n = 1,290) each having similar lithic counts. The S-Group (n = 555) has ~75% fewer lithics than the T-Group. Only five stone artifacts were found in the YBS tephra and two in the YBT tephra, all of which were recovered near the boundaries of the tephra units and are probably intrusive. Therefore, we consider the YBS and YBT tephras archaeologically sterile, and these artifacts have been removed from this analysis.

Minimum Number of Lithics

Faunal specialists have long recognized that the actual minimum number of individual (MNI) specimens represented within a dataset may differ from the actual total number of bone fragments at hand (White, 1953a; White, 1953b). These differences accrue because multiple, non-diagnostic bone fragments can originate from the same bone.

Lithic assemblages also undergo taphonomic processes similar to faunal assemblages, which can produce a fragmented assemblage. On the one hand, the fragmentation might occur at the time the assemblage is accrued. The knapper may not have had enough skill to control the flaking process properly, which could have resulted in more fragmentary pieces. Raw material could also be a factor. Quartzite, for instance, often shatters during flaking. On the other hand, the post-depositional process can also

fragment a stone artifact assemblage. If stone artifacts are exposed on the surface, then an increased likelihood occurs that these pieces might be walked upon by humans and/or animals, swept up and re-deposited by the occupants, or affected by fluvial or aeolian processes. In any one of these situations, lithic fragments, such as medial and lateral pieces, can be derived from a single artifact if it is broken. Therefore, such fragments can artificially drive up the total counts if each fragment is counted independently—a single fractured flake, shaped tool, or unshaped tool can produce a proximal and dorsal fragment, as well as multiple medial and lateral fragments.

The total lithic counts may therefore exaggerate (as in the case of shaped and unshaped tools and cores) or underestimate (as in the case of whole flakes) the true character of an assemblage. Adapting the faunal-based MNI approach to lithic analysis may be one way to more accurately count and analyze a lithic assemblage. Consequently, I introduce for this analysis the term "Minimum Number of Lithics" (MNL), which refers only to whole stone artifacts, conjoined artifacts and proximal flake fragments. Medial, distal, and lateral flake fragments and angular waste are therefore omitted from total lithic counts when using MNL.

Therefore, when only the MNL is used, the stone artifact count lowers to 1,715 total pieces (Table 7-2). The disparities in the total counts between stratigraphic groups are also equalized. The S-Group has 532 lithics, the T-Group Upper has 650 lithics, and the T-Group Lower has 526 lithics, which has important implications for understanding various artifact classes that are discussed in this chapter and the next chapter.

Hammerstones and Raw Material Nodules

To date, only one possible hammerstone fragment has been found in G10. This artifact (Bag Number (BN) 3115) (Figure 7-1) came from Level 23 (stratigraphic unit

DCC of the T-Group Upper) and it is made of basalt. A cavity within the nodule may be the reason that the stone broke in half. Table 7-3 provides the dimensions and weights for this possible artifact and the lithic raw material nodules that are described in the next section.

Only 15 possible raw material nodules came from G10, which are nearly, or fully, cortical. The small number of possible raw material nodules constitutes less than 1% of the cumulative (MNL) S-Group and T-Group lithic assemblage. However, it is doubtful that these 15 pieces can truly be called "raw material nodules." Most of these artifacts appear to be heavily aerated obsidian that have numerous cracks and irregularities, which would make these pieces unsuitable for knapping. Only one piece, a chalcedony nodule (BN 3105, Level 23) is not obsidian. Furthermore, they are small (Table 7-3) and the average weight is only ~1.22 grams each (SD = 1.48 g). Therefore, these pieces could have been collected with other raw materials, but deemed unsatisfactory and discarded with no intention of ever being used. Or they could also represent "manuports" (Leakey, 1971), natural stone pieces that were not collected for raw material but for some other purpose

Raw Materials

Five broad classes of raw materials were found in the G10 assemblage: obsidian, chert, quartzite, roof spall[23], and basalt. The most common raw material is obsidian, especially a homogenous jet black variety referred to here as "Common Black Obsidian" (CBO). Two sources of obsidian are found within 20 km of the site. S. Brandt and I visited these sites in 2007 and 2010. Preliminary results from an XRF analysis of the

[23] Naturally spalled rock from the rockshelter walls.

obsidian from these sites[24] show strong similarities to CBO at Moche Borago. The elemental spectra of the CBO show characteristics of very low strontium, with higher counts of other rare earth elements, elevated zinc, and high counts of both iron and zirconium (Figure 7-2). In lieu of a complete chemical analysis of all obsidian found at Moche Borago, I use CBO here to refer only to similarities in the external color (jet black) and appearance (homogenous) of the obsidian pieces. Obsidian source work is ongoing.

Within the G10 S-Group and T-Group assemblage, 90.5% of the obsidian found is CBO (n = 1,561). Gray obsidian represents 5.7% (n = 98) of the S-Group and T-Group assemblages, and both green and brown obsidian varieties constitute just over 0.5% combined (n = 10). Twenty artifacts were made from roof spall and 19 artifacts were made of basalt, which amounts to 2.3% of the entire dataset. Sixteen artifacts were made from multi-colored varieties of chert and chalcedony, which represent 0.9% of the entire assemblage. Only a single artifact was made of quartzite (core trimming flake BN 1794.21, Level 11 from the S-Group deposits).

Obsidian artifacts occur in all occupation layers within the deposits, but the non-obsidian raw materials have a much more limited distribution. Table 7-4 summarizes the MNL distribution of each raw material class within the major stratigraphic groups. Table 7-5 also provides MNL-based raw counts of each raw material type per excavation level.

These tables show that the entire assemblage of stone artifacts made from basalt and roof spall occur within the combined T-Group Lower and T-Group Upper deposits (n = 19 and n = 20, respectively). A similar distribution exists for the category of chert, and

[24] This analysis was conducted in the spring of 2010 using a Tracer III-V portable XRF. Final results of this analysis are pending.

93.0% of the chert assemblage is also found in the T-Group (n = 14). In fact, the only raw materials not represented in the T-Group Lower are quartzite and chalcedony, whereas multiple raw material types are absent from the T-Group Upper (Table 7-6).

Several explanations might account for the greater diversity of non-CBO artifacts in the T-Group Lower. The first, and perhaps the most obvious, explanation is that these patterns are simply the result of sampling bias. This assemblage is taken only from a single 50 cm^2 excavation unit. In adjacent areas at Moche Borago, the distribution of raw material types may be entirely different, owing to spatially distinct behavior patterns of the people who previously occupied this site. Further excavation and analysis should help to clarify these issues.

A second explanation for the greater diversity of non-CBO artifacts in the T-Group Lower is that these raw material patterns are evidence (although from a relatively limited sample size) for behavioral differences of the occupants of the rockshelter between the S-Group and T-Group. Specific raw materials may have been preferentially used for certain tool types. On the one hand, the earliest microlithic tools in East Africa are hypothesized to be related to an uptake in fine-grained raw material use (Ambrose, 2002). This pattern is even seen in Ethiopia at Porc Epic rockshelter. At Porc Epic, obsidian constitutes only 8.0% of the total assemblage, yet the majority of microliths, including 50% of all backed pieces, are made from this particular raw material. The nearest obsidian sources to Porc Epic are about 100 km from the site, which shows a clear preference to make these tools with obsidian (Pleurdeau, 2001).

On the other hand, little evidence is available from Moche Borago to suggest that non-CBO was used preferentially to make shaped and unshaped tools or cores. The

sample size of non-CBO is very small and the total count of minimal number of lithics (MNL) of non-CBO lithics within each of the three main stratigraphic aggregates never exceeds 10 pieces (T-Group Lower). Only 15 non-CBO (MNL) lithics were found in the S-Group, and nearly all these are debitage (Figure 7-3, 7-4, 7-5).

The relative percentages of non-CBO per artifact class within litho-stratigraphic groups are also small. In the case of the S-Group, the relative percentage of non-CBO artifacts is never above 1% per lithic group (e.g. shaped tools, unshaped tools, and cores). Therefore, if non-CBO was preferred for any lithic activity, then frequencies and percentages of non-CBO within the assemblage should be greater[25], but this pattern is not seen in the current dataset.

The distribution of CBO and non-CBO between shaped tools, unshaped tools, and cores is also similar in both the T-Group Upper and Lower (r^2 = 0.84 and 0.95, respectively, $p < .05$). The same distribution pattern is true for debitage. Regression analysis shows that the percentages of debitage (including flake fragments) made from CBO or non-CBO within each litho-stratigraphic group are similar (r^2 = S-Group: 0.98, T-Group Upper: 0.92, and T-Group Lower: 0.94, $p < .05$). If non-CBO was being used differently than CBO, differences should be evident in the number of artifacts made from either group of raw materials. What these distribution patterns suggest instead is that both raw material groups were being used for a variety of purposes, each with similar waste patterns.

The broader implications of these findings will be discussed in more detail at the end of this chapter and in Chapter 9. It is important to point out that the similarities

[25] Unless spatially distinct activity areas occur at the site, which is highly likely.

between the use of CBO and non-CBO raw materials likely refer to both social and technological reasons. On the one hand, if the development of microlithic tools during this period is linked to the availability and use of fine-grained raw materials, then the ready availability of CBO around Moche Borago may have meant little technological need to acquire other kinds of non-local, fine-grained raw materials. On the other hand, because the majority of non-CBO was found only on debitage (and still in small amounts), non-CBO tools may have been curated more thoroughly for non-technological, perhaps social, reasons.

In conclusion, four main points can be made about raw materials and raw material use in the G10 stone artifact assemblage. First, five different kinds of raw materials occur, but obsidian is far and away the most common. Second, the most frequent kind of obsidian is a homogenous jet black "CBO" variety. Third, CBO likely comes from a local source in the Sodo-Wolayta area. Fourth, the stone artifacts from the T-Group, especially T-Group Lower, are made on more types of raw materials than the S-Group, although this is still a very small percentage. However, no evidence shows that certain raw materials were preferentially used to make specific kinds of shaped and unshaped tools or cores.

Cores

The core sample is not very robust, with only 94 pieces. Single platform cores are most common in each litho-stratigraphic unit. Multiple platform cores are next most common and there are less than ten radial cores, including 3 Levallois cores, in the assemblages (Table 7-8). Nevertheless, the limited sample of cores provides interesting insights into the lithic reduction strategies employed at the site during early OIS 3. Two core characteristics stand out above all others: size and diversity.

Core Size

Small cores are not uncommon from Late Pleistocene sites in eastern Africa. Merrick (1975) found that mean core lengths from 14 "late MSA" and "early LSA" sites in Kenya and Tanzania were between only 3.4 cm and 1.5 cm (see Merrick's Figure 12:1, 400). By comparison, the average length[26] of all cores at Moche Borago is 2.3 cm (SD = 0.9 cm).

The largest cores at Moche Borago are flaked radially. Radial cores include the Levallois flaking method, discoids, and other miscellaneous radial core types. The mean volume for radial cores is 57.5 cm^3 (SD = 86.4) (Table 7-7).[27] Levallois radial cores, however, are generally small, with an average volume of 5 cm^3.

Single platform and multiple platform cores are also small. Single platform cores have a mean volume of 7.4 cm^3, whereas multiple platform cores have a mean volume of 5.1 cm^3.[28]

Several possible reasons arise why the cores, in general, at Moche Borago are small, including distance to raw material sources, size of original raw materials, and intensity of use. Distance to source materials is not expected to be a major factor in this area. Major obsidian sources are located within 20 km of Moche Borago, and they can be reached within a single day. It is also likely that other obsidian sources existed in the

[26] Dimensions of cores are notoriously difficult, hence the use of volumetric measures here. However, the core "length" measure is typically the distance perpendicular to the primary striking platform. In cases of multiple striking platforms, then the "length" is the longest distance of the piece.

[27] While still larger, these mean values for radial cores are skewed by a single large radial core in the T-Group Lower.

[28] These values are similar to a 1.7 cm equilateral cube. It is important to note here that the volumetric calculations suggest that all sides of the core are equilateral when in fact one or two sides may be significantly larger than the third side, depending on the type of core.

area due to volcanic activity in the region, but these sources are currently unknown to our research team.

The size of the raw materials is also not a primary factor regulating the size of the Moche Borago cores. In 2007 and 2010, S. Brandt and I observed that the local obsidian sources are broad, deep veins (often in excess of 20-30 cm wide), located over a broad geographic area. Primary core reduction flakes and large cores are in abundance at these sites. Therefore, it seems likely that raw materials were available locally to accommodate bigger cores, but the cores were probably reduced intentionally before they were transported to Moche Borago, or large nodules were broken into smaller ones at the quarry (or less likely at the site given the small size of site nodules).

It is also worth noting that the cores (and most other kinds of stone artifacts) most likely represent pieces that were discarded after being used, that is, the small sizes are an artifact of use and not inherent to the original artifact itself. Many of the cores at Moche Borago have hinge or step fractures (for example, see Figure 7-6), which indicates that these pieces were used extensively, developed defects or became too small, and were discarded.

The average volume of radial cores decreases by 51% from the T-Group Lower (M = 9.3 cm^3, SD = 3.7 cm^3) to the S-Group (M = 4.5 cm^3, SD = 2.9 cm^3). Therefore, decrease in core volume may indicate a general diachronic shift toward smaller cores and, by proxy, smaller shaped and unshaped tools and debitage.

Diversity of Single and Multiple Platform Cores

Merrick (1975), however, found little change in size between the late MSA and early LSA cores in Kenya and Tanzania. However, Merrick (1975: 396-398) pointed out

other qualitative core characteristics of the East Africa early LSA (i.e. Mode 4/5 technology) that include four points:

1. infrequent radial (discoidal, Levallois, and radial) cores
2. ≤ 11% prismatic and pyramidal core types
3. predominance (60-75%) of "non-regular" single platform and multiple platform cores
4. predominance of blade-flake removals on all core types

The core characteristics that Merrick (1975) identified with the early LSA are similar to those characteristics in the Moche Borago assemblage. Here, I will compare the Moche Borago core assemblage to Merrick's four points and note any dissimilarity with my findings.

Single platform cores

A shift in the design of cores emerges from the T-Group to the S-Group. The change is toward an emphasis on the production of single platform cores in lieu of other core types. In the T-Group Lower, single platform cores are most common (58.8%, n = 10), but relatively high percentages of radial cores (17.7%, n = 3) and multiple platform cores (23.5%, n = 4) (Table 7-8) still occur. In the T-Group Upper, the assemblage is composed almost uniformly of single platform cores (75%, n = 9). Only one radial core (8.3%) and two multiple platform cores in the T-Group Upper (16.7%) materialize.

Single platform cores represent 58.5% (n = 38) of the S-Group core types. These cores are made from a variety of core blank types, including flakes and cobbles. Concurrent increases in the frequency and diversity of multiple platform cores (17%, n = 11) also arise. Only four radial cores have been found in the S-Group, representing 6.2%. Therefore, from the T-Group to the S-Group more single platform cores appear in the

assemblage and multiple platform cores also become more common. In contrast, radial cores maintain consistent low frequencies throughout the assemblage.

Pyramidal and prismatic cores

Merrick (1975) found that formal pyramidal and prismatic cores types are less common in the early LSA than less formal single and multiple platform cores. A similar pattern exists at Moche Borago. Only four pyramidal/prismatic cores in the entire Moche Borago assemblage were found. In contrast, 52 single platform cores within the total assemblage (Table 7-8) appeared. In addition to the radial cores, the small numbers of pyramidal and prismatic cores suggests that core production at Moche Borago followed the more relaxed and informal designs common to single and multiple platform cores.

Core flake type

More frequently, early LSA cores have blade-flake removals, according to Merrick (1975). A similar pattern is again found at Moche Borago. The incidence of single platform cores with non-elongate flake removals is consistently high in the total assemblage (65%, n = 34). However, when flake removal type is analyzed across litho-stratigraphic groups, a statistically significant inverse correlation is evident between the increase of blade-flake removals and the decrease of ovate flake removals from the T-Group Lower to the S-Group ($r = -0.979$, sig(1-tailed) = .066) (Table 7-9). This inverse relationship would suggest a subtle shift from non-elongate flake removals to more elongate flake removals from the T-Group to the S-Group.

In summary, the qualitative and quantitative characteristics of the Moche Borago cores closely parallel Merrick's (1975) definition of early LSA cores, which are seen here to represent Mode 4/5 core technology. The main characteristics of a Mode 4/5 core assemblage, as found at Moche Borago, include:

1. Decreasing amounts of radial cores. The percentage of radial cores decreases across each litho-stratigraphic unit at Moche Borago.

2. Increased abundance of single platform cores. The S-Group is composed of (non-regularly patterned) more single-platform cores (58%).

3. Few formal cores designs, like radial, pyramidal, or prismatic cores. Pyramidal/prismatic cores constitute less than 10% in the entire Moche Borago core assemblage.

4. More abundant blade-flake removals from cores. The incidence of elongate flake scar removals on single and multiple platform cores increases in the S-Group.

These findings suggest that the S-Group assemblage, at least, is comparable to the early LSA or, more precisely, to Mode 4/5 technologies. In particular, increasing diversity is apparent in single and multiple platform core types from the T-Group to the S-Group. One explanation for this pattern is experimentation within the technological system at this time. The presence of Levallois and other radial core types throughout each of the three litho-stratigraphic groups suggests that the knowledge base underlying technologies during this time accessed both the prior Mode 3 technology and the newer Mode 4/5 technology. The development of new technological knowledge at this time therefore might include increased experimentation and non-fixation on standardized core morphologies, which may explain the high numbers of informal single and multiple platform cores. One way to test this hypothesis would be to look toward the R-Group, which overlies the S-Group and note the most common cores and the diversity of that assemblage.

Debitage

Two broad categories of debitage are described here. The first category of debitage consists of functional debitage types, such as core trimming flakes and burin spalls. These kinds of debitage often indicate specialized reduction activities. An abundance of

core trimming flakes, for example, might suggest a great deal of *in situ* core preparation and reduction at a site. Burin spalls denote the manufacture of burin tools, which may have been used for engraving/grooving of wood, bone, or antler. Other types of functional debitage include bifacial thinning flakes, but these are not represented within the current dataset.

The second category of debitage is non-functional. Non-functional flakes include whole, proximal, medial, distal, and lateral flake fragments, and angular waste. These lithics most often represent the condition of the assemblage, including whether or not the assemblage is biased due to post-depositional processes or human behavior. For example, fluvial activity can bias an assemblage by preferentially removing smaller debitage from the assemblage, whereas trampling can fracture whole flakes within an assemblage.

The relationship between functional debitage types (i.e. core trimming flakes and burin spalls) and non-functional debitage types (whole flakes and flake fragments) is one-sided in the current dataset. Throughout each litho-stratigraphic unit, non-functional debitage predominates. The functional debitage never occurs higher than 10% within any litho-stratigraphic unit. Also, no clear relationship exists between functional debitage and any other lithic type, such as cores or shaped tools. Linear regression shows no statistical relationship between the mean size of core trimming flakes in each excavation level (overall, the mean length of CTF is ~3.0 cm, SD = 1.24 cm) compared with mean volumetric dimensions of the cores found in the same levels ($r^2 = 0.006$, $p < .05$). This result indicates that the core trimming flakes were removed when the cores were larger and not at the end of their use life-cycle when the cores were smaller and discarded.

Both types of debitage (including non-MNL fragments) represent 83.4% (n = 2,423) of the combined S-Group and T-Group assemblage, making debitage the predominant lithic category. The T-Group Lower had 1,003 pieces of debitage (including non-MNL), amounting to ~94.5% of that assemblage (Table 7-10). The T-Group Upper had a slightly higher total count of debitage (n = 1,212, non-MNL), but the relative percentage of debitage is similar to the T-Group Lower (~94%), owing to more shaped and unshaped tools. Only 208 pieces of debitage were found in the S-Group, however, and this number amounted to only 37.5% of that assemblage.

Nearly three-fourths of the S-Group MNL debitage is comprised of whole flakes (74%, n = 154). This peculiar debitage pattern suggests taphonomic, activity-related, or even technological reasons, which may have influenced this assemblage. Taphonomic explanations, such as the fluvial actions known in the S-Group, seem unlikely. Fluvial actions are mass-oriented, hence smaller shaped and unshaped tools, debitage, and cores alike would all be removed. Numerous smaller shaped and unshaped tools and cores in the S-Group and the volumes of these pieces are, on average, smaller per excavation level in the S-Group than in the T-Group (Table 7-11). Furthermore, few of the artifacts are abraded in the S-Group (and T-Group). These results suggest that the S-Group debitage is not only *in situ* (a finding corroborated by the micromorphology and other litho-stratigraphic research), but no size-sorting of the assemblage has accounted for the predominance of whole flakes in the S-Group.

Comparisons between the number of fragmentary debitage found in the T-Group and S-Group suggest as much about the process affecting the T-Group as they do about the S-Group. One interpretation for the greater number of fragmentary debitage in the T-

Group may be due to these pieces being exposed on the surface longer and to the effects of foot traffic and trampling. The T-Group deposits are only slightly thicker in G10 compared to the S-Group deposits. Yet, the T-Group may span as much as 10,000 years (i.e. from ~60 ka - ~45 ka), whereas the S-Group deposits were deposited within ~3,000 years (from ~41 ka - ~44 ka if the minimum and maximum age errors are considered). Therefore, more fragmentary debitage in the T-Group was found because these stone artifacts were exposed on the surface longer.

Behavioral changes may also explain the differences between the T-Group and S-Group debitage patterns if different activities were conducted at the site or if the way certain activities were conducted. Raw material changes were not a likely factor, however, because only 15 non-CBO pieces were found within the S-Group MNL assemblage, which included multiple lithic types. The relatively sparse non-CBO pieces, as well as the diverse array of lithic types that these pieces represent, suggest no specialized raw material use in the S-Group that might indicate coincident changes in the way tools were being made or the way certain kinds of materials were used.

What then is the cause for the peculiar debitage patterns between the T-Group and S-Group? This period (early to mid OIS 3) is associated with the development and systematic adoption of Mode 4/5 microlithic and blade-based technologies across Africa. We therefore should expect to find changes in flake size and elongation that might relate to the development of Mode 4/5 stone tool technologies.

Mode 4/5 technology seems to be well represented in each litho-stratigraphic group at Moche Borago via diagnostic shaped tools such as microliths (see Chapter 8) and characteristics of the cores. The debitage also appears bladey overall and small. The

average length of all whole flakes is 1.6 cm (SD = 0.9 cm), and a subtle decrease occurs in the mean lengths of whole flakes across each litho-stratigraphic group (Figure 7-7).

However, the mean aspect ratios (length/width) of the whole flakes, which indicate elongation, remain largely unchanged across each excavation level (Figure 7-8). Furthermore, the weighted mean of the average aspect ratios per excavation level is only 1.24 (SE = 0.13), which would suggest a much more ovate whole flake planform and not an elongate, bladey planform. The unchanging aspect ratios belie the bladey appearance of the assemblage, as well as the subtle changes in whole flake length. Therefore, little actual information may be gleaned from the Moche Borago whole flake data about Mode 4/5 technology in the T-Group and S-Group if the trend is toward smaller and more elongate flakes. Perhaps because of the commonplace fine-grained raw materials (CBO), the stone artifacts were already being made small and more elongate with little reason to change at this time.

Furthermore, looking at flake length or aspect ratio might define the problem too narrowly. Other likely behavioral changes evident in the stone artifact assemblage might relate to the predominance of debitage in the T-Group and whole flakes in the S-Group. For example, while proportionally more debitage emerges in the T-Group (~94%, n = 1,040), more shaped tools, unshaped tools, and cores in the S-Group occur (~65%, n = 347) (Figure 7-9). In fact, 208% more shaped and unshaped tools materialize in the S-Group than in the T-Group (Figure 7-10 and Table 7-12).[29] In the S-Group, 60% (n = 128) of the shaped and unshaped tools are also made on end-struck whole flakes. Less than 5% of these pieces are made on either proximal, medial, or distal flake fragments

[29] Microliths increase 650%, burins 75%, points 111%, scrapers 235%, and unshaped tools 331% (see Chapter 8).

(combined, these categories amount to 13.7%) (Table 7-13). Therefore, when viewed within a broader context, the debitage patterns in the S-Group might relate to the manufacturing process of shaped and unshaped tools. Furthermore, a low, but statistically significant, relationship exists between whole flake striking platform type and aspect ratios ($r = .156$, p (one-tailed) $< .05$). Flakes with pointed, striking platforms also have the most elongate dimensions, suggesting that the production of whole flakes in the S-Group was systematic with a set standard of manufacture.

However, the average lengths of whole flakes in the S-Group are 50% smaller than the average lengths of shaped and unshaped tools ($M = 2.4$ cm, $SD = 0.85$ cm) (Figure 7-5). The average aspect ratios of whole flakes ($M = 1.4$, $SD = 0.8$) are also less than shaped and unshaped tools ($M = 1.6$, $SD = 0.6$), indicating the flakes are slightly more ovate than the shaped and unshaped tools. The discrepancies between the sizes and shapes of the whole flakes and shaped and unshaped tools may imply no relationship between these lithic types. Alternatively, the discrepancy may suggest that the whole unmodified flakes were rejected for various reasons, perhaps for being too small. I find it altogether unlikely that there is no relationship between the predominance of whole flakes in the S-Group and the concurrent increase in shaped and unshaped tools. However, based on the current dataset, only circumstantial morphological and metrical data connect these lithic types. The predominance of whole flakes suggests an intensified focus on the production of these lithics in the S-Group. Also, the predominance of whole flakes does not represent a biased sample due to actions such as fluvial processes. The frequent use of prepared, especially pointed, striking platforms also shows that the manufacture of these flakes was predetermined. Although the sizes and dimensions of

the whole flakes do not match the shaped and unshaped tools, these flakes may have been the rejects of the manufacturing process because they were, in fact, too small or not elongate enough at the outset.

Conclusions

The Moche Borago core and debitage samples show diachronic trends from the T-Group Lower to the S-Group, including the increased diversity of core types in the S-Group and a general trend toward the production of more elongate flakes. Raw material, not surprisingly, does not seem to be a big factor. CBO predominates across all levels. Only in the lowest litho-stratigraphic group (T-Group Lower) do more kinds and greater numbers of non-CBO raw materials occur, albeit in still very small percentages.

The diachronic technological patterns seen within the Moche Borago lithic assemblage also appears to parallel patterns, which are found in other assemblage across East Africa and the Horn of Africa (i.e. Porc Epic and Kenyan late MSA/early LSA sites) (Merrick, 1975; Pleurdeau, 2001). These patterns include increasing percentages of non-patterned single platform cores and decreasing percentages of radial cores.

The use of Mode 4/5 technologies at Moche Borago also does not appear to coincide with a shift in raw material use, which is seen in other sites in the region. The highest diversity and frequency of non-CBO raw materials are found within the oldest litho-stratigraphic group at the site. Perhaps hunter-gatherers living within and around Moche Borago at this time just did not need to expend effort procuring fine-grained raw materials from distant sources because they had abundant obsidian nearby. If this hypothesis is substantiated, then it may provide operational limitations on the use of raw material-based models for the development of Mode 4/5 microlith technologies at Moche Borago and the surrounding region.

Table 7-1: Summary of the major lithic groups by excavation level and stratigraphic group.

Stratigraphic Group	Level	Shaped Tools	Unshaped Tools	Cores	Debitage	Nodules	Total
	11	33	23	13	6	1	76
	12	14	16	9	6	1	46
	13	63	53	22	33	0	171
S-Group	14	37	28	11	59	0	135
	15	2	1	7	35	0	45
	16	5	5	3	69	0	82
	Total	154	126	65	208	2	555
	18	7	1	0	222	5	235
	19	7	2	1	80	0	90
	20	0	0	0	8	0	8
T-Group Upper	21	1	1	2	162	2	168
	22	7	2	2	227	1	239
	23	10	6	4	350	7	377
	24	5	3	2	163	0	173
	Total	37	15	11	1212	15	1290
	25	5	2	1	178	1	187
	26	0	0	1	58	0	59
	27	3	4	1	188	1	197
T-Group Lower	28	3	0	5	218	0	226
	29	2	3	2	74	0	81
	30	10	5	6	273	0	294
	32	2	0	1	14	0	17
	Total	25	14	17	1003	2	1061

Total Assemblage = 2,906

Notes: This table includes total lithic counts, including medial and lateral flake debitage. The seven lithics found in YBS and YBT have been removed from the total count.

Table 7-2: Summary of the major lithic groups by excavation level and stratigraphic group without medial or lateral flake debitage (MNL).

Stratigraphic Group	Level	Shaped Tools	Unshaped Tools	Cores	Debitage	Nodules	Total
	11	33	23	13	3	1	73
	12	14	16	9	5	1	45
S-Group	13	63	53	22	14	0	152
	14	37	28	11	59	0	135
	15	2	1	7	35	0	45
	16	5	5	3	69	0	82
	Total	154	126	65	185	2	532
	18	7	1	0	114	5	127
	19	7	2	1	47	0	57
	20	0	0	0	4	0	4
T-Group Upper	21	1	1	2	77	2	83
	22	7	2	2	110	1	122
	23	10	6	4	153	7	180
	24	5	3	2	67	0	77
	Total	37	15	11	572	15	650
	25	5	2	1	99	1	108
	26	0	0	1	26	0	27
T-Group Lower	27	3	4	1	86	1	95
	28	3	0	5	106	0	114
	29	2	3	2	41	0	48
	30	10	5	6	104	0	125
	32	2	0	1	6	0	9
	Total	25	14	17	468	2	526

Total Assemblage = 1,715

Figure 7-1: BN 3115.1, Level 23. Stratigraphic Unit DCC (T-Group Upper). This photo is a possible hammerstone fragment, as evidenced by peripheral pock-marking. Evidence also shows grinding on this piece.

Table 7-3**:** Metric information for nodules and hammerstones.

Bag Number	Excavation Unit	Level	Artifact Type	Weight (g)	Raw Material	Length (mm)	Breadth (mm)	Thickness (mm)	Volume (mm^3)
1796	G10	11	Nodule		CBO	19.23	12.08	7.88	1830.511
1799.7	G10	12	Nodule		CBO				
2254	G10	18	Nodule	0.63	CBO				
2571	G10	18	Nodule	0.93	CBO				
2572	G10	18	Nodule	0.18	CBO				
2129	G10	21	Nodule	1.29	CBO	19.21	13.97	7.37	1977.841
2129	G10	21	Nodule	5.58	CBO	29.8	30.11	10.87	9753.412
2133	G10	22	Nodule	0.52	CBO	23.07	9.8	3.36	759.649
3105	G10	23	Nodule	1.39	CBO				
3105	G10	23	Nodule	0.95	Grey Obsidian				
3105	G10	23	Nodule	0.18	CBO				
3105	G10	23	Nodule	0.19	CBO				
3105	G10	23	Nodule	0.05	CBO				
3730	G10	27	Nodule	0.18	CBO	12.77	8.1	2.85	294.7955
3105	G10	23	Nodule	3.88	Chalcedony				
3115.1	G10	23	Hammerstone	122.82	Basalt	65.05	47.16	36.03	110531.3

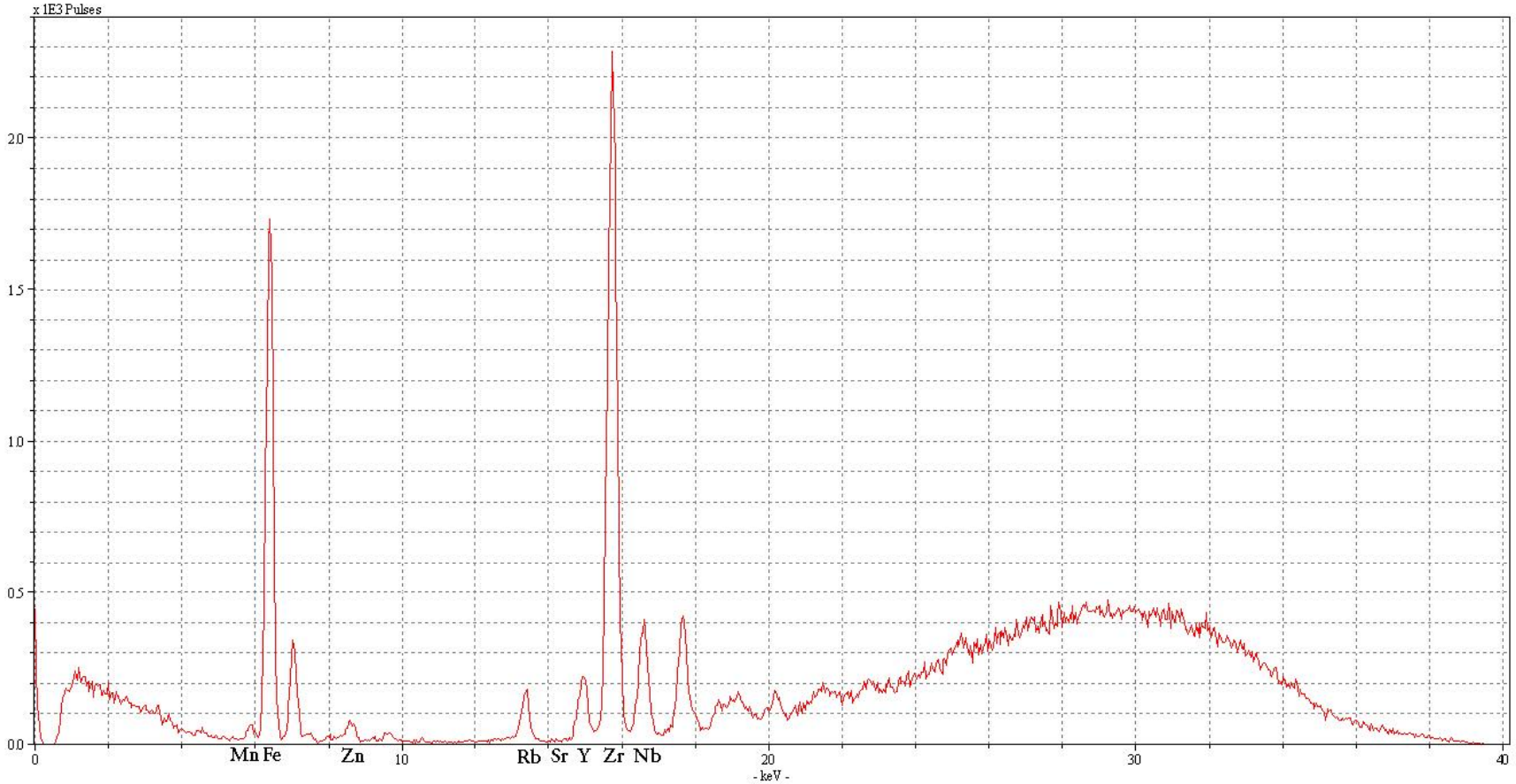

Figure 7-2: XRF spectra of Common Black Obsidian (CBO). CBO has high elemental counts of Fe and Zr, and most rare earth elements, including Rb, Y, and Nb. Sr is characteristically low.

Table 7-4: MNL Frequencies and percentages of the various raw material groups in the T-Groups and S-Group.

Stratigraphic Group	Raw Material Group	N	% of Total Count Within Stratigraphic Group	% of Total Count per Raw Material	% of Total Assemblage Count
S-Group	Obsidian	530	99.62%	31.87%	30.85%
	Chert	1	0.19%	6.67%	0.06%
	Basalt	0	0.00%	0.00%	0.00%
	Roof spall	0	0.00%	0.00%	0.00%
	Quartzitic	1	0.19%	100.00%	0.06%
	Stratigraphic Group Total	532			
T-Group Upper	Obsidian	636	97.55%	38.24%	37.02%
	Chert	2	0.31%	13.33%	0.12%
	Basalt	13	1.99%	68.42%	0.76%
	Roof spall	1	0.15%	5.00%	0.06%
	Quartzitic	0	0.00%	0.00%	0.00%
	Stratigraphic Group Total	652			
T-Group Lower	Obsidian	497	93.07%	29.89%	28.93%
	Chert	12	2.25%	80.00%	0.70%
	Basalt	6	1.12%	31.58%	0.35%
	Roof spall	19	3.56%	95.00%	1.11%
	Quartzitic	0	0.00%	0.00%	0.00%
	Stratigraphic Group Total	534			
	Total Assemblage Count	1718			

Total Count per Raw Material Type	
Obsidian	1663
Chert	15
Basalt	19
Roof spall	20
Quartzitic	1

Table 7-5: MNL Frequencies of raw material groups within the T-Group and S-Group deposits.

Stratigraphic Group	Level	Quartzitic	Basalt	Roof spall	Chert	Obsidian	Total Count per Level
S-Group	11	1				72	73
	12					45	45
	13					152	152
	14				1	134	135
	15					45	45
	16					82	82
	Total	1			1	530	
T-Group Upper	18				1	126	127
	19					57	57
	20					4	4
	21					85	85
	22		9			113	122
	23		3	1	1	175	180
	24		1			76	77
	Total		13	1	2	636	
T-Group Lower	25		1		2	107	110
	26			1	1	26	28
	27			7	2	88	97
	28			5	3	106	114
	29		3	4	1	43	51
	30		1	2	3	119	125
	32		1			8	9
	Total		6	19	12	497	

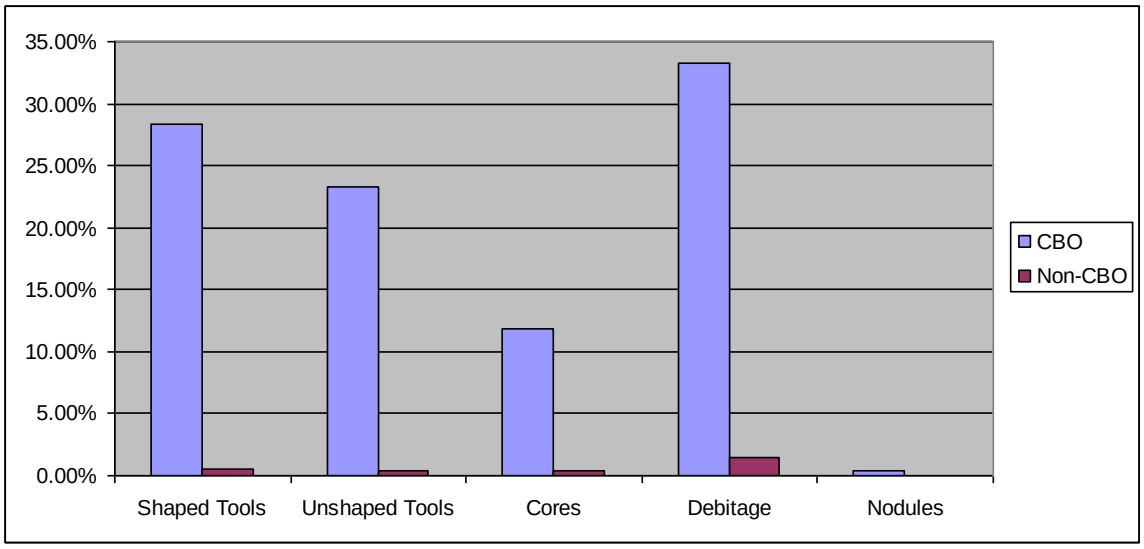

Figure 7-3: MNL proportions of CBO and non-CBO raw materials in the S-Group. The data are further subdivided by lithic group.

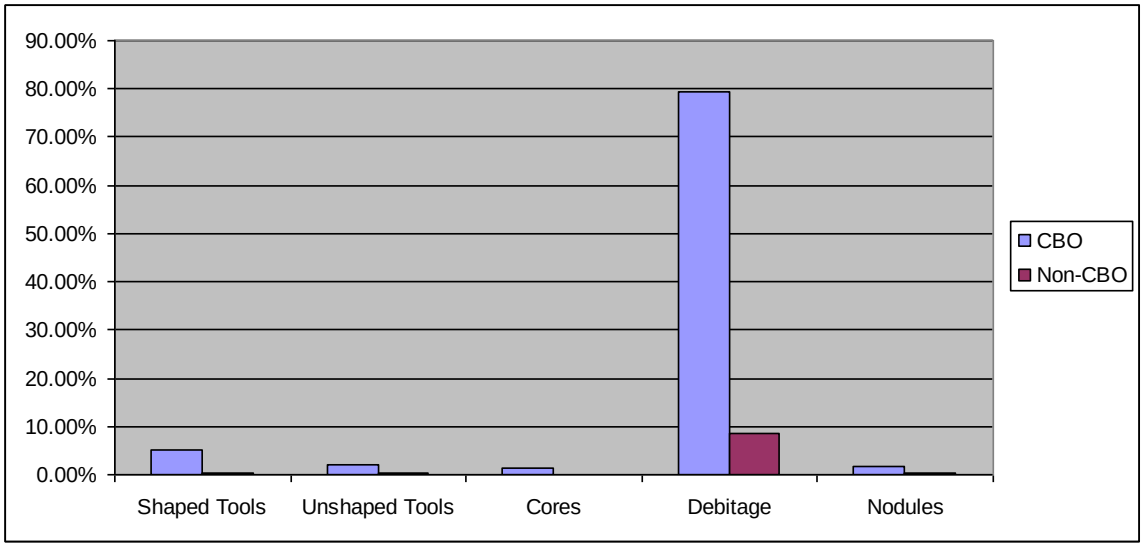

Figure 7-4: MNL proportions of CBO and non-CBO raw materials in the T-Group Upper. The data are further subdivided by lithic group.

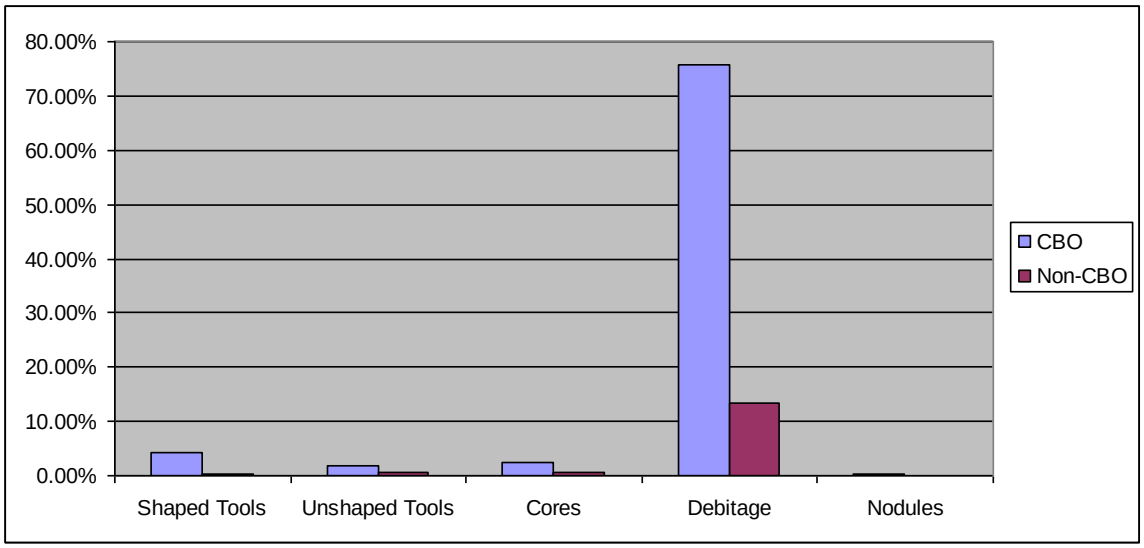

Figure 7-5: MNL proportions of CBO and non-CBO raw materials in the T-Group Lower. The data are further subdivided by lithic group.

Table 7-6: MNL Frequencies of individual raw material types organized by stratigraphic aggregate.

Raw Material Types	S-Group	T-Group Upper	T-Group Lower	Total
Quartzitic	1			1
Basalt		13	6	19
Roofspall		1	19	20
CBO	517	588	451	1556
Green Obsidian	2		2	4
Grey Obsidian	10	44	43	97
Brown Obsidian	1	4	1	6
Light Brown Chert			2	2
Dark Brown Chert			1	1
Grey Chert		1	5	6
Chalcedony		1		1
Red Chert	1		1	2
Pink Chert			2	2
White Chert			1	1
Total	532	652	534	1718

Table 7-7: Frequency and volumetric measurements for core types and core groups from each of the three litho-stratigraphic units discussed in the text (non-MNL).

	Core type	N	Mean volume (cm^3)	Std. Deviation
Radial Cores	Discoidal	2	22.3	14.8
	Levallois	3	5.1	1.4
	Misc. Radial	3	145	242.9
	Mean	8	57.5	86.4
Single Platform	Pyrimidal / Prismatic	4	6.1	5.7
	Single Platform	52	8.6	21.4
	Mean	56	7.4	13.5
Multiple Platform	Biconical	2	7.6	2.4
	Double Platform	2	3	3.2
	Opposed Platform, Same Face	5	5.6	1.9
	Mult. Platform	1	8.7	.
	Opposed Platform, Different Face	2	4.6	1.1
	Double Platform at right Angles	3	5.3	1.3
	Bipolar	1	2.4	.
	Acute Angle	1	5.7	.
	Two Platforms, Same Face at Right Angles	1	3.2	.
	Mean	18	5.1	2
Misc Core Types	Irregular	2	1.8	0.6
	Fragment	9	2.2	1.9
	Core Blank	1	4.3	.
	Mean	12	2.8	1.3

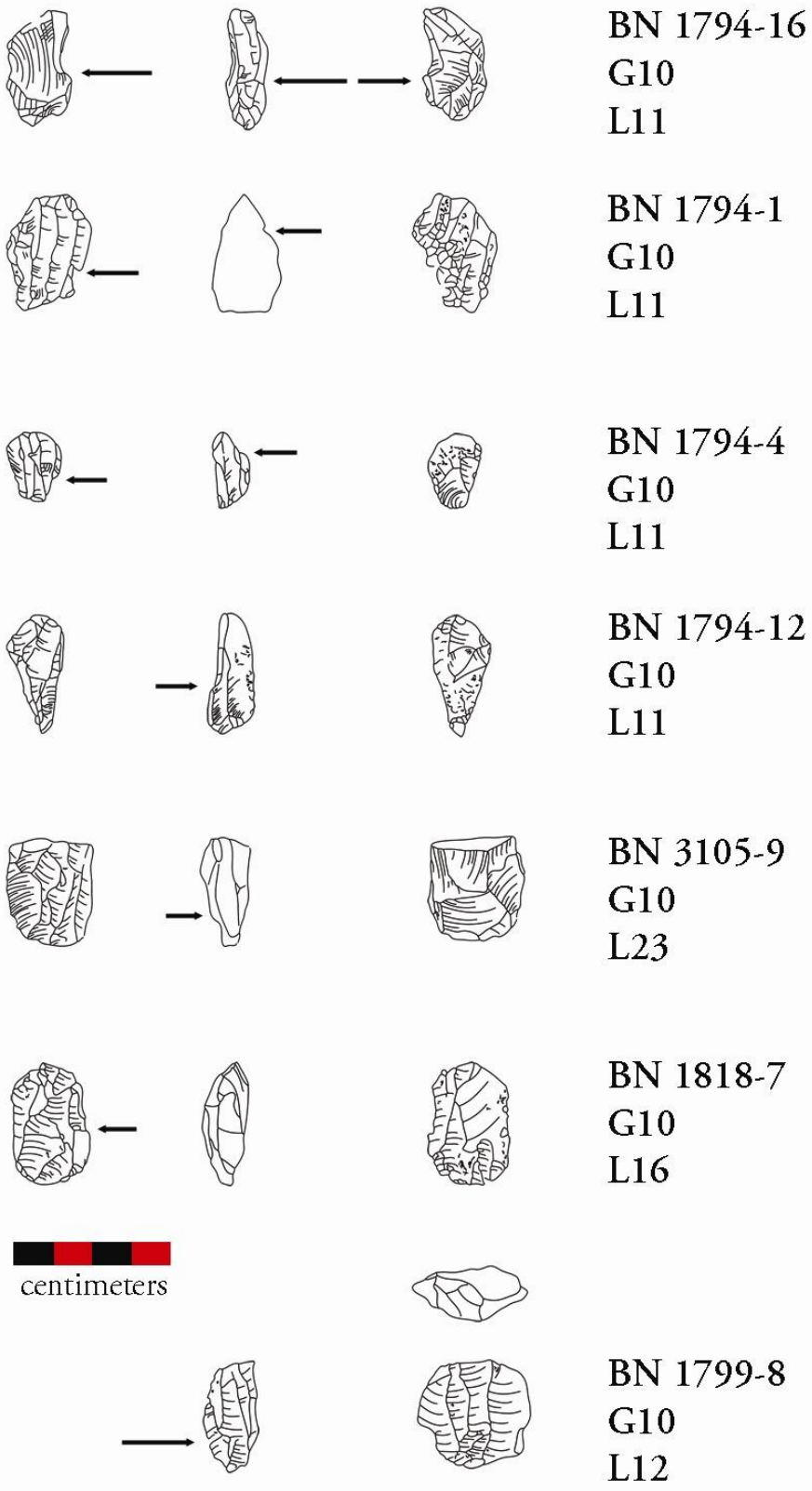

Figure 7-6**:** Selected single and multi-platform cores from the G10 assemblage. Arrows denote step or hinge fractures.

Table 7-8: Frequencies of core types in the S-Group and T-Group Upper and Lower (non-MNL).

		RADIAL			SINGLE PLATFORM			MULTIPLE PLATFORM								MISC.			
	Level	Discoidal	Levallois	Misc. Radial	Single Platform	Pyrimidal / Prismatic	Bipolar	Biconical	Double Platform	Opposed Platform, Same Face	Mult. Platform	Opposed Platform, Different Face	Double Platform at Right Angles	Acute Angle	Two Platforms, Same Face at Right Angles	Irregular	Fragment	Core Blank	Level Total
S-Group	11	0	0	1	8	1	0	1	0	0	0	0	0	0	1	0	1	0	13
	12	0	2	0	4	0	0	0	0	0	0	1	0	0	0	0	2	0	9
	13	0	0	0	12	0	1	0	1	1	0	0	1	0	0	2	4	0	22
	14	0	0	1	6	2	0	0	0	0	0	0	0	0	0	0	1	1	11
	15	0	0	0	3	0	0	0	1	1	0	0	0	1	0	0	1	0	7
	16	0	0	0	1	0	0	0	0	1	1	0	0	0	0	0	0	0	3
	Total	**0**	**2**	**2**	**34**	**3**	**1**	**1**	**2**	**3**	**1**	**1**	**1**	**1**	**1**	**2**	**9**	**1**	
	Group Total	**4**			**38**			**11**								**12**			
T-Group Upper	17	0	0	0	0	1	0	0	0	0	0	0	0	0	0	0	0	0	1
	19	0	0	0	1	0	0	0	0	0	0	0	0	0	0	0	0	0	1
	21	1	0	0	1	0	0	0	0	0	0	0	0	0	0	0	0	0	2
	22	0	0	0	2	0	0	0	0	0	0	0	0	0	0	0	0	0	2
	23	0	0	0	2	0	0	0	0	2	0	0	0	0	0	0	0	0	4
	24	0	0	0	2	0	0	0	0	0	0	0	0	0	0	0	0	0	2
	Total	**1**	**0**	**0**	**8**	**1**	**0**	**0**	**0**	**2**	**0**	**0**	**0**	**0**	**0**	**0**	**0**	**0**	
	Group Total	**1**			**9**			**2**								**0**			
T-Group Lower	25	0	0	0	1	0	0	0	0	0	0	0	0	0	0	0	0	0	1
	26	0	0	0	1	0	0	0	0	0	0	0	0	0	0	0	0	0	1
	27	0	0	0	1	0	0	0	0	0	0	0	0	0	0	0	0	0	1
	28	0	0	0	3	0	0	0	0	0	0	1	1	0	0	0	0	0	5
	29	1	0	0	1	0	0	0	0	0	0	0	0	0	0	0	0	0	2
	30	0	1	0	3	0	0	1	0	0	0	0	1	0	0	0	0	0	6
	32	0	0	1	0	0	0	0	0	0	0	0	0	0	0	0	0	0	1
	Total	**1**	**1**	**1**	**10**	**0**	**0**	**1**	**0**	**0**	**0**	**1**	**2**	**0**	**0**	**0**	**0**	**0**	
	Group Total	**3**			**10**			**4**								**0**			
								Total per core Type											
		2	**3**	**3**	**52**	**4**	**1**	**2**	**2**	**5**	**1**	**2**	**3**	**1**	**1**	**2**	**9**	**1**	

Table 7-9: Relative percents of core flake removal types per excavation levels (non-MNL).

	Level	Flake	Blade	Levallois	Multiple	Indet.	Total
S-Group	11	50.00%	33.30%	0.00%	16.70%	0.00%	12
	12	44.40%	44.40%	11.10%	0.00%	0.00%	9
	13	63.60%	27.30%	0.00%	0.00%	9.10%	22
	14	36.40%	63.60%	0.00%	0.00%	0.00%	11
	15	28.60%	42.90%	0.00%	14.30%	14.30%	7
	16	33.30%	66.70%	0.00%	0.00%	0.00%	3
		48.40%	40.60%	1.60%	4.70%	4.70%	64
T-Group Upper	19	100.00%	0.00%	0.00%	0.00%	0.00%	1
	21	100.00%	0.00%	0.00%	0.00%	0.00%	2
	22	50.00%	50.00%	0.00%	0.00%	0.00%	2
	23	75.00%	25.00%	0.00%	0.00%	0.00%	4
	24	100.00%	0.00%	0.00%	0.00%	0.00%	2
		81.80%	18.20%	0.00%	0.00%	0.00%	11
T-Group Lower	25	100.00%	0.00%	0.00%	0.00%	0.00%	1
	26	100.00%	0.00%	0.00%	0.00%	0.00%	1
	27	0.00%	100.00%	0.00%	0.00%	0.00%	1
	28	100.00%	0.00%	0.00%	0.00%	0.00%	5
	29	100.00%	0.00%	0.00%	0.00%	0.00%	2
	30	83.30%	0.00%	16.70%	0.00%	0.00%	6
	32	100.00%	0.00%	0.00%	0.00%	0.00%	1
		88.20%	5.90%	5.90%	0.00%	0.00%	17

Notes: A statistically significant inverse correlation exists between the increase of blade-flake removals from the T-Group Lower to the S-Group and the decrease in flake removals ($r = -0.979$, sig (one-tailed) = .066).

Table 7-10: Percentages of the major lithic groups by stratigraphic aggregates for the entire assemblage (upper) and MNL only (lower).

Frequencies and Relative Percentages of Lithics based on the Full Assemblage						
	Shaped Tools	Unshaped Tools	Cores	Debitage	Nodules	Total
S-Group	154	126	65	208	2	555
	27.75%	22.70%	11.71%	37.48%	0.36%	
T-Group Upper	37	15	11	1212	15	1290
	2.87%	1.16%	0.85%	93.95%	1.16%	
T-Group Lower	25	14	17	1003	2	1061
	2.36%	1.32%	1.60%	94.53%	0.19%	
Total	216	155	94	2424	19	2908

Frequencies and Relative Percentages of Lithics based on the MNL Assemblage						
	Shaped Tools	Unshaped Tools	Cores	Debitage	Nodules	Total
S-Group	154	126	65	185	2	532
	28.95%	23.68%	12.22%	34.77%	0.38%	
T-Group Upper	37	15	11	572	15	650
	5.69%	2.31%	1.69%	88.00%	2.31%	
T-Group Lower	25	14	17	468	2	526
	4.75%	2.66%	3.23%	88.97%	0.38%	
Total	216	155	93	1225	19	1708

Table 7-11: Average volume (mm^3) of cores, shaped and unshaped tools per excavation level and litho-stratigraphic group (non-MNL).

	Level	N	Mean Volume (mm^2)	Std. Deviation	Group Mean Volume (mm^2)	Group Std. Deviation
S-Group	10	5	4751.06	3124.08	2802.05	2937.27
	11	69	3679.08	4385.7		
	12	39	2730.53	2034.75		
	13	138	2566.17	2582.75		
	14	76	2239.93	2040.49		
	15	10	2814.58	1847.16		
	16	13	4142.32	3384.49		
	17	1	14007.45	.		
T-Group Upper	18	7	1434.98	1309.89	8934.95	22388.49
	19	8	4090.18	1603.54		
	21	3	13262.59	16901.61		
	22	9	9547.99	6567.7		
	23	14	5361.14	5697.38		
	24	7	26476.56	56594.97		
	25	6	5514.21	4679.17		
	26	1	9689.42	.		
T-Group Lower	27	4	3875.99	1979.03	14771.93	64984.95
	28	8	3890.43	2671.18		
	29	4	8192.59	2806.29		
	30	16	4223.84	2254.58		
	32	3	143555.7	244133.59		
Total		441	4657.08	21645.93		

Notes: The calculation of the group mean volume was made using the raw data values derived from the level means.

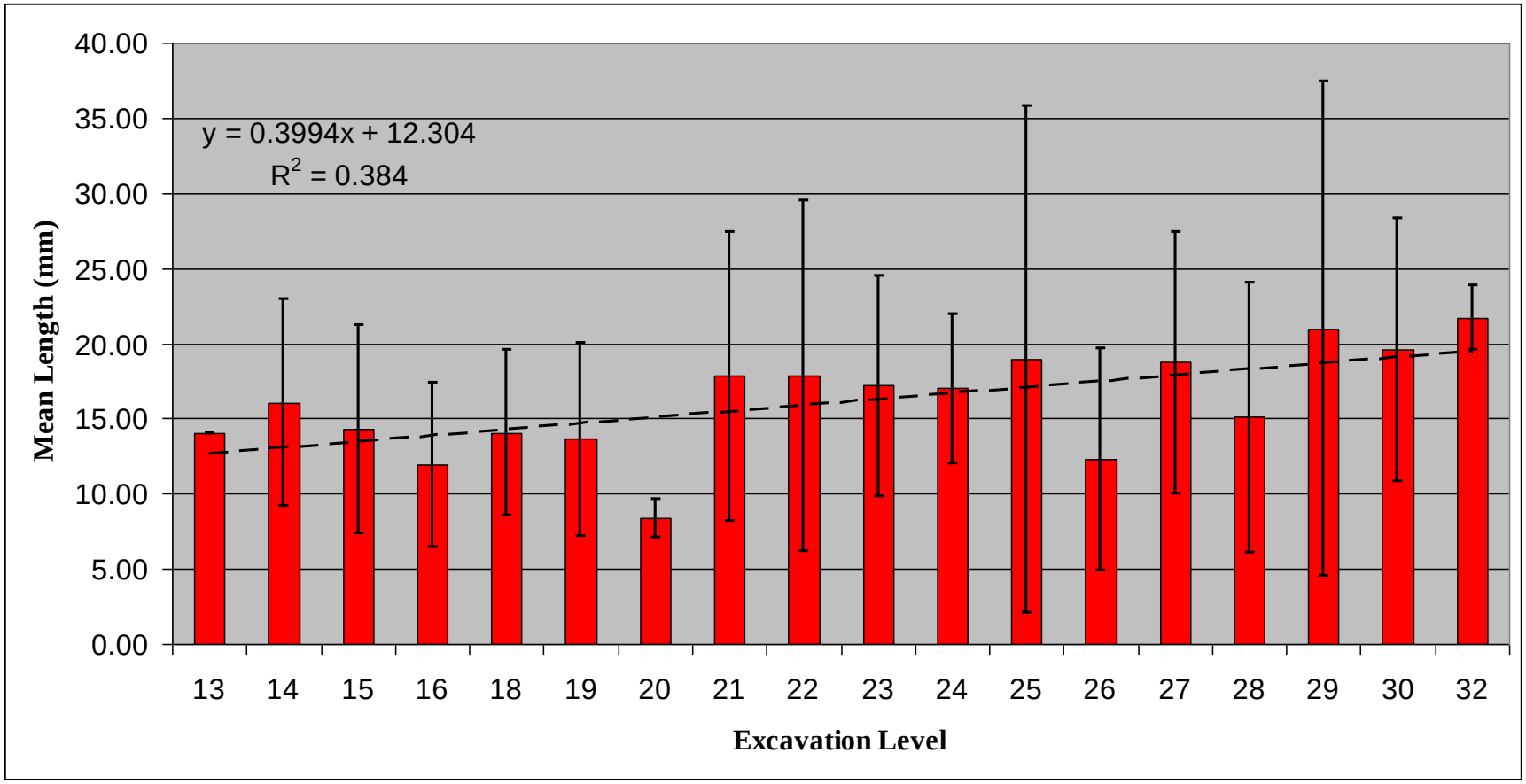

Figure 7-7: Bar chart showing the mean length of whole flakes per excavation level (MNL). Standard deviation and a linear trend line have been superposed for reference. This graph shows a subtle, but evident, decrease in the mean length of whole flake from the T-Group Lower (levels 32-25) and the S-Group (levels 16-11). Level 11 and 12 are absent from this chart due to a lack of whole flakes in these levels.

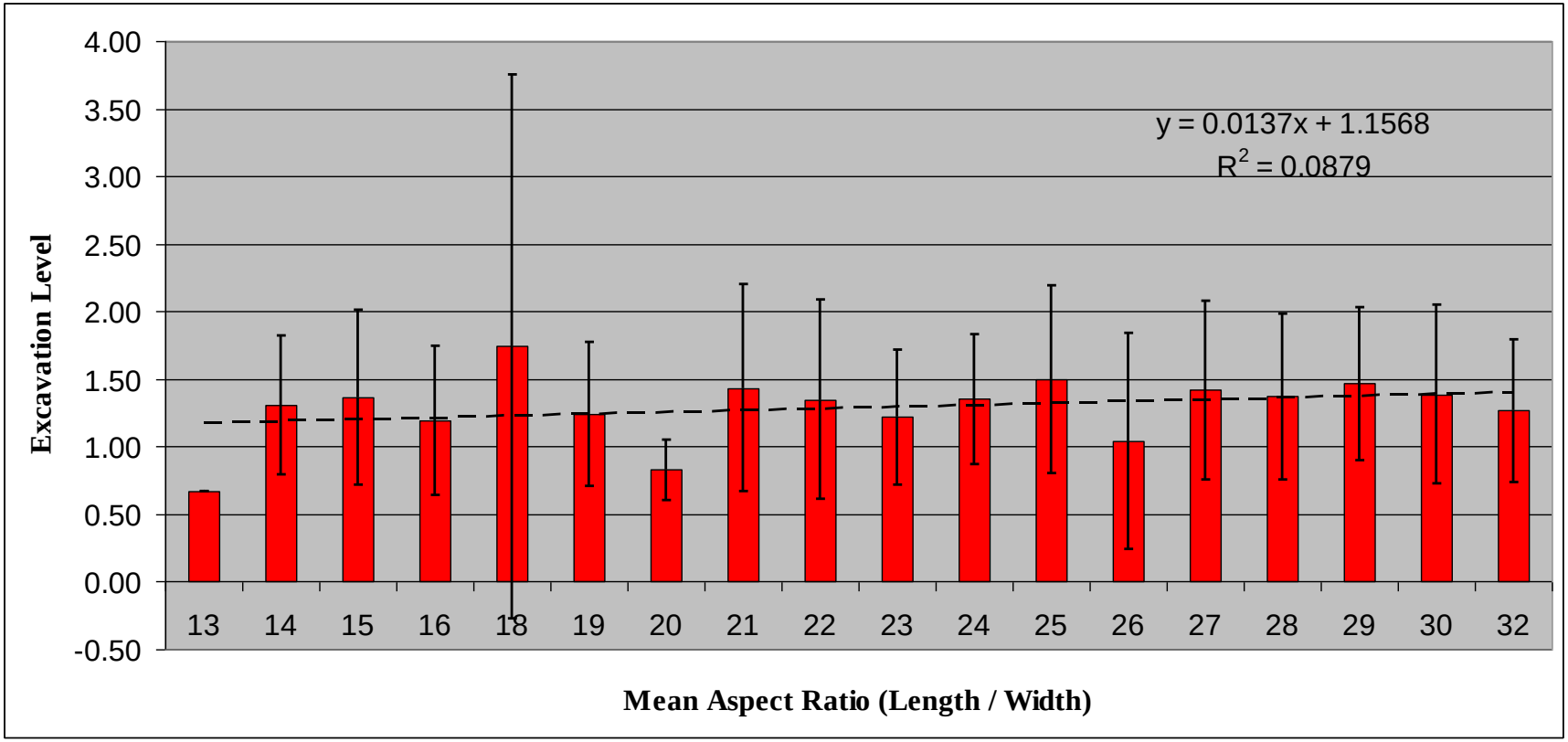

Figure 7-8: Bar chart showing the mean aspect ratio (length/width) of whole flake per excavation level (MNL). This graphs a slight decrease in aspect ratio from the T-Group Lower to the S-Group, but the trend is actually almost indiscernible. For comparison, an aspect ratio value of "1" is equivalent to a perfect circle and value of "2" is twice as long as it is wide.

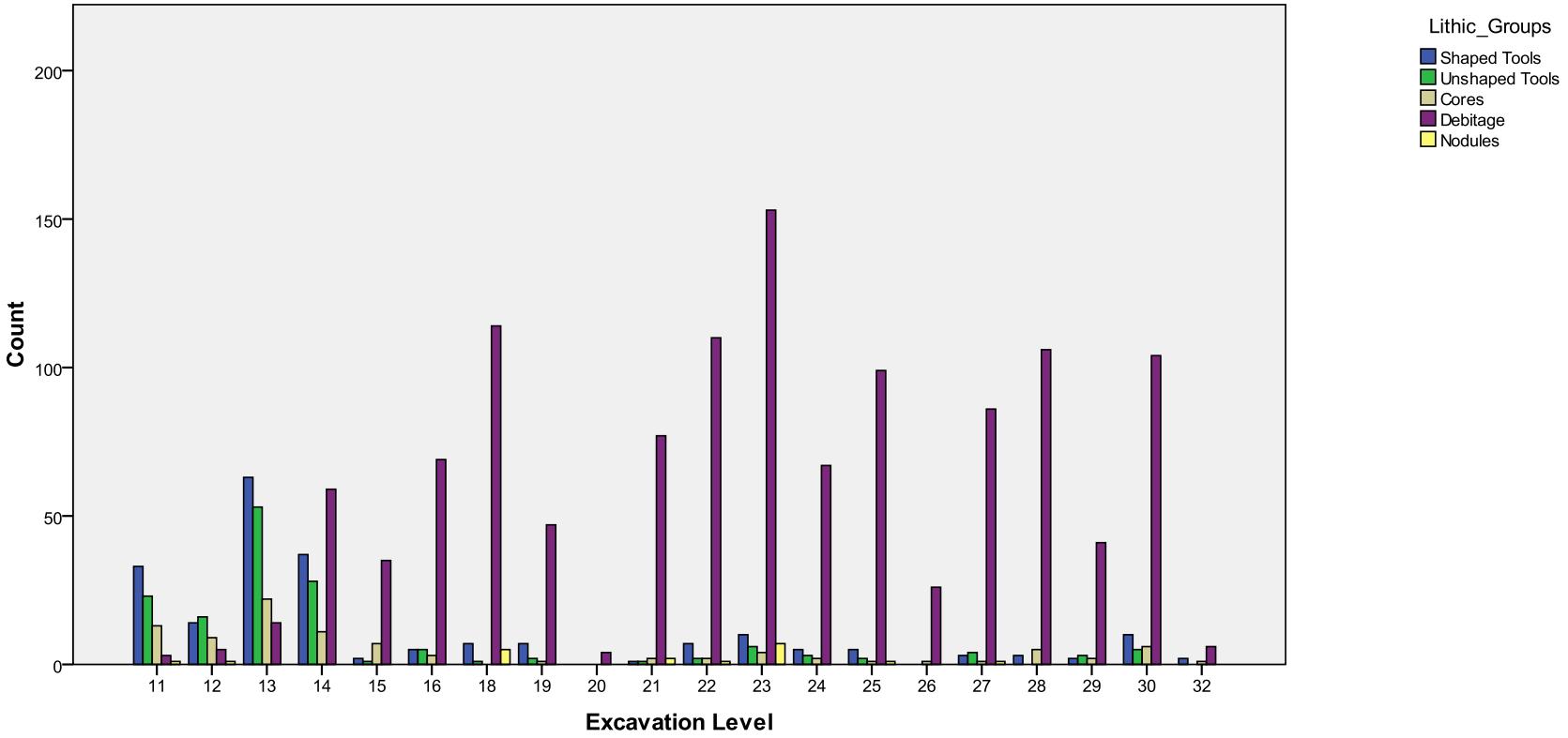

Figure 7-9: MNL frequency of raw material groups from excavation level 11 to 32. The patterns of lithic types suggest a turnover from debitage dominance in the T-Group (level 32-18) to shaped and unshaped tool dominance in the S-Group (level 16-11).

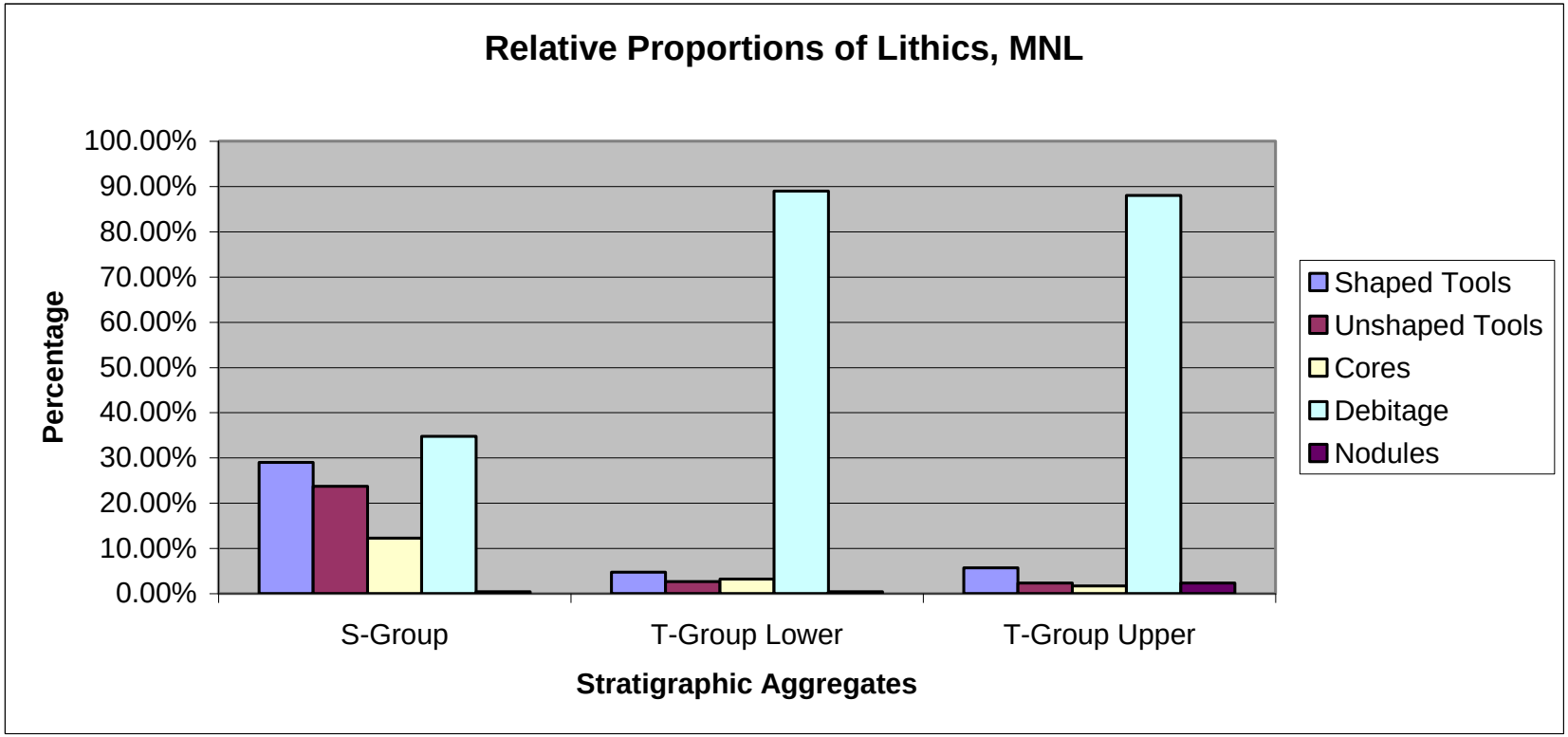

Figure 7-10: Relative proportions of lithic groups in the S-Group and T-Group stratigraphic aggregates.

Table 7-12: Total frequencies and percentages of various shaped and unshaped tool categories (non-MNL).

Stratigraphic Aggregate		Misc Unshaped	Burins	Microliths	Points / Unifaces / Bifaces	Scrapers	Utilized	Modified	Total
S-Group	Frequency	14	7	15	72	47	61	64	280
	Percent	5.00%	2.50%	5.36%	25.71%	16.79%	21.79%	22.86%	0.00%
T-Group Upper	Frequency	5	3	2	20	7	9	6	52
	Percent	9.62%	5.77%	3.85%	38.46%	13.46%	17.31%	11.54%	0.00%
T-Group Lower	Frequency	3	1	0	14	7	7	7	39
	Percent	7.69%	2.56%	0.00%	35.90%	17.95%	17.95%	17.95%	0.00%
	Total	22	11	17	106	61	77	77	371

Table 7-13: MNL proportions of the blank types used to make shaped and unshaped tools within each litho-stratigraphic unit.

	End-Struck Flake	Side-struck flake	Flake Fragments	Other	Total
S-Group	60.38%	3.30%	13.68%	22.64%	212
T-Group Lower	68.75%	3.13%	9.38%	18.75%	32
T-Group Upper	59.57%	6.38%	10.64%	23.40%	47

CHAPTER 8
DESCRIPTIVE AND STATISTICAL ANALYSIS OF THE T-GROUP AND S-GROUP ASSEMBLAGES AT MOCHE BORAGO: UNSHAPED AND SHAPED TOOLS

As discussed in Ch 7, lithic raw materials, cores, and debitage from the T-Group and S-Group assemblages suggest diachronoic changes in the frequencies of artifact types and core reduction strategies. This chapter considers the evidence for temporal changes in unshaped and shaped tools from the T-Group and S-Group assemblages. The chapter first focuses on the description and analysis of the unshaped tools, followed by the five broad classes of shaped tools: 1) microliths; 2) miscellaneous shaped tools such as becs, awls, and drills; 3) scrapers; 4) burins; and 5) points (unifacial, parti-bifacial and bifacial).

Overview of the Unshaped and Shaped Tools

Unshaped tools (also referred to as informal tools) are flaked stone artifacts that display shallow or irregular retouch along one or more edges without intentional alteration of the original shape of the edge(s). Unshaped tools come in two types: "utilized" unshaped tools have marginal (< 3 mm) edge alteration caused by use and "modified" unshaped tools, where edge alteration is more invasive but the shape of the original un-worked edge is still maintained.

Shaped tools (or "formal" tools) display more invasive and patterned retouch that alters the original shape of the edge(s). The edge alteration on shaped tools is often semi-invasive (5-10 mm) to fully invasive (> 10 mm), regularly spaced, and patterned. Shaped tools such as drills, awls, scrapers, or points are made to suite specific functional and/or social tasks.

A total of 369 unshaped and shaped whole and broken tools were recovered from the S-Group and T-Group assemblages. Table 8-1 provides the frequency and percentages of shaped and unshaped tools relative to the total number of artifacts in this class. Among all stone artifacts, the highest frequencies of unshaped and shaped tools are found in the S-Group (9.6%, n = 279) while T-Group tools account for 3.1 % (n = 90). In the S-Group alone, unshaped and

shaped tools account for 50.5% of the assemblage whereas in the T-Group these tools only account for 3.9%. The higher percentage of unshaped and shaped tools in the S-Group parallels the percentage of cores from the S-Group.

Table 8-2 shows the relative percentages of shaped and unshaped tools per stratigraphic group, which indicated that there was a fairly consistent distribution of scrapers, points, and unshaped tools within each litho-stratigraphic group. These findings suggest that although the total number of unshaped and shaped tools increases in the S-Group, the relative proportions remain largely unchanged between the two groups. Microliths are the only tool class not found within all three litho-stratigraphic groups.

When a Minimum Number of Lithics (MNL) filter (see Chapter 7) is applied to the dataset, the total amount of unshaped and shaped tools drops to 201, which is 54% lower than the non-MNL counts (Table 8-3). More unshaped and shaped tools are still found in the S-Group, but the proportions of different tool types change. For example, the frequency of points in the S-Group drops from 72 to 29, representing a 59.7% decrease. In comparison, the frequency of points in the T-Group Upper decreases by 80% and by 50% in the T-Group Lower.

Unshaped Tools

The frequency and relative percentage of utilized and modified unshaped tools are provided in Table 8-4. MNL counts show that unshaped tools represent 30 to 40% of all tools in the T-Group and 35% of all tools in the S-Group. The high percentage of unshaped tools suggest that during early OIS 3 the occupants of Moche Borago during the T-Group and S-Group may have engaged in similar, and perhaps opportunistic, tasks that required relatively quick and informal tools.

Unifacial dorsal edge damage is found on 72% of all unshaped tools (Table 8-5). Inverse (ventral) edge damage or retouch accounts only for 12% of all unshaped tools. Retouch and

edge damage occurs primarily on one or both lateral edges, but less commonly on the distal edge and almost never on the proximal edge. Incidences of step fracturing are also low, and 57% of dorsal flake scars are neither stepped nor hinged (Table 8-6). The low amount of step and hinge flake fractures suggest that the unshaped tools, as a whole, may have been used only briefly and moderately before they were discarded.

Modified and utilized unshaped tools were made on similar types of flake-blanks. End-struck whole flake-blanks account for 71% of modified tools and 84% of utilized unshaped tools (Table 8-7). Flake fragments are the next most common blank type, while side-struck flake-blanks represent only 5% and 1% of the modified and utilized unshaped tools, respectively.

The size and elongation of unshaped tools vary between modified and utilized tools and also between the T-Group and the S-Group. Utilized tools are longer than modified tools by 13%. Furthermore, the longest unshaped tools are found in the T-Group Upper compared to the S-Group (Table 8-8). However, the aspect ratios of unshaped tools, which is illustrated in Figure 8-1, shows a clear trend towards elongation from the T-Group Lower to the S-Group.

Miscellaneous Shaped Tools

There are only ten miscellaneous shaped stone artifacts like becs, awls, and outil ecaille. Table 8-9 provides basic metric and descriptive information about these artifacts. All of these artifacts are made on CBO and all but one piece is found in the S-Group, which is BN 3105.11, an irregularly shaped artifact from the T-Group Upper. Only a single possible drill-like implement has been identified (BN 1794.15) due to dihedral lateral retouching. There are five possible awls, one bec, and two possible outil ecaille. Since most of these stone artifacts come from the S-Group it is possible that they indicate more diverse kinds of on-site activities at that time than during the T-Group.

Microliths

Microliths first appear in the T-Group Upper. The S-Group and T-Group deposits contained 17 whole and fragmented microliths, representing ~5% of the total unshaped and shaped tools assemblage. Additional microliths have been recovered from the S-Group and T-Group deposits in units H9 and G9, but they have yet to be analyzed. The sample size is limited, but we can make a few diachronic observations. Table 8-10 provides basic metric information for each microlith recovered from G10. Photos and illustrations for most of the microliths are provided in Figure 8-2, and each piece is described in detail in Appendix C.

All the microliths in the current sample are manufactured using common black obsidian (CBO). They are all elongate and most are straight-backed with obverse backing. The average microlith aspect ratio is 2.1 (SD = 1.0), which shows that these artifacts are twice as long as they are wide. Straight-backing accounts for 29.4% (n = 5) of the total microlith assemblage, and many of these pieces are obversely-backed (41.2%, n = 7). Bidirectional flaking is the next most common type of backing (23.5%, n = 4).[30]

The backing angle is also relatively steep on each piece, which would be expected for backed tools. The average backing angle is 81.3° (SD = 13.3°). Also, no statistically significant relationship occurs between the backing angle and backing type ($r = .202$, sig(1-tailed) = .454, $p < .01$), but obversely-backed microliths, in general, have the steepest edge angles (84.6°, SD = 11.44). Finally, no statistically significant relationship occurs between the microlith type and type of backing ($r = .202$, sig(1-tailed) = .227, $p < .01$).

[30] Bidirectional flaking differs from alternating flaking patterns because bidirectional flaking is less standardized. But an alternating flaking pattern is a series of inverse flake scars followed by a series of obverse flake scars in a repetitive fashion along the backed edge of the tool.

The current sample is too small to reveal any statistically-significant quantitative patterning in the microliths from the T-Group to the S-Group. However, two pieces of qualitative evidence suggest that microlithic technology at this time may have been in a state of flux. The first piece is artifact BN 2571.1 from Level 18. While most microliths are straight-backed, BN 2571.1 is a crescent, which shows that Mode 4/5 geometric microlith designs had been developed by ~45 ka. Geometric microliths become common in Ethiopia in the Holocene Mode 4/5 technologies (Brandt, 1982) and BN 2571.1 is one of the earliest Mode 4/5 crescents known in the area. Furthermore, in overlying S-Group deposits, another microlith is made on a Levallois flake (BN 1818.6, Level 16), which is significant because the artifacts shows that prior Mode 3 Levallois flaking techniques were used in combination with Mode 4/5 tool design.

Scrapers

All the scrapers are made from CBO. More than three-quarters of all scrapers or scraper fragments are found in the S-Group (77%, n = 47), compared to just seven each in the T-Group Upper and Lower deposits (Tables 8-11 and 8-12). Several scrapers were fragmented, and the dataset has been filtered for MNL (Table 8-13 and 8-14). Metrical data for all scrapers is provided in Table 8-15.

End scrapers are the most common scraper type before and after MNL. The most end scrapers are found in the S-Group representing 41.4% (n = 17) of that assemblage whereas there are two scrapers in the T-Group Upper (40%) and only a single end scraper in the T-Group Lower (25%) (Tables 8-13 and 8-14). Notched scrapers are the next most common type, but are significantly reduced in frequency, representing 22% (n = 9) of the S-Group and 20% (n = 1) of the T-Group Upper. No notched scrapers were present in the T-Group Lower. Side scrapers are also poorly represented, accounting for 12% (n = 5) of the S-Group, 0% of the T-Group Upper,

and 25% (n = 1) of the T-Group Lower. Other categories of scrapers, such as scraper side-combinations, represent a combined 28.0% (n = 14) of the total assemblage.

The scrapers are all fairly elongate with aspect ratios exceeding 1.0 (Table 8-16), but there are minimal diachronic differences in elongation. The most elongate scrapers are found in the T-Group Upper (M = 1.7, SD = 0.6), and the least elongate scrapers are found in the T-Group Lower (M = 1.3, SD = 0.2). End scrapers are also ~10% less elongate than the mean elongation values calculated from the entire assemblage (Table 8-17).

Most scrapers are retouched on the dorsal face (Table 8-18). End scrapers are retouched most commonly along the distal edge (52.6%), as are scrapers with multiple retouched edges (e.g. end and side, end and double side). Side scrapers are retouched with equal frequency along either the left lateral or both laterals (33.3%) (Table 8-19).

The working edge angles for side and end scrapers are all fairly steep with an average of 73.9° (SD = 4.6). Edge angles appear lowest in the T-Group Lower (68.5°, SD = 0.7) and highest in the S-Group (77.2° (SD = 2.7) (Table 8-20). However, these observations are made from only four artifacts in the T-Group Lower. Only two end scrapers are in the T-Group Upper.

Straight working edges are also most common among end scrapers (45%, n = 9) and convex working edges are next most common (30%, n = 6) (Table 8-21). Serrated edges or irregular edges, such as burs or use-wear defects, occur in relatively low frequency within the entire scraper assemblage, which suggests that these artifacts were not used intensively before being discarded.

Of the nine notched pieces, all but one are found in the S-Group, and of those pieces, 55% (n = 6) come from Level 13. Notching is most common along the right lateral edges of flakes (66.7%). The notches are also typically obversely-flaked (75%). Table 8-22 provides basic

metrics on the notched pieces. The average notch width is 10.5 mm (SD = 2.5), and the average notch depth is 3.8 mm (SD = 0.8).

Burins

Only 12 burins were identified, and basic descriptive information for each piece is provided in Table 8-23. Two noteworthy specimens are illustrated in Figures 8-3 and 8-4. Burins occur in each litho-stratigraphic group, but they are most common (67%, n = 8) in the S-Group. All the burins are made of common black obsidian (CBO) except for BN 1818.12, which is made of gray obsidian. Of these burins, 83% (n = 10) are made on end-struck flakes. The burins are also often elongate with a mean aspect ratio of 2.2 (SD = 0.9). However, T-Group burins appear slightly more elongate (M=2.6, SD = 1.2) than S-Group burins (M=2.0, SD = 0.6).

Angle burins (42%, n = 5) and dihedral burins (33%, n = 4) are the most common types. Dihedral and angle burins are found in both the T-Group and S-Group. The average width of the burin edges is 6.2 mm (SD = 1.8) and angle burins have a more oblique edge angle (M=86º, SD = 9.3) than dihedral burins (M=54º,SD = 2.9).

Two of the burins are especially noteworthy with detailed descriptions as follows:

BN 1802.98
Level 13
G10
S-Group
Figure 8-3

BN 1802.98 is a backed flake but with a series of burin spalls on the distal left lateral edge. The tool is made on an end-struck whole flake. The backing is found along the right lateral edge. The distal edge has also been snapped off, likely to create an oblique striking platform for the burin spalls. Two spalls were removed along the right lateral edge to create an angle burin at the intersection of the right lateral and distal faces. It appears that the burins spalls overlie the backing retouch.

BN 4906.2
Level 30
G10
T-Group Lower
Figure 8-4

BN 4906.2 is a dihedral burin. The tool is made on the distal section of an end-struck flake. It appears that the flake blank was snapped (lateral-lateral), and a single burin spall was removed from the left lateral edge. This spall was then truncated with two additional obverse flake removals along the proximal left lateral edge. The obverse flake removals may have been to reinforce this face as a striking platform. Subsequently, three or four more burin

spalls were removed from the proximal right lateral edge using the former burin surface as the striking platform. The angle of the resulting dihedral burin is 52º.

Points

Points are a major component of most Late Pleistocene archaeological assemblages in East Africa and the Horn. Numerous studies have described the diverse inter-regional and intra-regional variations of points (Cole, 1954; Clark, 1954; Clark, 1970; Kurashina, 1978; Brandt, 1986; Mehlman, 1989; Pleurdeau, 2001; Brooks et al., 2006), and some authors even see cultural patterning emerge from point types (Clark 1988). Morphologically, points are flake or flake fragments that have convergent lateral edges to make a pointed end. A point can be created using prepared core techniques which do not require retouching, or using unifacial, parti-bifacial, or fully bifacial retouch.

Points are problematic for two reasons. The first is determining function. On the one hand, points may be part of projectile technologies, such as spears or the bow and arrow that relied on hand-thrusted, hand-thrown, or mechanically projected implements. On the other hand, points may have been used as knives, drills, or other kinds of implements that emphasized the convergent morphology of the tool and the sharp lateral edges. Macrowear analysis, including size and morphology studies, may not be able to differentiate between points that were used for different functions because they can produce similar macroscopic use-wear. Microwear analysis may be able to suggest point functions, but these studies rely on in-depth experimental analysis of specific raw materials and point types.[31]

The second problem is that the lack of well-dated and continuous archaeological sequences across East Africa and the Horn provide little information about how point type and function

[31] Microwear analysis is on-going for Moche Borago (V. Rotts per comm.).

change over time and how point types between regions relate to each another. For instance, in the Horn of Africa, Clark's (1954) typology of Late Pleistocene bifacial and unifacial points was based on artifacts from open-air sites or sites that had short, discontinuous sequences. The longest sequence Clark was able to use came from Porc Epic (Ethiopia), which is now known to have a major unconformity and problematic dating. Consequently, Clark (1954; 1988) and others such as Pleurdeau (2001) were still unable to accurately describe temporal changes in point technology and style during the Late Pleistocene, and especially the change from Mode 3 to Mode 4/5 technologies.

Moche Borago, however, provides the Horn with the first well-dated sequence of Late Pleistocene points, though the assemblage is still small overall. The T-Group and S-Group have Mode 3 Levallois points, as well as Mode 4/5 unifacial, parti-bifacial, and bifacial foliate points.[32] While the size of the assemblage limited the breadth of the analysis, there were qualitative patterns that relate to technology and typology, which are described here. Functional and quantitative differences are still being analyzed.

The points are divided into two sub-sections: The first provides metric information for the T-Group and S-Group points, while the second focuses on a subset of the best examples of unifacial and bifacial points from the T-Group, the S-Group, and R-Group. The R-Group points are included to discern the broader diachronic trends within the point assemblage as a whole. Relevant contextual information for the R-Group is provided as needed. Summaries of technological and typological changes in the points are provided at the end of this chapter.

[32] There is no evidence for point preforms in the current assemblage.

The Point Assemblage

The 105 points or point fragments (non-MNL) from the T-Group and S-Group represent 28.6% of the total unshaped and shaped tools. Whole and point fragments are more common in the S-Group (68.5%, n = 72) compared to the T-Group Upper (18.1%, n = 19) or T-Group Lower (13.3%, n = 14). Compared to other unshaped and shaped tools, the proportions of points in each litho-stratigraphic group range from 25.7% (n = 72) in the S-Group to 38.5% in the T-Group Upper (Table 8-1).

The majority of points in the total assemblage are flaked unifacially with proportions ranging from 57% in the T-Group Lower to 73% in the T-Group Upper (Tables 8-24 and 8-25). Point fragments are also more common than whole points (Table 8-26), which may indicate that the points were used and then discarded. Further evidence for point use is found in the type of fragments seen in the assemblage. Proximal point fragments (15%, n = 16) are twice as frequent as either medial or distal fragments. At Moche Borago, many of the points are made on flakes with the proximal edge (i.e. the platform) located at the widest part of the tool, which is the butt, opposite the pointed edge. The proximal edge becomes contained in the haft when the point is oriented platform/base. Therefore, if a point is broken during use, the proximal edge still in the haft may be more likely to be removed and discarded on-site when the tool is repaired. However, orienting point platforms down also means that the thicker width around the bulb of percussion might prevent a secure haft. Bulbar thinning is found on some points, but more than three-quarters (78.9%) of points at Moche Borago do not show evidence for bulbar thinning (Tables 8-27 and 8-28).[33]

[33] Bifacial flaking is not included in these tables.

Basic metric data for whole points is provided in Table 8-29, which shows a slight decrease in the mean lengths of points from the T-Group Lower (M = 31.3 mm, SD = 14.1) to the S-Group (M = 25.9 mm, SD = 9.1) (Figure 8-5). Mean aspect ratios, however, do not change much, although the whole points in the T-Group Lower are slightly more elongate than either the T-Group Lower or S-Group points (Figure 8-6).

Point Descriptions

This section provides detailed technological and typological descriptions of a sample of 20 Moche Borago points[34]. The sample is derived primarily from G10 (n = 15), but points from H9 (n = 3), G9 (n = 1), and TU2 (n = 1) are also added to increase the sample size. R-Group points are also included to broaden the diachronic depth of the analysis. Each point is illustrated in Figure 8-7. Detailed descriptions of each point are also provided in Appendix D.

Technological Summary of the Moche Borago Points

Two different technological traditions are represented within the Moche Borago points, as shown in Figure 8-8. Mode 3 points, characterized by the use of Levallois flaking methods, were found in both the T-Group and S-Group, but there are only four Mode 3 points in the entire assemblage (BN 3114.1, 3132.1, 1799.12, 1818.1). Each of these artifacts has a triangular platform, radial or convergent dorsal scars, and facetted flake-blank platforms, which indicate that they were removed from prepared cores. BN 3132.1 is unique in that the dorsal scar pattern is opposed to the striking platform such as the Nubian Type 1 technique (Vermeersch, 2001).

Mode 4/5 points are most clearly characterized by unifacial, parti-bifacial, or fully bifacial retouching techniques. Intensive retouch is found on each piece, and the retouch pattern

[34] The points included in this sample were chosen because they were whole, but in some cases, like Toora points, the flake blank is snapped, which indicates that these tool are either fragmentary or the tools were made on blanks that were snapped intentionally.

is most commonly semi-circular to fully circular. Bifacial points are usually retouched more finely on one face. Furthermore, the planform shapes of points vary according to retouch type. Unifacial points appear to have the most triangular planform shapes and bifacial points have the most ovate planforms. One interpretation for the ovate bifacial point shape may be that these points were used and reworked more heavily prior to being discarded.

BN 1818.1 appears to be a mix of both Mode 3 and Mode 4/5 techniques. The piece is made on a transverse flake with Levallois elements, including a radial dorsal scar pattern and facetted platform, which indicates that the flake-blank was derived from a prepared core. The flake has been retouched along the proximal and distal edges (which are equivalent to the lateral edges of the point) to create a sub-triangular teardrop planform. The retouching, shape, and size of BN 1818.1 are similar to other unifacial and parti-bifacial Mode 4/5 points, including BN 1693.3, 1802.90, 3477.3, 3575.3, and 2043.1. Each of these pieces was also made from end-struck whole flakes, and each piece shares with BN 1818.1 bilateral or semi-circular dorsal retouch that forms straight convergent lateral edges that expand outward before contracting on a rounded point butt.

Bulbar or basal thinning is evident on six parti-bifacial points. Five of these points are retouched ventrally along the butt edge, as well as the ventral right lateral edges of the tool.[35] The right lateral ventral retouching always extends halfway up the axis of the tool. The purpose of the right lateral retouching, if significant, is currently unknown.

Notches are present on four pieces (BN 4889.1, 2268.2, 1794.36, 1799.13), but it is uncertain if all of the notches relate to hafting. The notching is most commonly shallow, unifacial, and present on only one lateral edge (possibly the flake-blank right lateral). On BN

[35] Orientation via the tool should not to be confused with the orientation of the flake-blank.

4889.1, bilateral notches are located equidistantly approximately one-half to two-thirds from the point base. The left lateral notch is formed by a single large facet with several smaller auxiliary flake facets. The right lateral notch is formed by a single flake facet, but it also exhibits an abraded edge. The location of notching is similar across each of the four pieces.

Six points (BN 1693.3, 3477.3, 3575.3, 4258.1, 4889.1, 1818.1) also have finer and more intensive retouching along the lateral edges, approximately one-half to two-thirds from the point base. The retouching is so intensive on four points (BN 1693.3, 3477.3, 3575.3, 1818.1) that the lateral edge became slightly concave. In another two instances (BN 1818.1 and 4258.1), the lateral angle at the tip may have become more oblique due to more intensive retouching from the tip to midsection. These retouching patterns are believed to be related to hafting, and further evidence for hafting is found in BN 4889.1, which has bilateral notching at approximately the same location where the differential retouch on the other pieces begins. Therefore, if these points were hafted, then it is possible that the hafts obstructed the basal section of the point, meaning that only the exposed part of the point nearer the tip was retouched.

Bifacially flaked points appear to be retouched much more intensively than either unifacial or part-bifacial flaked points. Bifacial points BN 1799.16 and 1799.13 are especially retouched and their planforms are uncharacteristically ovate with more oblique tip angles. The other two bifacial points (BN 2116.2 and 4854.1), however, are slightly more elongate, and in the case of BN 2116.2, clearly have a teardrop planform, which might imply that BN 1799.16 and 1799.13 may have been used more heavily than BN 2116.2 and BN 4854.1 before being discarded.

In summary, the technological analysis of the Moche Borago whole points shows two technological traditions represented in the point assemblage. Mode 3 points are less frequent and are characterized by Levallois flaking techniques. Mode 4/5 points are made using either

unifacial, parti-bifacial, or fully bifacial techniques, and notching and basal/bulbar thinning techniques can also occur. BN 1818.1 appears to be a mix of both Mode 3 and Mode 4/5 techniques.

Typological Summary of the Moche Borago Points

Based on qualitative similarities observed in planform shapes (e.g. triangular, ovate, or teardrop) and styles of manufacture (e.g. notches, bulbar thinning, end-struck flake-blanks), I have been able to discern four possible typological groups within the Moche Borago points, which are named here for convenience. Figure 8-9 shows the distribution of the typological groups and the relationships between each group. Groups of points are first described individually and synchronically before being ordered chronologically to discuss typical point changes diachronically.

Group 1: Levallois: Levallois is a method of flake manufacture, which gives this group more affinity to aspects of technology than typology, but the Levallois technique is also a shared characteristic among several of the points. There are three pieces in the Levallois Group: BN 3114.1; 3132.1; 1799.12. This group is defined by use of the Levallois point flaking method, which includes the use of facetted platforms and convergent flaking/dorsal scars on prepared cores. Levallois points are also not intensively retouched, which means that BN 1818.1 is not included within the Levallois Group even though it is made on a transverse Levallois flake.

Group 2: Irra Xoketta Points: Irra Xoketta[36] is Wolaytiña for "teardrop," which is the characteristic shape of this point type. Irra Xoketta points are identified by two primary characteristics: their shape and retouch type. Irra Xoketta points are often made on end-struck whole flakes. Most Irra Xoketta points appear to be retouched more intensively on a single

[36] Pronounced as "Iræ Tokɛtta" following the International Phonetic Alphabet.

surface of the tool, typically the flake-blank dorsal surface. Bulbar/basal thinning is also common, which results in characteristic moderate-to-intensive ventral retouch, as well as a biconvex/lenticular profile.

The retouching pattern is often bilateral (lateral-lateral) along the lateral edges of the tool and semi-circular along the periphery of the point butt. This method of retouching creates a distinctive shape of the point, which is typically like a teardrop, but with subtle differences in the shape of Irra Xoketta points:

Irra Xoketta Type I points (BN 3477.3, 3575.3, 2116.2, 1818.1, 1693.3, 2043.1) have a sub-triangular planform with straight convergent lateral edges, expanding outward that terminate at a rounded butt. Finer retouching from approximately one-half to two-thirds up from the point butt often creates a slightly concave lateral edge form. Irra Xoketta Type I points are frequently made on end-struck whole flakes. Bulbar/basal thinning is common on both dorsal and ventral surfaces along the proximal edge, which doubles as the base of the point. The proximal edge retouching forms a distinctive rounded butt shape that distinguishes Type I points from Type II points.

Irra Xoketta Type II points (BN 1887.1, 2072.1) have straight or slightly convex lateral edges, but they do not appear to expand outward as obliquely as Type I points. As a result, Type II points often appear more elongate, even foliate. Type II points are also commonly made on end-struck flake-blanks, and bulbar/basal thinning is common. Unlike Type I points, Type II points are also characterized by more angular, trapezoidal butts.

Group 3: Tona Points (BN 4854.1, 1802.90, 1799.16, 1799.13, 4258.1): Tona points are bifacial with retouch that is characteristically finer and more intensive on one surface. Most of the Tona points within the current sample also seem to be heavily re-worked. Thus, the majority

of the Tona points tend to be typically smaller than Irra Xoketta points with sub-triangular or ovate platforms. Tona points are characterized by bilateral (tip-butt)/convergent flaking of the most heavily retouched point surface. The other surface often has a single large basal flake scar, which may originate from the original flake-blank ventral surface. Finer retouch is common along the tip and basal edges.

Group 4: Toora Points (BN 4889.1, 3574.1, 1794.36, 2268.2): Toora points are characterized by their shared triangular planform which is often produced by snapping (lateral-lateral) the flake-blank and retouching the distal lateral edges. Dorsal retouching is bilateral, and it seems to be most commonly lateral-lateral oriented, though BN 3574.1 has bilateral tip-butt retouch. Basal thinning is not present on Toora points. All four points within the current sample exhibit strong indications of hafting, including unilateral or bilateral shallow notching approximately one-half to two-thirds up from the tool and differential retouch patterns. In most cases, retouching of the dorsal surface (and in one case, the ventral surface: BN 2268.2) is finer beyond approximately one-half to two-thirds up from the point butt creating more oblique tip angles.

Diachronic Technological and Typological Point Patterns

Mode 3 points belonging to the Levallois Group are currently known only from the oldest and deepest strata at Moche Borago, which is the T-Group Lower. The Mode 3 Levallois technique is still present in overlying S-Group deposits, but at this time it is also associated with Mode 4/5 retouching and morphology (on both points and microliths). For example, one distinct typological characteristic of Mode 4/5 Irra Xoketta points is the use of bilateral dorsal scars to produce a medial ridge that may be related to prior Mode 3 techniques. More than 70% of Irra Xoketta points have a medial ridge, which increases the thickness of the points, although its functional value is unknown. Bifacial thinning is also evident in some points, such as BN 4854.1

and 1799.13, which shows that the technical means to remove medial ridges was present at that time.

Mode 3 points in the assemblage (BN 3114.1 and BN 3132.1) also have medial ridges due to Levallois convergent and radial flaking techniques. Furthermore, the only point in the assemblage, which shares Mode 3 and Mode 4/5 characteristics (BN 1818.1), also has a medial ridge because it was removed from a prepared core that created the semi-radial/convergent dorsal scar pattern. On other Irra Xoketta points the dorsal scars were made after the flake-blank was removed from the core. Therefore, the presence of a medial ridge on Irra Xoketta points, via the dorsal flaking technique, may represent a purposely maintained technical tradition that was carried over from prior Mode 3 technologies. Otherwise, we might expect to see more bifacial thinning techniques, such as on BN 4854.1 and 1799.13, which make thinner points that are easier to haft.

The use of Mode 3 and Mode 4/5 techniques to make microliths, such as BN 1818.6, suggests that continuity between technologies was not limited to points alone. In BN 1818.6, symmetry of the two technological traditions occurs; the former Mode 3 Levallois technique to produce the flake and the latter Mode 4/5 backing to create the tool. Therefore, it does not seem likely that a discrete break occurs between technological modes at Moche Borago. Gradual changes among types, such as the morphological variations that define Type I and Type II Irra Xoketta points, may also reflect similar processes of continuous technological change that resulted in subtle typological variations over time.

Conclusions

How do the points articulate with other aspects of the lithic assemblage? Based on the qualitative differences in point shape and design, there may be continuous technological changes that resulted in subtle typological changes in point morphology over time. Future quantitative

analysis on a larger sample of points is expected to provide statistically significant point changes over time.

In contrast, the other shaped tools, unshaped tools, and cores reveal differences in the types and frequencies of these artifacts between the S-Group and the T-Group. On the one hand, the points show subtle changes and inferred continuity, and on the other hand, the other artifacts suggest discontinuity or rapid change. How do these observations co-relate? First, it is important to account for cultural traditions at this time, including social and symbolic practices that may not be easily identified in the archaeological record. Clark (1988) suggested that hunter-gatherers in the Horn of Africa had developed cultural traditions and regional identities by the Late Pleistocene, which included unique point types. Many of the points in the Horn are small and have foliate shapes, and this regional pattern is substantiated by newer studies at sites such as at Aduma (Ethiopia) (Yellen et al., 2005; Brooks et al., 2006) and Porc Epic (Pleurdeau, 2001; Pleurdeau, 2005). Moche Borago's points fit within this regional cultural tradition, and the precise dating of the site's deposits provides a diachronic perspective often lacking at open-air (e.g. Aduma) sites or sites with questionable dating (e.g. Porc Epic). Many of the "transitional MSA/LSA" points described by Pleaurdeu (2001) also show strong similarities to the Moche Borago points, which may indicate similar ages, even though their actual age is questionable. Therefore, the points show that the Moche Borago T-Group and S-Group assemblages were probably made by groups of hunter-gatherers with similar cultural traditions, which may also relate to a broader cultural tradition found across the Horn.

Second, while cultural patterns may have remained largely unchanged that does not mean that people's use of the site or their adaptation to environments also did not change. For example, residency time at the site may have influenced the breadth of on-site activities, and

longer stays might account for more diverse stone artifact types in the S-Group versus shorter stays and fewer artifact types in the T-Group. Shorter stays during the T-Group may also account for the lack of curated tools from these levels. Simply put, the lack of formal shaped tools coupled with large amounts of debitage might indicate that the shaped tools were being repaired or modified on site at this time for the purposes of being used elsewhere. In lieu of using their shaped tools then, the occupants of the site relied on informal and expedient unshaped tools during their time at the site.

Therefore, while the points may imply cultural or, at least, technological continuity between the T-Group and the S-Group, these observations are not at odds with data about the other shaped tools, unshaped tools and cores. Stone artifacts other than the points appear to be influenced by different factors than the points, namely site use and mobility, which may be due to ecological changes in the area between the T-Group and S-Group.

Table 8-1: Frequency (upper) and percentages (lower) of the unshaped and shaped tools per total number of artifacts in this class.

	Backed	Scrapers	Points	Burins	Misc. Shaped	Unshaped Tools	Total
S-Group	15	47	70	8	14	125	279
T-Group Upper	2	7	19	3	5	15	51
T-Group Lower	0	7	14	1	3	14	39
Total	17	61	103	12	22	154	369

	Backed	Scrapers	Points	Burins	Misc. Shaped	Unshaped Tools
S-Group	4.07%	12.74%	18.97%	2.17%	3.79%	33.88%
T-Group Upper	0.54%	1.90%	5.15%	0.81%	1.36%	4.07%
T-Group Lower	0.00%	1.90%	3.79%	0.27%	0.81%	3.79%

Note: These values include tool fragments.

Table 8-2: Percentage of unshaped and shaped tools per stratigraphic aggregate.

	Backed	Scrapers	Points	Burins	Misc. Shaped	Unshaped Tools	Total
S-Group	5.38%	16.85%	25.09%	2.87%	5.02%	44.80%	279
T-Group Upper	3.92%	13.73%	37.25%	5.88%	9.80%	29.41%	51
T-Group Lower	0.00%	17.95%	35.90%	2.56%	7.69%	35.90%	39

Table 8-3: MNL frequency (upper) and percentages (lower) of the unshaped and shaped tools in the S-Group and T-Group.

	Backed	Scrapers	Points	Burins	Misc. Shaped	Unshaped Tools	Total
S-Group	8	41	29	8	9	57	152
T-Group Upper	2	5	7	3	3	10	30
T-Group Lower	0	4	4	1	3	7	19
Total	10	50	40	12	15	74	201

	Backed	Scrapers	Points	Burins	Misc. Shaped	Unshaped Tools
S-Group	3.98%	20.40%	14.43%	3.98%	4.48%	28.36%
T-Group Upper	1.00%	2.49%	3.48%	1.49%	1.49%	4.98%
T-Group Lower	0.00%	1.99%	1.99%	0.50%	1.49%	3.48%

Table 8-4: Frequency and percentage per stratigraphic group of unshaped tools based on non-MNL counts (above) and MNL counts (below).

	Modified		Utilized		Total
S-Group	64	51.20%	61	48.80%	61
T-Group Upper	6	40.00%	9	60.00%	10
T-Group Lower	7	50.00%	7	50.00%	8
Total	77	50.00%	77	50.00%	79

	Modified		Utilized		Total
S-Group	26	45.61%	31	54.39%	57
T-Group Upper	4	40.00%	6	60.00%	10
T-Group Lower	4	57.14%	3	42.86%	7
Total	34	45.95%	40	54.05%	74

Table 8-5: Percentages of edge damage on unshaped tools (MNL) based on the location of edge damage.

	Dorsal						
	Left Lateral	Right Lateral	Both Laterals	Distal	Distal Combo.	Proximal Combo.	Semi-Circular
S-Group	13.5%	13.5%	17.6%	5.4%	5.4%	0.0%	1.4%
T-Group Upper	1.4%	0.0%	4.1%	2.7%	1.4%	1.4%	0.0%
T-Group Lower	2.7%	0.0%	0.0%	0.0%	1.4%	0.0%	0.0%

	Ventral		
	Left Lateral	Right Lateral	Both Laterals
S-Group	2.7%	2.7%	2.7%
T-Group Upper	1.4%	0.0%	0.0%
T-Group Lower	0.0%	2.7%	0.0%

	Bifacial					
	Left Lateral	Right Lateral	Both Laterals	Distal Combo.	Indet.	Lateral Combo.
S-Group	4.1%	1.4%	1.4%	0.0%	0.0%	5.4%
T-Group Upper	0.0%	0.0%	0.0%	1.4%	0.0%	0.0%
T-Group Lower	0.0%	0.0%	0.0%	0.0%	1.4%	1.4%

Edge Damage Face	Percentage	Total
Dorsal	71.6%	53
Ventral	12.2%	9
Both	16.2%	12
Total		74

Table 8-6: Edge damage type on unshaped tools (MNL).

	Dorsal			Ventral			Bifacial/Parti-bifacial		
	Simple	Stepped	Combo	Simple	Stepped	Combo	Simple	Combo	Total
S-Group	56.9%	1.7%	19.0%	8.6%	0.0%	0.0%	8.6%	5.2%	58
T-Group Upper	70.0%	0.0%	10.0%	10.0%	0.0%	0.0%	10.0%	0.0%	10
T-Group Lower	42.9%	0.0%	0.0%	14.3%	14.3%	14.3%	14.3%	0.0%	7
Total Percent	57.3%	1.3%	16.0%	9.3%	1.3%	1.3%	9.3%	4.0%	75
Group Percent			74.7%			12.0%		13.3%	

Table 8-7: Relative percentage of blank types used for modified and utilized unshaped tools (non-MNL).

	Level	Side-Struck Flake	End-Struck Flake	Flake Fragments	Levallois flake	Levallois Point	Indet.	CTF	Burin	Total
Modified Tools	S-Group Percentage	6.30%	68.80%	15.60%			6.30%	3.10%		64
	T-Group Upper Percentage		83.30%			16.70%				6
	T-Group Lower Percentage		85.70%				14.30%			7
	Modified Tools Group Percentage	5.20%	71.40%	13.00%		1.30%	6.50%	2.60%		77
Utilized Tools	S-Group Percentage	1.60%	83.60%	6.60%	1.60%		1.60%	3.30%	1.60%	61
	T-Group Upper Percentage		88.90%			11.10%				9
	T-Group Lower Percentage		85.70%	14.30%						7
	Utilized Tools Group Percentage	1.30%	84.40%	6.50%	1.30%	1.30%	1.30%	2.60%	1.30%	77

Table 8-8: Mean aspect ratio and length values for whole modified and utilized unshaped tools (MNL).

Modified, n = 34			
		Aspect Ratio	Length
S-Group	Mean	1.71	23.9
	Std. Deviation	0.84	11.21
T-Group Upper	Mean	1.82	33.35
	Std. Deviation	0.85	13.83
T-Group Lower	Mean	1.44	28.54
	Std. Deviation	0.75	8.7

Utilized, n = 40			
		Aspect Ratio	Length
S-Group	Mean	2.2	26.2
	Std. Deviation	0.9	7.51
T-Group Upper	Mean	1.71	36.51
	Std. Deviation	0.92	7.57
T-Group Lower	Mean	1.28	33.4
	Std. Deviation	0.34	5.31

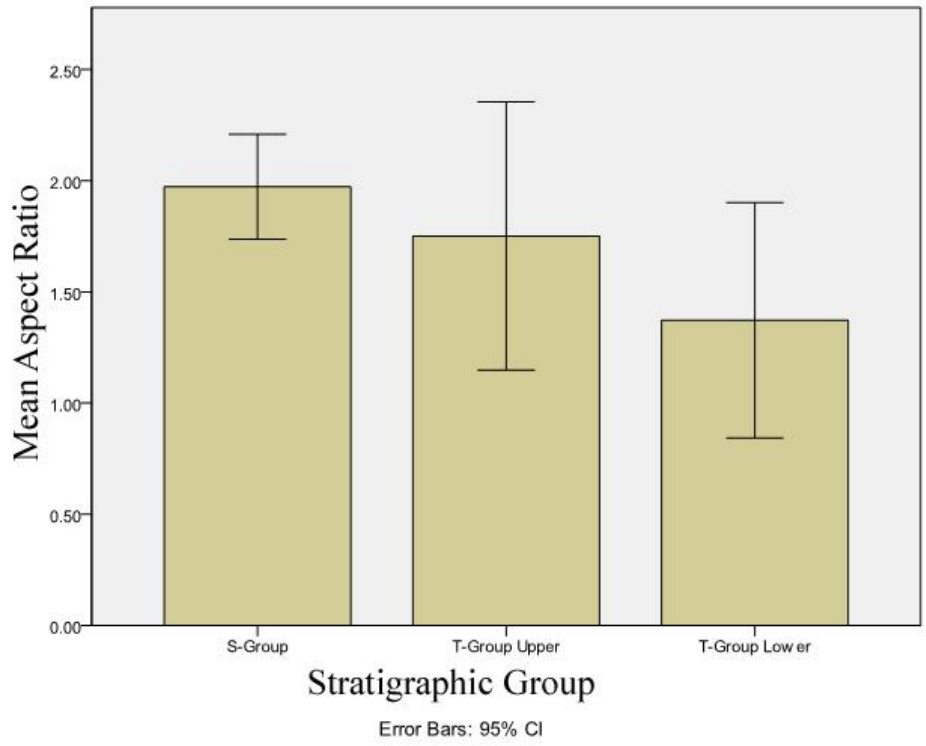

Figure 8-1: Average aspect ratio of unshaped (modified and utilized) whole flake-blanks between the three litho-stratigraphic groups.

Table 8-9: Basic metrical data and descriptions for miscellaneous shaped tools in the S-Group and T-Group (MNL).

Bag Number	Excavation Unit	Level	Stratigraphic Aggregate	Artifact Type	Raw Material	Length (mm)	Breadth (mm)	Thickness (mm)
1794.15	G10	11	S-Group	Drill	CBO	35.18	29.47	12.12
1794.27	G10	11	S-Group	Outil ecaille	CBO	27	27.85	8.69
1794.29	G10	11	S-Group	Awl	CBO	29.87	13.44	5.44
1794.39	G10	11	S-Group	Awl	CBO	19.4	9.17	5.1
1799.17	G10	12	S-Group	Outil ecaille	CBO	27.36	27.33	6.56
1802.102	G10	13	S-Group	Bec	CBO	30.86	14.19	9.67
1802.136	G10	13	S-Group	Awl	CBO	17	11.65	6.25
1802.82	G10	13	S-Group	Awl	CBO	26.34	16.18	10.32
1805.69	G10	14	S-Group	Awl	CBO	15.69	13.85	3.42
3105.11	G10	23	T-Group Upper	Irregular	CBO	27.68	23	3.75

Table 8-10: Basic metrical data and descriptions of the microliths found in the S-Group and T-Group.

Bag Number	Excavation Unit	Level	Stratigraphic Aggregate	Artifact Type	Raw Material	Length (mm)	Breadth (mm)	Thickness (mm)	Type of Backing	Angle of Backing
1799.15	G10	12	S-Group	Straight Back	CBO	25.22	11.01	3.77	Bidirectional	88
1799.42	G10	12	S-Group	Straight Back	CBO	21.92	15.68	3.93	Inverse	95
1802.2	G10	13	S-Group	Microlith Fragment	CBO	11.64	6.61	4.43	Obverse	100
1802.4	G10	13	S-Group	Collateral Backed	CBO	27.18	7.34	5.42	Bidirectional	68
1802.54	G10	13	S-Group	Orthogonal Truncation	CBO	15.71	9.21	7.06	Inverse	68
1802.98	G10	13	S-Group	Backed Blade	CBO	26.27	18.37	4.92	Obverse	65
1805.54	G10	14	S-Group	Curved Back	CBO	21.85	12.25	6.9	Bidirection	90
1805.58	G10	14	S-Group	Backed Blade	CBO	20.42	13.43	6.45	Natural	60
1805.73	G10	14	S-Group	Microlith Fragment	CBO	15.11	8.1	5.32	Natural	90
1805.75	G10	14	S-Group	Microlith Fragment	CBO	13.54	10.13	5.5	Obverse	82
1805.77	G10	14	S-Group	Microlith Fragment	CBO	15.46	8.97	2.66	Obverse	85
1805.78	G10	14	S-Group	Straight Back	CBO	18.25	10.75	3.34	Obverse	78
1805.83	G10	14	S-Group	Curved Back	CBO	11.04	10.14	2.39	Obverse	95
1818.5	G10	16	S-Group	Collateral Backed	CBO	20.35	5.25	4.68	Bidirectional	55
1818.6	G10	16	S-Group	Straight Back	CBO	31.81	15.78	3.87	Inverse/Alt	88
2571.1	G10	18	T-Group Upper	Crescent	CBO	30.1	7.83	2.93	Obverse/Alt	88
3105.12	G10	23	T-Group Upper	Straight Back	CBO	13.34	7.39	3.11	natural	87

Note: Microliths listed are complete unless otherwise noted in artifact type.

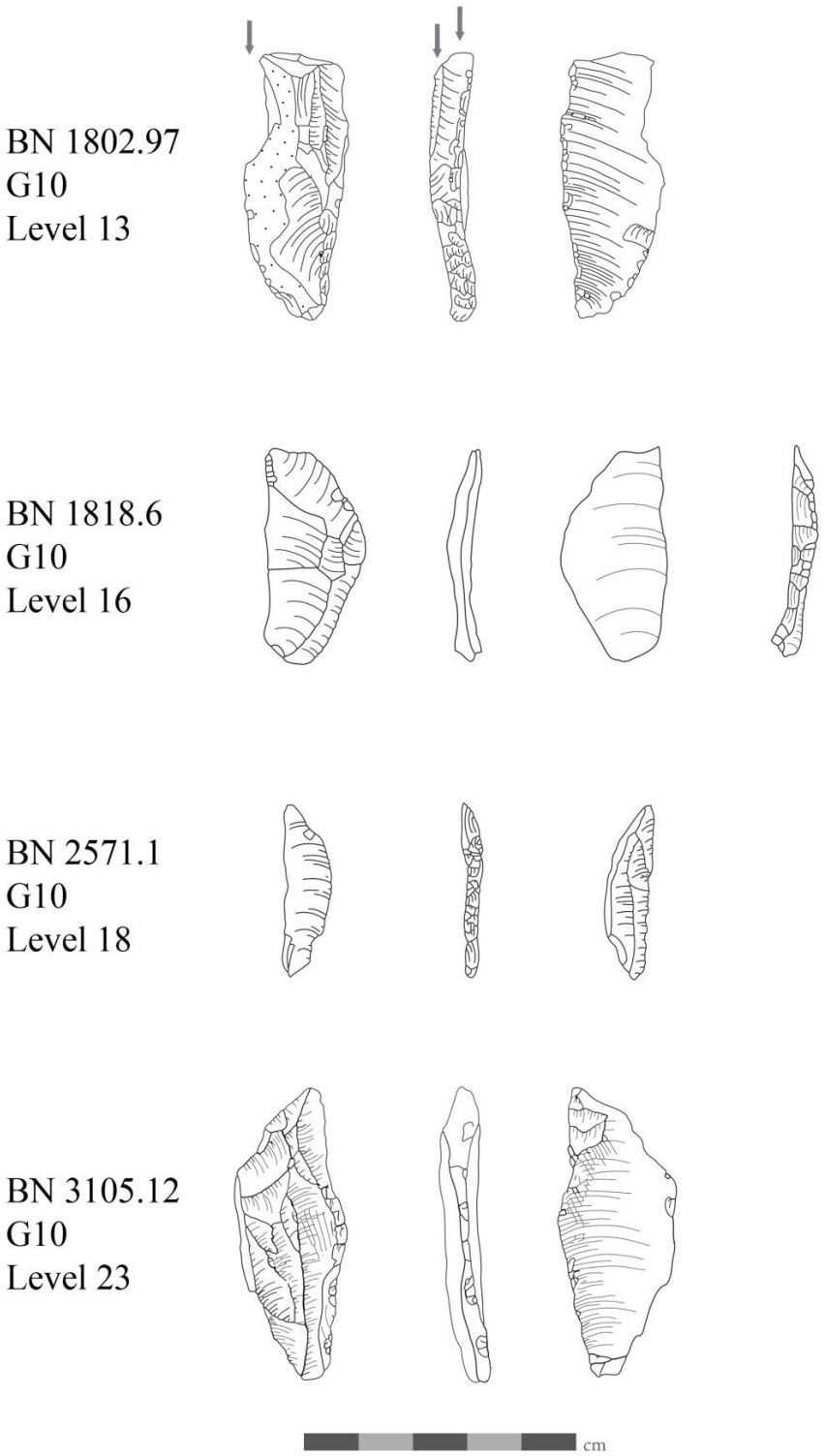

Figure 8-2: Microliths from the BXA T-Group and S-Group deposits.

Table 8-11: Frequency of scrapers and scraper fragments by type within each level and stratigraphic aggregate.

		End Scraper	Side Scraper	End and Single Side	End and Double Side	Double Side	Opposite side Dorsal/ Ventral	Notch and End or Side Scraper	Convergent Scraper	Notched Scraper	Irregular	Fragment	Total
S-Group	11	8	2	0	0			0	1	2	1		14
	12	1	0	1	1			0	0	0	0		3
	13	7	2	1	3			0	4	6	0		23
	14	2	1	0	0			1	0	3	0		7
	Total	18	5	2	4			1	5	11	1		47
T-Group Upper	18	2	0	0						0	0		2
	19	0	0	1						0	0		1
	21	1	0	0						0	0		1
	22	0	1	0						0	0		1
	23	0	0	0						0	1		1
	24	0	0	0						1	0		1
	Total	3	1	1						1	1		7
T-Group Lower	25	0	1		0	0	0	0				0	1
	27	1	0		0	1	0	0				0	2
	28	0	0		0	0	0	0				1	1
	29	0	0		0	0	0	1				0	1
	30	0	0		1	0	1	0				0	2
	Total	1	1		1	1	1	1				1	7

Note: Counts are not filtered for MNL.

Table 8-12: Relative percentage of scraper types and scraper fragments per level.

		End Scraper	Side Scraper	End and Single Side	End and Double Side	Double Side	Opposite side Dorsal/ Ventral	Notch and End or Side Scraper	Convergent Scraper	Notched Scraper	Irregular	Fragment
	11	57.10%	14.30%						7.10%	14.30%	7.10%	
	12	33.30%		33.30%	33.30%							
	13	30.40%	8.70%	4.30%	13.00%				17.40%	26.10%		
S-Group	14	28.60%	14.30%					14.30%		42.90%		
	Total	38.30%	10.60%	4.30%	8.50%			2.10%	10.60%	23.40%	2.10%	
	18	100.00%										
	19			100.00%								
	21	100.00%										
	22		100.00%									
T-Group	23										100.00%	
Upper	24									100.00%		
	Total	42.90%	14.30%	14.30%						14.30%	14.30%	
	25		100.00%									
	27	50.00%				50.00%						
	28											100.00%
T-Group	29							100.00%				
Lower	30				50.00%		50.00%					
	Total	14.30%	14.30%		14.30%	14.30%	14.30%	14.30%				14.30%

Note: Percentages are not based on MNL counts.

Table 8-13: MNL frequency of scrapers and scraper fragments by type within each level and stratigraphic aggregate.

		End Scraper	Side Scraper	End and Single Side	End and Double Side	Double Side	Convergent Scraper	Notched Scraper	Notch and End or Side Scraper	Irregular	Total
S-Group	11	8	2	0	0		1	2	0		13
	12	1	0	1	1		0	0	0		3
	13	6	2	0	3		3	5	0		19
	14	2	1	0	0		0	2	1		6
	Total	17	5	1	4		4	9	1		41
T-Group Upper	18	2		0				0		0	2
	19	0		1				0		0	1
	23	0		0				0		1	1
	24	0		0				1		0	1
	Total	2		1				1		1	5
T-Group Lower	25	0	1		0	0					1
	27	1	0		0	1					2
	30	0	0		1	0					1
	Total	1	1		1	1					4

Table 8-14: Relative percentage of scraper types and scraper fragments per level based on MNL counts.

		End Scraper	Side Scraper	End and Single Side	End and Double Side	Double Side	Convergent Scraper	Notched Scraper	Notch and End or Side Scraper	Irregular	Total
S-Group	11	61.50%	15.40%				7.70%	15.40%			13
	12	33.30%		33.30%	33.30%						3
	13	31.60%	10.50%		15.80%		15.80%	26.30%			19
	14	33.30%	16.70%					33.30%	16.70%		6
	Total	41.50%	12.20%	2.40%	9.80%		9.80%	22.00%	2.40%		41
T-Group Upper	18	100.00%									2
	19			100.00%							1
	23									100.00%	1
	24							100.00%			1
	Total	40.00%		20.00%				20.00%		20.00%	5
T-Group Lower	25		100.00%								1
	27	50.00%				50.00%					2
	30				100.00%						1
	Total	25.00%	25.00%		25.00%	25.00%					4

Table 8-15: Basic metrical data and descriptions of the scrapers (non-MNL) found in the S-Group and T-Group.

Bag Number	Level	Stratigraphic Group	Raw Material	Scraper Type	Length (mm)	Breadth (mm)	Thickness (mm)	Angle Left	Angle Right	Angle Proximal	Angle Distal
1794.10	11	S-Group	CBO	Side Scraper	32.63	14.57	14.18	89			
1794.18	11	S-Group	CBO	End Scraper	29.95	17.72	12.56			95	
1794.20	11	S-Group	CBO	End Scraper	34.58	23	10.19				71
1794.24	11	S-Group	CBO	Convergent Scraper	23.87	12.58	9.4	85	65		
1794.28	11	S-Group	CBO	End Scraper	20.28	14.49	6.59			45	78
1794.33	11	S-Group	CBO	Irregular	11.79	9.74	4.48	78	78	61	76
1794.34	11	S-Group	CBO	End Scraper	10.99	12.68	7.43				91
1794.35	11	S-Group	CBO	End Scraper	16.01	16.01	5.26				98
1794.38	11	S-Group	CBO	End Scraper	26.27	20.09	9.96				83
1794.41	11	S-Group	CBO	Side Scraper	30.91	12.29	6.22	70	68		
1794.51	11	S-Group	CBO	Notched Scraper	16.39	19	4.45	73	78		88
1794.54	11	S-Group	CBO	End Scraper	18.37	12.37	4.76				85
1794.71	11	S-Group	CBO	End Scraper	23.49	20.08	4.28			88	
1794.76	11	S-Group	CBO	Notched Scraper	23.77	14.43	6.08		56		90
1799.29	12	S-Group	CBO	End and Double Side	22.24	15.89	6.43	58	65		70
1799.32	12	S-Group	CBO	End and Single Side	24.11	14.32	5.7		68	66	
1799.45	12	S-Group	CBO	End Scraper	17.93	22.49	6.84				83
1802.104	13	S-Group	CBO	End Scraper	23.78	12.18	6.15				75
1802.112	13	S-Group	CBO	Notched Scraper	24.71	18.98	7.64		52		
1802.115	13	S-Group	CBO	End Scraper	20.48	13.37	5.42				80
1802.116	13	S-Group	CBO	End Scraper	16.62	17.25	8.03				82
1802.118	13	S-Group	CBO	End Scraper	19.28	11.92	6.06				88
1802.123	13	S-Group	CBO	Side Scraper	19.3	15.42	7.2				
1802.124	13	S-Group	CBO	Notched Scraper	18.98	14.03	3.17	61	60		

Table 8-15: Continued.

Bag Number	Level	Stratigraphic Group	Raw Material	Scraper Type	Length (mm)	Breadth (mm)	Thickness (mm)	Angle Left	Angle Right	Angle Proximal	Angle Distal
1802.126	13	S-Group	CBO	End and Double Side	19.64	11.7	7.6	64	84		88
1802.127	13	S-Group	CBO	Convergent Scraper	17.23	10.44	5.6	69	90	86	
1802.25	13	S-Group	CBO	Convergent Scraper	37.08	15.57	8.14	71	55		35
1802.26	13	S-Group	CBO	Notched Scraper	25.82	14.11	4.38	70	68		
1802.301	13	S-Group	CBO	End Scraper	31.77	13.68	4.6				
1802.34	13	S-Group	CBO	Convergent Scraper	18.39	15.97	7.03		75	80	
1802.41	13	S-Group	CBO	End Scraper	15.16	12.75	5.16				80
1802.57	13	S-Group	CBO	End and Double Side	18.53	11.88	4.84	82	67		93
1802.65	13	S-Group	CBO	Side Scraper	13.95	19.45	8.56	75			
1802.67	13	S-Group	CBO	End and Single Side	13.66	11.76	5.93	68			80
1802.68	13	S-Group	CBO	End Scraper	36.73	20.53	8.01				40
1802.80	13	S-Group	CBO	Notched Scraper	27.48	21.18	6.69				70
1802.87	13	S-Group	CBO	Convergent Scraper	32.8	17.07	8.25		75		
1802.88	13	S-Group	CBO	End and Double Side	23.97	22.78	6.46	72	71	75	
1802.91	13	S-Group	CBO	Notched Scraper	42.58	17.09	6.3	68	65		
1802.92	13	S-Group	CBO	Notched Scraper	22.68	14.93	3.81	44	52		

Table 8-15: Continued.

Bag Number	Level	Stratigraphic Group	Raw Material	Scraper Type	Length (mm)	Breadth (mm)	Thickness (mm)	Angle Left	Angle Right	Angle Proximal	Angle Distal
1805.24	14	S-Group	CBO	End Scraper	16.23	13.7	5.63			82	
1805.5	14	S-Group	CBO	Notched Scraper	37.19	24.02	5.72	68	81		
1805.57	14	S-Group	CBO	Side Scraper	14.43	12.99	4.9	85	98		
1805.70	14	S-Group	CBO	Notch and end or side scraper	19.25	12.17	6.77	83	60	75	
1805.74	14	S-Group	CBO	Notched Scraper	14.72	10.92	3.87		81		78
1805.80	14	S-Group	CBO	Notched Scraper	23.23	15.22	6.27		81		
1805.82	14	S-Group	CBO	End Scraper	23.63	13.24	4.28				82
3574.1	25	T-Group Lower	CBO	Side Scraper	38.16	26.29	9.7	56	74		
3730.3	27	T-Group Lower	CBO	End Scraper	17.32	15.49	5.86				68
3730.4	27	T-Group Lower	CBO	Double Side	32.02	21.58	8.75	50	55		

Table 8-15: Continued.

Bag Number	Level	Stratigraphic Group	Raw Material	Scraper Type	Length (mm)	Breadth (mm)	Thickness (mm)	Angle Left	Angle Right	Angle Proximal	Angle Distal
4109.6	28	T-Group Lower	CBO	Fragment, Indet.	15.36	16.5	4.68	71			
4100.2	29	T-Group Lower	CBO	Notch and end or side scraper	27.36	24.56	7.65	55	56		
4105.2	30	T-Group Lower	CBO	Opposite side dorsal / ventral	31.31	23.98	5.06	47	50		
4906.7	30	T-Group Lower	CBO	End and Double Side	24.45	18.8	7.41	82	74		85
2254.3	18	T-Group Upper	CBO	End Scraper	16.28	14.37	5.07				70
2254.7	18	T-Group Upper	CBO	End Scraper	30.2	16.8	8.47				80
2116.8	19	T-Group Upper	CBO	End and Single Side	34.65	17.57	7.84		83		75
2129.3	21	T-Group Upper	CBO	End Scraper	23.44	20.65	7.48				67
2133.3	22	T-Group Upper	CBO	Side Scraper	32.51	25.57	15.29	68			
3105.12	23	T-Group Upper	CBO	Irregular	50.93	19.99	6.14				
3575.7	24	T-Group Upper	CBO	Notched Scraper	31.54	25.84	6.41		77		

Table 8-16: Mean aspect ratios of all scrapers types (MNL) subdivided by litho-stratigraphic group.

	Aspect Ratio		
	Mean	Std. Deviation	N
S-Group	1.53	0.45	41
T-Group Upper	1.73	0.58	5
T-Group Lower	1.34	0.17	4

Table 8-17: Mean aspect ratios of MNL end scrapers only subdivided by litho-stratigraphic group.

	Aspect Ratio		
	Mean	Std. Deviation	N
S-Group	1.43	0.41	17
T-Group Upper	1.47	0.47	2
T-Group Lower	1.12	.	1

Table 8-18: Distribution of retouch location per scraper type (MNL).

	Dorsal	Ventral	Bifacial	Parti-bifacial	Total
End Scraper	95.00%	5.00%			20
Side Scraper	100.00%				6
End and Single Side	100.00%				2
End and Double Side	100.00%				5
Convergent Scraper	50.00%	25.00%		25.00%	4
Notched Scraper	80.00%	10.00%		10.00%	10
Irregular			100.00%		1
Double Side	100.00%				1
Notch and End or Side Scraper			100.00%		1

Table 8-19: Location of retouch per scraper type.

	Left Lateral	Right Lateral	Both Laterals	Distal	Distal Combination	Proximal	Proximal Combination	Semi-Circular	Circular	Total
End Scraper			5.30%	52.60%	21.10%	10.50%	5.30%		5.30%	20
Side Scraper	33.30%		33.30%	16.70%				16.70%		6
End and Single Side					50.00%		50.00%			2
End and Double Side					80.00%		20.00%			5
Convergent Scraper		50.00%			50.00%					4
Notched Scraper		25.00%	37.50%	12.50%	25.00%					10
Irregular										1
Double Side			100.00%							1

Note: End scrapers are retouched more frequently on the distal rather than the proximal, and side scrapers are retouched on either the left lateral or both laterals, but infrequently on the right lateral. The categories for "distal combination" and "proximal combination" refer to a combination of the specified edge and at least one other edge.

Table 8-20: Angle of the working edges for end and side scrapers.

	End Scraper						Side Scraper		
	Distal			Proximal			Left		
	Mean	Std. Deviation	N	Mean	Std. Deviation	N	Mean	Std. Deviation	N
S-Group	79.69	13.75	13	77.5	22.31	4	74.37	10.60	8
T-Group Upper	75.00	7.07	2						
T-Group Lower	68.00	-	1				69.00	17.01	3

Note: Derived from MNL filtered data.

Table 8-21: Frequency of working edge form for end scrapers (above) and side scrapers (below).

End Scraper Working Edge Form

Level	Straight	Convex	Serrated	Straight-Convex	Irregular	Total
11	2	5	0	1	0	8
12	1	0	0	0	0	1
13	2	1	1	2	0	6
14	2	0	0	0	0	2
18	1	0	0	0	1	2
27	1	0	0	0	0	1
Total	9	6	1	3	1	20
Total Percentage	45.0%	30.0%	5.0%	15.0%	5.0%	

Side Scraper Working Edge Form

Level	Straight	Convex	Concavo-Convex	Straight-Convex	Total
11	1	0	0	1	2
13	1	1	0	0	2
14	0	1	0	0	1
25	0	0	1	0	1
Total	2	2	1	1	6
Total Percentage	33.3%	33.3%	16.7%	16.7%	

Note: The data are based on MNL counts.

Table 8-22: Basic metric information on notched flakes from the S-Group and T-Group.

Bag Number	Level	Length (mm)	Width (mm)	Thickness (mm)	Retouch Class	Notch Width (mm)	Notch Depth (mm)	Notch Location
1794.76	11	23.77	14.43	6.08	Obverse	7.68	1.2	Distal Dorsal
1794.51	11	16.39	19	4.45	Inverse	11.25	1.95	Ventral Rt. Lat
1802.92	13	22.68	14.93	3.81	Obverse	7.06	2.14	Dorsal Rt. Lat
1802.124	13	18.98	14.03	3.17	Obverse			Dorsal Both Laterals
1802.26	13	25.82	14.11	4.38	Obverse	7.1	2.71	Dorsal Distal Rt. Lat
1802.80	13	27.48	21.18	6.69	Obverse	10.2	2.62	Distal Dorsal
1802.112	13	24.71	18.98	7.64	Inverse	7.44	2.42	Ventral right
1802.91	13	42.58	17.09	6.3	Part-Bifacial	15.99	3.63	Prox Left Lat Ventral
1805.80	14	23.23	15.22	6.27	Obverse			Dorsal Right Lateral
1805.5	14	37.19	24.02	5.72	Obverse	10.25		Dorsal Left Prox
1805.74	14	14.72	10.92	3.87	Obverse			Dorsal Distal and Right Lat
3575.7	24	31.54	25.84	6.41	Obverse	17.14	3.31	Dorsal Right Lateral

Note: All pieces are made of CBO. All artifacts listed are made on whole flakes except for BN 1802 .26 and 1805.74.

Table 8-23: Basic descriptive information of burins.

Bag Number	Level	Strat Group	Artifact Type	Raw Material	Length (mm)	Breadth (mm)	Thickness (mm)	Number of Burin Spalls	Width of Burin Cutting Edge (mm)	Angle of Burin
1794.5	11	S-Group	Other	CBO	27.22	16.09	6.4	1	7	65
1802.99	13	S-Group	Angle	CBO	28.75	29.64	9.25	1	9	75
1802.134	13	S-Group	Angle	CBO	34.83	11.96	5.25	1	4	89
1802.98	13	S-Group	Angle	CBO	46.42	18.41	5.89	1		
1805.11	14	S-Group	Angle	CBO	40.23	22.48	9.92	1	7	97
1805.19	14	S-Group	Dihedral	CBO	30.21	13.57	8.22	1	9	57
1805.5	14	S-Group	Dihedral	CBO	37	24	6	1		
1818.12	16	S-Group	Dihedral	Grey Obs.	31.98	12.3	11.2	3	5	52
2116.1	19	T-Group Upper	Other	CBO	44.46	10.01	7.43	1	6	
2116.4	19	T-Group Upper	Angle	CBO	36.6	20.1	5.28	1	4	83
2133.11	22	T-Group Upper	Multiple	CBO	50.69	23.2	10.79	4	6	95
4906.2	30	T-Group Lower	Dihedral	CBO	20.39	10.1	4.83	6	5	52

Note: All tools are whole, but some burins are made on flake fragments.

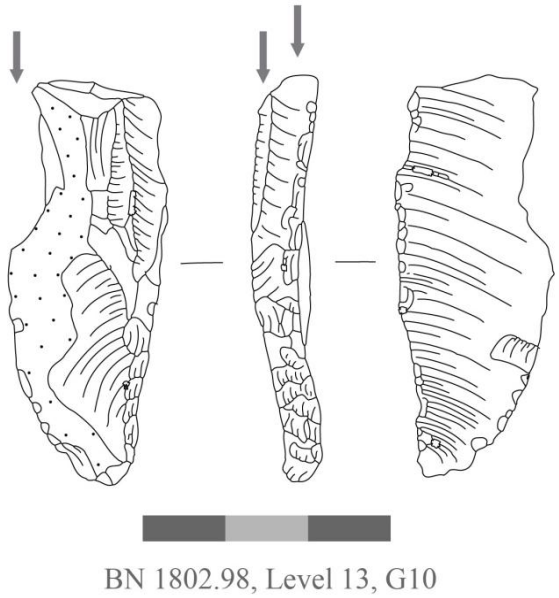

Figure 8-3: Angle burin from Level 13 with possible backing along the right lateral edge.

Figure 8-4: Dihedral burin recovered from Level 30.

Table 8-24: Frequencies of point retouch type.

	Level	Unifacial	Parti-Bifacial	Bifacial	Total
S-Group	11	10	3	1	14
	12	3	1	4	8
	13	18	7	1	26
	14	14	5	1	20
	15	2	0	0	2
	16	2	0	0	2
	Total	49	16	7	72
T-Group Upper	18	2		0	2
	19	3		1	4
	22	4		1	5
	23	2		2	5
	24	3		0	3
	Total	14		4	19
T-Group Lower	25	3	0	0	3
	28	1	0	1	2
	29	0	1	0	1
	30	4	2	1	7
	32	0	1	0	1
	Total	8	4	2	14

Note: Data derived from non-MNL counts.

Table 8-25: Percentages of point retouch type.

	Unifacial	Parti-Bifacial	Bifacial
S-Group	68.1%	22.2%	9.7%
T-Group Upper	73.7%		21.1%
T-Group Lower	57.1%	28.6%	14.3%

Note: Data derived using non-MNL counts.

Table 8-26: Completeness of the points (non-MNL) within the T-Group and S-Group.

	Whole	Broken Indet.	Proximal Fragment	Medial Fragment	Distal Fragment	Total
S-Group	29	22	11	2	6	70
T-Group Upper	7	4	3	5	1	19
T-Group Lower	4	3	2	2	3	14
Total	40	29	16	9	10	103
	38.8%	28.2%	15.5%	8.7%	9.7%	

Table 8-27: Frequency of bulbar thinning on points.

	Level	Absent	Marginal	Marginal to Semi-Invasive	Semi-Invasive	Invasive	Total
S-Group	11	5	0	1	0	0	6
	12	2	1	0	0	0	3
	13	11	1	1	1	1	15
	14	8	0	1	0	1	10
	15	2	0	0	0	0	2
	16	2	0	0	0	0	2
	Total	30	2	3	1	2	38
T-Group Upper	18	0	0		0		0
	19	2	0		0		2
	22	1	0		0		1
	23	1	0		0		1
	24	0	1		1		2
	Total	4	1		1		6
T-Group Lower	25	1		0		0	1
	28	0		0		0	0
	29	1		0		0	1
	30	2		1		1	4
	32	0		0		0	0
	Total	4		1		1	6

Note: Pieces with no evident bulb of percussion have been omitted from this table.

Table 8-28: Percentage of bulbar thinning found on points.

	Level	Absent	Marginal	Marginal to Semi-Invasive	Semi-Invasive	Invasive
S-Group	11	83.3%		16.7%		
	12	66.7%	33.3%			
	13	73.3%	6.7%	6.7%	6.7%	6.7%
	14	80.0%		10.0%		10.0%
	15	100.0%				
	16	100.0%				
	Total	78.9%	5.3%	7.9%	2.6%	5.3%
T-Group Upper	18					
	19	100.0%				
	22	100.0%				
	23	100.0%				
	24		50.0%		50.0%	
	Total	66.7%	16.7%		16.7%	
T-Group Lower	25	100.0%				
	28					
	29	100.0%				
	30	50.0%		25.0%		25.0%
	32					
	Total	66.7%		16.7%		16.7%

Note: Pieces with no evident bulb of percussion have been omitted from this table.

Table 8-29: Basic metric information for whole points.

Bag Number	Level	Group	Point Retouch Type	Raw Material	Physical Condition	Length (mm)	Breadth (mm)	Thickness (mm)
1794.25	11	S-Group	Unifacial Point	CBO	Fresh	48.16	22.54	6.18
1794.44	11	S-Group	Parti-Bifacial Point	CBO	Fresh	21.6	13.78	4.98
1794.48	11	S-Group	Parti-Bifacial	CBO	Fresh	16.75	14.53	4.12
1794.49	11	S-Group	Bifacial Point	CBO	Fresh	38.06	20.62	8.62
1794.52	11	S-Group	Unifacial Point	CBO	Fresh	36.63	16.51	6.69
1799.12	12	S-Group	Parti-Bifacial Point	CBO	Fresh	31.36	24.68	8.23
1799.13	12	S-Group	Parti-Bifacial	CBO	Fresh	24.16	18.43	4.69
1799.16	12	S-Group	Bifacial Point	CBO	Fresh	24.99	21.99	6.96
1802.105	13	S-Group	Parti-Bifacial	CBO	Fresh	36.4	16.26	5.4
1802.108	13	S-Group	Unifacial Point	CBO	Fresh	31.39	17.62	8.43
1802.121	13	S-Group	Unifacial Point	CBO	Fresh	18.18	14.46	5.04
1802.135	13	S-Group	Parti-Bifacial	CBO	Fresh	20.02	17.76	5.93
1802.85	13	S-Group	Parti-Bifacial	CBO	Fresh	30.92	22.12	6.25
1802.86	13	S-Group	Unifacial Point	CBO	Fresh	23.95	27.55	9.11
1802.9	13	S-Group	Unifacial Point	CBO	Fresh	20.63	29.27	8
1805.37	14	S-Group	Unifacial Point	CBO	Fresh	22.47	12.29	4.95
1805.55	14	S-Group	Unifacial Point	CBO	Slightly Abraded	19.65	10.29	5.68
1805.62	14	S-Group	Unifacial Point	CBO	Moderately Abraded	23.37	14.41	8.31
1805.63	14	S-Group	Unifacial Point	CBO	Fresh	11.76	10.7	4
1806.1	15	S-Group	Unifacial Point	CBO	Fresh	12.7	11.02	4.83
1806.9	15	S-Group	Unifacial Point	CBO	Fresh	23.46	16.81	7.69
1818.1	16	S-Group	Unifacial Point	CBO	Fresh	45.11	27.85	7.17
1818.4	16	S-Group	Unifacial Point	CBO	Fresh	8.88	12.41	3.65

Table 8-29: Continued.

Bag Number	Level	Group	Point Retouch Type	Raw Material	Physical Condition	Length (mm)	Breadth (mm)	Thickness (mm)
2116.2	19	T-Group Upper	Bifacial Point	CBO	Fresh	30.92	19.31	5.96
2116.3	19	T-Group Upper	Parti-Bifacial	CBO	Fresh	25.37	36.5	7.25
2116.7	19	T-Group Upper	Unifacial Point	CBO	Fresh	31.94	20.21	7.63
2133.2	22	T-Group Upper	Parti-Bifacial	CBO	Fresh	49.68	34.69	13.72
3132.1	29	T-Group Upper	Parti-Bifacial Point	CBO	Fresh	51.03	20.57	6.98
3477.3	24	T-Group Upper	Parti-Bifacial	CBO	Fresh	40.17	22.2	8.25
3575.3	24	T-Group Upper	Parti-Bifacial	CBO	Fresh	33.61	19.98	8.89
4564.3	25	T-Group Lower	Unifacial Point	CBO	Slightly Abraded	27.6	17.29	3.27
4105.7	30	T-Group Lower	Parti-Bifacial Point	CBO	Fresh	17.66	12.06	5.03
4854.1	30	T-Group Lower	Parti-Bifacial	CBO	Fresh	29	18.46	6.38

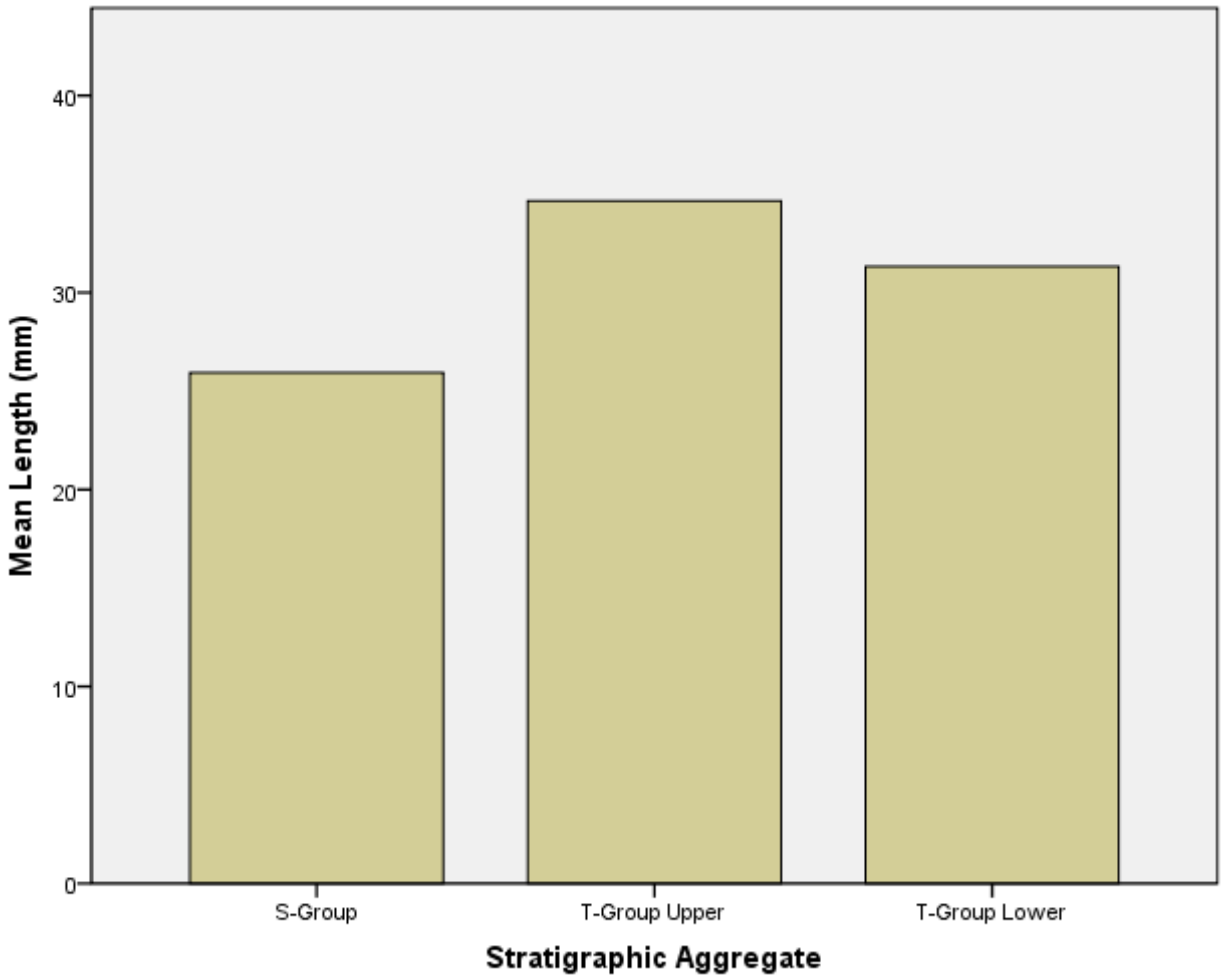

Figure 8-5: Histogram of the mean lengths of whole points per stratigraphic aggregate.

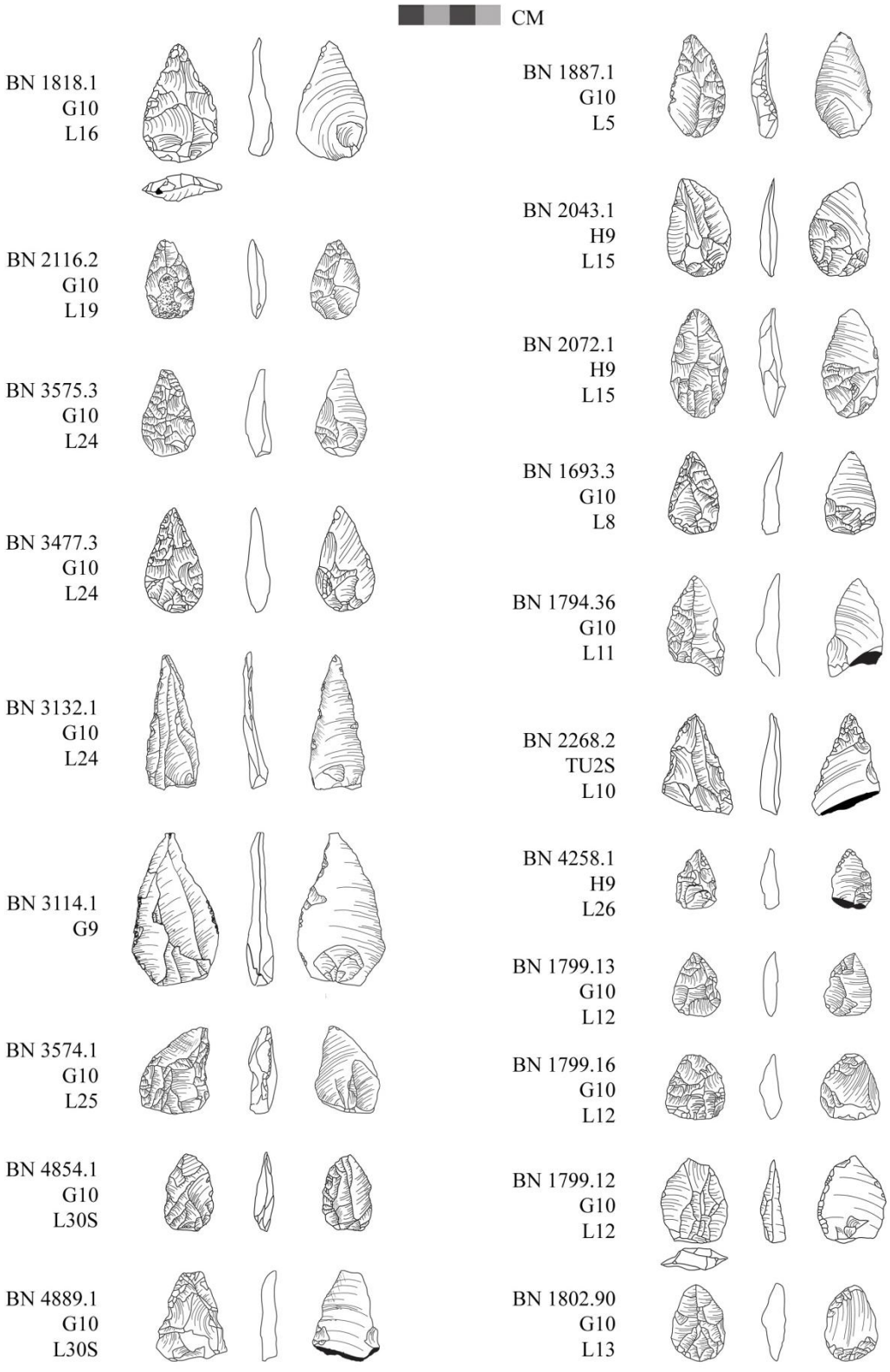

Figure 8-7: Points from the Moche Borago OIS 3 deposits. These points come from the BXA and TU2 areas, as well as the T-Group, S-Group, and the R-Group.

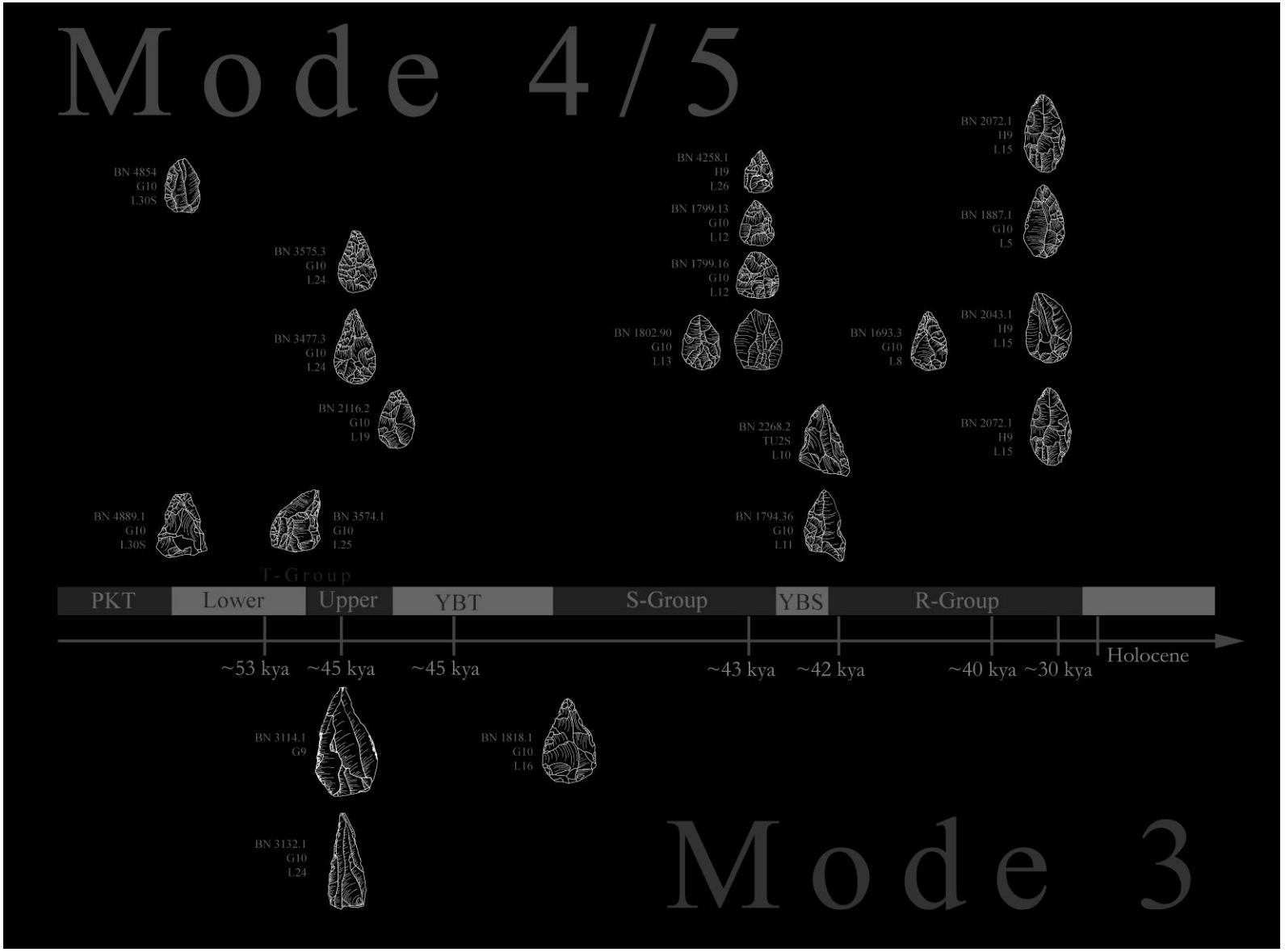

Figure 8-8: Point technological traditions represented at Moche Borago.

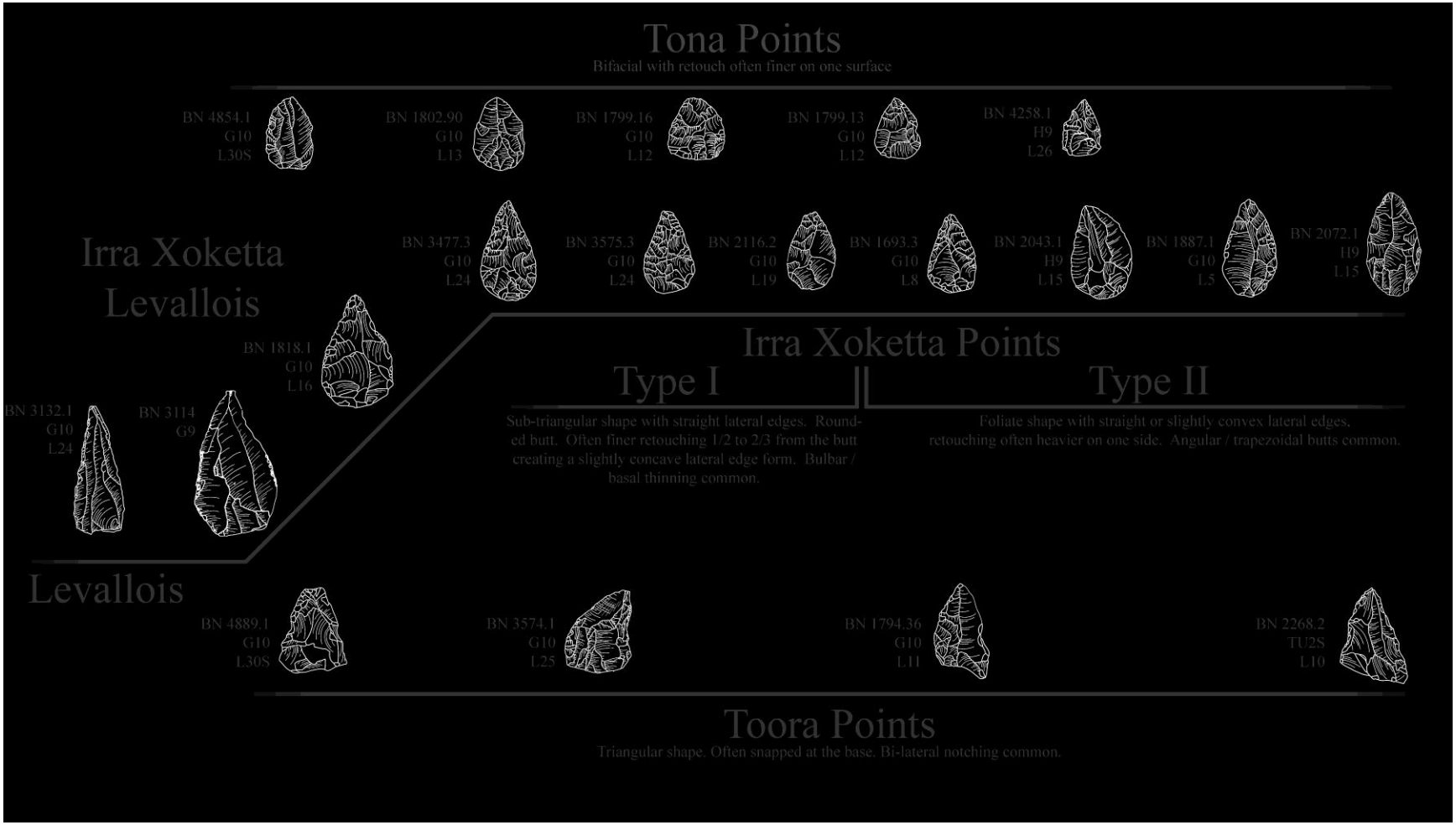

Figure 8-9: Point typology for Moche Borago. The points represented are ordered in a roughly chronological sequence.

CHAPTER 9
SYNTHESIS

This dissertation has studied human behavioral change during a known period of climatic flux, Oxygen Isotope Stage 3 (OIS 3), dated 59.4 to 27.8 ka. My study focused primarily on the frequencies and kinds of flaked stone artifacts that were used at the site from ~60 ka to ~43 ka to infer changes in hunter-gatherer subsistence strategy and site use. Based upon these findings, and drawing upon a top-down, multi-scalar methodology that described global and hemispheric climatic changes that likely affected regional and local environments, I have suggested that humans living in and around Moche Borago may have altered their behaviors in response to ecological changes brought on by monsoonal flux during OIS 3.

In Chapter 1, I posed four research questions:

1) What is the evidence at global, continental, and local scales for climatic fluctuations during early and middle OIS 3?
2) How might these climatic changes have affected the local ecology around Moche Borago?
3) If evidence exists at various scales for climatic and environmental fluctuations during OIS 3, how did the mobility patterns, subsistence strategies, and social organization of hunter-gatherers vary in response to paleoenvironmental instability?
4) If evidence exists at various scales for climatic and environmental fluctuations during OIS 3, how did hunter-gatherer stone tool technology vary in response to paleoenvironmental fluctuations?

I now attempt to provide succinct answers to these questions by drawing upon the discussions and analytical results presented in the previous chapters.

What is the Evidence at Global, Continental, and Local Scales for Climatic Fluctuations during Early and Middle OIS 3? How Might these Changes Have Affected Local Ecology Around Moche Borago?

Numerous multi-proxy data sources, such as speleothems, marine cores, and Nile paleohydrology records, indicate that the African and SW Asian monsoons reacted similarly and synchronously to high-latitude climatic changes above Greenland. Nile paleohydrology records, in particular, provide a direct link to monsoon-driven climatic changes in the Ethiopian highlands (Revel et al., 2010). At Moche Borago, fluvial activity peaks ~43 ka, which is contemporaneous to Dansgaard-Oeschger 11, when monsoons are expected to be more intense.

The catalyst behind monsoonal flux in the Horn appears to be related to broader climatic changes across the Northern Hemisphere at this time. Beginning in OIS 4, ~75 ka, Northern Hemisphere climates became increasingly unstable (Sanchez-Gone and Harrison, 2010; Wolff et al., 2010; Hessler et al., 2010). Heinrich events may have slowed or shut down the North Atlantic thermohaline circulation, which regulates oceanic temperatures and, by proxy, terrestrial temperatures and precipitation, creating cooler and more arid conditions (Hemming, 2004). Cooler sea surface temperatures would have reduced the land-sea thermal gradient and shifted the location of the Inter-Tropical Convergence Zone, minimizing the intensity of monsoonal winds across Africa and SW Asia (Vidal and Arz, 2004; Tierney et al., 2008). In contrast, the rapid warming associated with Dansgaard-Oeschger (D-O) events would have increased Northern Hemisphere insolation, which intensified the land-sea thermal gradient and strengthened the monsoons from West Africa to Western Asia (Wang et al., 2001; Burns et al., 2003; Burns et al., 2004; Cai et al., 2006; Cosford et al., 2008; Revel et al., 2010).

Numerous multi-proxy records show contemporaneous African and SW Asian monsoonal variability, which is in sync with high-latitude temperature anomalies above Greenland, such as D-O events. Marine core records from the Gulf of Guinea show African monsoonal flux during

D-O events (Weldeab et al., 2007). Unpublished new data from the same location demonstrate that the monsoons are tightly linked to high-latitude temperature anomalies during OIS 3 (S. Weldeab per comm.). Sapropel events seen in the Soreq cave speleothem records reveal similar variations in the African monsoons across the eastern Mediterranean region (Bar-Matthews et al., 2000). In the Indian Ocean, the Moomi cave record from Socotra Island, as well as Arabian Sea marine cores, provides detailed accounts of SW Asian monsoonal flux during D-O events (Schulz et al., 1998; Burns et al., 2003; Burns et al., 2004).

The highlands of Ethiopia, and in particular the SW Highlands, are uniquely positioned to receive both West African and SW Asian monsoonal precipitation, and this area would have experienced increased monsoonal precipitation during D-O events. Nile paleohydrology records are linked to climatic fluctuations affecting the source waters in the Ethiopian highlands, and these records show increases in monsoonal activity in the Ethiopian highlands during OIS 3 (Revel et al., 2010). The orographic effects of the highlands on monsoonal air masses (Mohammed et al., 2004) may have even increased rainfall in SW Ethiopia, as those air masses similarly do today.

At Moche Borago, S-Group or similar deposits in each of the three excavation areas show clear geomorphic evidence that the local area was wetter ~43 ka. In the BXA, the LVDBS deposits of the S-Group represent channel-fill deposits of a fluvial feature that cut into tephra YBT. Sections of tephra YBT were even missing in the BXA, which is likely due to cut-and-fill activity from the BXA channel. In TU2, fluvial activity truncated and undercut the TU2 L-Group. In N42, size-sorted channel-fill deposits unconformably overlie the L-Group deposit (ULF) in that area.

Stratigraphic correlations and radiometric dates from the BXA and TU2 showed that the S-Group fluvial features in those two excavation areas were contemporaneous. Geochemical and stratigraphic correlations link these features to fluvial features also found in N42. The YBT (underlying) and YBS (overlying) tephras bracket the S-Group deposits in the BXA and TU2, providing the maximum and minimum weighted mean age estimate of the fluvial activity: 43,403 ± 1,213 cal. BP to 43,121 ± 692 cal. BP, respectively. The weighted mean age of radiocarbon samples on charcoal taken directly from the BXA and TU2 S-Group deposits fit the YBT-YBS chronology, 43,480 ± 443 cal. BP.

Therefore, from ~44 ka to ~43 ka, a series of high and low energy fluvial features were present at Moche Borago. The source of the water was likely due to percolation from joints within the rear rockshelter walls. A similar phenomenon is seen at Esay rockshelter today, which has an active stream channel in that site. The morphology of the channel features and condition of associated stone artifacts suggest that the energy of the stream flows on-site were lower around the BXA and greatest at N42. Size-sorting or abrasion is not indicated on the stone artifacts in the BXA, and these stone artifacts are currently believed to be *in situ*. The presence of the freshwater at this time may have been a major incentive for occupation of the site.

The timing of the fluvial activity at Moche Borago coincides closely with wetter and warmer climatic conditions that would have occurred during D-O 11, 43.4 ka. The D-O 11 event is evident in both high-latitude ice cores and regional records surrounding the Horn of Africa. Above Greenland, D-O 11 is associated with the greatest increase in mean annual temperatures known during OIS 3, 15°C (Wolff et al., 2010). Across Africa, monsoonal activity may also have increased at this time. West African Atlantic marine core records indicate that African monsoonal precipitation was greater at 43 ka just prior to a dry event at 42.5 ka, though the

changes are subtle (S. Weldeab per comm.). The Moomi cave records show a similar, subtle pattern of monsoonal increase ~43 ka (Burns et al., 2003; Burns et al., 2004). Nile paleohydrology records also indicate a broad period of pluvial conditions at this time, which show wetter conditions in the Ethiopian highlands (Revel et al., 2010).

In summary, a chain of evidence suggests that high-latitude climatic changes affected low-latitude climates and environments. In the Horn of Africa, climatic changes impacted the monsoon systems, which account for much of the annual moisture in the area. At Moche Borago, on-site fluvial activity peaked ~43 ka. The timing of this fluvial activity is concurrent to the well-dated and well-studied D-O 11 event, which had the second highest temperature flux during OIS 4 and OIS 3 (+15°C) (Wolff et al., 2010). As with other D-O events during this time, D-O 11 probably had a significant impact on monsoon intensity across the Horn, and I currently believe that the increased fluvial activity at Moche Borago ~43 ka is linked to the D-O 11 event.

If Evidence Exists at Various Scales for Climatic and Environmental Fluctuations during OIS 3, How Did the Mobility Patterns, Subsistence Strategies, and Social Organization of Hunter-Gatherers Vary in Response to Paleoenvironmental Instability?

The frequency and type of stone artifacts represented in the Moche Borago assemblages change from the T-Group to the S-Group litho-stratigraphic units. The T-Group assemblage is composed largely of debitage, and more kinds of raw materials may have been collected and used during the T-Group than in the S-Group. These raw materials may indicate that hunter-gatherers were traveling farther across the landscape, collecting different raw materials, and staying at the site for only brief periods of time. In contrast, the S-Group assemblage is almost completely made from locally available common black obsidian (CBO). The S-Group has more stone artifacts and more diverse types of stone artifacts, which might be due to longer occupation time in the rockshelter. The lack of fragmentary debitage in the S-Group may indicate residential activities like waste management.

Today, Moche Borago is located within the Afromontane woodlands on the volcano massif of Mt. Damota. The site is also within a day's walk to lowland grassy woodlands at the base of the volcano and Southern Rift Valley, as well as lacustrine resources from nearby Lake Abaya and other lowland resources in the Omo gorge. However, lake core and pollen records from across eastern Africa indicate that the montane woodlands would have moved to higher elevations during arid phases of the Terminal Pleistocene and Holocene due in part to decreased monsoonal precipitation at lower elevations (Maitima, 1991; Hildebrand, 2003; Kiage and Liu, 2006). Holocene lake level records from the Ziway-Shala basin north of Lake Abaya also reveal that lake levels across the region would have fallen during arid phases as a result of decreased monsoonal rains (Gillespie et al., 1983; Lamb et al., 2000; Chalie and Gasse, 2002; Benvenuti et al., 2002). The distances separating each ecological zone would have increased during arid phases of weakened monsoonal precipitation. Therefore, during arid periods, it may have been more advantageous for hunter-gatherers to live in lowland woody grasslands below Mt. Damota, which may have been more centrally located to other ecological zones and resources in the area. Precipitated freshwater probably still collected atop the mountain and drained into the surrounding valleys during arid periods similarly to drought conditions in the region today (Borena, 2008).

The stone artifact assemblages from the T-Group may date to one such period of aridity though more precise dating and geomorphological work still needs to be done. Current evidence suggests that the T-Group Upper deposits were laid down in a humid environment (P. Goldberg, per comm.), and I think it is likely that the T-Group Upper deposits may date to D-O 12, which began 46.8 (Svensson et al., 2008; Wolff et al., 2010). But, the absence of fluvial channels

throughout the T-Group deposits suggests that the climatic conditions were unlikely to be as wet as the S-Group, even if some of the deposits do date to D-O 12.

The T-Group stone artifacts appear to have accumulated at the site via repeated brief trips where only limited activities were undertaken. If the site was only briefly occupied throughout the T-Group, due to marginalization or no *in situ* freshwater supply, then the range of on-site activities represented in the stone artifacts might be smaller than in the S-Group when extended occupation was more likely. The T-Group assemblages are dominated by debitage (> 85%) and there are 130% fewer cores and 200% fewer shaped and unshaped tools in the T-Group compared to the S-Group. Furthermore, there are only seven scrapers and four burins in the T-Group compared to 47 scrapers and 8 burins in the S-Group. The most diverse kinds of raw materials are also found in the T-Group (and especially T-Group Lower), which includes multiple kinds of obsidian, chalcedony, basalt, quartzite, and chert. The sources of these raw materials remain speculative, however, but the volcanic geology of the immediate area makes it highly unlikely that the chalcedonies and cherts were available locally.

The relatively sparse amount of cores, shaped tools, and unshaped tools in the T-Group suggests 1) there were relatively fewer activities on site than in the S-Group, due to the lack of burins, scraper, or other specialized tools and 2) that if shaped and unshaped tools or cores were brought into the site during the T-Group, then they were likely modified and taken away. This pattern of curation would also help to explain the large amount of T-Group debitage: Stone tools were being repaired or modified on-site and then taken away. The more diverse raw material types in the T-Group may indicate that more raw material sources were encountered and used at this time as hunter-gatherers were foraging for resources farther across the landscape due to increased separation between ecological zones (cf. Ambrose, 2002).

In contrast, during time periods when monsoonal intensity increased, hunter-gatherer mobility around Moche Borago may have decreased. More resources may have been available locally, especially if the montane woodlands moved toward lower elevations. Moche Borago may have been located between highland woodlands and lowland grassy woodlands, with supplemental resources coming from Lake Abaya and the Omo Gorge. Another source of *in situ* freshwater, which is evident in the S-Group geomorphology, would have been an added attraction to occupy the site for longer periods of time.

During the S-Group, Moche Borago may have offered an ideal balance between protection from the elements, convenience to resources (including locally available obsidian), and ecotone resource diversity and abundance. Most of the stone artifacts in the S-Group appear to be made of CBO, assumed to be locally available. Two sources of CBO are known within 15 km of the site. The large amounts of shaped tools, unshaped tools, and cores indicate that frequent activities were performed on-site during the S-Group. Tools such as burins and drills may have been used to work wood or bone for hunting or foraging implements such as spear shafts or digging sticks. Scrapers show that animal hides were processed on-site. Numerous points suggest that at this time hunting forays were also based out of the site.

In addition, evidence shows that the people living at the site at this time managed the site by possibly removing waste by-products of stone tools production. The size of the S-Group assemblage is 50% smaller than the T-Group Upper or Lower. Hypothetically, more intensive occupation of a site should generate more stone tools debris, but less debris might indicate that the site was also actively maintained. It is unrealistic to assume that behaviorally modern humans, their families, and their children living in Moche Borago wanted to walk on razor sharp stone debris. The rockshelter was their home. Therefore, one possible explanation worth further

study, is that the smaller S-Group assemblage may indicate that occupants at the site were collecting and redistributing lithic debitage outside of the cave. Further evidence for site management may be found in the lack of S-Group fragmentary debitage. More than three-fourths of the S-Group debitage is comprised of whole flakes, which may have been produced to make shaped and unshaped tools. No evidence suggests that the lack of fragmentary debitage is due to fluvial sorting or other natural processes. Therefore, while whole flakes may have been collected for shaped and unshaped tools, the fragmentary debitage could have been intentionally discarded.

In summary, the Moche Borago stone artifact assemblage shows patterns that give evidence to hunter-gatherer site use, mobility, and subsistence strategy. The debitage dominated T-Group assemblage contrasts with the abundant shaped tools, unshaped tools, and cores in the S-Group. The emerging picture of hunter-gatherer life ways may be due to varying amounts of aridification and separation between ecological zones and resources. The site may have been marginally located to numerous ecological zones during arid periods, and hunter-gatherers infrequently relied on the rockshelter at these times, perhaps as they ranged far and wide across the landscape for resources. Wetter times meant that woodlands moved into lower elevations. The Rift Valley lakes probably also expanded, and the site may have been centrally located to numerous resources. An on-site source of freshwater may have lured people to this location. S-Group stone artifacts attest to a wide range of on-site activities at this time, which relate to foraging and hunting activities, as well as domestic activities such as hide scraping.

If Evidence Exists at Various Scales for Climatic and Environmental Fluctuations during OIS 3, How Did Hunter-Gatherer Stone Tool Technology Vary in Response to Paleoenvironmental Fluctuations?

Hunter-gatherers living in and around Moche Borago may have altered their way of life and their technologies in accordance with suspected ecological changes caused by monsoonal

flux and broader climatic instability. In addition to suspected changes in subsistence economy and mobility, these hunter-gatherers began relying on Mode 4/5 stone tool technology that had similarities to Mode 3 techniques and knowledge. The timing of the newer Mode 4/5 technology at Moche Borago and probably at other sites, such as Enkapune Ya Muto in Kenya and Mumba rockshelter in Tanzania, coincides with unstable climatic conditions during OIS 3. These erratic conditions would have affected monsoon systems across the region and the distribution of ecological zones and natural resources. The switch to Mode 4/5 technology was an adaptation to the social and economic requirements of the OIS 3 hunter-gatherers as climates and environments fluctuated across the region and over time.

Modern hunter-gatherers living in unpredictable environments such as deserts employ flexible behavior strategies that enable them to adapt to, and exploit, numerous available resources in varying ecological zones (Yellen, 1977). During OIS 3, climatic instability across the Horn may have created environmental conditions where resource availability and location were similarly unknowable and unpredictable. More abundant or diverse resources during wetter periods of OIS 3 may have made collecting resources from known sources easier. But, the variable conditions would have required repeated re-learning of the natural environments, thus finding new resources would have cost valuable time and energy (Kelly, 1995). The development at this time of new tool types (e.g. microliths) for new technologies (e.g. the bow and arrow) with lightweight, portable, and multi-component designs would have allowed hunter-gatherers to range more freely across the landscape to find and utilize diverse resources.

Evidence suggests that certain technological developments, which are found more frequently in the S-Group, begin in the T-Group Upper[37] when several new types of stone

[37] Analysis is ongoing to assess culture-stratigraphic divisions within the assemblage, but in this dissertation I relied strictly on litho-stratigraphic breaks to avoid confusion.

artifacts first appear, including Mode 4/5 Type I Irra Xoketta points and microliths. But Mode 3 Levallois cores and points are also still present. Both Mode 3 and Mode 4/5 stone artifacts in the T-Group Upper suggest that hunter-gatherers were adjusting their stone tool technologies at this time, but still retaining tried and true methods. Technological development toward smaller and multi-component stone artifacts, such as microliths, suggests that hunter-gatherers at this time desired less wieldy tools that could be repaired and applied flexibly and to various applications. If the T-Group Upper dates more precisely to D-O 12, as I have speculated, then it means that hunter-gatherers may have begun developing new technologies as early as the T-Group Upper to contend with variable and unpredictable climatic and environmental conditions associated with monsoonal flux during OIS 3. The mobility patterns of these people during the T-Group Upper were still fairly mobile, however, perhaps due to long distances between resources.

While new tool types appear in the T-Group Upper, the prior Mode 3 technology does not disappear completely, and its sustained presence in the S-Group indicates that the technological innovation of Mode 4/5 tools was a prolonged and complex process. Several tools (e.g. BN 1818.1 and 1818.6) show that Levallois techniques were used to make Mode 4/5 tools in the S-Group, and Irra Xoketta points may also derive aspects of their unique morphology from Mode 3 technology. The mixing of techniques implies that hunter-gatherers had not completely abandoned the older knowledge base (Mode 3), but were incorporating it into the new system, possibly in innovative ways and contexts.

Ongoing technological innovation might also account for the increase in less formal single platform core designs within the assemblage. Single platform cores become the dominant core type in the T-Group Upper, and this pattern is similarly seen in the S-Group. The single platform cores are made casually, and they appear to be based on informal designs, which is unlike

pyramidal or prismatic core types commonly seen in later periods. It is possible that old technological traditions were being revised or abandoned at this time, while new technological traditions were still in formative stages. Therefore, the informality of single platform core designs may be because technologically or culturally specific formal core designs had not yet been settled upon at this time.

In summary, ~45 ka, T-Group hunter-gatherers at Moche Borago began to develop and use new types of Mode 4/5 stone artifacts, such as microliths and Irra Xoketta points. Warmer climates due to D-O 12 may have brought wetter conditions to the area, though these conditions were still likely drier than during the later periods represented by S-Group deposits. The development of Mode 4/5 technologies at this time could have been a coping mechanism to the destabilized environments and unpredictable resources brought about by the monsoonal fluctuations. The designs of the new tools may have prioritized efficiency and portability, which would have been essential if the locations and types of resources in an area were changing. Individual pieces used in multi-component tools could be repaired separately and the use of microlithic technology was lightweight.

By ~43 ka, added monsoonal moisture may have increased resource diversity around Moche Borago, especially if the montane woodlands moved toward lower elevations and the distances to other resources, like Lake Abaya, shortened. Coupled with an on-site freshwater supply, and Moche Borago may have been an ideal residential base to utilize highland woodland, lowland grassland, and numerous other resources. The more intensive occupation of the site at this time (S-Group) gives a more in-depth glimpse into hunter-gatherer life ways and behaviors, and stone tools suggest on-site activities related to hunting, foraging, and domestic tasks.

But the environment would have still been in a state of flux due to increased monsoonal rains and the locations and types of resources may have been largely unpredictable. Stone artifacts from this time suggest that hunter-gatherers continued to utilize Mode 3 technological knowledge and skills along with the newer Mode 4/5 system. Even though more diverse resources may have been available at this time, which likely affected mobility patterns, the long-term unpredictability of the resources and their locations may have sustained technological innovation. The continued innovation of Mode 4/5 tools into the S-Group, therefore, suggests that the development of Mode 4/5 tools, like microliths, at this time was not a direct product of increased mobility, but rather a by-product that enabled hunter-gatherers to become more mobile, dependent on the circumstances. Thus I believe that the development and continued innovation of Mode 4/5 technology found at Moche Borago shows that these people were adapting primarily to the variable environments and unpredictable resources in early OIS 3.

Moche Borago in Broader Perspective

Three variables place Moche Borago into its regional context: time period, environment, and culture. The timing of the earliest Mode 4/5 technology across eastern Africa is perhaps the most contentious of the three variables due to dating issues at other sites like Mumba (Mehlman, 1989; Prendergast et al., 2007) and Enkapune Ya Muto (Ambrose, 1998a) rockshelters,. However, the ages of the Mode 4/5 deposits from these sites suggests to me that OIS 3 is emerging as the consensus for this region (see Chapter 4).

Last Glacial environments and climates may have heavily influenced hunter-gatherers living in both highland and lowland environments of the Horn and East Africa. Ambrose (2002), for example, has hypothesized that unpredictable environments in savanna environments of East Africa during the Last Glacial required hunter-gatherers to develop more mobile subsistence strategies and tool kits and also exchange systems. However, lowland climates in East Africa

may have been even drier than highland Ethiopia at that time, and detailed paleoenvironmental records for the Horn and East Africa are generally lacking. Therefore, comparisons between highland and lowland sites must be made cautiously.

Throughout this dissertation, I have argued that the development of Mode 4/5 technology occurred during early OIS 3 at Moche Borago. While I am confident in my conclusions, I am also aware of the limitations of my data, which is only an early OIS 3 stone artifact assemblage. Currently, no earlier *in situ* archaeological deposits are known at Moche Borago. It is equally plausible that Mode 4/5 technology could have developed earlier during OIS 4 in response to monsoonally-driven climatic fluctuations and environment instability, if my theory is correct. D-O events occurred in OIS 4 as early as ~76 ka (D-O 20) (Wolff et al., 2010). D-O 19, dated ~72.3 ka, was associated with the biggest temperature anomaly of the Late Pleistocene above Greenland (+16°C) (Landais et al., 2004), and it could have had a significant impact on monsoonal patterns across the Horn and East Africa. But my main point is that whether or not Mode 4/5 was developed during OIS 4 or OIS 3, the key factor may have been that hunter-gatherers were adapting more toward regional climatic instability and resource unpredictability rather than to a broad period of aridification, resource depletion, and ecological niche narrowing.

The idea of regional cultural traditions in the Horn and East Africa during the Late Pleistocene can be traced back to Leakey (1931; 1936) and Clark (1954; 1988), who maintained that artifact morphology and frequency, especially in points, reflected distinctive styles that were expressions of cultural variability. The Type 1 and 2 points from Moche Borago, which in the previous chapter I have tentatively named "Irra Xoketta," may also be found to be stylistically and culturally distinct.

Local evidence for regional cultural traditions around Moche Borago may be seen in stone artifacts predating and postdating the YBT eruption at the site. Similarities between point typologies before and after YBT show that the reoccupation of Moche Borago after YBT was by hunter-gatherers who shared a culture with prior occupants at the site. Irra Xoketta, Tona, and Toora points each occur in the T-Group Upper and the S-Group. Microliths and single platforms cores, which occur for the first time in the T-Group Upper, are also similarly seen in the S-Group. If our estimates of the YBT eruption are accurate, then YBT may have been on par with the Mount St. Helens eruption of 1980 in that it took over a decade for plant and animal communities around Mount St. Helens to make a comeback (del Moral and Lacher, 2005). YBT may have had a similar effect on the area surrounding Mt. Damota. The lack of artifacts from within the YBT ash at Moche Borago suggests that the eruption was very likely devastating, destroying local flora and fauna resources and forcing people out of the area. Entire hunter-gatherer groups may have even been killed. Therefore, the similarity of stone artifact styles from layers, which were dated before and after the YBT eruption, may indicate that these hunter-gatherers were part of a broader regional cultural tradition, or at least a tradition that surpassed the local influence of the YBT eruption. Larger stone artifact assemblages from Moche Borago and coeval assemblages from other sites in the area are expected to provide further useful information to test this hypothesis in the future.

As a topic of future study, the Irra Xoketta points and associated artifacts from Moche Borago should be compared in more depth to the assemblages from other local and regional sites. For example, based on a rather subjective comparison of shape, size, and design attributes, I find that Irra Xoketta points are very similar to points found in central Ethiopia and Somalia formerly referred to as “Somaliland Stillbay” (Clark, 1954). At Hargeisa in Somalia, Clark (1954:193)

believed that Somaliland Stillbay points derived from earlier Levallois-based techniques, and the points were frequently made on end-struck flakes, exhibited bulbar thinning, and had sub-triangular to foliate shapes with rounded butts—characteristics that are common to Irra Xoketta points at Moche Borago. Furthermore, in Locality 5 at the Ethiopian Central Rift site of K'one, unifacial to fully bifacial points,[38] most of which are made from the Levallois method, are similar morphologically to Moche Borago points, and the K'one points are also found in association with backed tools, (Kurashina, 1978). A similar assemblage is found at Porc Epic in east-central Ethiopia where numerous "Somaliland Stillbay" points were found in Stratum 4[39] (Clark et al., 1984), and are now considered to be Late Pleistocene "transitional MSA/LSA," in age and typology (Pleurdeau, 2001). These points are also found with the earliest microliths at Porc Epic, which parallels the situation at Moche Borago and at K'one.

Conclusions

This dissertation has provided the first detailed description of a well-dated and continuous early OIS 3 archaeological assemblage in the Horn of Africa. The stone artifact assemblages from Moche Borago dating to early OIS 3 show changes that may reflect alterations in hunter-gatherer subsistence economy, mobility, site use, and technology. To explain the changes in flaked stone artifacts, I have explored the possibility that hunter-gatherers were adapting to local environmental fluctuations, which may relate to broader climatic and monsoonal variability during OIS 3.

There has been very little research in general directed at understanding hunter-gatherer behavioral adaptations to OIS 3 paleoclimates in Africa. Consequently, many of the ideas

[38] Kurashina (1978) implied the points are "Somaliland Stillbay," but he preferred to use technological terminology instead.

[39] Referred to as Ensemble III in Pleurdeau (2001).

proposed in this dissertation remain untested, and some untestable, due to the lack of available data. Much more research is required in order to answer such basic questions as:

- What is the current actual ratio of precipitation delivered from the African and SW Asian Monsoons in SW Ethiopia? Did this ratio ever vary in the past?
- Were there latitudinal gradients in the Horn affecting the contributions from the African and SW Asian monsoons (Kebede et al., 2009)?
- Did the monsoon systems vary similarly and synchronously to broader climatic changes or were there other factors which influenced monsoonal intensity during OIS 3?
- Were the orographic effects of the Ethiopian highlands that today act upon monsoonal moisture similar in the past?

Furthermore, how did highland ecological zones in SW Ethiopia change during OIS 3? Hildebrand's (2003) study provides useful hypotheses about Holocene paleoenvironmental changes in the western highlands of SW Ethiopia. To date, however, there are no archaeological studies from SW Ethiopia, or for that matter anywhere in the Horn, which describe environmental fluctuations during OIS 4, OIS 3, or OIS 2. And, what few lake cores and pollen assemblages that are available, they are poorly dated beyond 40 ka.

How did hunter-gatherers living in the lowland areas of the Horn adapt to climatic flux during OIS 3? If these areas were already drier than highland areas, how did fluctuations in monsoonal rains affect lowland ecology? My interpretation of the flaked stone artifacts from the T-Group suggests that while hunter-gatherers developed new technologies to perform activities required of unstable climates and variable resources, aridity and distance between resources may be a primary factor driving mobility patterns. Therefore, if lowland areas were generally drier

than the highlands during OIS 3, then hunter-gatherers in these areas may have continued to rely on a high degree of mobility unlike their S-Group counterparts in the highlands.

Many of these questions should be resolvable with continued research. At a local level, the SWEAP team is continuing to work at Moche Borago and surrounding areas on a variety of related issues. During the recent 2010 field season, SWEAP researchers visited several other open air and rockshelter sites in the area, which can be compared to the archaeology of Moche Borago. New radiocarbon samples have also been submitted, which we hope will improve the current dating of the site and area. We are also exploring the use of other dating techniques like luminescence in volcanic sediments. Lithic microwear and faunal analyses will also provide cogent data on the function of stone artifacts, the local wildlife during early OIS 3, and hunting strategies.

On a regional level, new lake cores from Ethiopia and sediment cores from the Indian Ocean and Gulf of Guinea (Atlantic Ocean) may provide new data about paleoenvironmental and paleoclimatic changes during the Late Pleistocene, including monsoonal fluctuations. Research at additional archaeological sites across the Horn, like at Aduma (Middle Awash, Ethiopia) or around the Bulbula / Ziway area in central Ethiopia could yield comparative data to Moche Borago about lowland hunter-gatherer adaptations during the Last Glacial.

Above all, I hope that this dissertation provides useful information to other researchers studying Late Pleistocene hunter-gatherer behavioral adaptations in Eastern Africa and at continental and global scales.

APPENDIX A
LIST OF ABBREVIATIONS AND DEFINITIONS USED IN THE TEXT

14C	Carbon-14 used for radiocarbon dating.
AMH	Anatomically Modern Humans
AMS	Accelterator Mass Spectrometry
BP	Before Present (i.e. 1950)
BXA	Block Excavation Area at Moche Borago
D-O	Dansgaard-Oeschger event (i.e. D-O 12)
East Africa	Kenya, Tanzania, Uganda, Rwanda, Burundi
GEPCA	Groupe d'étude de la Protohistoire dans la Corne de l'Afrique (English: Protohistoric study group in the Horn of Africa)
Horn of Africa	Ethiopia, Eritrea, Somalia, Djibouti
ITCZ	InterTropcial Convergence Zone
ka	kilo anum
Last Glacial	Geological period lasting from 73.5 ka to 14.7 ka
LGM	Last Glacial Maximum (27.2-23.5 ka)
LSA	Late Stone Age
MNL	Minimum Number of Lithics
MSA	Middle Stone Age
mtDNA	Mitchrondrial DNA
North Africa	Morocco, Algeria, Tunisia, Libya, Egypt, Sudan, Chad
OIS	Oxygen Isotope Stage
PE-PC	Paleoenvironment and Paleoclimate
SST	Sea Surface Temperature

SWAP Sodo-Wolayta Archaeological Project

SWEAP SouthWest Ethiopia Archaeological Project

APPENDIX B

LIST OF ARCHAELOGICAL SITES FROM THE HORN OF AFRICA, EAST AFRICA, AND NORTH AFRICA, DATING TO THE LAST GLACIAL PERIOD WHICH HAVE DEPOSITS CONTAINING MODE 3 AND MODE 4/5 LITHICS

Country	Site Name	Locality	Total Depth of Deposits	Stratigraphic Context	Age	Calibrated Age	Depth (cm) / Stratigraphic Association
Kenya	Lukenya Hill	GvJm62	Area 2: 4.4 meters	Alluvial fan deposits adjacent to Lukenya Hill	21,535 ± 980	25924 ± 1294	220 - 230
		GvJm46				~30,000	
	Prolonged Drift			Weakly developed paleosols stratigraphically above sand and silt deposits from aggrading stream channel. Deposit capped by disconformable Makalia ash, dated ~30 ka		>40,000	
	Prospect Farm	Locality 1-4	~15 meters	Interstratified volcanic ash layers		21,800 - 32,500 46,500 - 53,100 ~50,000	
	Kisese II			Upper Mode 5 assemblage (Levels 1 - 12)	18,190 ± 300	21852 ± 440	Spit 9 at base of microlithic rich deposits
				Lower Mode 5 assemblage (Levels 13 - 36)	31,480 ± 1,350	36235 ± 1619	Level 14

Country	Site Name	Locality	Total Depth of Deposits	Stratigraphic Context	Age	Calibrated Age	Depth (cm) / Stratigraphic Association
Kenya	Enkapune Ya Muto		5.54 meters	Loam	16,300 ± 1000		DBL1.2
					29,300 ± 750		DBL1.2
					35,800 ± 550		DBL1.2
					37,000 ± 1,100		DBL1.3
					39,900 ± 1,600		DBL1.3
					>26,000		RBL4.1
					41,400 ± 700		RBL4.1
					29,280 ± 540		RBL4.1 + 4.2
						35348 ± 2183	DBL1.3
						46406 ± 2758	GG1.3
						32,548 ± 1247	RBL4.2
Tanzania	Mumba		>10 meters	Stratified sand and loam deposits		33,460 ± 900[a]	Level IV
						20,995 ± 680 to 65,680+6049 / -5426[a]	Level V
	Naisusu Beds	Olduvai Gorge		Aeolian tuffs	17,550 ± 1,000	21048 ± 1206	
				Aeolian tuffs		42,000 ± 1,000	
Ethiopia	Porc Epic		~2.5 meters	cemented breccia capped by unconformable Holocene dripstone		61,202 ± 958 61,640 ± 1,083 77,565 ± 1,575	60 - 200 cm; ensemble 3 / 4a
	K'one	G4, Area A	~10 meters	Loam	14,670 ± 200		Upper Loam
	Bulbula River		Not Excavated	Stratified paleosols	27,050 ± 1,540		paleosol
	Liben Bore		>2 meters	Silty clay		UNDATED	

Country	Site Name	Locality	Total Depth of Deposits	Stratigraphic Context	Age	Calibrated Age	Depth (cm) / Stratigraphic Association
Somalia	Midhishi 2		0.7 meters	7 lithostratigraphic units	>40,000 18,790 ± 340		uppermost Mode 3 bearing unit Deposits overlying Mode 3
	Gud-Gud		2 meters	1.4 meters of archaeologically sterile deposits overlying thin occupation horizon	>40,000		
	Gogoshiis Qabe		~1.8 meters			UNDATED	

Country	Site Name	Locality	Technique / Material	Lithic Assemblage	Comments	References
Kenya	Lukenya Hill	GvJm62	14C on apatite	Mode 5	Kusimba (2001) cautions 14C ages are inaccurate because of modern carbon contamination. Ambrose (1988) suggests GvJm62 and GvJm46 date to ~39,000 ka.	Kusimba 2001
		GvJm46	14C on apatite	Mode 5		
	Prolonged Drift			Mode 3	Artifact density very low - estimated only 50 lithics / 0.01 cubic meters	Merrick 1975; Ambrose 2001
	Prospect Farm	Locality 1-4	Obsidian hydration	Mode 5 Mode 3 Mode 3		Michels et al. 1983; Ambrose 2001
			14C on OES	Mode 5	More abundant microliths than lower deposit	
	Kisese II		14C on OES	Mode 5	Microliths rare. Assemblage similar to Nasera and Mumba rockshelters were early Mode 5 is scraper dominated with few backed pieces	Inskeep 1962; Barut 1997

Country	Site Name	Locality	Technique / Material	Lithic Assemblage	Comments	References
Kenya	Enkapune Ya Muto		14C on charcoal	Mode 5 / Sakutiek	Age reported for the earliest Mode 5 at EYM is >46 ka but this is based is an estimate based on sediment deposition rate using obsidian hydration ages.	Ambrose 1998, 2001
				Mode 3 / Endingi		
			Obsidian hydration	Mode 5 / Sakutiek Mode 5 / Nasampolai Mode 3 / Endingi		
			14C on tufa and achatina shell		Archaeologically sterile	
Tanzania	Mumba		14C and Th-230 on bone apatite, OES, shell	Mode 3 and Mode 5	Assemblage is heavily biased and existing analyses are based on a limited sample from the original Kohl-Larson excavation.	Mehlman 1989; Prendergast et al. 2007; Marks and Conard 2006
	Naisusu Beds	Olduvai Gorge	14C on OES	Mode 3 and Mode 5	Dating inconsistency between radiocarbon and Argon/Argon	Leakey et al. 1972; Barut 1997
			40Ar / 39Ar on biotite			Manega 1993

Country	Site Name	Locality	Technique / Material	Lithic Assemblage	Comments	References
Ethiopia	Porc Epic		Obsidian hydration	Mode 3 and Mode 5	Context and dating are problematic and there is a large disparity between radiocarbon and obsidian hydration age estimates. Some of the MSA deposits are also eroded by fluvial activity.	Assefa 2002; Pleurdeau 2001; Clark et al. 1984; Michels and Marean 1984)
	K'one	G4, Area A	14C	Mode 3 and Mode 5	11 meter sequence and only the topmost section of the stratigraphically highest loam deposit has been dated. Lithics in the upper Loam include backed Levallois flakes but the deposits may be secondary context.	Kurashina 1978; Clark and Williams 1978; Brandt 1986, Brandt and Brook 1984

Country	Site Name	Locality	Technique / Material	Lithic Assemblage	Comments	References
Ethiopia	Bulbula River		14C	Mode 5	Site is unexcavated. Lithics include non-geometric microliths and blades made on obsidian.	Gasse and Street 1978; Gasse et al. 1980; Brandt 1986
	Liben Bore			Mode 3 with increasing abundance of Mode 5 higher in the sequence	Deposits appear to span the Mode 3 to Mode 4/5 transition, however, the site is currently undated.	Brandt 2000; Kinahan 2004; Fisher 2005; Negash 2004
Somalia	Midhishi 2		14C on charcoal	Mode 3 Mode 3 and Mode 5		Brandt and Brook 1984; Brandt 1986; Gresham 1984
	Gud-Gud		14C on charcoal	Likely not Mode 3	Assemblage is less than 50 pieces.	Brandt 1986; Brandt and Brook 1984
	Gogoshiis Qabe			Mode 3 and Mode 5	Mode 3 deposits are stratified under terminal Pleistocene (Eibian) and Holocene (Bardaale) assemblages, but the Mode 3 deposits themselves are undated	Brandt 1986

Country	Site Name	Locality	Total Depth of Deposits	Stratigraphic Context	Age	Calibrated Age	Depth (cm) / Stratigraphic Association
Egypt	Bir Sahara	BS-11 and BS-15		Upper Lake: basal unit of sandy silt	30,870 ± 1,000 >44,700 32,780 ± 900		
	Bir Tarfawi			white limestone unit	40,710 ± 3,270 >41,450		
				middle of grey silt	44,190 ± 1,380		
	Taramsa Hill			Aeolian sands		55,500 ± 3.7	aeolian deposits surrounding location of Taramsa I skeleton
	Nazlet Safaha	Sector 89/03			38,100 ± 1,400 37,200 ± 1,300		
	Nazlet Khater	.Nazlet Khater I		Gravel and wadi deposits		UNDATED	
		Nazlet Khater 2					
		Nazlet Khater 3		Sand and gravel deposits	31,320 ± 2,310		
		Nazlet Khater 4			30,980 ± 2,850 30,360 ± 2,310 33,280 ± 1,280		

Country	Site Name	Locality	Total Depth of Deposits	Stratigraphic Context	Age	Calibrated Age	Depth (cm) / Stratigraphic Association
Egypt	Sodmein		>4 meters		25,200 ± 500		MP1 / Top of Layer D
					>30,000		MP2
					>45,000		MP3 / Interface between Layers F and F
					>44,500		MP4
						118,000 ± 8,000	MP5
Libya	Jebel Gharbi	Wadi Ghan		Three main units (from bottom to top): 7-12 m alluvial gravel capped by calcrete; 3-6 m of red aeolian sand grading into loess; 3-4 m light pink aeolian sand grading into loess		UNDATED	
		Ain Zargha		Colluvial silt overlain by aeolian sands. Sequence topped by two more layers of colluvial silts with interstratified paleosols			Lower paleosol within the upper colluvial silt layer

Country	Site Name	Locality	Total Depth of Deposits	Stratigraphic Context	Age	Calibrated Age	Depth (cm) / Stratigraphic Association
Libya				3 main stratigraphic units representing aeolian sediments deflated from nearby wadi	27,310 ± 320		Upper Deposit
	Jebel Gharbi	Ain Shakshuk			24740 ± 140 30,870 ± 200 25500 ± 400		
					44,600 ± 2,430		Charcoal bearing layer in middle of sequence
					43,450 ± 2,110		Lowest Deposit
	Haua Fteah		13 meters		28,500 ± 800 33,100 ± 400 >35,950 43,400 ± 1,300 47,000 ± 3,200		

Country	Site Name	Locality	Total Depth of Deposits	Stratigraphic Context	Age	Calibrated Age	Depth (cm) / Stratigraphic Association
Morroco	Mugharet el 'Aliya			eolian sands		56,000 ± 5,000[t]	Layer 6
						47,000 ± 5,000	Layer 6
						51,000 ± 5,000	Layer 9
						81,000 ± 9,000	Layer 10
	Grotte de Pigeons (Taforalt)		~10 meters			20,200 - 37,400	Phase C
						40,600 - 52,300[b]	Phase 03 Top
						67,500 - 79,200[b]	Phase 03 Middle
						46,600 - 88,900[b]	Sequence 05 Upper
						77,400 - 112,900[b]	Phase Group F
	Dar es soltan	DeS 1	7.5 meters			~49,000 - 57,000c	G4
						~62,000 - 140,000c	G3
						~72,000 - 100,000c	G2

Country	Site Name	Locality	Technique / Material	Lithic Assemblage	Comments	References
Egypt	Bir Sahara	BS-11 and BS-15		Mode 3 / Aterian	several deposits at the site are deflated	
	Bir Tarfawi		14C on *Melanoides*	Mode 3 / Mousterian	several deposits at the site are deflated and some show dessication cracks	Wendorf 1977
				Mode 3 / Aterian		
	Taramsa Hill		Weighted mean estimate of multi-aliquot OSL ages	Mode 3 characterized by Nubian Levallois technique	Vermeersch et al. 1998 find the "Late Middle Paleolithic" assemblage to be transitional to the systematic production of blades	Vermeersch et al. 1998; Vermeersch et al. 1995
		Sector 89/03	AMS on charcoal	"Transitional" Mode 3 / Mode 4/5		Van Peer 1998
	Nazlet Safaha			"Transitional" Mode 3 Levallois		Van Peer 1998
		.Nazlet Khater I		Mode 3	Nubian Style Levallois	
		Nazlet Khater 2		Mode 3	Nubian Style Levallois	
	Nazlet Khater	Nazlet Khater 3		Mode 3	Nubian Style Levallois	Vermeersch et al. 1982
		Nazlet Khater 4	14C on charcoal	Mode 3 overlaid by Mode 4	Shows persistence of Levallois technology into Upper Paleolithic in Egypt	

Country	Site Name	Locality	Technique / Material	Lithic Assemblage	Comments	References
Egypt	Sodmein		14C	Mode 5	Abundant blades with few retouched tools	Moeyersons et al. 2001; Mercier et al. 1999
			14C	Mode 3? / Possible Aterian		
			14C	Mode 3	Disconformity between layers F and G characterized by thick lens of ground based hymenoptera nests. Assemblage includes classic levallois and Nubian levallois as well as some truncated, facetted pieces	
			14C	Mode 3	Assemblage similar to MP3	
			weighted mean estimate of thermoluminesence ages derived from flint blocks	Mode 3	Assemblage predominantly Nubian Levallois	

Country	Site Name	Locality	Technique / Material	Lithic Assemblage	Comments	References
Libya	Jebel Gharbi	Wadi Ghan			Alluvial gravel and calcrete contain Mode 3; lowest loess unit contains Aterian and Mode 5 lithics	Garcea and Giraudo 2006; Barich and Garcea 2008
		Ain Zargha	14C on charcoal	Mode 5 and Aterian	Undated Mode 3 lithics in lower colluvial silt layer.	
			14C on charcoal	Mode 5		
		Ain Shakshuk	14C on charcoal	Mode 5		
			14C on charcoal			
	Haua Fteah		14C on charcoal	Mode 3 / Aterian Mode 5 Mode 3 and Mode 5 Mode 3 Mode 3 Mode 3	Ages are considered underestimates. Low artifact density during Mode 3 to Mode 4/5 transition. Rapid appearance of Mode 4/5 has led to speculation the technology was not indigenous to the region.	McBurney 1967; Moyer 2003

Country	Site Name	Locality	Technique / Material	Lithic Assemblage	Comments	References
Morroco	Mugharet el 'Aliya		ESR on tooth enamel	Mode 3 / Aterian	Low artifacts counts. Level deposits may be disturbed	Wrinn and rink 2003
				Mode 3 / Mousterian	Low artifact counts. Instursive artifacts from higher deposits	
	Grotte de Pigeons (Taforalt)		OSL and 14C	Mode 3 with Mode 4/5 near the top of the deposit		Bouzouggar et al. 2007
			OSL, TL, 14C	Mode 3		
				Mode 3 / Aterian		
				Mode 3		
	Dar es soltan	DeS 1	Multi-Grain OSL	Mode 3 / Aterian		Barton et al. 2009

APPENDIX C
DETAILED DESCRIPTIONS OF THE MICROLITHS AT MOCHE BORAGO

Level 12

BN 1799.15: Medial flake fragment with semi-collateral backing on the right lateral. The flake blank has a parallel dorsal scar structure and the right lateral edge is modified lightly.

BN 1799.42: Proximal flake fragment with straight backing on the right lateral edge. The flake blank has a dihedral platform with a parallel dorsal scar pattern. The left lateral edge is utilized.

Level 13

BN 1802.2: Flake with obverse backing along the right lateral edge. Flake blank has a parallel dorsal scar pattern.

BN 1802-97: Flake with obverse backing along the right lateral edge. The most intensive backing retouch is from the proximal edge to ½ the length of the flake. The distal edge of the flake blank has been snapped off and the distal, right lateral edge may be burinated.

Level 14

BN 1805-77: Microlith fragment with limited obverse backing on the left lateral edge. The right lateral edge is utilized. The planform of the piece is reminiscent of an obliquely truncated geometric microlith but there is no modification along the distal edge.

BN 1805-73: Flake with natural backing on the left lateral edge. There is use-wear and modification on the right lateral edge opposite the backing. Distal and proximal sections of flake blank are snapped off creating a sub-triangular plan form.

BN 1805-75: Flake with obverse backing on the left lateral edge. Similar in overall morphology to BN 1805-73.

BN 1805-78: Flake with obverse backing on the right lateral edge. Right lateral ventral surface has step-fracturing indicating possible use wear.

Level 16

BN 1818.5: Medial flake fragment with semi-collateral retouching. The cross-section of this piece is almost equilaterally triangular

and the dorsal surface is bifacial. The retouching begins along the medial ridge of the dorsal surface and extends to the left lateral edge.

BN 1818.6: Levallois flake with backing on the left lateral. The flake has a radial dorsal scar pattern and a facetted platform. The backing is predominantly inverse except along a limited distance near the proximal edge of the left lateral edge where there appears to be several obverse oriented flake scars. This would indicate that the retouching is not due to core trimming activities and was intentionally retouched along the lateral edge.

Level 18:

BN 2571.1: Crescent. There is an alternating backing pattern on the left lateral edge of the flake blank. The backing angle is 88° and the retouching forms a convex left lateral planform. There is a large flake scar near the proximal dorsal left lateral edge and two scars on the proximal ventral right lateral edge that may be use-wear damage. There is utilization along the right lateral edge.

Level 23:

BN 3105.15: Utilized flake with curved, possibly crescentic, obverse / natural backing along the left lateral edge. The utilization is located on the right lateral edge extending from the proximal edge to around 2/3 the length of the tool. Micro-facets along the ventral right lateral edge and two larger flake facets on the ventral right lateral near the distal edge may be use wear.

APPENDIX D
DETAILED DESCRIPTIONS OF THE POINTS AT MOCHE BORAGO

BN 4889.1
G10
Level 30
T-Group
DCC

This is a small, unifacial point with a triangular planform that is made on an end-struck flake. The point may be broken at the base but this seems unlikely. It is possible also that the proximal edge of the flake bank was snapped off prior to retouching of the dorsal surface in a crude method of bulbar thinning. This is supported by flake scars along the break which were likely produced after the break occurred. The retouching is mainly on the distal surface producing a circular dorsal scar pattern. The retouching is distinctly finer along the distal left lateral edge of the dorsal surface. The tip is broken and retouched, but there is similar fine retouching here also. There are shallow bi-lateral notches half way up from the base of the tool. These are interpreted to be mainly caused by, or for, hafting purposes.

BN 4854.1
G10
L30
T-Group Lower
DCC

BN4854.1 is a small semi-ovate point that has been bifacially retouched. Retouching is fully invasive and there is no indication which surface was originally ventral or dorsal. Surface 1 primarily has a unidirectional flake scar pattern though. The left lateral edge is retouched more intensively than the right lateral edge. On the obverse face (Surface 2) the flake scar pattern is more convergent. It is also opposed to the direction of the flake scars on Surface 1. The base of the point on Surface 2 is retouched more heavily than the other faces and when viewed in profile, the point is distinctly lenticular. This suggests that the Surface 2 retouching was bifacial thinning and very likely for hafting purposes.

BN 3574.1
G10
L25
T-Group Lower
CTT / HLB

The piece is made on an end-struck flake blank and it has been retouched mainly unifacially on the dorsal surface - there is a large flake scar on the ventral proximal surface. Retouch along the dorsal surface is mainly unidirectional (proximal - dorsal) but there are several opposing flake scars along the distal edge, near the tip that may be due to impact fractures meaning that the tip of the piece is effectively missing. There is finer retouch along the left lateral edge near the striking platform and the right lateral is retouched concavely. If the opposing distal dorsal flake scars (distal to proximal) are due to impact fracturing then it is likely that the original planform of this piece was sub-triangular with a semi-convex base.

BN 3575.3
G10
L24
T-Group Upper
DCC

BN 3575.3 is a parti-bifacial point made on an end-struck flake. The planform is distinctly tear-drop in shape and the lateral edges widen at the base to produce a characteristic wide, and rounded, butt. The flake blank platform is not facetted. The bulbar thinning is located primarily on the right lateral ventral surface and extends half-way up the right lateral edge. At least 75% of the bulb is missing. The dorsal surface is retouched

heavily. The dorsal scar pattern is technically circular but is more accurately described as bi-lateral because the majority of flake scars were struck from the lateral edges and not the proximal or distal edges. The dorsal left lateral surface is retouched more finely than the right lateral surface and is just slightly concave form the medial lateral to the tip.

BN 3477.3
G10
L24
T-Group Upper
DCC

BN 3477.3 is a parti-bifacial point made on an end struck flake. The point planform is teardrop shaped and the lateral edges expand at the base to produce a wide, rounded butt. The ventral right lateral surface has been retouched fairly intensively. This appears to be bulbar thinning, but it is actually basal thinning because the point itself is actually made on the distal end of the flake blank. The point profile is lenticular. The dorsal surface retouch is semi-circular with fine retouching along the butt and right lateral edge near the tip - which is narrowly concave.

BN 3132.1
G10
T-Group Upper
DCC

BN 3132.1 is a Levallois point. The flake blank platform surface is facetted. The dorsal scar pattern is convergent but the flake scars themselves show that the striking platforms alternated end-to-end. There is moderate edge damage along the dorsal left lateral and also the ventral right lateral edges. The style of manufacture - especially the dorsal scars oriented from the distal edge - is reminiscent of Nubian type I technology (Vermeersch 2001).

BN 3114.1
G9
T-Group Upper

BN 3114.1 was recovered from the profile wall during the 2007 field season. It was plotted *in situ* but not excavated as such. It is a Levallois point with a convergent dorsal scar pattern. Unlike BN 3132.1, which has an alternating convergent dorsal scar pattern the flake scars on BN 3114.1 are unidirectional. Dorsal scar flaking is finer along the proximal dorsal surface and the platform is facetted. There is edge damage along the left lateral edge near the base and along both lateral edges equidistant from the butt - this may be evidence of hafting. There is right lateral edge damage on the ventral surface.

BN 2116.2
G10
L19
T-Group Upper
DCC

BN 2116.2 is a small bifacial point. Retouching along both faces is intensive but there is a small patch of cortex remaining on the distal surface. The point has a tear-drop shape plan form with a rounded but the lateral edges do not expand outwards very much creating almost an ovate shape. The ventral surface retouching is semi-circular - most bi-lateral though - and the flake scars themselves are broad and poorly refined. In contrast, the dorsal surface flaking is much more refined and circular. Retouching along the butt is especially fine, though it is along fairly non-invasive. The tip-end is broken off.

BN 1818.1
G10

BN 1818.1 is a unifacial point made on a transverse flake. The flake blank platform is facetted. The dorsal scar pattern is semi-circular but the

L16
S-Group
VDBS

flake scars are predominantly oriented bi-laterally (in this case proximal - dorsal). The dorsal surface flaking is fairly coarse but there is irregular, shallow lateral retouching from the medial to the tip forming slightly serrated lateral edges. Technologically, this pieces appears to be Levallois but the retouching and plan form suggest it shares technological elements in common with other, smaller tear-drop shaped points within the assemblage.

BN 1802.90
G10
L13
S-Group
VDBS

BN 1802.90 is a small parti-bifacial point made on the medial section of a flake. The dorsal scar pattern is bi-lateral (lateral - lateral). The base of the point appears to be the left lateral edge. The left lateral flake scars are slightly finer than those on the right lateral. There is also slightly more intensive flaking along the ventral surface of the left lateral edge to form a thinner profile. Furthermore, there is moderate right lateral ventral retouching to make a more convergent edge. The plan form of the point is reminiscent of other tear-drop shaped points within the assemblage though BN 1802.90 is clearly more ovate.

BN 1799.12
G10
L12
S-Group
VDBS

BN 1799.12 is an end-struck flake with a parallel / convergent dorsal scar pattern - the two flake scars at the distal edge, and along the right lateral edge are opposed to the uniform direction of all other flake scars. The flake blank platform is facetted. This piece is reminiscent of Levallois technology. Whether this piece is a point, however, can be questioned. There is non-invasive utilization along the ventral right lateral edge. This may indicate that this edge was, in fact, the primary working edge of the tool and not the tip.

BN 1799.16
G10
L12
S-Group
VDBS

BN 1799.16 is a small bifacial point with intensive retouching on both faces. The retouching on Surface 1 is more intensive than on Surface 2. Surface 1 retouching itself is more intensive along the point butt and left lateral edges. Retouching on Surface 2 is more intensive along the right lateral edge. The point has a semi-lenticular profile but the profile is ovate and the tip is also rounded. This may suggest the piece was retouched heavily during use and is thus the end-product of a much different initial point shape, possibly being more elongate and tear-drop shaped like bifacial point BN 2116.2.

BN 1799.13
G10
L12
S-Group
VDBS

BN 1799.13 is a small bifacial point with intensive retouching on both faces. Similar to 1799.16, Surface 1 is retouched more heavily than Surface 2. Retouching along Surface 1 is circular and there is a intensive retouching along the medial right lateral edge that may be a shallow notch. The retouching on Surface 2 is largely bi-directional and it is much coarser than on Surface 1, except at the tip / right lateral edge where there are finer flake scars. There is no equivalent retouching on Surface 2 adjacent to the possible Surface 1 notch. Due to the medial location on the piece, the notch may relate to hafting. The point has a lenticular profile

and the plan form is tear-drop. There is similarity in design with BN 1799.16 and this may be an example of a bifacial point that was not retouched as heavily (due to use?) as BN 1799.16.

BN 1794.36
G10
L11
S-Group
VDBS

BN 1794.36 is made on the distal edge of an end-struck flake. It is possible that this piece is incomplete (being broken at the butt) but this seems unlikely because some dorsal scars emanate from the existing butt edge. The original dorsal scar pattern was likely parallel and opposed to the flake blank platform. The retouching pattern is semi-circular. The point is retouched most heavily along the dorsal left lateral and butt edges. There is some retouching adjacent to a shallow divot on the medial right lateral, which is reminiscent of a notch for hafting purposes (see BN 1799.13). There is no equivalent ventral retouching around the notch. The point has an irregular / semi-lenticular profile and a triangular planform.

BN 4258.1
H9
L26
S-Group
VDBS

BN 4258.1 is a small parti-bifacial made on an end-struck flake. The dorsal scar pattern is circular and retouching intensity is similar along all edges. There are two large flake scars at the butt of the piece that terminate in step-fractures medially along the axis of the tool. In profile, this creates a biconvex shape with basal thinning. There is retouching along the ventral left lateral edge near the proximal edge as well as retouching or possible edge damage / use wear along the ventral right lateral edge near the tip. The point planform is sub-triangular - almost tear drop - with straight convergent edges at the tip that morph into parallel straight edges for the medial section of the tool to the butt. The butt is convex.

BN 2268.2
TU2S
S-Group
VDBS - YBS

BN 2268.2 is a parti-bifacial point made on the distal edge of an end-struck flake. The flake blank was snapped medially (lateral - lateral) similar in design to BN 17944.36. BN 2268.2 is retouched most heavily along the dorsal surface. The dorsal scar pattern is circular and there is equivalent retouching intensity along each edge. There is edge damage / utilization on the dorsal left lateral edge. The ventral surface is retouched most heavily at the tip where there are bi-lateral (lateral - lateral) flake scars. There is edge damage / utilization along the ventral right lateral edge. The point has a rhomboidal profile and the plan form is triangular.

BN1693.3
G10
R-Group
RGCB

BN 1693.3 is a part-bifacial point made on an end struck flake. There is intensive semi-circular bulbar thinning on the ventral proximal surface which has completely removed the bulb of percussion. The dorsal scar pattern is circular and retouching is finest along both lateral edges medially towards the point tip. The lateral edges expand towards the butt, which is rounded, forming a tear drop shape.

BN 1887.1
G10
L5
R-Group
RGCA

BN 1887.1 is an elongate unifacial point made on an end-struck flake. There is no bulbar thinning. The point is retouched most heavily along the right lateral edge, but there is also fine retouching along the distal, left lateral edge at the tip. The original dorsal scar pattern of the flake blank may have been parallel. The proximal left lateral edge is naturally convergent but the proximal right lateral edge has been intentionally retouched similarly to produce a characteristic trapezoidal butt shape.

BN 2043.1
H9
L15
R-Group
RCA

BN 2043.1 is a parti-bifacial point made on an end-struck (possibly transverse) whole flake. The flake blank dorsal scar pattern was parallel and opposed to the striking platform. The dorsal surface is retouched most heavily along the butt. The ventral surface is also retouched most heavily along the butt - and extending along the ventral right lateral edge- for bulbar thinning. The point has a lenticular profile. The lateral edges are slightly convex (and skewed to the left lateral) forming an ovate planform with a rounded base.

BN 2072.1
H9
L15
R-Group
RCA

BN 2072.1 is a parti-bifacial point made on an end-struck flake. The retouching is heaviest on the dorsal surface. The dorsal scar pattern is semi-circular and the butt is retouched heaviest. There is intensive bi-lateral (lateral-lateral) / semi-circular bulbar thinning on the ventral surface. The point has a lenticular profile. The plan form is elongate with characteristic slightly convex lateral edges that expand outwards towards a more steeply rounded - semi-trapezoidal - butt. The semi-trapezoidal butt shape is reminiscent of BN 1887.1.

REFERENCE LIST

Allen, J.R.M., Brandt, U., Brauer, A., Hubberten, H.W., Huntley, B., Keller, J., Kraml, M., Mackensen, A., Mingram, J., Negendank, J.F.W., Nowaczyk, N.R., Oberhansli, H., Watts, W.A., Wulf, S., and Zolitschka, B., 1999. Rapid environmental changes in southern Europe during the last glacial period, Nature 400, 740-743.

Ambrose, S., 2001. Middle and Later Stone Age settlement patterns in the Central Rift Valley, Kenya: comparisons and contrasts. in: Conard, N. (Ed.), Settlement Dynamics of the Middle Paleolithic and Middle Stone Age. Kerns Verlag, Tubingen, pp. 21-43.

Ambrose, S.H., 1998a. Chronology of the Later Stone Age and food production in East Africa, Journal of Archaeological Science 25, 377-392.

Ambrose, S.H., 1998b. Late Pleistocene human population bottlenecks, volcanic winter, and differentiation of modern humans, Journal of Human Evolution 34, 623-651.

Ambrose, S.H., 2002. Small things remembered: origins of early microlithic industries in Sub-Saharan Africa, Archeological Papers of the American Anthropological Association 12, 9-29.

Ambrose, S.H., 2003. Did the super-eruption of Toba cause a human population bottleneck? Reply to Gathorne-Hardy and Harcourt-Smith, Journal of Human Evolution 45, 231-237.

Ambrose, S.H., Elston, R.G., and Kuhn, S.L., 2002. Small things remembered: Origins of early microlithic industries in Sub-Saharan Africa. Thinking Small: Global Perspectives on Microlithization, pp. 9-29.

Andersen, K.K., Svensson, A., Johnsen, S.J., Rasmussen, S.O., Bigler, M., Rothlisberger, R., Ruth, U., Siggaard-Andersen, M.L., Steffensen, J.P., Dahl-Jensen, D., Vinther, B.M., and Clausen, H.B., 2006. The Greenland Ice Core Chronology 2005, 15-42 ka. Part 1: constructing the time scale, Quaternary Science Reviews 25, 3246-3257.

Anovitz, L.M., Elam, J.M., Riciputi, L.R., and Cole, D.R., 1999. The failure of obsidian hydration dating: sources, implications, and new directions, Journal of Archaeological Science 26, 735-752.

Arnold, J.R. and Libby, W.F., 1949. Age determinations by radiocarbon content - checks with samples of known age, Science 110, 678-680.

Assefa, Z., 2006. Faunal remains from Porc-Epic: Paleoecological and zooarchaeological investigations from a Middle Stone Age site in southeastern Ethiopia, Journal of Human Evolution 51, 50-75.

Bar-Matthews, M., Ayalon, A., and Kaufman, A., 2000. Timing and hydrological conditions of Sapropel events in the Eastern Mediterranean, as evident from speleothems, Soreq cave, Israel, Chemical Geology 169, 145-156.

Bard, E., 2003. Indian Ocean sea surface temperature reconstruction. IGBP PAGES/World Data Center for Paleoclimatology, Data Contribution Series #2003-027. , NOAA/NGDC Paleoclimatology Program, Boulder Colorado.,

Bard, E., Rosteck, F., and Sonzogni, C., 1997. Interhemispheric synchrony of the last deglaciation inferred from alkenone palaeothermometry, Nature 385, 707-710.

Barham, L. and Mitchell, P., 2008. The first Africans: African archaeology from the earliest toolmakers to the most recent foragers, Cambridge University Press, New York.

Barton, R.N.E., Bouzouggar, A., Collcutt, S.N., Schwenninger, J.L., and Clark-Balzan, L., 2009. OSL dating of the Aterian levels at Dar es-Soltan I (Rabat, Morocco) and implications for the dispersal of modern Homo sapiens, Quaternary Science Reviews 28, 1914-1931.

Basell, L.S., 2008. Middle Stone Age (MSA) site distributions in eastern Africa and their relationship to Quaternary environmental change, refugia and the evolution of Homo sapiens, Quaternary Science Reviews 27, 2484-2498.

Baumgartner, S., Beer, J., Masarik, J., Wagner, G., Meynadier, L., and Synal, H.A., 1998. Geomagnetic Modulation of the 36Cl Flux in the GRIP Ice Core, Greenland, Science 279, 1330-1332.

Beckingham, C.F. and Huntingford, G.W.B., 1954. Some records of Ethiopia, 1593-1646. Hakluyt Society, London, p. lxxx.

Benvenuti, M., Carnicelli, S., Belluomini, G., Dainelli, N., Di Grazia, S., Ferrari, G.A., Iasio, C., Sagri, M., Ventra, D., Atnafu, B., and Kebede, S., 2002. The Ziway-Shala lake basin (main Ethiopian rift, Ethiopia): a revision of basin evolution with special reference to the Late Quaternary, Journal of African Earth Sciences 35, 247-269.

Berna, F., Matthews, A., and Weiner, S., 2004. Solubilities of bone mineral from archaeological sites: the recrystallization window, Journal of Archaeological Science 31, 867-882.

Binford, L.R., 1962. Archaeology as anthropology, American Antiquity 28, 217-225.

Binford, L.R., 1965. Archaeological systematics and the study of culture process, American Antiquity 31, 203-210.

Binford, L.R., 1980. Willow's smoke and dogs' tails: Hunter-gatherer settlement systems and archaeological site formation, American Antiquity 45.

Blanckenhorn, M., 1901. Das Pliocän und Quartärzeitalter in Aegypten ausschliesslich des Rothen Meergebietes. Neues zur Geologie und Palaeontology Aegyptens IV Zeitschrift der Deutschen geologischen Gesellschaft, Jahrgang, pp. 307-502.

Bond, G., Broecker, W., Johnsen, S., McManus, J., Labeyrie, L., Jouzel, J., and Bonani, G., 1993. Correlations between climate records from North Atlantic sediments and Greenland ice, Nature 365, 143-147.

Bond, G., Showers, W., Cheseby, M., Lotti, R., Almasi, P., deMenocal, P., Priore, P., Cullen, H., Hajdas, I., and Bonani, G., 1997. A Pervasive millennial-scale cycle in North Atlantic Holocene and glacial climates, Science 278, 1257-1266.

Borena, A., 2008. Project proposal on natural resource conservation in Mt. Damota area, International NGO Journal 3, 48-56.

Bowler, J.M., Johnston, H., Olley, J.M., Prescott, J.R., Roberts, R.G., Shawcross, W., and Spooner, N.A., 2003. New ages for human occupation and climatic change at Lake Mungo, Australia, Nature 421, 837-840.

Bradley, R.S., 1999. Paleoclimatology: Reconstructing climates of the Quaternary, Academic Press, San Diego.

Brandt, S.A. and Brook, G.A., 1984. Archaeological and paleoenvironmental research in Northern Somalia, Current Anthropology 25, 119-121.

Brandt, S.A., 1982. A Late Quaternary cultural / environmental sequence from lake Besaka, southern Afar, Ethiopia. Ph.D. thesis, University of California, Berkeley, Ann Arbor: University microfilms

Brandt, S.A., 1986. The Upper Pleistocene and early Holocene prehistory of the Horn of Africa, African Archaeological Review 4, 41-82.

Brandt, S.A., 1988. Early Holocene mortuary practices and hunter-gatherer adaptations in Southern Somalia, World Archaeology 20, 40-56.

Brandt, S.A., Fisher, E., Hildebrand, E., and Wang, H., 2010. Archaeological and paleoenvironmental implications of >40 ka charcoal radiocarbon dates from Moche Borago, Ethiopia. 2010 Paleoanthropology Society Meeting, St. Louis, Missouri

Brandt, S.A.A.-P., Hildebrand, E.E.-P., Negash, A., Marshall, F., Lesure, J., Lamb, H., Mohammed, M.U., Ambrose, S., Abate, A., Demissew, S., Rots, V., Unbushe, D., Denu, D., Renne, P., and Fisher, E., 2006. SW Ethiopia as a Late Quaternary refugium: archaeology and paleoenvironment. National Science Foundation,

Brandt, S., 2000. Emergency archaeological fieldwork and capacity building at the Gilgel Gibe hydroelectric project, Deneba, southern Ethiopia. Unpublished report to the Ethiopia tourism commission and Center for Research and Conservation of Cultural Heritage.

Broecker, W., Bond, G., Klas, M., Clark, E., and McManus, J., 1992. Origin of the northern Atlantic's Heinrich events, Climate Dynamics 6, 265-273.

Broecker, W.S., 1994. Massive iceberg discharges as triggers for global climate change, Nature 372, 421-424.

Brooks, A.S., Nevell, L., Yellen, J.E., and Hartman, G., 2006. Projectile technologies of the African MSA. Transitions Before the Transition, pp. 233-255.

Brooks, C.E.P., 1914. The meteorological conditions of the ice sheet and their bearing on the desiccation of the Globe., Quarterly Journal of the Royal Meteorological Society xi.

Burns, S.J., Fleitmann, D., Matter, A., Kramers, J., and Al-Subbary, A.A., 2003. Indian Ocean climate and an absolute chronology over Dansgaard/Oeschger Events 9 to 13, Science 301, 1365-1367.

Burns, S.J., Fleitmann, D., Matter, A., Kramers, J., and Al-Subbary, A.A., 2004. CORRECTIONS AND CLARIFICATIONS, Science 305, 1567a.

Cai, Y., An, Z., Cheng, H., Edwards, R.L., Kelly, M.J., Liu, W., Wang, X., and Shen, C.C., 2006. High-resolution absolute-dated Indian Monsoon record between 53 and 36 ka from Xiaobailong Cave, southwestern China, Geology 34, 621-624.

Capron, E., Landais, A., Lemieux-Dudon, B., Schilt, A., Masson-Delmotte, V., Buiron, D., Chappellaz, J., Dahl-Jensen, D., Johnsen, S., Leuenberger, M., Loulergue, L., and Oerter, H., 2010. Synchronising EDML and NorthGRIP ice cores using d18O of atmospheric oxygen (d18Oatm) and CH4 measurements over MIS5 (80-123 kyr), Quaternary Science Reviews 29, 222-234.

Cayre, O., Lancelot, Y., Vincent, E., and Hall, M., 1999. Paleoceanograpic reconstructions from planktonic formainifera of the Iberian margin: temperature, salinity, and Heinrich events, Paleoceanography 14, 384-396.

Cerulli, E., 1956. Part III: North Eastern Africa: Peoples of Southwest Ethiopia and its borderland, International African Institute, London.

Chalie, F. and Gasse, F., 2002. Late Glacial-Holocene diatom record of water chemistry and lake level change from the tropical East African Rift Lake Abiyata (Ethiopia), Palaeogeography, Palaeoclimatology, Palaeoecology 187, 259-283.

Chiu, T.C., Fairbanks, R.G., Cao, L., and Mortlock, R.A., 2007. Analysis of the atmospheric C-14 record spanning the past 50,000 years derived from high-precision Th-230/U-234/U-238, Pa-231/U-235 and C-14 dates on fossil corals, Quaternary Science Reviews 26, 18-36.

Clark, J.D., 1960. Human ecology during Pleistocene and later times in Africa South of the Sahara, Current Anthropology 1, 307-324.

Clark, J.D., 1963. The evolution of culture in Africa, The American Naturalist 97, 15.

Clark, J.D., 1964. The prehistoric origins of African culture, The Journal of African History 5, 161-183.

Clark, J.D., 1965. The later Pleistocene cultures of Africa, Science 150, 833-847.

Clark, J.D., 1970. The prehistory of Africa, Praeger, New York.

Clark, J.D., 1988. The Middle Stone Age of East Africa and the beginnings of regional identity, Journal of World Prehistory. 2, 235-305.

Clark, J.D. and Williams, M.A.J., 1978. Recent archaeological research in Southeastern Ethiopia, Annales d'Ethiopie 19-44.

Clark, J.D., Williamson, K.D., Michels, J.W., and Marean, C.W., 1984. A Middle Stone Age occupation site at Porc Epic cave, Dire Dawa (east-central Ethiopia), The African Archaeological Review 2, 37-71.

Clark, J.D., 1954. The prehistoric cultures of the Horn of Africa: an analysis of the stone age cultural and climatic succession in the Somalilands and eastern parts of Abyssinia, Cambridge University Press, Cambridge.

Clark, J.G.D., 1971. World prehistory, A New Outline, Cambridge University Press, Cambridge.

Close, A.E., Straus, L.G., Eriksen, B.V., Erlandson, J.M., and Yesner, D.R., 1996. Plus Ca Change: The Pleistocene-Holocene Transition in Northeast Africa. Humans at the End of the Ice Age: The Archaeology of the Pleistocene-Holocene Transition Plenum Press, New York, pp. 43-60.

Cohen, A.S., Stone, J.R., Beuning, K.R.M., Park, L.E., Reinthal, P.N., Dettman, D., Scholz, C.A., Johnson, T.C., King, J.W., Talbot, M.R., Brown, E.T., and Ivory, S.J., 2007. Ecological consequences of early Late Pleistocene megadroughts in tropical Africa, Proceedings of the National Academy of Sciences 104, 16422-16427.

Cole, S., 1954. The prehistory of East Africa, American Anthropologist 56, 1026-1050.

Cornelissen, E., 2002. Human responses to changing environments in Central Africa between 40,000 and 12,000 B.P, Journal of World Prehistory 16, 197-235.

Cosford, J., Qing, H., Yuan, D., Zhang, M., Holmden, C., Patterson, W., and Hai, C., 2008. Millennial-scale variability in the Asian monsoon: Evidence from oxygen isotope records from stalagmites in southeastern China, Palaeogeography, Palaeoclimatology, Palaeoecology 266, 3-12.

Dansgaard, W., 1964. Stable isotopes in precipitation, Tellus 16, Medium.

Dansgaard, W., Johnson, S.J., Clausen, H.B., hl-Jensen, D., Gudenstrup, N.S., Hammer, C.U., Hvidberg, C.S., Steffensen, J.P., Sveinbjornsdottir, A.E., Jouzel, J., and Bond, G., 1993. Evidence for general instability of past climate from a 250-kyr Ice core record, Nature 364, 218-220.

del Moral, R. and Lacher, I.L., 2005. Vegetation patterns 25 years after the eruption of Mount St. Helens, Washington, USA, American Journal of Botany 92, 1948-1956.

Di Paola, G., 1972. The Ethiopian rift valley, Bulletin of Volcanology 36, 517-560.

Fisher, E.C., 2005. A complex systems theory of technological change: a case study involving a morphometrics analysis of stone age flake debitage from the Horn of Africa. University of Florida,

Fisher, E.C., Bar-Matthews, M., Jerardino, A., and Marean, C.W., 2010. Middle and Late Pleistocene paleoscape modeling along the southern coast of South Africa, Quaternary Science Reviews 29, 1382-1398.

Fletcher, W.J., Sanchez-Gone, M.F., llen, J.R.M., Cheddadi, R., Combourieu-Nebout, N., Huntley, B., Lawson, I., Londeix, L., Magri, D., Margari, V., Mnller, U.C., Naughton, F., Novenko, E., Roucoux, K., and Tzedakis, P.C., 2010. Millennial-scale variability during the last glacial in vegetation records from Europe, Quaternary Science Reviews In Press, Corrected Proof.

Flint, R.F., 1959. On the basis of Pleistocene correlation in East Africa, Geological Magazine XCVI, 265-284.

Flores, J.A., Barcena, M.A., and Sierro, F.J., 2000. Ocean-surface and wind dynamics in the Atlantic Ocean off Northwest Africa during the last 140 000 years, Palaeogeography, Palaeoclimatology, Palaeoecology 161, 459-478.

Forster, P., Harding, R., Torroni, A., and Bandelt, H.J., 1996. Origin and evolution of native American mtDNA variation: a reappraisal, American Journal of Human Genetics 59, 935-945.

Galbraith, R.F. and Laslett, G.M., 1993. Statistical-Models for Mixed Fission-Track Ages, Nuclear tracks and radiation measurements 21, 459-470.

Galbraith, R.F., Roberts, R.G., Laslett, G.M., Yoshida, H., and Olley, J.M., 1999. Optical dating of single and multiple grains of quartz from Jinmium rock shelter, northern Australia, part 1: Experimental design and statistical models, Archaeometry 41, 339-364.

Galbraith, R.F., Roberts, R.G., and Yoshida, H., 2005. Error variation in OSL palaeodose estimates from single aliquots of quartz: a factorial experiment, Radiation Measurements 39, 289-307.

Garcea, E.A.A. and Giraudi, C., 2006. Late Quaternary human settlement patterning in the Jebel Gharbi, Journal of Human Evolution 51, 411-421.

Gasse, F., 1977. Evolution of Lake Abhe (Ethiopia and TFAI), from 70,000 b.p., Nature 265, 42-45.

Gasse, F., 2000. Hydrological changes in the African tropics since the Last Glacial Maximum, Quaternary Science Reviews 19, 189-211.

Gasse, F. and Street, F.A., 1978. Late Quaternary lake-level fluctuations and environments of the Northern Rift Valley and Afar Region (Ethiopia and Djibouti), Palaeogeography, Palaeoclimatology, Palaeoecology 24, 279-325.

Genty, D., Blamart, D., Ouahdi, R., Gilmour, M., Baker, A., Jouzel, J., and Van-Exter, S., 2003. Precise dating of Dansgaard-Oeschger climate oscillations in western Europe from stalagmite data, Nature 421, 833-837.

Gillespie, R., Street-Perrott, F.A., and Switsur, R., 1983. Post-glacial arid episodes in Ethiopia have implications for climate prediction, Nature 306, 680-683.

Greenland Ice-core Project, M., 1993. Climate instability during the last interglacial period recorded in the GRIP ice core, Nature 364, 203-207.

Grootes, P.M., Stuiver, M., White, J.W.C., Johnsen, S., and Jouzel, J., 1993. Comparison of oxygen isotope records from the GISP2 and GRIP Greenland ice cores, Nature 366, 552-554.

Grousset, F.E., Labeyrie, L., Sinko, J.A., Cremer, M., Bond, G., Duprat, J., Cortijo, E., and Huon, S., 1993. Patterns of ice-rafted detritus in the glacial North Atlantic (40-55 -ºC), Paleoceanography 8, 175-192.

Guiot, J., de Beaulieu, J.L., Cheddadi, R., David, F., Ponel, P., and Reille, M., 1993. The climate in Western Europe during the last Glacial/Interglacial cycle derived from pollen and insect remains, Palaeogeography, Palaeoclimatology, Palaeoecology 103, 73-93.

Gutherz, X., Jallot, L., Lesur, J., Pouzolles, G., and Sordoillet, D., 2001. The Moche Borago (Soddo-Wolayta) Rock-shelter: December 2001 Excavation. Report on file, SNNPR Office of Culture and Information, Awassa, Ethiopia.,

Gutherz, X., Jallot, L., Poisblaud, B., Sordoillet, D., Pouzolles, G., Asfaw, A., Lakew, B., and Aba, G., 2000a. The Moche Borago Rock-shelter: January-February 2000 Excavation. Reports on file, SNNPR Office of Culture and Information, Awassa, Ethiopia.,

Gutherz, X., Said.H., and Lakew, B., 2000b. The Moche Borago Rock-shelter: November 2000 Excavation. Report on file, SNNPR office of Culture and Information, Awassa, Ethiopia.,

Hedges, R.E.M. and Vanklinken, G.J., 1992. A Review of Current Approaches in the Pretreatment of Bone for Radiocarbon Dating by Ams, Radiocarbon 34, 279-291.

Hemming, S.R., 2004. Heinrich events: Massive late Pleistocene detritus layers of the North Atlantic and their global climate imprint, Reviews of Geophysics 42.

Henshilwood, C., D'Errico, F., Vanhaeren, M., van Niekerk, K., and Jacobs, Z., 2004. Middle Stone Age shell beads from South Africa, Science 304, 404.

Henshilwood, C.S. and Marean, C.W., 2003. The origin of modern human behavior: a critique of the models and their test implications, Current Anthropology 44.

Herries, A.I.R. and Fisher, E.C., Multi-dimensional modelling of magnetic mineralogy as a proxy for fire use and spatial patterning: evidence from the Middle Stone Age bearing sea cave of Pinnacle Point 13B (Western Cape, South Africa). Submitted, In Press.

Hessler, I., Dupont, L., Bonnefille, R., Behling, H., Gonzales, C., Helmens, K.F., Hooghiemstra, H., Lebamba, J., Ledru, M.P., Lazine, A.-M., Maley, J., Marret, F., and Vincens, A., 2010. Millennial-scale changes in vegetation records from tropical Africa and South America during the last glacial, Quaternary Science Reviews In Press, Corrected Proof.

Hildebrand, E., 2003. Enset, yams, and honey: ethnoarchaeological approaches to the origins of horticulture in southwest Ethiopia. Washington University, St. Louis, Missouri

Hildebrand, E., Brandt, S.A., Fisher, E.C., Mohammed, M.U., Wang, H., Ambrose, S., Roberts, R., Grun, R., Morgan, L., and Lesure, J., 2008. Late Pleistocene environments and technological change in a northeast African refugium: current research at Moche Borago rockshelter, southwestern Ethiopia. Paleoanthropology society meeting, 2008 Paleoanthropology Society,

Huber, C., Leuenberger, M., Spahni, R., Fluckiger, J., Schwander, J., Stocker, T.F., Johnsen, S., Landais, A., and Jouzel, J., 2006. Isotope calibrated Greenland temperature record over Marine Isotope Stage 3 and its relation to CH4, Earth and Planetary Science Letters 243, 504-519.

Hughen, K., Lehman, S., Southon, J., Overpeck, J., Marchal, O., Herring, C., and Turnbull, J., 2004. 14C activity and global carbon cycle changes over the past 50,000 Years, Science 303, 202-207.

Hughen, K., Southon, J., Lehman, S., Bertrand, C., and Turnbull, J., 2006. Marine-derived C-14 calibration and activity record for the past 50,000 years updated from the Cariaco Basin, Quaternary Science Reviews 25, 3216-3227.

Hull, K.L., 2001. Reasserting the utility of obsidian hydration dating: A temperature-dependent empirical approach to practical temporal resolution with archaeological obsidians, Journal of Archaeological Science 28, 1025-1040.

Jacobs, Z., Duller, G.A.T., Wintle, A.G., and Henshilwood, C.S., 2006. Extending the chronology of deposits at Blombos Cave, South Africa, back to 140 ka using optical dating of single and multiple grains of quartz, Journal of Human Evolution 51, 255-273.

Jacobs, Z., Roberts, R.G., Galbraith, R.F., Deacon, H.J., Grun, R., Mackay, A., Mitchell, P., Vogelsang, R., and Wadley, L., 2008. Ages for the Middle Stone Age of southern Africa: implications for human behavior and dispersal, Science 322, 733-735.

Jallot, L. and Pouzolles, G., 2000. Test-pit 1 extension: excavation results. in: Gutherz, X., Jallot, L., Lesur, J., Pouzolles, G., Sordoillet, D., Said, H., and Lakew, B. (Eds.), The Moche Borago Rockshelter: November 2000 Excavation.

Kamenov, G.D., Brenner, M., and Tucker, J.L., 2009. Anthropogenic versus natural control on trace element and Sr-Nd-Pb isotope stratigraphy in peat sediments of southeast Florida (USA), similar to 1500 AD to present, Geochimica et Cosmochimica Acta 73, 3549-3567.

Kebede, S., Travi, Y., Asrat, A., Alemayehu, T., Ayenew, T., and Tessema, Z., 2008. Groundwater origin and flow along selected transects in Ethiopian rift volcanic aquifers, Hydrogeology Journal 16, 55-73.

Kebede, S., Travi, Y., and Rozanskic, K., 2009. The delta O-18 and delta H-2 enrichment of Ethiopian lakes, Journal of Hydrology 365, 173-182.

Kebede, S., 2004. Approaches isotopique et geochemique pout l'etude Nil Bleu et du rift Ethiopien. University of Avignon, France,

Kebede, S., Travi, Y., Alemayehu, T., and Ayenew, T., 2005. Groundwater recharge, circulation and geochemical evolution in the source region of the Blue Nile River, Ethiopia, Applied Geochemistry 20, 1658-1676.

Kelly, R.L., 1995. The Foraging Spectrum, Smithsonian Institution Press, Washington D.C.

Kiage, L.M. and Liu, K., 2006. Late Quaternary paleoenvironmental changes in East Africa: a review of multiproxy evidence from palynology, lake sediments, and associated records, Progress in Physical Geography 30, 633-658.

Kurashina, H., 1978. An Examination of Prehistoric Lithic Technology in East-Central Ethiopia. (Ph.D. thesis, University of California, Berkeley)., University Microfilms, Ann Arbor.

Labeyrie, L.D., Juillet-Leclerc, A., Kallel, N., and Blanc, P.L., 1991. Sea level and oceanic thermohaline circulation: changes over a glacial/interglacial cycle. in: Frenzel, B. (Ed.), Klimageschichtliche Probleme der letzten 130'000 Jahre Fischer Verlag, Mainz, Stuttgart, pp. 197-214.

Lamb, A.L., Leng, M.J., Lamb, H.F., and Mohammed, M.U., 2000. A 9000-year oxygen and carbon isotope record of hydrological change in a small Ethiopian crater lake, The Holocene 167-177.

Lamberti, M. and Sottile, R., 1997. The Wolaytta Language, Rudiger Koppe Verlag, Cologne.

Landais, A., Barnola, J.M., Masson-Delmotte, V., Jouzel, J., Chappellaz, J., Caillon, N., Huber, C., Leuenberger, M., and Johnsen, S.J., 2004. A continuous record of temperature evolution over a sequence of Dansgaard-Oeschger events during Marine Isotopic Stage 4 (76 to 62 kyr BP), Geophysical Research Letters 31.

Le Gal, E. and Molinier, N., 2006. Agricultural and economic analysis-diagnosis of Obe Jage (Damot Gale, Wolayta). Institut National Agronomique Paris-Grignon,

Leakey, L.N. and Solomon, J.D., 1929. East African Archaeology, Nature 124.

Leakey, L.S.B., 1931. The Stone Age cultures of Kenya colony, Cambridge University Press, Cambride.

Leakey, L.S.B., 1936.
Stone age Africa: An outline of prehistory in Africa, Oxford University Press, Oxford.

Leakey, M.D., 1971. Olduvai Gorge Volume III: Excavations in beds I and II, 1960-1963, Cambridge University Press, Cambridge.

Lee, R.B. and DeVore, I., 1968. Man the Hunter, Aldine, Chicago.

Lesur, J., 2000. Moche Borago's Fauna. in: Gutherz, X., Jallot, L., Lesur, J., Pouzolles, G., Sordoillet, D., Said, H., and Lakew, B. (Eds.), The Moche Borago rock-shelter: November 2000 Excavation

Lesur-Gebremariam, J., 2008. Climatic changes in Holocene Horn of Africa and animals exploitations by human societies. Society of Africanist Archaeologists

Leuschner, D.C. and Sirocko, F., 2000. The low-latitude monsoon climate during Dansgaard-Oeschger cycles and Heinrich Events, Quaternary Science Reviews 19, 243-254.

Lezine, A.M. and Casanova, J., 1991. Correlated oceanic and continental records demonstrate past climate and hydrology of North Africa (0-140 ka), Geology 19, 307-310.

Libby, W.F., 1951. Radiocarbon dates 2, Science 114, 291-296.

Libby, W.F. and Arnold, J.R., 1950. Radiocarbon Dates, Science 112, 453.

Livingstone, D.A., 1975. Late Quaternary climatic change in Africa, Annual Review of Ecology and Systematics 6, 249-280.

Lundblad, K. and Holmgren, K., 2005. Paleoclimatological survey of stalagmites from coastal areas in Tanzania., Geografiska Annaler: Series A, Physical Geography 87, 125-140.

MacAyeal, D.R., 1993. Binge/purge oscillations of the Laurentide ice sheet as a cause of the North Atlantic's Heinrich events, Paleoceanography 8.

Maitima, J.M., 1991. Vegetation response to climatic change in Central Rift Valley, Kenya, Quaternary Research 35, 234-245.

Marean, C.W. and Assefa, Z., 2005. The middle and upper Pleistocene African record for the biological and behavioral origins of modern humans. in: Stahl, A. (Ed.), African Archaeology: A Critical Introduction Blackwell Publishing Ltd., pp. 93-129.

Marean, C.W., Bar-Matthews, M., Bernatchez, J., Fisher, E., Goldberg, P., Herries, A.I.R., Jacobs, Z., Jerardino, A., Karkanas, P., Minichillo, T., Nilssen, P.J., Thompson, E., Watts, I., and Williams, H.M., 2007. Early human use of marine resources and pigment in South Africa during the Middle Pleistocene, Nature 449, 905-908.

Marks, A. and Conard, N., 2006. Technology vs. typology: the case for and against a transition from the MSA to the LSA at Mumba Cave, Tanzania. in: Aubry, T., Almeida, F., Aranjo, A.C., and Tiffagom, M. (Eds.), XV World Congress UISPP BAR Press, Lisbon

Marlowe, F., 2010. The Hadza: Hunter-Gatherers of Tanzania, University of California Press, Berkeley.

Maslin, M.A., Seidov, D., and Lowe, J., 2001. Synthesis of the nature and causes of sudden climate transitions during the Quaternary. in: Seidov, Haupt, and Maslin, M.A. (Eds.), The Oceans and Rapid Climate Change: Past, Present and Future

Mazer, J.J., Stevenson, C.M., Ebert, W.L., and Bates, J.K., 1991. The experimental hydration of obsidian as a function of relative humidity and temperature, American Antiquity 56, 504-513.

McBrearty, S. and Brooks, A.S., 2000. The revolution that wasn't: a new interpretation of the origin of modern human behavior, Journal of Human Evolution 39, 453-563.

Meese, D.A., Gow, A.J., Grootes, P., Stuiver, M., Mayewski, P.A., Zielinski, G.A., Ram, M., Taylor, K.C., and Waddington, E.D., 1994. The accumulation record from the GISP2 Core as an indicator of climate change throughout the Holocene, Science 266, 1680-1682.

Mehlman, M.J., 1989. Later Quaternary Archaeological Sequences in Northern Tanzania. University of Illinois at Urbana-Champaign,

Merrick, H., 1975. Change in Later Pleistocene Lithic Industries in Eastern Africa. Ph.D. Dissertation, University of California, Berkeley., University Microfilms Intl., Ann Arbor.

Milankovitch, M., 1941. [New English Translation, 1998], Canon of Insolation and the Ice Age Problem. With introduction and biographical essay by Nikola Pantic, Alven Global.

Mitchell, P., 2002. The Archaeology of Southern Africa, Cambridge University Press, Cambridge.

Mohammed, U., Legesse, D., Gasse, F., Bonnefille, R., Lamb, H.F., and Leng, M.J., 2004. Late Quaternary climate changes in the Horn of Africa. in: Battarbee, R.W., Gasse, F., and Stickley, C.E. (Eds.), Past Climate Variability through Europe and Africa Springer, Dordrecth, pp. 159-175.

Muscheler, R., Beer, J., Kubik, P.W., and Synal, H.A., 2005. Geomagnetic field intensity during the last 60,000 years based on 10Be and 36Cl from the Summit ice cores and 14C, Quaternary Science Reviews 24, 1849-1860.

National Meteorlogical Agency, F.D.R.o.E., 2010. National Meteorlogical Agency City Index.

Neev, D. and Emery, K.O., 1967. The Dead Sea, depositional processes and environments of evaporites. Geolical Survey of Israel Bulletin, p. 147.

Negash, A., 2004. Unpublished report on the lithic analysis at Liben Bore, Ethiopia.

Nilsson, E., 1929. Preliminary Report on the Wuaternary Geology of Mount Elgon and some Parts of the Rift Valley.

Nilsson, E., 1949. The pluvials of East Africa. An attempt to correlate Pleistocene changes of climate, Geografiska Annaler 31, 204-211.

North Greenland Ice Core Project, 2004. High-resolution record of Northern Hemisphere climate extending into the last interglacial period, Nature 431, 147-151.

Olago, D.O., Street-Perrott, F.A., Perrott, R.A., Ivanovich, M., and Harknessm D.D., 2001. EU/Th and 14C Isotope Dating of Lake Sediments from Sacred Lake and Lake Nkunga, Kenya, African Journal of Science and Technology.Science and Engineering Series 2, 36-46.

Oppenheimer, S., 2003. Out of Africa's Eden: The Peopling of the World, Jonathan Ball Publishers, Johannesburg.

Pleurdeau, D., 2001. Gestion des Matieres Premieres et Comportements Techniques dans le Middle Stone Age Africain: Les Assemblages Lithiques La Grotte Du Porc Epic (Dire Dawa, Ethiopie). Ph.D. Dissertation, Museum National D'Histoire Naturelle., Museum National D'Histoire Naturelle.

Pleurdeau, D., 2005. Human Technical Behavior in the African Middle Stone Age: The Lithic Assemblage of Porc-Epic Cave (Dire Dawa, Ethiopia), African Archaeological Review 22, 177-197.

Poisblaud, B., 2000. Preliminary study of lithic implements of the U.S. 1010 and comparisons with cuttings 7 and 9 of test pit 1. in: Gutherz, X., Jallot, G., Poisblaud, B., Sordoillet, D., Pouzolles, G., Asfaw, A., Lakew, B., and Aba, G. (Eds.), The Moche Borago Rock-shelter: January - February 2000 Excavation. Report on File, SNNPR Office of Culture and Information, Awassa, Ethiopia., pp. 40-43.

Prendergast, M.E., Luque, L., Dom+¡nguez-Rodrigo, M., ez-Mart+¡n, F., Mabulla, A.Z.P., and Barba, R., 2007. New excavations at Mumba rockshelter, Tanzania, Journal of African Archaeology 5, 217-243.

Reimer, P.J., Baillie, M.G.L., Bard, E., Bayliss, A., Beck, J.W., Blackwell, P.G., Ramsey, C.B., Buck, C.E., Burr, G.S., Edwards, R.L., Friedrich, M., Grootes, P.M., Guilderson, T.P., Hajdas, I., Heaton, T.J., Hogg, A.G., Hughen, K.A., Kaiser, K.F., Kromer, B., McCormac, F.G., Manning, S.W., Reimer, R.W., Richards, D.A., Southon, J.R., Talamo, S., Turney, C.S.M., van der Plicht, J., and Weyhenmeye, C.E., 2009. Intcal09 and Marine09 radiocarbon age calibration curves, 0-50,000 years cal BP, Radiocarbon 51, 1111-1150.

Revel, M., Ducassou, E., Grousset, F.E., Bernasconi, S.M., Migeon, S., Revillon, S., Mascle, J., Murat, A., Zaragosi, S., and Bosch, D., 2010. 100,000 Years of African monsoon variability recorded in sediments of the Nile margin, Quaternary Science Reviews In Press, Corrected Proof.

Roberts, R.G., Galbraith, R.F., Laslett, G.M., Olley, J.M., and Yoshida, H., 1999. Optical dating of single and multiple grains of quartz from Jinmium Rock Shelter, northern Australia: Part II, results and implications, Archaeometry 41, 365-395.

Rogers, A.K., 2008. Obsidian hydration dating: accuracy and resolution limitations imposed by intrinsic water variability, Journal of Archaeological Science 35, 2009-2016.

Rostek, F., Bard, E., Beaufort, L., Sonzogni, C., and Ganssen, G., 1997. Sea surface temperature and productivity records for the past 240 kyr in the Arabian Sea, Deep Sea Research Part II: Topical Studies in Oceanography 44, 1461-1480.

Ruddiman, W.F., 1977. Late Quaternary deposition of ice-rafted sand in the subpolar North Atlantic (lat 40° to 65°N), Geological Society of America Bulletin 88, 1813-1827.

Sanchez-Gone, M.F. and Harrison, S.P., 2010. Millennial-scale climate variability and vegetation changes during the Last Glacial: Concepts and terminology, Quaternary Science Reviews In Press, Corrected Proof.

Sanchez-Gone, M.F., Landais, A., Fletcher, W.J., Naughton, F., Desprat, S., and Duprat, J., 2008. Contrasting impacts of Dansgaard-Oeschger events over a western European latitudinal transect modulated by orbital parameters, Quaternary Science Reviews 27, 1136-1151.

Schulz, H., von, R., Erlenkeuser, H., and von, R., 1998. Correlation between Arabian Sea and Greenland climate oscillations of the past 110,000 years, Nature 393, 54-57.

Shea, J.J., 2006. The origins of lithic projectile point technology: evidence from Africa, the Levant, and Europe, Journal of Archaeological Science 33, 823-846.

Shinn, D.H. and Ofcansky, T.P., 2004. Historical Dictionary of Ethiopia, The Scarecrow Press, Lanham.

Sordoillet, D. and Pouzolles, G., 2000. Stratigraphical and sedimentological survey of Moche Borago infilling. in: Gutherz, X., Jallot, L., Lesur J., Pouzolles, G., Sordoillet, D., Said, H., and Lakew, B. (Eds.), The Moche Borago Rock-shelter: November 2000 Excavation.

Sowers, T., Bender, M., Labeyrie, L., Martinson, D., Jouzel, J., Raynaud, D., Pichon, J.J., and Korotkevich, Y.S., 1993. A 135,000-Year Vostok-Specmap common temporal framework, Paleoceanography 8.

Stein, M., Goldstein, S.L., Schramm, M., Katz, A., and Starinsky, A., 1998. Lake Lisan sediments (paleo-Dead Sea) as monitors of the last glacial history. PAGES Past Global Changes and their Significance for the Future University of London, p. 21.

Stuiver, M. and Grootes, P.M., 2000. GISP2 Oxygen isotope ratios, Quaternary Research 53, 277-284.

Stuiver, M. and Polach, H.A., 1977. Reporting of C-14 Data - Discussion, Radiocarbon 19, 355-363.

Svensson, A., Andersen, K.K., Bigler, M., Clausen, H.B., Dahl-Jensen, D., Davies, S.M., Johnsen, S.J., Muscheler, R., Parrenin, F., Rasmussen, S.O., Roethlisberger, R., Seierstad, I., Steffensen, J.P., and Vinther, B.M., 2008. A 60 000 year Greenland stratigraphic ice core chronology, Climate of the Past 4, 47-57.

Svensson, A., Andersen, K.K., Bigler, M., Clausen, H.B., Dahl-Jensen, D., Davies, S.M., Johnsen, S.J., Muscheler, R., Rasmussen, S.O., Rothlisberger, R., Steffensen, J.P., and Vinther, B.M., 2006. The Greenland ice core chronology 2005, 15-42 ka. Part 2: comparison to other records, Quaternary Science Reviews 25, 3258-3267.

Thorne, A., Grun, R., Mortimer, G., Spooner, N.A., Simpson, J.J., McCulloch, M., Taylor, L., and Curnoe, D., 1999. Australia's oldest human remains: age of the Lake Mungo 3 skeleton, Journal of Human Evolution 36, 591-612.

Tierney, J.E., Russell, J.E., Huang, Y., Damste, J.S.S., Hopmans, E.C., and Cohen, A.S., 2008. Northern hemisphere controls on tropical Southeast African climate during the past 60,000 Years, Science 1160485.

Trigger, B., 1989. A History of Archaeological Thought, Cambridge University Press, New York.

Van Campo, E., Duplessy, J.C., Prell, W.L., Barratt, N., and Sabatier, R., 1990. Comparison of terrestrial and marine Temperature estimates for the past 135 Kyr off Southeast Africa: A test for Gcm simulations of paleoclimate, Nature (London) 348, 209-212.

Van der Touw, J.W., Galbraith, R.F., and Laslett, G.M., 1997. A logistic truncated normal mixture model for overdispersed binomial data, Journal of Statistical Computation and Simulation 59, 349-373.

Van Peer, P., 1998. The Nile corridor and the out-of-Africa model: an examination of the archaeological record, Current Anthropology 39, 115-140.

Van Peer, P. and Vermeersch, P.M., 2000. Nubian complex and the dispersal of modern humans in North Africa. in: Krzyzaniak, L., Kroeper, K., and Kobusiewicz, M. (Eds.), Recent Research into the Stone Age of Northeastern Africa Poznan Archaeological Museum, Poznan, pp. 47-60.

Vermeersch, P.M., 2001. 'Out of Africa' from an Egyptian point of view, Quaternary International 75, 103-112.

Vidal, L. and Arz, H., 2004. Oceanic climate variability at millenial time scales: models of climate connections. in: Battarbee, R.W., Gasse, F., and Stickley, C.E. (Eds.), Past climate Variability through Europe and Africa Springer, Dordrecht, pp. 31-40.

Vincent, A.S., 1984. Plant foods in savanna environments: a preliminary report of tubers eaten by the Hadza of northern Tanzania, World Archaeology 17, 131-147.

Voelker, A.H.L., 2002. Global distribution of centennial-scale records for Marine Isotope Stage (MIS) 3: a database, Quaternary Science Reviews 21, 1185-1212.

Wadley, L., 2001. What is cultural modernity? A general view and a South African perspective from Rose Cottage Cave, Cambridge Archaeological Journal 11, 201-221.

Wang, Y.J., Cheng, H., Edwards, R.L., An, Z.S., Wu, J.Y., Shen, C.C., and Dorale, J.A., 2001. A High-Resolution Absolute-Dated Late Pleistocene Monsoon Record from Hulu Cave, China, Science 294, 2345-2348.

Wayland, E.J., 1929. African Pluvial Periods and Prehistoric Man, Man 29, 118-121.

Wayland, E.J., 1930. African Pluvial Periods and Prehistoric Man, Man 30, 236.

Wayland, E.J., 1934. Rifts, rivers, rains and early Man in Uganda, The Journal of the Royal Anthropological Institute of Great Britain and Ireland 64, 333-352.

Wayland, E.J. and Burkitt, M.C., 1932. The Magosian culture of Uganda, Journal of the Royal Anthropological Institute 1, 369-390.

Weldeab, S., Lea, D.W., Schneider, R.R., and Andersen, N., 2007. 155,000 years of West African monsoon and ocean thermal evolution, Science 316, 1303-1307.

Wendorf, F. and Schild, R., 1989. Summary and synthesis. in: Wendorf, F., Schild, R., and Close, A. (Eds.), The Prehistory of Wadi Kubbaniya, volume 3: Late Paleolithic Archaeology Southern Methodist University Press, Dallas

Wendorf, F. and Schild, R., 1992. The Middle Paleolithic of North Africa: a status report. New light on the Northeast African past Heinrich-Barth Institute, Cologne, pp. 42-78.

Weninger, B. and Joris, O., 2008. A C-14 age calibration curve for the last 60 ka: the Greenland-Hulu U/Th timescale and its impact on understanding the Middle to Upper Paleolithic transition in Western Eurasia, Journal of Human Evolution 55, 772-781.

White, L., 1959. The Evolution of Culture, McGraw-Hill, New York.

White, T.D., Asfaw, B., Degusta, D., Gilbert, H., Richards, G.D., Suwa, G., and Clark Howell, F., 2003. Pleistocene Homo sapiens from Middle Awash, Ethiopia, Nature 423, 742-747.

White, T.E., 1953a. A method of calculating the dietary percentage of various food animals utilized by aboriginal peoples, American Antiquity 18, 396-398.

White, T.E., 1953b. Observations on the butchering technique of some aboriginal peoples, no. 2, American Antiquity 19, 160-164.

Wiessner, P., 1982. Beyond willow smoke and dogs' tails: a comment on Binford's analysis of hunter-gatherer settlement systems, American Antiquity 47, 171-178.

Wiessner, P., 1977. Hxaro: A regional system of reciprocity for reducing risk among the !Kung San. University of Michigan, Ann Arbor, University Microfilms

Wiessner, P., 1980. Risk, reciprocity and social influence on !Kung San economies. in: Leacock, E.R. and Lee, R.B. (Eds.), Politics and History in Band Societies Cambridge University Press, London

WoldeGabriel, G., Aronson, J.L., and Walter, R.C., 1990. Geology, geochronology, and rift basin development in the central sector of the Main Ethiopia Rift, Geological Society of America Bulletin 102, 439-458.

Wolff, E.W., Chappellaz, J., Blunier, T., Rasmussen, S.O., and Svensson, A., 2010. Millennial-scale variability during the last glacial: The ice core record, Quaternary Science Reviews In Press, Corrected Proof.

Woodburn, J., Lee, R.B., and DeVore, I., 1968. An introduction to Hadza ecology. Man the Hunter, pp. 49-55.

Yellen, J., Brooks, A., Helgren, D., and Tappen, M., 2005. The Archaeology of Aduma Middle Stone Age Sites in the Awash Valley, Ethiopia, PaleoAnthropology 25-100.

Yellen, J.E. and Harpending, H., 1972. Hunter-gatherer populations and archaeological inference, World Archaeology 4, 244-253.

Yellen, J.E., 1977. Long Term Hunter-Gatherer Adaptation to Desert Environments: A Biogeographical Perspective, World Archaeology 8, 262-274.

Zilhão, J., 2006. Aurignacian, behavior, modern: issues of definition in the emergence of the European Upper Paleolithic. Towards a Definition of the Aurignacian, pp. 53-69.

Zilhão, J., Trinkaus, E., Constatin, S., Milota, S., Gherase, M., Sarcina, L., Danciu, A., Rougier, H., Quiles, J., and Rodrigo, R., 2007. The Pestera cu Oase people, Europe's earliest modern humans. in: P.Mellars, K.Boyle, O.Bar-Yosef, and C.Stringer (Eds.), Rethinking the Human Revolution McDonald Institute, Cambridge

BIOGRAPHICAL SKETCH

Erich Christopher Fisher was born Colorado. The oldest of two children, Erich and his family moved to Houston, Texas when he was in second grade. Although not a native, Erich considers Texas home. Erich received his B.A. in anthropology with a minor in cartography / GIS from Southwest Texas State University (known now as Texas State University, San Marcos) in 2002. That same year he began graduate school at the University of Florida and he earned his Master of Arts degree in 2005.